NASA CR–135011
144
TECH LIBRARY KAFB, NM
0062772
LOAN COPY: RETUR
AFWL TECHNICAL LI
KIRTLAND AFB, N.

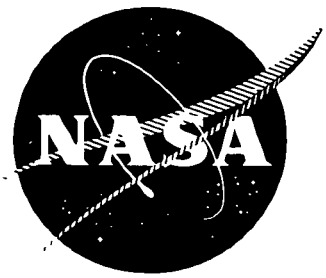

THRUSTER ENDURANCE TEST

FINAL REPORT

MAY 1976

BY

ION PHYSICS DEPARTMENT STAFF

HUGHES RESEARCH LABORATORIES
A DIVISION OF HUGHES AIRCRAFT COMPANY
3011 MALIBU CANYON ROAD
MALIBU, CALIFORNIA 90265

PREPARED FOR

NATIONAL AERONAUTICS AND SPACE ADMINISTRATION
NASA LEWIS RESEARCH CENTER

CONTRACT NAS 3 - 15523

TECH LIBRARY KAFB, NM
0062772

1 Report No	2. Government Accession No	3 R
NASA-CR-135011		

4 Title and Subtitle	5 Report Date
THRUSTER ENDURANCE TEST	May 1976
	6. Performing Organization Code

7 Author(s)	8 Performing Organization Report No.
C. Collett, et al.	
	10. Work Unit No.

9. Performing Organization Name and Address	11 Contract or Grant No
Hughes Research Laboratories 3011 Malibu Canyon Road Malibu, CA 90265	NAS 3-15523
	13 Type of Report and Period Covered
12. Sponsoring Agency Name and Address National Aeronautics and Space Administration Cleveland, OH 44135	Contractor Report
	14 Sponsoring Agency Code

15 Supplementary Notes

Project Managers; Nelson Milder, James S. Sovey,
NASA-Lewis Research Center, Cleveland, Ohio

16 Abstract

The original goal of this program was to conduct a 6000-hour endurance test of a 30-cm Electron Bombardment Ion Thruster. At the time the program was initiated, the 400 series thruster had been developed under Contract NAS 3-14140 and it was this version of thruster which was intended to be evaluated. By the time this program was concluded, the 400 series thruster had been superceded by the 700 series engineering model thruster and a 10,000-hour test of thruster 701 was underway. (The 10,000-hour test was completed under Contract NAS 3-17803.)

At the beginning of this program a test system was built and several short term tests were completed. The test system included, in addition to the 30-cm ion thruster, a console for powering the thruster and monitoring performance, a vacuum facility for simulating a space environment, and a storage and feed system for the thruster propellant. This system was used to perform three short term tests (one 100-hour and two 500-hour tests), an 1108-hour endurance test which was aborted by a vacuum facility failure, and finally the 10,000-hour endurance test.

In addition to the two 400 series thrusters which were used in the short term and 1100-hour tests, four more 400 series thrusters were fabricated, checked out and delivered to NASA. Three consoles similar to the one used in the test program were also fabricated and delivered.

17 Key Words (Suggested by Author(s))	18 Distribution Statement
Electric Propulsion Ion Propulsion 30-cm Ion Thruster Testing Power Conditioning for Ion Thruster	UNCLASSIFIED - Unlimited

19 Security Classif (of this report)	20 Security Classif (of this page)	21 No of Pages	22 Price*
UNCLASSIFIED	UNCLASSIFIED	276	

* For sale by the National Technical Information Service, Springfield, Virginia 22151

FOREWORD

The work described herein was performed by personnel of the Hughes Research Laboratories, Malibu, California and Space and Communications Group of Hughes Aircraft Company, El Segundo, California. The work at Hughes Research Laboratories was performed in the Ion Physics Department managed by Mr. J.H. Molitor; the test consoles were designed and built in the Power Electronics Department of S&CG managed by P.S. DuPont; the endurance tests were conducted at Hughes Space Simulation Laboratory managed by H. Allgauer. The work was performed under Contracts NAS 3-15523 monitored by Mr. Nelson Milder and NAS 3-17803 monitored by Mr. James S. Sovey of NASA Lewis Research Center. Major technical contributions to this effort were C.R. Collett, Program Manager for NAS 3-15523 and NAS 3-17803; D.R. Garth, Test Console Project Manager; H.J. King, Thruster Project Manager; D.E. Schnelker, Thruster Fabrication; E. A. Volkoff, Test Facility Supervision; and R. L. Poeschel, Thruster 701 post-test analysis.

Page intentionally left blank

Page intentionally left blank

SUMMARY

The original goal of this program was to conduct a 6000-hour endurance test of a 30-cm Electron Bombardment Ion Thruster. At the time the program was initiated, the 400 series thruster had been developed under Contract NAS3-14140 and it was this version of thruster which was intended to be evaluated. By the time this program was concluded, the 400 series thruster had been superceded by the 700 series engineering model thruster and a 10,000-hour test of thruster 701 was underway. (The 10,000-hour test was completed under Contract NAS3-17803.)

At the beginning of this program a test system was built and several short term tests were completed. The test system included, in addition to the 30-cm ion thruster, a console for powering the thruster and monitoring performance, a vacuum facility for simulating a space environment, and a storage and feed system for the thruster propellant. This system was used to perform three short term tests (one 100-hour and two 500-hour tests), an 1108-hour endurance test which was aborted by a vacuum facility failure, and finally the 10,000-hour endurance test.

The short term tests served the useful purpose of identifying several life limiting factors in the thruster. As a result, thruster modifications were incorporated which were subsequently confirmed to be successful by the results of the 10,000-hour test. The 10,000-hour endurance test, in turn, demonstrated the need for further thruster changes to overcome the effects of erosion within the discharge chamber. The effectiveness of these changes are still to be evaluated in an endurance test to be conducted under Contract NAS3-18914.

In addition to the two 400 series thrusters which were used in the short term and 1100-hour tests, four more 400 series thrusters were fabricated, checked out and delivered to NASA. Three consoles similar to the one used in the test program were also fabricated and delivered.

Page intentionally left blank

Page intentionally left blank

TABLE OF CONTENTS

SECTION		PAGE
	SUMMARY	v
I.	INTRODUCTION	1
II.	TEST SYSTEM DESCRIPTION	3
	A. Thruster	3
	B. Test Console	9
	C. Vacuum Test Facility	27
	D. Mercury Feed System	31
III.	TEST RESULTS	33
	A. Short Term Tests	33
	B. Endurance Tests	61
IV.	CONCLUSIONS	83
	A. Insulators	83
	B. Eroded Components	84
	APPENDIX A	87
	REFERENCES	269

Page intentionally left blank

Page intentionally left blank

LIST OF ILLUSTRATIONS

FIGURE		PAGE
II-1	400 series thruster design	4
II-2	400 series thruster	6
II-3	700 series thruster design	7
II-4	700-series thruster with ground screen	8
II-5	Test console used during endurance test program	10
II-6	Pullout drawers with mounted thruster power supplies	11
II-7	Test console power processor block diagram	13
II-8	Basic inverter circuit	16
II-9	Screen supply block diagram	17
II-10	Accelerator supply block diagram	19
II-11	Discharge supply block diagram	20
II-12	Heater/keeper supply control circuitry	22
II-13	Control system block diagram	23
II-14	Control system functional diagram	25
II-15	Test console automatic start up sequence	26
II-16	Test facility with thruster (mounted on dome) being lifted to top of vacuum chamber	30
II-17	Test facility showing location of thrusters, beam probe, cryoshrounds, and frozen mercury collector	31
II-18	Mercury storage and feed system	32

FIGURE		PAGE
III-1	Beam profiles taken at 4 accel voltages with probe located 2.7 m downstream	42
III-2	Time history of principal thruster operating parameters during 50 hour test No. 1	45
III-3	Center section of accel electrode after 500 hour test No. 1	48
III-4	Locking screw from center support of 500 hour test No. 1 optics and new unused locking screw	49
III-5	Time history of the principal thruster operating parameters during 500 hour test No. 2	52
III-6	After 500 hour test No. 2	57
III-7	Cathode thermal radiators after 500 hour tests. .	58
III-8	Cross sections of cathode tip heater and thermal radiator after 500 hour test No. 2	59
III-9	Time history of selected thruster operating parameters during the 1,100 hour endurance test	63
III-10	Thrusters at test hours 1800, 8600, and 10,000 showing flakes on optics and eroded baffle . . .	74
III-11	Photograph of optics showing flakes on screen electrode and localized erosion of accelerator electrode apertures caused by flakes (Accelerator aperture diameter is 0.15 cm)	75
III-12	Beam current time history profile for 10,000 hour test.	77

LIST OF TABLES

TABLE		PAGE
II-1	Test Console Power Processor Rating	15
II-2	Test Console Alarms	28
III-1	Summary of Test Results	34
III-2	Summary of Thruster Characteristics	35
III-3	Summary of Thruster Performance	36
III-4	Thruster Performance During 100-Hour Test . .	40
III-5	Thruster Performance During 100-Hour Test No. 1	44
III-6	Pre-Test and Post-Test Heater Resistances for 500 Hour Test No. 2 Thruster	60
III-7	Summary of Thruster Performance During 10,000 Hour Test	66
III-8A	Performance Summary of 10,000 Hr Test Thruster 701	67
III-8B	Performance Summary of 10,000 Hour Test Thruster 701	69

I. INTRODUCTION

The 30-cm electron bombardment ion thruster presently under development at Hughes Research Laboratories (under Contracts NAS3-17803 and NAS3-19703) is expected to form the basis of near future prime propulsion systems, both for interplanetary vehicles and orbit raising of synchronous satellites. An essential prerequisite to spacecraft application of these thrusters is the demonstration of extended periods of uninterrupted operational testing.

The principal goal of this program, when first initiated, was to conduct a 6000-hour endurance test of what, at that time, was the latest model of a 30-cm Kaufman thruster, the 400 series design. The purpose of the test was to demonstrate the lifetime capability of such critical components as cathodes, vaporizers, and isolators, as well as to demonstrate that recent thruster modifications had eliminated or substantially reduced the problems of neutralizer erosion due to impingement by beam ions and erosion of the accelerator electrode in the region of the neutralizer. The final result of this program was the initiation of a 10,000-hour endurance test of the first of the engineering model 30-cm thrusters, the 700 series design. The 10,000-hour test was initiated under this program and concluded under Contract NAS3-17803.

The endurance test was the culmination of a program which included the development of an ion engine life test support system as well as the performance of several preliminary tests of shorter duration. The principal elements of the support system were (1) a test console consisting of a flight prototype transistorized high frequency power processor (the predecessor of the thermal-vacuum breadboard, power processor developed under Contract NAS3-17223), the control logic and the data acquisition equipment for powering, controlling, and monitoring the thruster during the endurance test, (2) a vacuum facility capable of operating unattended for the duration of the endurance test which was designed to minimize sputter deposition on the thruster through the incorporation of a frozen mercury collector, and (3) a laboratory type mercury feed system which included provisions for

measuring the propellant flowrate either by weight change or volume change. Descriptions of the thruster, test console, vacuum facility, and feed system are presented in Section II.

The short term tests conducted prior to the endurance test were designed to uncover any thruster life limiting factors which could be detected after 500 hours of operation and also demonstrate the readiness of the test facility for the endurance test. The short term tests did result in modifications which were included in the endurance test thruster. These modifications are identified and evaluated in terms of the endurance test results in Section III.

The endurance test began on February 22, 1974 and was concluded (under Contract NAS3-17803) on May 12, 1975. The initial contractual operating point was a beam current of 1.5 A, 1100 V beam voltage, 500 V accelerator voltage, and 37 V discharge voltage. During the course of the test the test objectives were modified to raise the beam current in steps to 2 A. Thruster performance at each beam current level which was achieved is presented herein, including electrical efficiency, propellant efficiency (based on main, cathode, and neutralizer flowrate), and high voltage trip rate. Finally, in the interest of completeness, the results of an extensive post-test analysis of the endurance test thruster are provided in Section III and Appendix A.

II. TEST SYSTEM DESCRIPTION

The test system utilized throughout this program consisted of four principle subsystems: (1) the 30-cm ion thruster being tested, (2) a test console which provides electrical power to the thruster, controls the operation of the thruster and provides data for assessing the performance of the thruster, (3) a vacuum facility for simulating the thermal-vacuum environment of space to test the thruster, and (4) a mercury storage and distribution system to provide propellant to the thruster. Each of these subsystems is described individually in the sections that follow.

A. Thruster

The thrusters tested under this program were dual-grid 30-cm hollow cathode electron bombardment mercury fueled Kaufman thrusters. The major elements of this type of thruster are (1) a discharge chamber with permanent magnets and a variable magnetic field baffle, (2) dual-grid multiple aperture accelerator system, (3) main isolator-vaporizer assembly, (4) cathode isolator-vaporizer assembly, (5) hollow cathode plasma bridge neutralizer, and (6) outer ground screen.

During the course of this program three thrusters were tested; the first two were 400 series thrusters, S/N 401 and 402, the third was a 700 series thruster, S/N 701. The 400 series thruster design was developed under Contract NAS 3-14140. The 400 series 30-cm thruster design is shown in Fig. II-1. The thruster is designed so that a small number of major subassemblies are fabricated as separate units and assembled into a final configuration requiring only mechanical assembly and final wiring. The subassemblies which go into making up a thruster are as follows:

- Thruster shell with mounting provisions for all other subassemblies
- Main isolator vaporizer (MIV)

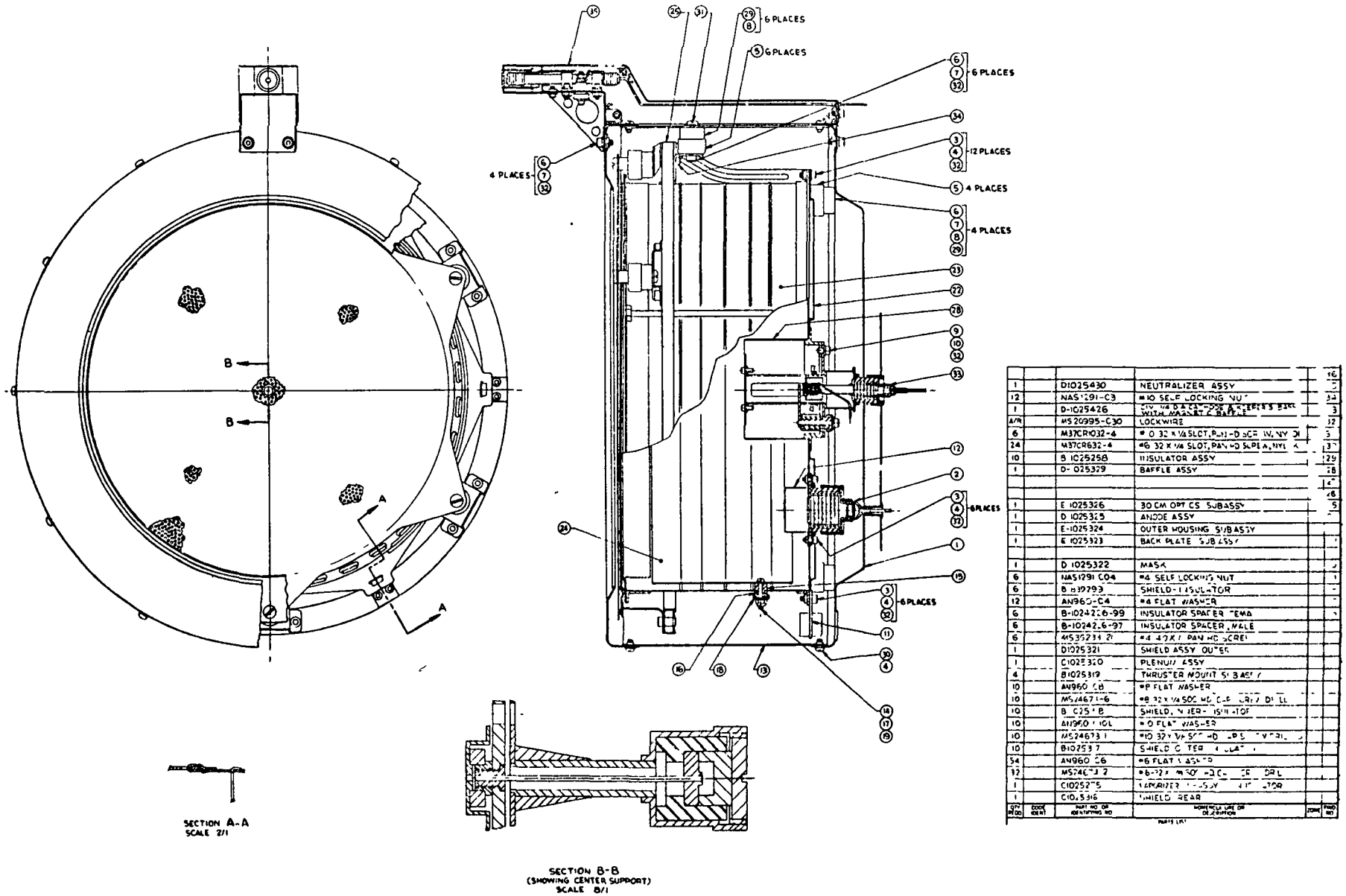

1		D1025430	NEUTRALIZER ASSY	16
12		NAS1291-C3	#10 SELF LOCKING NUT	34
1		D-1025426	CUP W/4 DATA PLATES & RIVETS SIZE WITH MAGNETIC BAFFLE	3
A/R		MS20995-C30	LOCKWIRE	32
6		M37CR1032-4	#10-32 X 1/4 SLOT, PAN HD SCREW, NYL	5
24		M37CR632-4	#6-32 X 1/4 SLOT, PAN HD SCREW, NYL	31
10		B 1025258	INSULATOR ASSY	29
1		D-1025329	BAFFLE ASSY	18
				4
				16
1		E 1025326	30 CM OPT CS SUBASSY	5
1		D 1025325	ANODE ASSY	2
1		E-1025324	OUTER HOUSING SUBASSY	
1		E 1025323	BACK PLATE SUBASSY	
1		D 1025322	MASK	1
6		NAS1291 C04	#4 SELF LOCKING NUT	1
6		B 1039799	SHIELD-INSULATOR	
12		AN960-C4	#4 FLAT WASHER	
6		B-10242.6-99	INSULATOR SPACER, FEMALE	
6		B-10242.6-97	INSULATOR SPACER, MALE	
6		MS35234-21	#4-40X1 PAN HD SCREW	
1		D1025321	SHIELD ASSY OUTER	
1		C1025320	PLENUM ASSY	
4		B1025319	THRUSTER MOUNT SUBASSY	
10		AN960-C8	#8 FLAT WASHER	
10		MS24671-6	#8-32 X 3/8 SOC HD CAP SCREW DRILL	
10		B 1025318	SHIELD, INSULATOR	
10		AN960-10L	#10 FLAT WASHER	
10		MS24673-1	#10-32 X 1/4 SOC HD CAP SCREW	
10		B102537	SHIELD CENTER FLAT	
54		AN960-C6	#6 FLAT WASHER	
32		MS24671-2	#6-32 X 3/16 SOC HD CAP SCREW DRILL	
1		C1025275	NEUTRALIZER SUBASSY	
1		C10.5316	SHIELD REAR	

QTY PER UNIT	CODE IDENT	PART NO. OR IDENTIFYING NO.	NOMENCLATURE OR DESCRIPTION	ZONE	FIND NO.

PARTS LIST

Figure II-1. 400 series thruster design.

- Cathode isolator vaporizer (CIV)
- Ion extraction system
- Neutralizer
- Ground screen.

Design details of these subassemblies are available in the final report of Contract NAS 3-14140.[1] A completed 400 series thruster ready for testing is shown in Fig. II-2.

The 700-series thruster which was introduced into the test program at the beginning of the 10,000 hour endurance test was developed under Contract NAS 3-16528. The 700 series design is shown in Fig. II-3. Substantial mechanical design differences exist between the 400-series and 700-series thruster. The primary mechanical changes included in the 700 series are as follows:

- Dished grids to replace flat grids with center support
- Improved ion optical system mounting structure
- Structural additions to allow two point gimbal mounting of the thrusters
- Stiffening across the back plate to prevent "oil canning"
- Substitution of titanium for stainless steel ion discharge chamber to reduce weight
- Substitution of flame sprayed cathode heaters for brazed on coaxial heaters
- Relocation of the CIV to a cooler location
- Addition of terminals for all internal wiring.

Details of these design differences are available in references 2 and 3. Some of the design differences listed above, e.g., dished optics in place of flat optics, were introduced and evaluated during the series of tests conducted under this program which preceded the 10,000 hour test of thruster 701. These changes are identified in Section III, Test Results (see Table III-1). Figure II-4 shows a 700-series thruster with the ground screen removed.

M8374

Figure II-2. 400 series thruster.

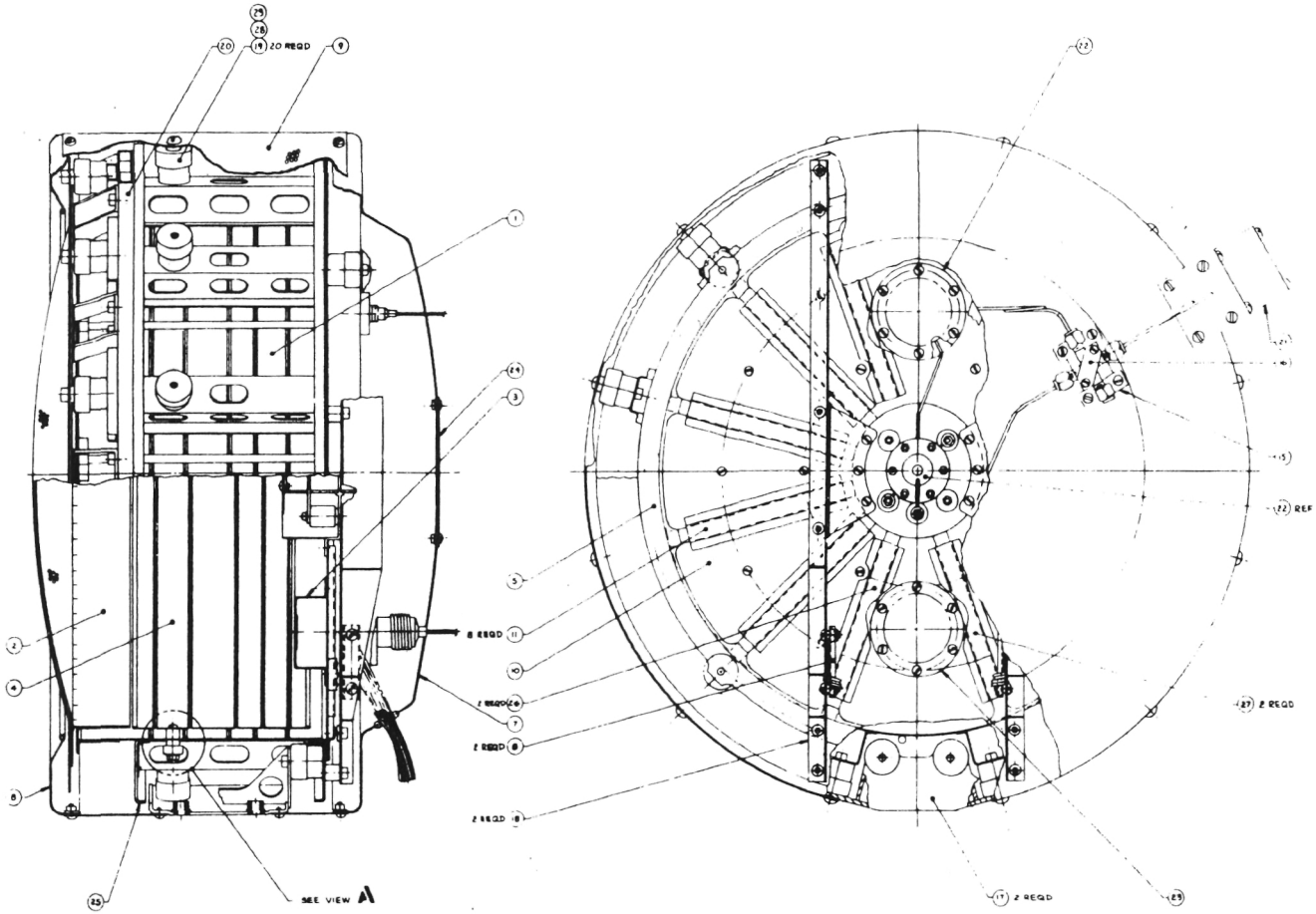

Figure II-3. 700 series thruster design.

M9963

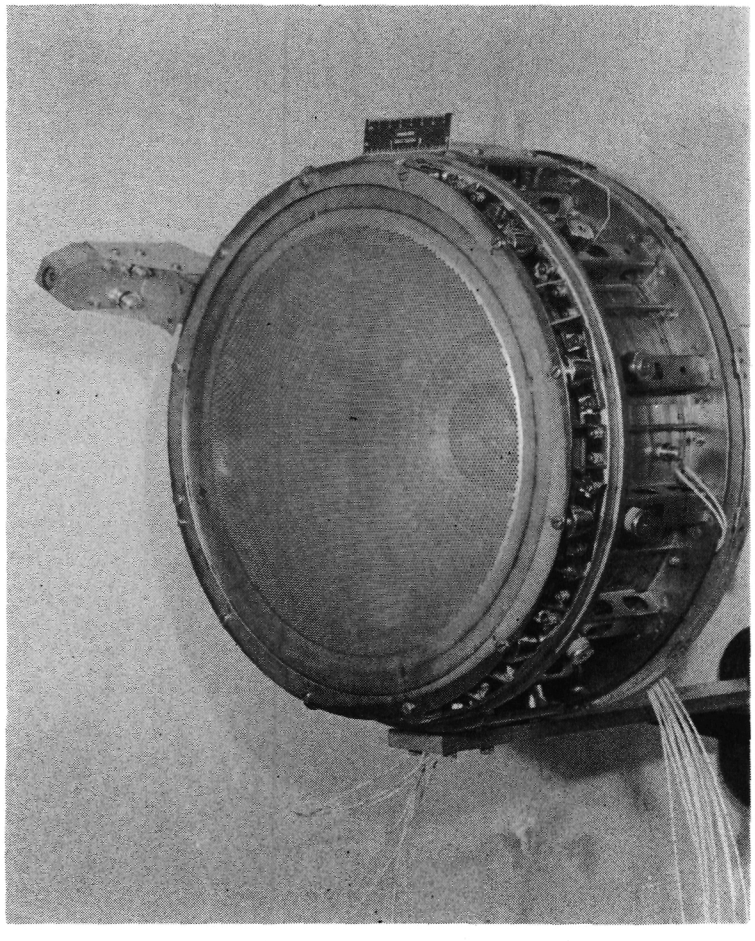

(a) front view

M9959

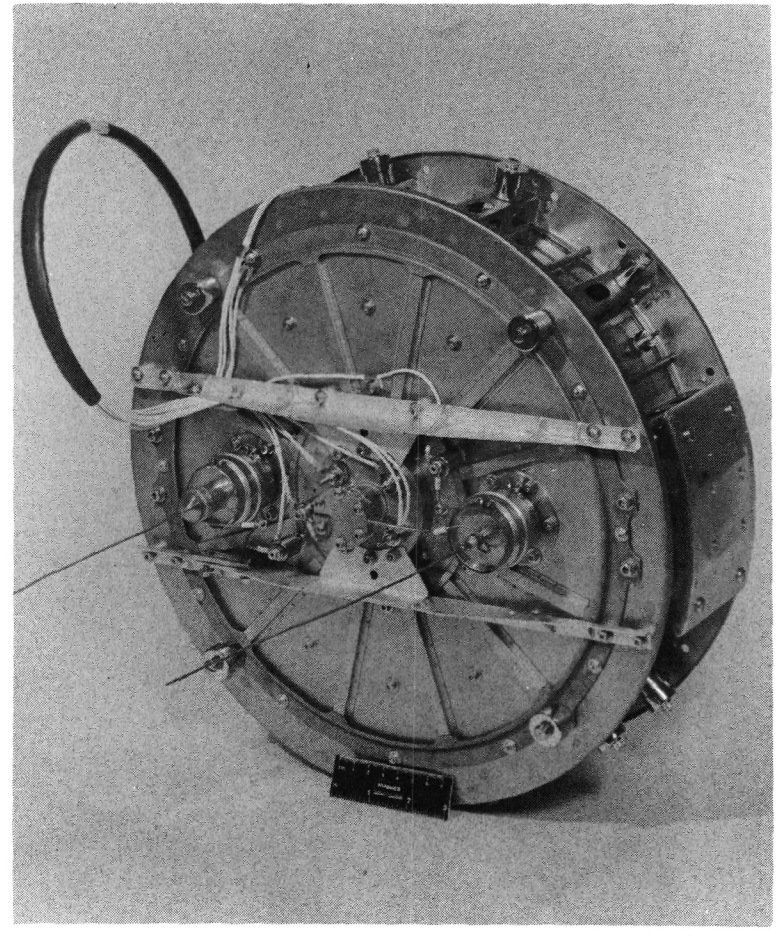

(b) rear view

Figure II-4. 700-series thruster with ground screen removed.

B. Test Console

In order to perform the endurance test and precursor short term tests it was necessary to provide power conditioning equipment and control circuitry for the thruster. A test console was designed which contains the power supplies, thruster control circuitry, indicator/alarm provisions and data acquisition equipment necessary for safe stable long term unattended thruster operation. Four test consoles were built; S/N 1 (shown in Fig. II-5) was used for all the tests conducted under this program, S/N 2 and S/N 3 were delivered to Lewis Research Center and S/N 4 will be the backup power processor for the 30-cm thruster endurance test to be conducted under Contract NAS 3-18914.

The locations of the major sections of the test console are indicated in Fig. II-5. The thruster power supplies are mounted on pull-out drawers which are shown extended in Fig. II-6. The power supplies are constructed on 19-in. rack panels which can be easily removed if required.

1. Power Processor

The various voltage and current levels required for thruster operation are provided by high frequency transistorized supplies operating from a regulated 250 Vdc power bus. Functionally, the power processor design follows the modular configuration concept used in earlier HAC systems; the circuit designs utilized were initially evaluated under Contract NAS 3-14140.[1]

The power processor system block diagram is shown in Fig. II-7. This system is constructed with basic building-block inverters. Eight such inverters with their rectified dc outputs connected in series are used in the screen supply. The discharge supply employs three inverters with their ac output in series. The accelerator supply consists of a single inverter preceded by regulated switching in the 250 V line to provide closed loop control. All of the above supplies operate at an inverter switching frequency of approximately 10 kHz. Heater and keeper power is supplied by map-amp controllers that regulate, in a constant current mode, the output of a single inverter operating at 5 kHz.

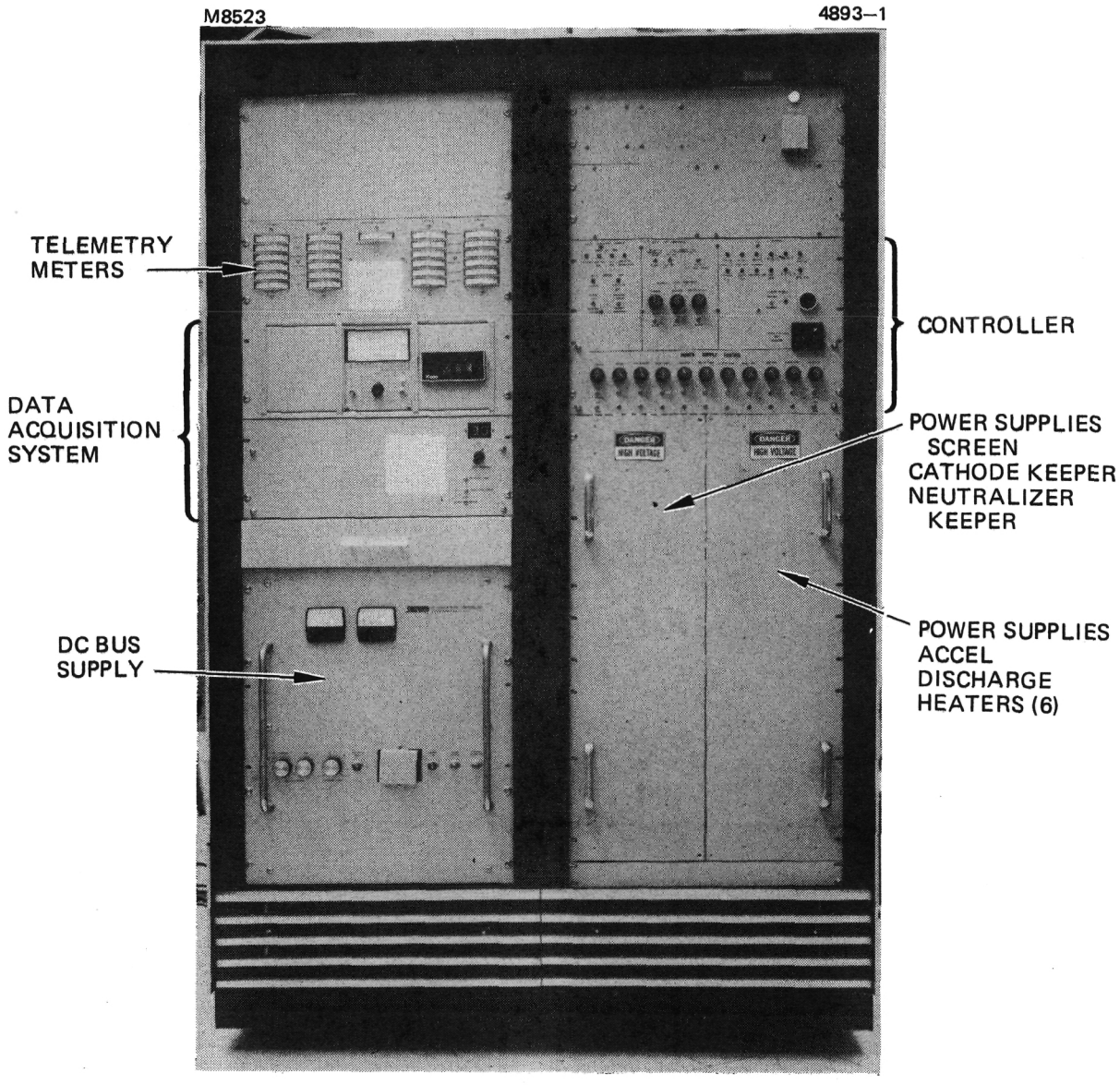

Figure II-5. Test console used during endurance test program.

4R27681

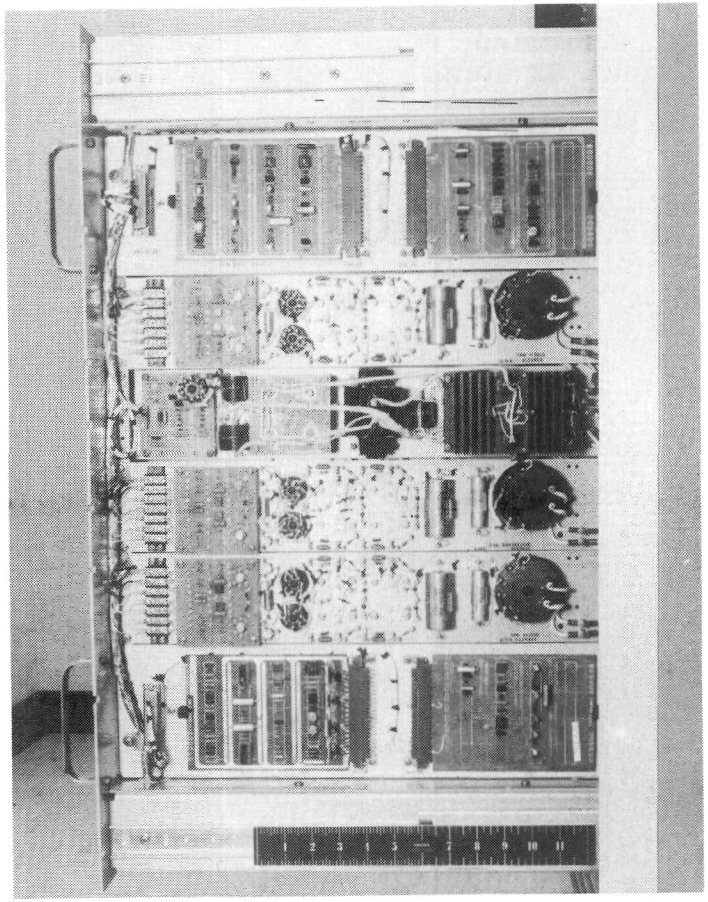

4R27679

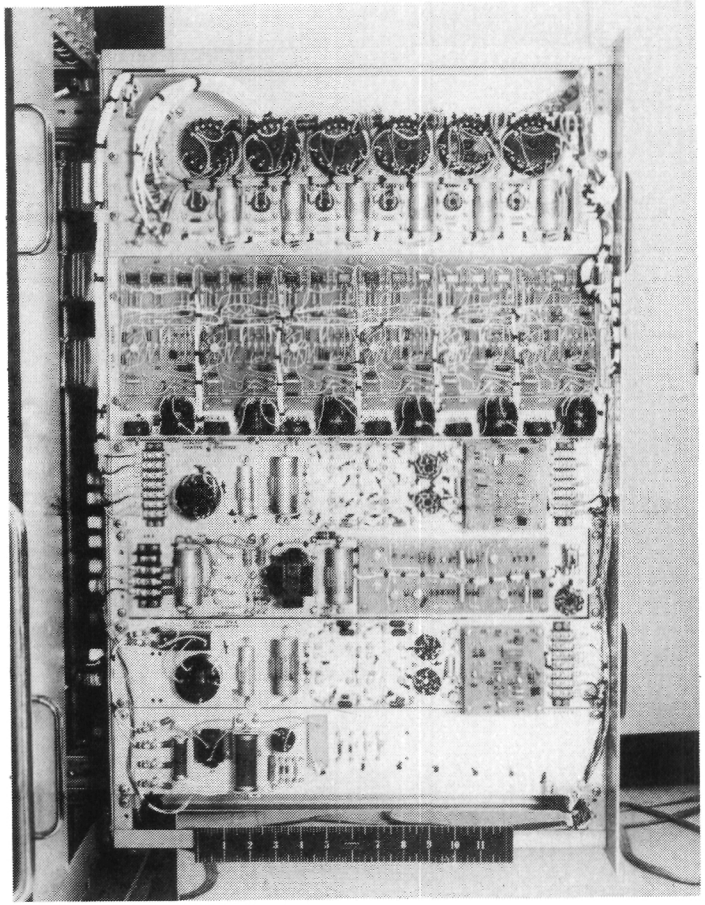

(a)

Figure II-6. Pullout drawers with mounted thruster power supplies.

4R2768

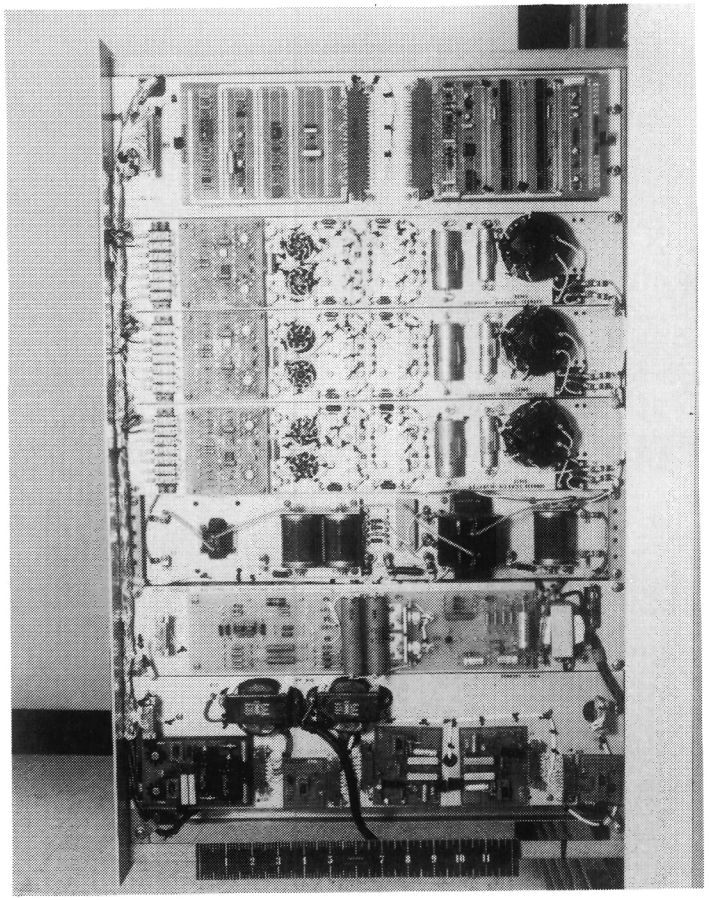

4R27682

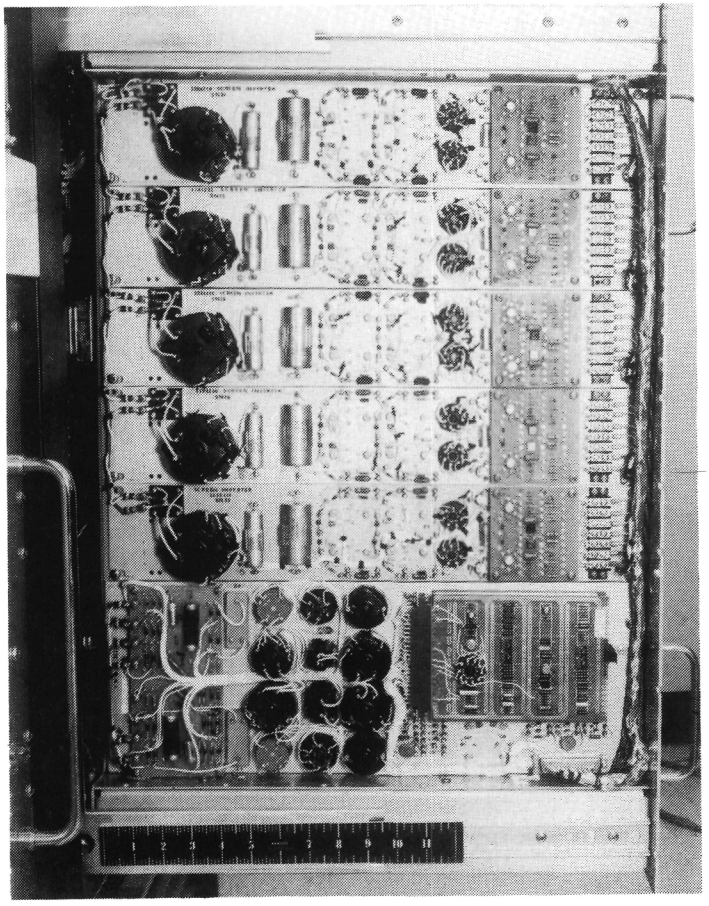

(b)

Figure II-6. (Continued)

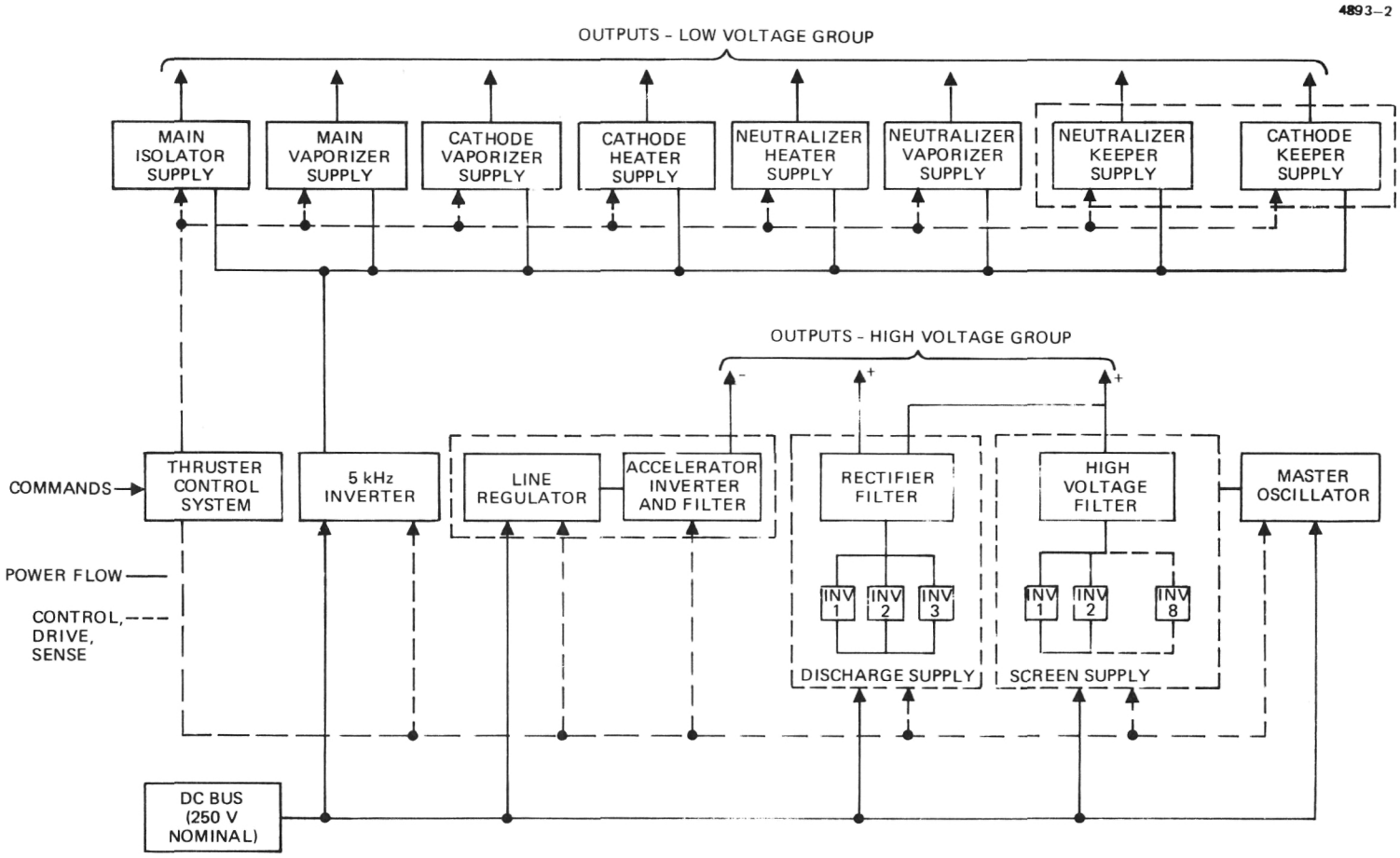

Figure II-7. Test console power processor block diagram.

Individual supply ratings and regulation modes are listed in Table II-1. During normal thruster operation most of the supplies were operated below their maximum capability.

a. Basic Inverter Circuit – The basic building-block inverter circuit is shown in Fig. II-8. The circuit used is a transistor bridge driven by a pair of energy storage converters. The drive power is alternately provided to pairs of opposing bridge transistors from separate windings on the drive transformers T_1 and T_2. The pulse width drive commands enter the inverter at terminals 1 and 3 in the form of 0 or +5 V signals and are buffered by a low level stage which incorporates cross coupling to prevent both sides of the bridge from being inadvertently turned on at the same time, plus overlap protection. The overlap protection signal is derived from the output transformer and prevents the off transistors from turning on until the on transistors have turned off. The width of the drive command pulses are determined in the pulsewidth modulator circuitry (not shown) where the supply feedback level (voltage or current sensing) is compared with a setpoint reference level to establish supply closed loop regulation.

The output bridge stages of this system utilize 3 A, 400 V transistors. The output transformers, which are constructed of ferrite core materials, are ac coupled to eliminate the dc current path that could cause transformer saturation due to asymmetry in the switching waveforms. Total output power capability of each inverter is in excess of 400 W, but are run typically at levels less than 270 W.

b. Screen Supply – The screen supply consists of eight inverters, connected as shown in Fig. II-9. All inverters are driven from one common pulsewidth modulator, and the supply output is voltage programmed with a remote reference signal in the range of 0 to 5 Vdc. An integral overload detector is provided with the supply for protection. During normal thruster operation, however, the overload detection and recycle circuitry in the control system takes precedent in processing high voltage supply overloads.

Table II-1. Test Console Power Processor Ratings

	Minimum Open Circuit, Volt	Maximum Ratings		Nominal Ratings		Regulation, (± %)
		E (V)	I (A)	E (V)	I (A)	
Main Vaporizer[1]	20	20	7	10	3	I, 5
Cathode Vaporizer[1]	20	20	7	5	2	I, 5
Cathode Heater[1]	20	20	7	12	6	I, 5
Main Isolator[1]	20	20	7	9	2	I, 5
Neutralizer Heater[1]	20	20	7	8	4	I, 5
Auxiliary Heater[1]	20	20	7	6	4	I, 5
Neutralizer Keeper	1000	1000/40	0.005/3.0	20	2.0	I, 5
Cathode Keeper	1000	1000/50	0.005/1.0	30	0.5	I, 5
Discharge	85	60	20	45	12	I, 3
Accelerator[2]	2000	2000	0.2	1000	0.02	E, 2
Screen	1500	1500	2.0	1330	1.5	E, 2

(1) To obtain maximum values tap changes are required on output transformers.

(2) Capable of short term transients to 400 mA without recycling.

T1844

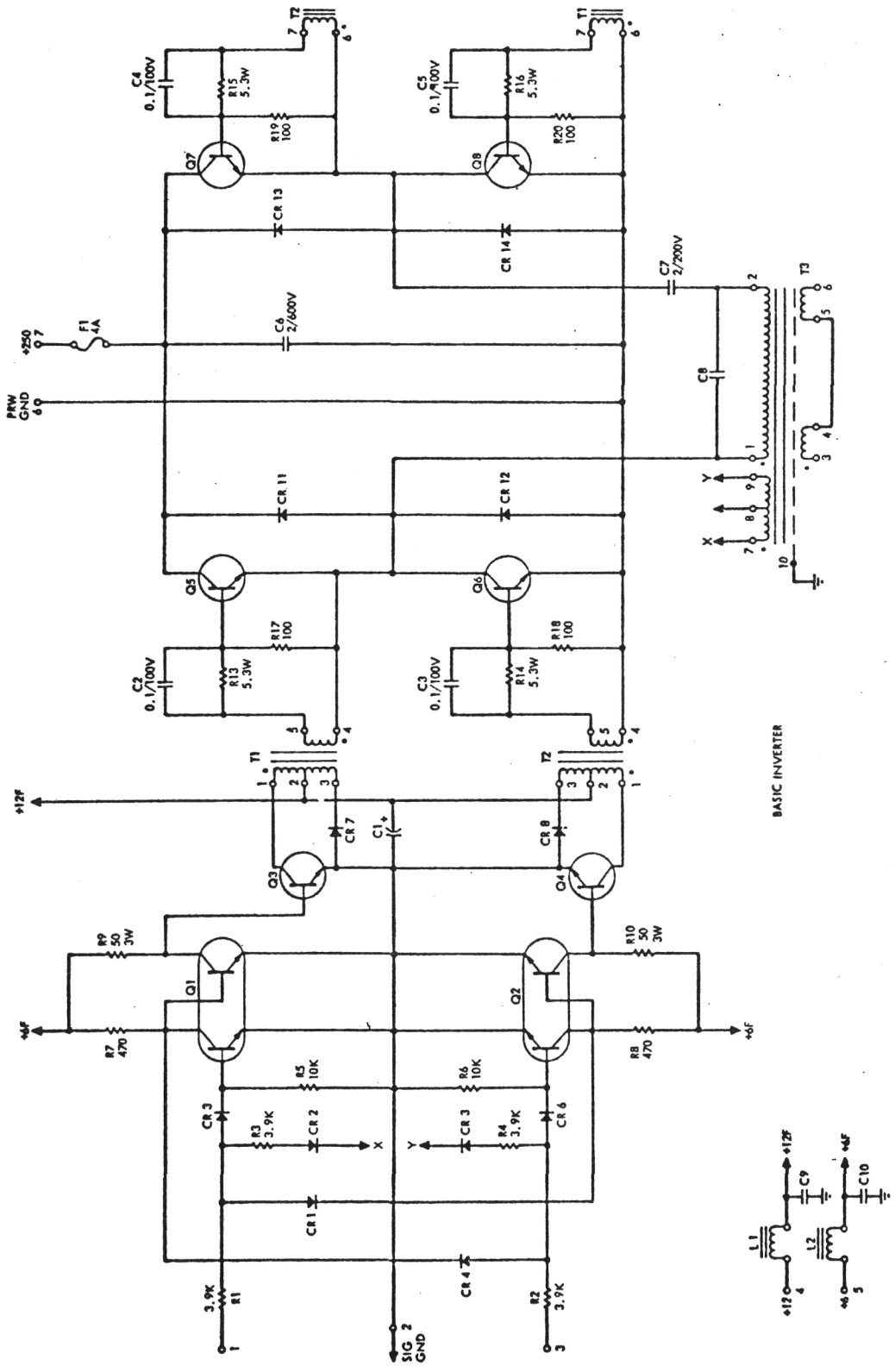

Figure II-8. Basic inverter circuit.

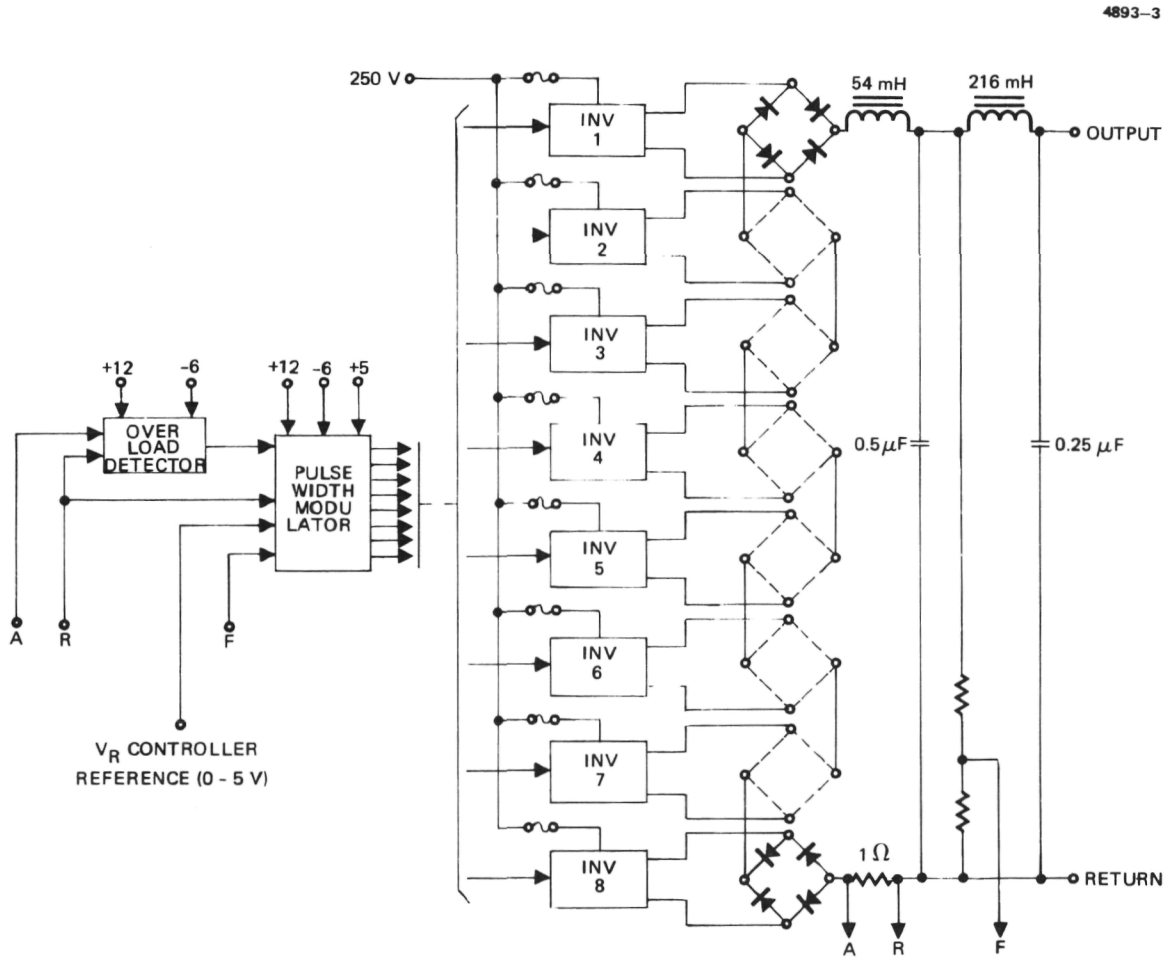

Figure II-9. Screen supply block diagram.

The output filter is constructed with two L-C sections. The additional section placed past the feedback voltage divider provides ripple reduction, but more importantly buffering from transient overloads common to thruster operation. Both filter chokes are fabricated using silicon steel C cores.

c. Accelerator Supply – The accelerator supply is mechanized as shown in Fig. II-10. The line regulator is controlled by an external reference signal to program the accelerator voltage. There are two regulation control loops. The minor loop prevents the output of the line regulator from increasing above the level required to achieve a preset output voltage from the inverter. The major loop is dominant and controls when the output reaches the preset level. The effect of the minor loop is to improve transient response. An integral overload circuit is provided, as with the screen supply, for current overload protection. The output filter is composed of a T section with the output inductor provided to limit the surge and circulating current when the screen and accelerator supplies are shorted together. Regulation for load variations from 0 to 100 mA is better than +1% and maintains an accuracy of ±2% for loads in excess of 200 mA.

d. Discharge Supply – Discharge power is generated by a series connection of the output of three inverters as shown in Fig. II-11. The inverter's pulsewidth modulator and remote control capability are typical of supplies already discussed. An additional amplifier is, however, required in the regulation circuitry to provide both current and voltage control functions. Current feedback is generated by a magnetic amplifier type current sensor, which requires an external excitation source. The advantages of the current sensor are the high voltage isolation capability plus good linearity. A voltage transformer (with high voltage isolation) in combination with L-C filtering is used to sense the output voltage. During system operation, the supply functions as a current regulated supply with the output voltage determined by the cathode vaporizer control loop. Current regulation is approximately ±1% over its normal operating range.

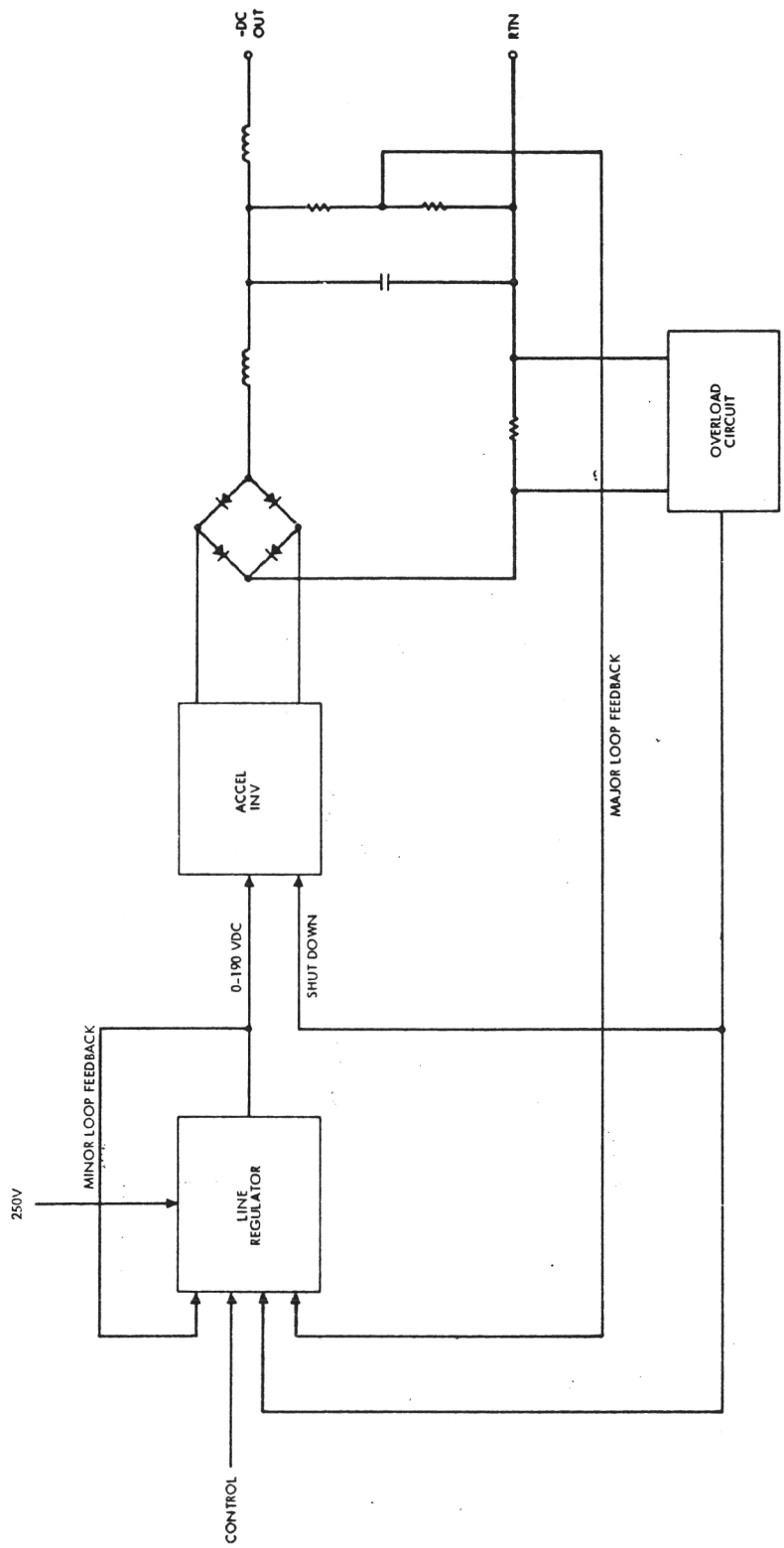

Figure II-10. Accelerator supply block diagram.

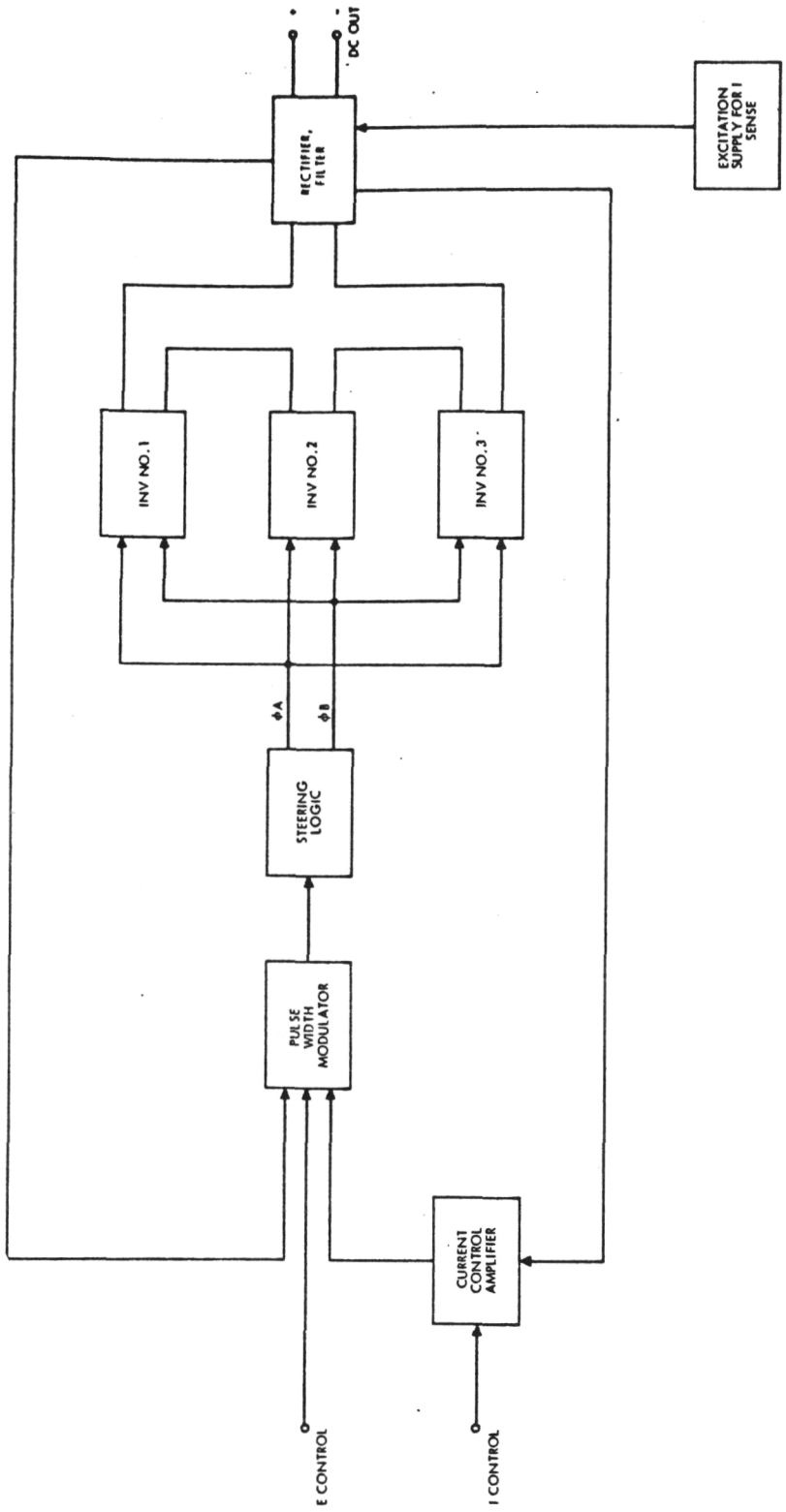

Figure II-11. Discharge supply block diagram.

e. Heater and Keeper Supplies – The heater and keeper power is controlled by magnetic amplifiers driven by square wave ac from the 5 kHz inverter. Figure II-12 shows a schematic of the control circuitry used. The magnetic amplifier is controlled by the differential amplifier formed by Q1 and Q2, which compares the control signal with the feedback. Feedback is generated by a current transformer followed by an rms shaping network.

The keeper supplies contain additional circuitry for rectifying the output to the required dc. Also included in each keeper supply is a high voltage/low current (1000 V/5 mA) section which provides the initial ignition voltage for the keepers.

2. Controller

The requirement for long periods of continuous unattended operation during the thruster endurance test dictated that special functions be included in the control system developed for the test console. In addition to providing control of the thruster power supplies during normal operation the controller also provides

- Automatic startup from all thruster power off to full beam closed loop operation
- Continuous monitoring of critical voltage and current levels with generation of corrective commands and/or alarm annunciation if preselected threshold conditions are reached
- Automatic shutdown from full beam operation to all thruster power off either upon operator command or certain alarm conditions.

The block diagram of Fig. II-13 illustrates how the principal control functions were implemented in the test console controller. Voltage or current level control signals are supplied to each of the ten power supplies from the associated buffer amplifier. The source of these control signals depends on the operational mode, either manual or auto, selected for the particular supply. In the manual mode the supply output level is determined by the setting of a front panel control. In the auto mode the supply output level for all but the three vaporizer supplies is determined by the setting of an internal trimpot. Several

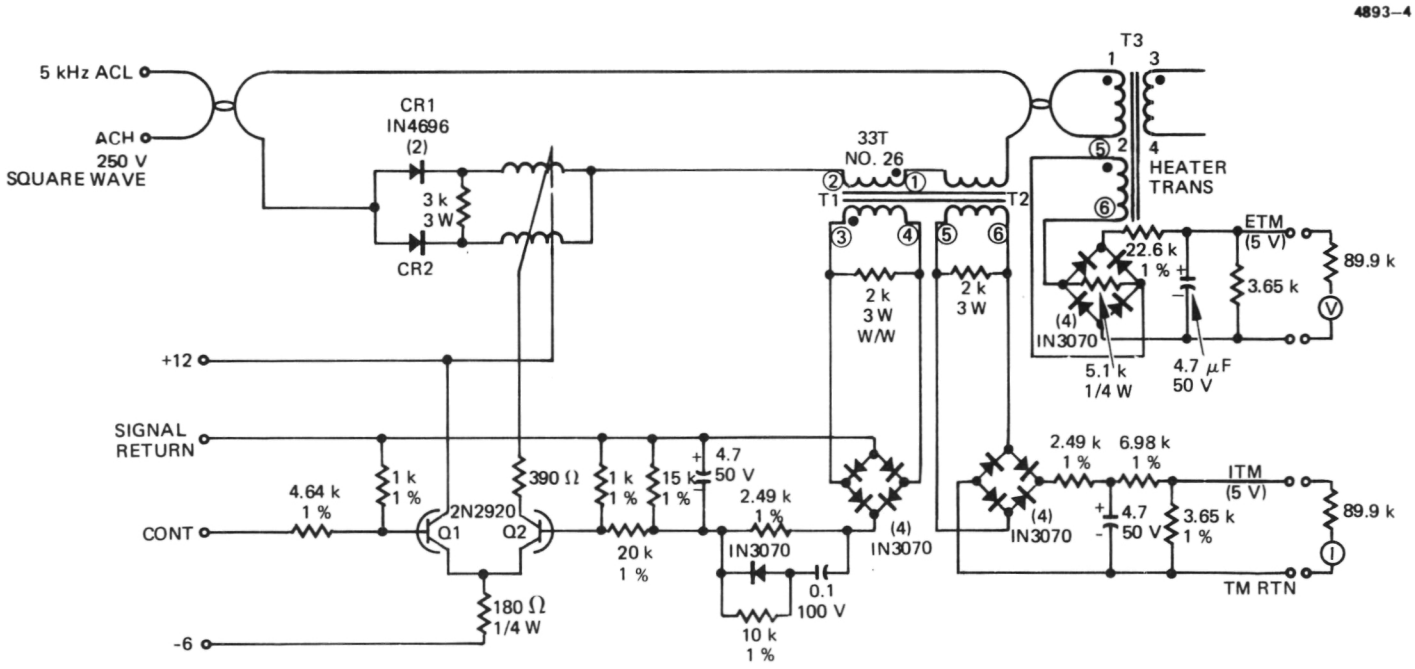

Figure II-12. Heater/keeper supply control circuitry.

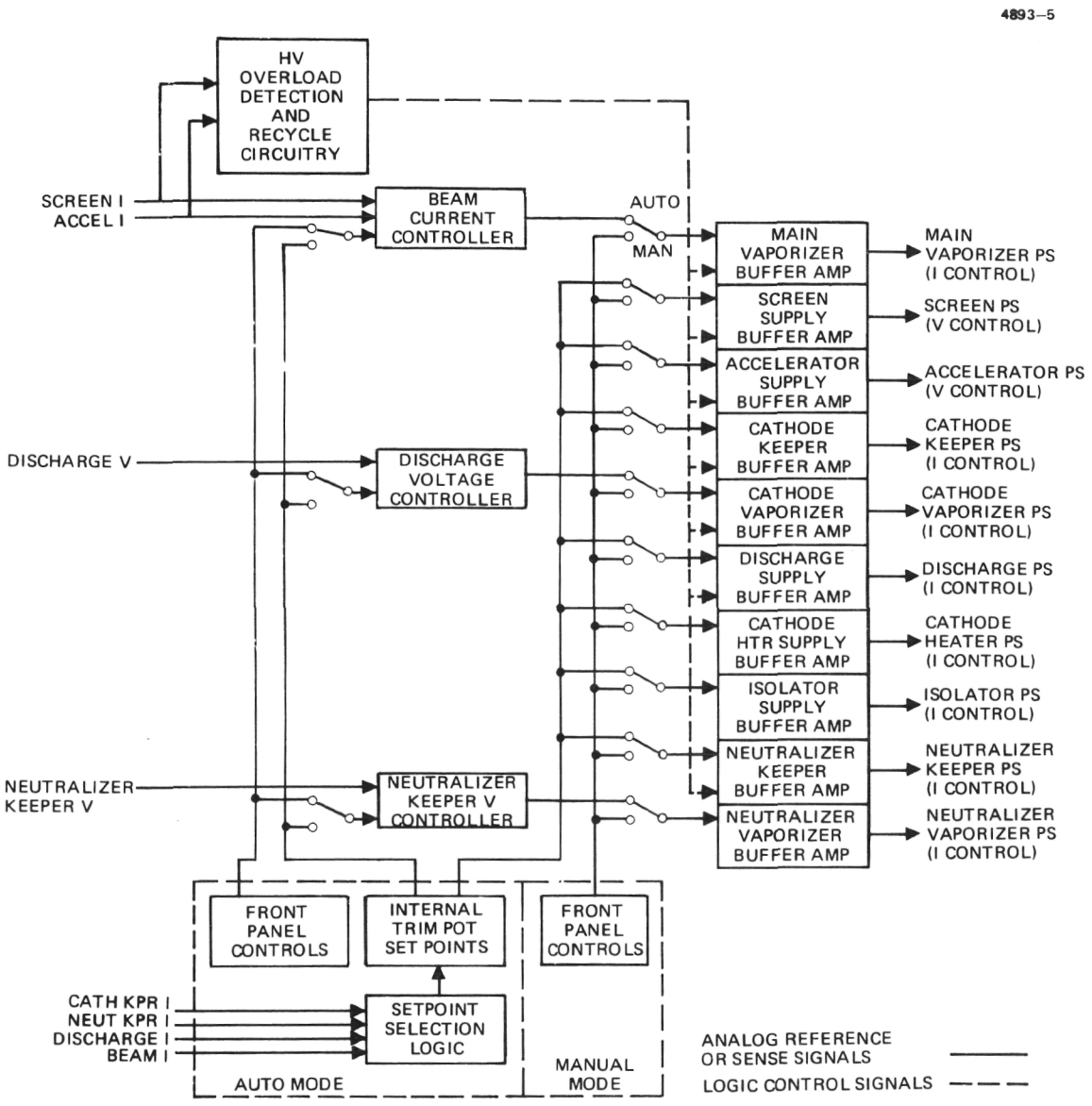

Figure II-13. Control system block diagram.

supplies have more than one trimpot associated with them in order to provide different output levels during startup, run, and shutdown. Selection of the correct trimpot is controlled by logic circuits within the controller, depending on the operating mode requested and the existing levels of certain thruster parameters, e.g., keeper current and beam current. In the auto mode the three vaporizer supplies operate closed loop; each is attempting to maintain a different thruster parameter (beam current, discharge voltage, neutralizer keeper voltage), at some selected level. As shown in Fig. II-13, the level command may come from either an internal trimpot or a front panel control with the choice being an operator option. Operation of the control system in the normal closed loop mode is shown functionally in Fig. II-14.

The controller also provides the function of screen or accel current overload protection. The most common cause of a current overload of one or both of these supplies is a temporary voltage breakdown between the thruster screen and accelerator electrodes. When either the screen or accel current exceeds preset levels for a prescribed length of time, a high voltage recycle sequence is initiated. The screen and accel supplies are momentarily switched off, the discharge current is decreased, the cathode keeper current and neutralizer keeper current are increased, and the main vaporizer is set to a cutback level. The screen and accel voltages are then reapplied and if another current overload is not sensed the other supplies are commanded back to their normal operating levels.

Automatic startup is achieved by combining timed commands with sensed operating parameters. A flow diagram of the test console automatic startup sequence is presented in Fig. II-15. The time between commands necessary to permit warmup of certain thruster elements is provided by internal solid state counters. At other decision points in the sequence, advancement can only occur when certain thruster operating conditions are satisfied, e.g., neutralizer keeper current and cathode keeper current both present. A rapid advance mode is also available which converts minutes to seconds for quickly restarting

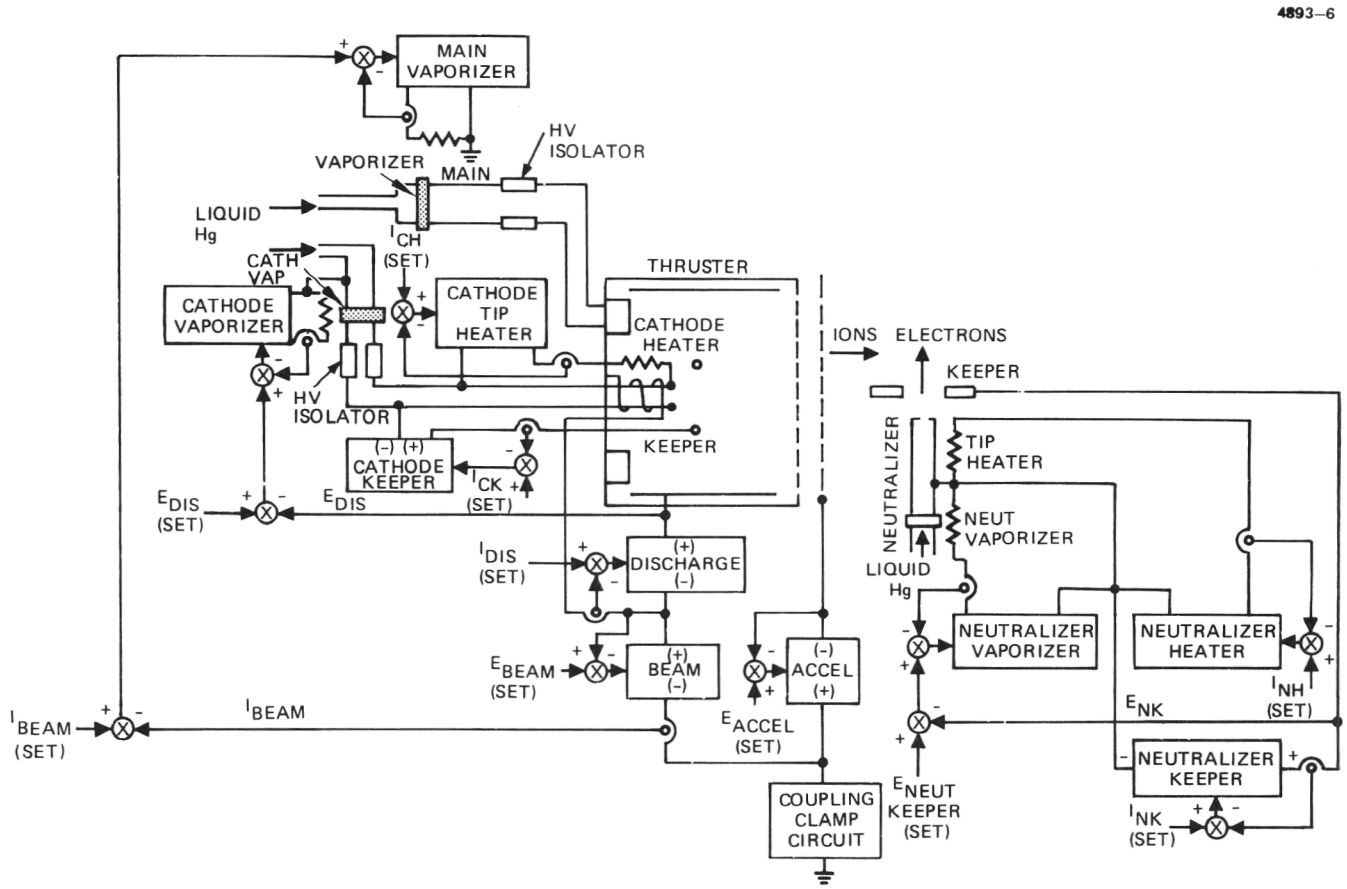

Figure II-14. Control system functional diagram.

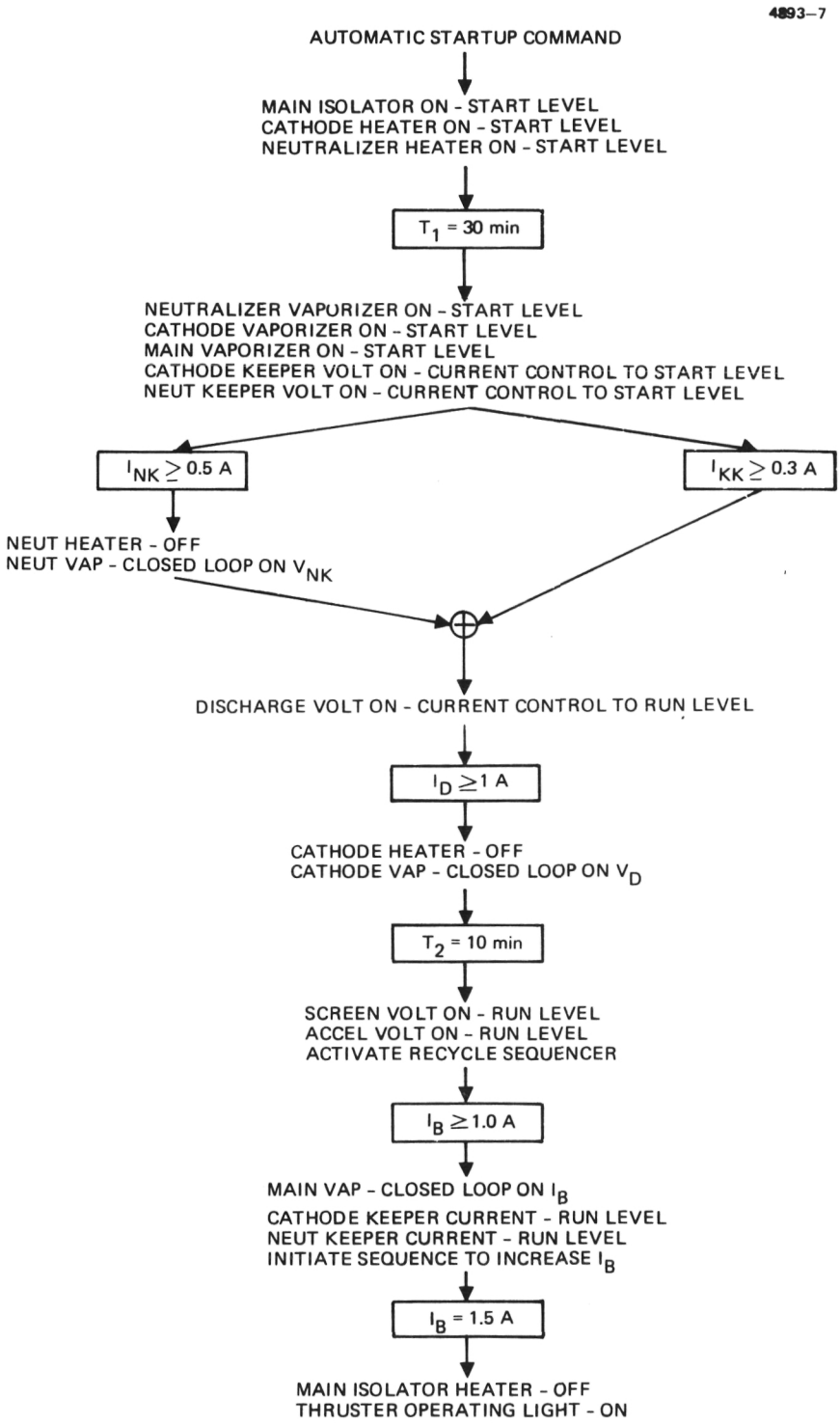

Figure II-15. Test console automatic start up sequence.

a thruster which is already at or near operating temperature. The automatic shutdown sequence included in the test console is controlled by timed commands only; no sensed thruster operating parameters are involved.

Another important function provided by the test console controller is the generation of alarms if certain thruster, power supply, or vacuum chamber parameters shift outside of predetermined limits. To preclude transients erroneously activating an alarm, most of the alarms require the out of bounds condition to exist for five minutes before an alarm is sounded. Several of the more critical alarm conditions, e.g., loss of chamber vacuum, generate commands within the controller to turn off power to the thruster in order to prevent damage to the thruster. Table II-2 lists the alarm conditions and resultant actions that are implemented in the test console.

3. Data Acquisition System

The primary purpose of the test console was to provide a system which would permit the thruster endurance test to run unattended. Therefore, it was necessary that the test console include a means of automatically acquiring and storing test data. For this purpose a data system was built into the test console to provide periodic sampling of all of the output voltages and currents of the power conditioner plus the neutralizer emission current, voltage and current to ground and the weight of mercury in the three feed system reservoirs. The sampled data is converted to teletype code for storage on both punched tape and teletype printout. In addition to the automatic data acquisition capability, the system is mechanized so that real time data can be acquired at remote locations, such as Lewis Research Center, via a telephone-teletype linkup.

C. Vacuum Test Facility

All thruster tests described in this report were conducted at the Hughes Space Simulation Laboratory in a vacuum chamber specially modified for mercury ion thruster endurance testing. The vacuum test

Table II-2. Test Console Alarms

Parameter	Limits	Time Permitted
A. Audio Alarm Only		
1. Screen Voltage	V_s < 1.0 or >1.2 kV[a]	5 min
2. Beam Current	I_B < 1.4 or >1.6 A[a]	5 min
3. Accel Voltage	V_A < 0.4 or > 0.6 kV[a]	5 min
4. Discharge Voltage	V_o < 35 or > 39 V[a]	5 min
5. Voltage to Ground	V_G > 20 V[a]	5 min
6. Current to Ground	I_G > 0.5 A[a]	5 min
7. Hg Level in Main Reservoir	< 10%	5 min
8. Chamber Pressure 1	P ≥ 5 x 10^{-6} Torr	5 min
9. Arc Rate 1	≥10 per hour	——
B. Turn off Screen and Accel Voltage + Audio Alarm		
1. Accel Current	I_A > 10 mA	5 min
2. Chamber Pressure 2	P ≥ 1 x 10^{-5} Torr	5 min
3. Arc Rate 2	≥ 10 per min	——
C. Turn Off all Thruster Power + Audio Alarm		
1. Pressure 3	P ≥ 1 x 10^{-4} Torr	0

[a]Typical valves; limits are settable to bracket selected operating level.

T1913

facility (Fig. II-16) is a vertical chamber 5.6 m long and 2.7 m in diameter with LN_2 cryoshrouds. The thruster is suspended from the top of the chamber. The beam is directed into a 2.4 m diameter frozen mercury collector at the bottom of the chamber 4 m downstream from the thruster (see Fig. II-17). Mercury is employed as the beam collecting surface so that the material back sputtered on the thruster will be mercury which then evaporates from the hot surfaces of the thruster. The thruster fuel is mercury, therefore back sputtered mercury cannot create any new material compability problems.

Four viewing ports are available in the chamber. From three of the ports the thruster can be viewed and photographed at different angles. The mercury collector can be viewed from two of the ports and photographed from different angles. A movable Faraday cup probe is mounted in the chamber so that beam profiles can be measured at approximately 2.7 m downstream from the thruster face. A retractable flood lamp is provided for internal illumination of the chamber. The lamp can be rotated to illuminate the mercury collector or the thruster. The retracting feature is provided so that the lamp can be withdrawn from the chamber when not in use to prevent mercury deposition on the lamp lens.

The test facility is instrumented with numerous thermocouples on the collector pan, cryoshrouds, and the vacuum system. Readings from all of these thermocouples are recorded periodically. A continuous strip chart recording of the chamber pressure is also made. The sensor for the pressure recording is mounted in the top dome of the chamber and "looks" down at the mercury collector. Certain critical test facility parameters are monitored continuously. If preselected limits are exceeded an alarm is sounded and an equipment protection sequence initiated.

Figure II-16. Test facility with thruster (mounted on dome) being lifted to top of vacuum chamber.

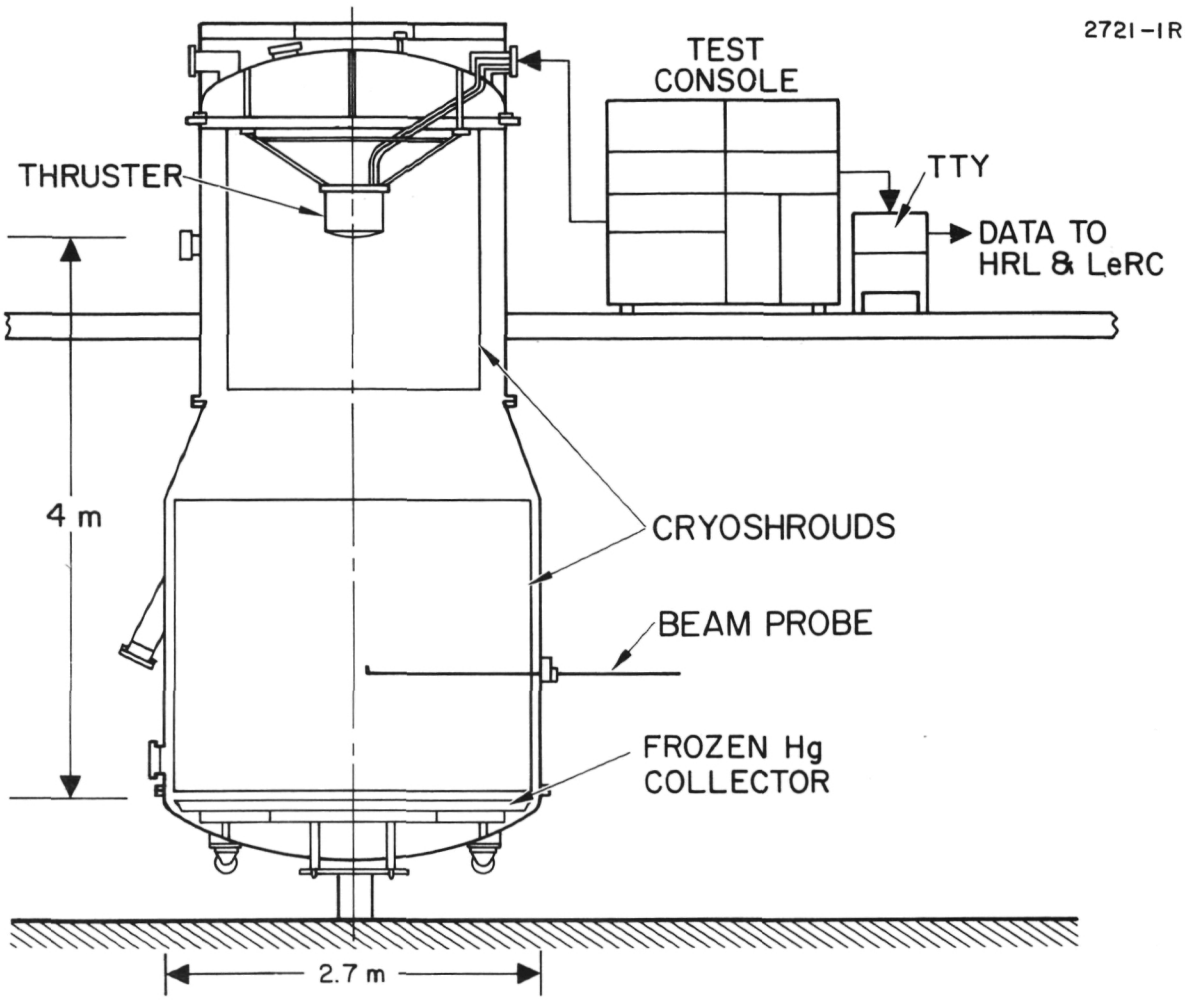

Figure II-17. Test facility showing location of thrusters, beam probe, cryoshrouds, and frozen mercury collector.

D. Mercury Feed System

A laboratory-type feed system (Fig. II-18) which provides two methods for measuring mercury flow was designed and built for this program. The feed system consists of three similar sections which differ only in the sensitivity of the measuring devices. One section supplies the main flow, another feeds the cathode, and the third section supplies the neutralizer. Each section consists of a storage reservoir, graduated pipettes for measuring volumetric flow rate, a small reservoir mounted on a load cell for measuring flow rate by the weight of mercury used, and the necessary feed lines and valves for filling and transferring mercury within the feed system and to the thruster.

M8524

4893–122

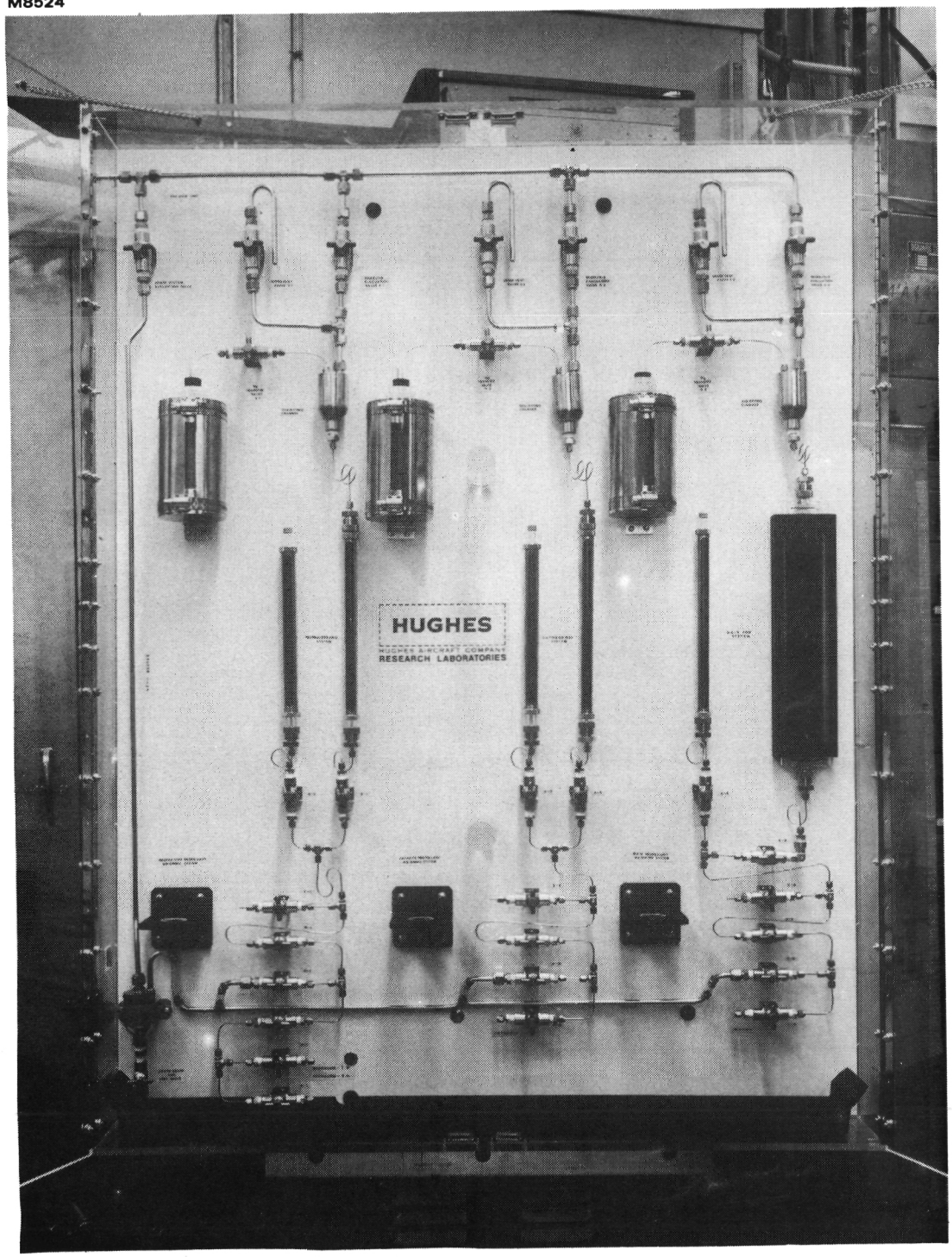

Figure II-18. Mercury storage and feed system.

III. TEST RESULTS

Five major thruster tests were conducted or initiated under this program; three short term tests, an 1100 hour endurance test, and a 10,000 hour endurance test. The first four of these tests were completed under this contract, NAS 3-15523; the last test (10,000 hours) was initiated under this contract and completed under contract NAS 3-17803. However, in the interest of completeness the test results, including post-test analysis, of the entire 10,000 hour endurance test are included in this report.

As a result of the series of tests described herein several life limiting problems were identified and fixes implemented. Table III-1 summarizes the performance results, problems identified and changes adopted for the entire five-test series. The changes to the thruster are more fully identified in Table III-2 where the thruster characteristics are summarized for each test. A comparison of thruster performance for the five tests is presented in Table III-3. The results of each test are presented separately in the pages that follow.

A. Short Term Tests

This section describes three short term tests that were conducted prior to initiating the first endurance test of a 30-cm electron bombardment thruster. The three tests that are described herein were a 100-hour attended test and two 500-hour unattended tests. The 100-hour test demonstrated the compatibility of the thruster, test console, including power conditioner, and test facility with frozen mercury collector. No design changes were made between the 100-hour test and first 500-hour test.

Thruster performance during the first 500-hour test exceeded the contract goal; however, this test did reveal the need for two changes. Localized erosion on the accel electrode in the region surrounding the insulated cap on the center support led to a switch to dished electrode optics which do not require a center support. The existence of cathode isolator leakage current after 350 hours of the test resulted in a change

Table III-1. Summary of Test Results

Test	Performance Results	Problems Identified	Changes Adopted Prior to Next Test
100 Hour	Good thruster, power conditioner and facility performance.	None	None
500 Hour No. 1	Good thruster, power conditioner and facility performance. η_M = 87%, η_E = 81%	1. Localized optics erosion due to insulated cap on center support 2. Cathode feedline H. V. isolator developed leakage current	1. Replace flat electrode optics with dished electrode optics which do not require center support 2. Change isolator alumina to AL 300 and add exterior glaze
500 Hour No. 2	Good thruster, power conditioner and facility performance. η_M = 89%, η_E = 82% Optics erosion and cathode isolator electrical leakage problems nonexistent	1. Cathode heater sheaths damaged by reaction with excessive braze	1. Replace sheathed cathode heaters with plasma sprayed heaters similar to ones used on 5 cm and SERT II thrusters 2. Grind exterior of cathode isolator
1100 Hour Endurance Test	Good thruster, power conditioner and facility performance until vacuum system electrical feedthrough failure. η_M = 87%, η_E = 82%	1. Backsputtering from vacuum chamber due to wide beam of uncompensated dished electrode optics 2. Cathode feedline H. V. isolator developed leakage current	1. Incorporate compensated dished electrodes to reduce beam angle 2. Relocate cathode isolator to same thermal environment as main isolator. Modify sputter shielding and fabrication techniques
10,000 Hour Endurance Test	Good thruster, power conditioner and facility performance until baffle erosion became excessive. η_M^* = 88%, η_E^* = 83% *for J_B = 1.5 A	1. High level of doubly charged ions caused excessive erosion of baffle, cathode pole piece and screen electrode 2. Sputter deposited material in discharge chamber flaked off on to optics 3. Neutralizer cathode exhibited mode shifting	1. Modify baffle assembly geometry to Ⓐ reduce number of doubly charged ions. Add tantalum to erosion sites in discharge chamber 2. Cover deposition sites with stainless steel mesh and grit blast 3. Change cathode insert from rolled foil to impregnated porous tungsten

Ⓐ Implemented in 900 series thrusters under Contract NAS 3-17803.

T1845

Table III-2. Summary of Thruster Characteristics

Thruster	Test				
	100 Hour	500 Hour No. 1	500 Hour No. 2	1100 Hour Endurance Test	10,000 Hour Endurance Test
Serial Number	401	402	402	402	701
Optics					
Type	Flat with center support	Flat with center support	Dished, no center support	Dished, no center support	Dished, no center support
Aperture Spacing (CTR-CTR)	0.254 cm	0.254 cm	0.254 cm	0.279 cm	0.221 cm
Aperture Diameter, Screen	0.208	0.208	0.216	0.241	0.190
Accel	0.193	0.193	0.173	0.193	0.152
Electrode Thickness, Screen	0.051	0.051	0.038	0.038	0.038
Accel	0.127	0.127	0.076	0.076	0.051
Open Area Screen	61%	61%	66%	68%	67%
Accel	52%	52%	42%	44%	43%
Interelectrode Spacing					
Center	0.063 cm	0.069 cm	0.081 cm	0.066 cm	0.061 cm
Edge	0.190-0.249	0.211-0.236	0.081-0.089	0.076-0.101	0.056-0.084
Compensation	N/A	N/A	None	None	0.4%
Cathode-Isolator-Vaporizer (CIV)					
Cathode Orifice	0.076 cm	0.076 cm	0.076 cm	0.076 cm	0.076 cm
Keeper Spacing	0.15 cm	0.15 cm	0.15 cm	0.15 cm	0.15 cm
Cathode Heater	Sheathed htr brazed on	Sheathed htr brazed on	Plasma sprayed	Plasma sprayed	Flame sprayed
Isolator Body	McDanel Alumina	McDanel Alumina	Wesgo Al 300 Alumina with exterior glaze	Wesgo Al 300 Alumina, Exterior ground after fabrication	Wesgo Al 300 Alumina, Exterior ground after fabrication①
Neutralizer					
Cathode Orifice	0.038 cm	0.038 cm	0.038 cm	0.038 cm	0.038 cm
Keeper Spacing	0.15 cm	0.15 cm	0.076 cm	0.15 cm	0.15 cm
Cathode Heater	Sheathed htr brazed on	Sheathed htr brazed on	Plasma sprayed	Plasma sprayed	Flame sprayed

① Cathode Isolator relocated to same thermal environment as main isolator.

T1847

Table III-3. Summary of Thruster Performance

Parameter	Contract Goal	First 500-Hr Test	Second 500-Hr Test	1100 Hr Endurance Test	10,000 Hr Endurance Test			
Total Input Power	2.6 kW	2.5	2.4	2.4	2.0	2.2	2.3	2.4
Net Extraction Voltage	1330 V	1330	1330	1330	1100	1100	1100	1100
Accelerator Voltage	≤1000 V	600	500	600	500	500	500	500
Beam Current	1.5 A	1.5	1.5	1.5	1.5	1.6	1.7	1.75
Effective Specific Impulse (1)	3100 sec	3170	3250	3180	2920	2980	3050	3080
Thrust (1)	112 mN	112	112	112	102	109	115	119
Electrical Efficiency	77%	81	82	82	83	84	84	84
Mass Utilization Efficiency (1)	85%	87	89	87	88	90	92	93
Total Efficiency (1)	65%	70	73	71	73	76	77	78
eV/Ion	–	262	235	236	185	185	185	185

(1) Uncorrected for doubly charged ions or beam divergence in this and subsequent data unless otherwise noted.

T1848

in isolator material and addition of a glaze to the exterior of the isolator for the second 500-hour test.

Thruster performance during the second 500-hour test also exceeded the contract goal. The problems of accel erosion and cathode isolator leakage which had been experienced during the first 500-hour test did not occur during the second 500-hour test. Post test examination of the thruster did reveal a problem which was not experienced earlier. An interaction had occurred between the NICRO braze and the tantalum components of the main and neutralizer cathodes. The components affected were the heater sheath, neutralizer tube and cathode thermal radiator. As a result, a change to plasma sprayed heaters for the main and neutralizer cathodes was incorporated before proceeding with the endurance test. This change eliminated the NICRO braze from the main and neutralizer cathodes.

1. 100-Hour Test

After the installation and integration of the thruster and test console in the test facility, the short-term test of 100-hours duration was performed to obtain the following information.

a. Measurement of thruster performance

b. Measurement of the beam angle

c. Measurement of sputtering deposition

d. Check data acquisition

e. Measurement of temperature profiles in the facility

f. Obtain pressure versus time curve.

The 100-hour test was continuously manned throughout the test. The facility and test console automatic alarm and corrective action circuits were also operational. Both automatic and manual data acquisition were utilized in order to gain the maximum information concerning thruster and test system performance.

The thruster was operated at the performance point specified in the contract with one exception. The accel voltage was varied from 1000 V to 500 V in order to determine an acceptable minimum value. The three dynamic control loops built into the test console were operated closed loop. Thus, the main vaporizer flow was controlled by the beam current setting (1.5 A), the cathode vaporizer flow was controlled by the discharge voltage setting and the neutralizer vaporizer flow was controlled by the neutralizer keeper voltage setting (set to achieve a coupling voltage of less than 20 V and a neutralizer mass flow of 50 mA or less).

Thruster electrical performance was determined by recording once an hour the 26 electrical parameters which are monitored by the test console data acquisition system. In addition, the beam and accel current were continuously monitored. Data for calculating the propellant efficiency of the thruster was obtained from the mass flow and volume flow from the calibrated pipettes provided by the data acquisition system.

Beam profiles were taken with the movable Faraday cup probe. Profiles were taken at the beginning of the test, near the midpoint and at the conclusion of the test. When not in use, the probe was pulled out of the beam. The Faraday cup was biased negatively to reject any electrons which came from the neutralizer.

Four sputter deposition "cameras" were mounted around the periphery of the thruster approximately in the plane of the accel. These "cameras" as suggested by LeRC were closed stainless steel cylinders of varying length (varying f number) with glass discs mounted inside at one end and a small aperture drilled in the other end. Three of the cameras pointed down toward the mercury collector to collect material sputtered back from the lower section of the chamber. The fourth camera pointed toward the top of the chamber to collect any material that came from that region of the chamber.

Early during the 100-hour test photographs were taken in order to evaluate the internal illumination. Photos were taken through all four viewing ports with different camera settings and different power and angle settings of the internal light. Additional photos were taken near the end of the test for comparison purposes.

Thruster number 401 was used for the 100-hour test. The principal physical characteristics of this thruster are identified in Table III-2.

a. Test Results — Thruster start up for the 100-hour test was performed with the automatic startup mode of the test console. The final step of the sequence, application of high voltages, was manually delayed 8 minutes to permit the LN_2 to cool the upper shroud of the vacuum chamber. When the high voltages were applied the beam came on in the normal manner. The beam current was brought up to 1.5 A and left at that level throughout the test.

During the 100-hour test thruster performance was measured over a range of accel voltages and discharge voltages. The accel voltage, V_a, was varied from -1000 V to -500 V; the discharge voltage, V_I, was varied from 40 V to 42 V. The beam current and discharge current were maintained at 1.5 A and 9.8 A, respectively, throughout the test. Thus, the eV/ion changed when the discharge voltage was varied. The mass utilization and eV/ion for each combination of operating parameters is presented in Table III-4. The lower than normal mass utilization which was experienced was attributed to improper spacing of the grids. This conclusion was confirmed following the 100-hour test when the grids were respaced, put back on the thruster and retested. At V_A = -800 V, V_I = 40 V and an eV/ion of 262 the discharge mass utilization was 92.4%. It was possible to run as low as 242 eV/ion and still achieve a mass utilization in the discharge of 88%.

At approximately the midpoint of the test, the cathode high voltage isolator began to show some leakage current. By the end of the 100 hours, this current had risen to 27 μamps. The main isolator leakage current was 0.1 μamp at the end of the test.

The vacuum test facility performed without any problems during the test. The pressure at the beginning of the test was 2.9×10^{-6} Torr and by the conclusion of the test the pressure had decreased to 1×10^{-6} Torr. Photographs of the thruster and frozen mercury collector were taken at the beginning and end of the test which demonstrated that

Table III-4. Thruster Performance During 100 Hour Test
(Thruster S/N 401, Optics S/N 402)

Time, Hours	V_A, V	V_I, V	$\dot{m}_{MAIN}$ (Eq. A)	$\dot{m}_{CATH}$ (Eq. A)	$\dot{m}_{NEUT}$ (Eq. A)	$\eta_{m_{DIS}}$, %	$\eta_{m_{TOTAL}}$, %	eV/ION
0 to 23.5	-800	40	1.629	0.136	0.047	85.0	82.7	261
23.5 to 31	-1000	40	1.575	0.137	0.053	87.5	85.0	261
31 to 49	-1000	42	1.538	0.129	0.044	90.0	87.6	274
49 to 61.5	-800	42	1.545	0.121	0.058	90.0	87.0	274
61.5 to 68.5	-800	41	1.582	0.126	0.059	87.8	84.9	268
68.5 to 78	-700	41	1.611	0.125	0.060	86.4	83.5	268
78 to 87.5	-600	41	1.611	0.121	0.057	86.5	83.9	268
87.5 to 90	-500	41	1.629	0.121	0.054	85.7	83.1	268
90 to 101	-600	42	1.562	0.120	0.062	89.2	86.0	274
V_S = +1330 V , J_I = 9.8 A , J_B = 1.5 A								

T1849

the location of the viewing ports and the internal illumination system were satisfactory. Beam profiles were taken with the beam probe three times during the test. Figure III-1 shows the profiles obtained at four different accel voltages with the probe mounted 2.7 m downstream of the thruster.

b. Post Test Analysis – Post test examination of the thruster following the 100-hour test revealed the thruster to be in good shape. Of particular interest was the condition of the cathode isolator in view of the isolator leakage current which had developed as the test progressed. When the sputter shields were removed from around the isolator body, a gray coating was observed on the surface of the isolator. Since sandblasting had eliminated isolator leakage in previous cases it was decided to sandblast the exterior of the isolator body and use the same CIV in the 500-hour test. Following a light sandblasting the resistance measured ∞ with a 1000 V megger.

Thruster 401 had been used for the test console integration testing in the 3-meter chamber at HRL and the system integration of the test facility at the Space Simulation Laboratory. Therefore, in order to get a true measure of the effect of operating in the test facility which incorporates a frozen mercury collector it was planned to use a new thruster, S/N 402, for the 500-hour test and endurance test. No design changes to the thruster were deemed necessary as a result of the post-test examination of the 100-hour test thruster. Also, the test facility and test console were judged to be ready for the 500-hour test at the conclusion of the 100-hour test.

2. 500-Hour Test No. 1

The first 500-hour test followed the post test evaluation of the 100-hour test thruster. Thruster S/N 402 which was used for this test was of the same design as thruster S/N 401 which was used for the 100-hour test. In fact, the same optics and CIV were used for both tests. The physical characteristics of thruster 402 for this test are given in Table III-2.

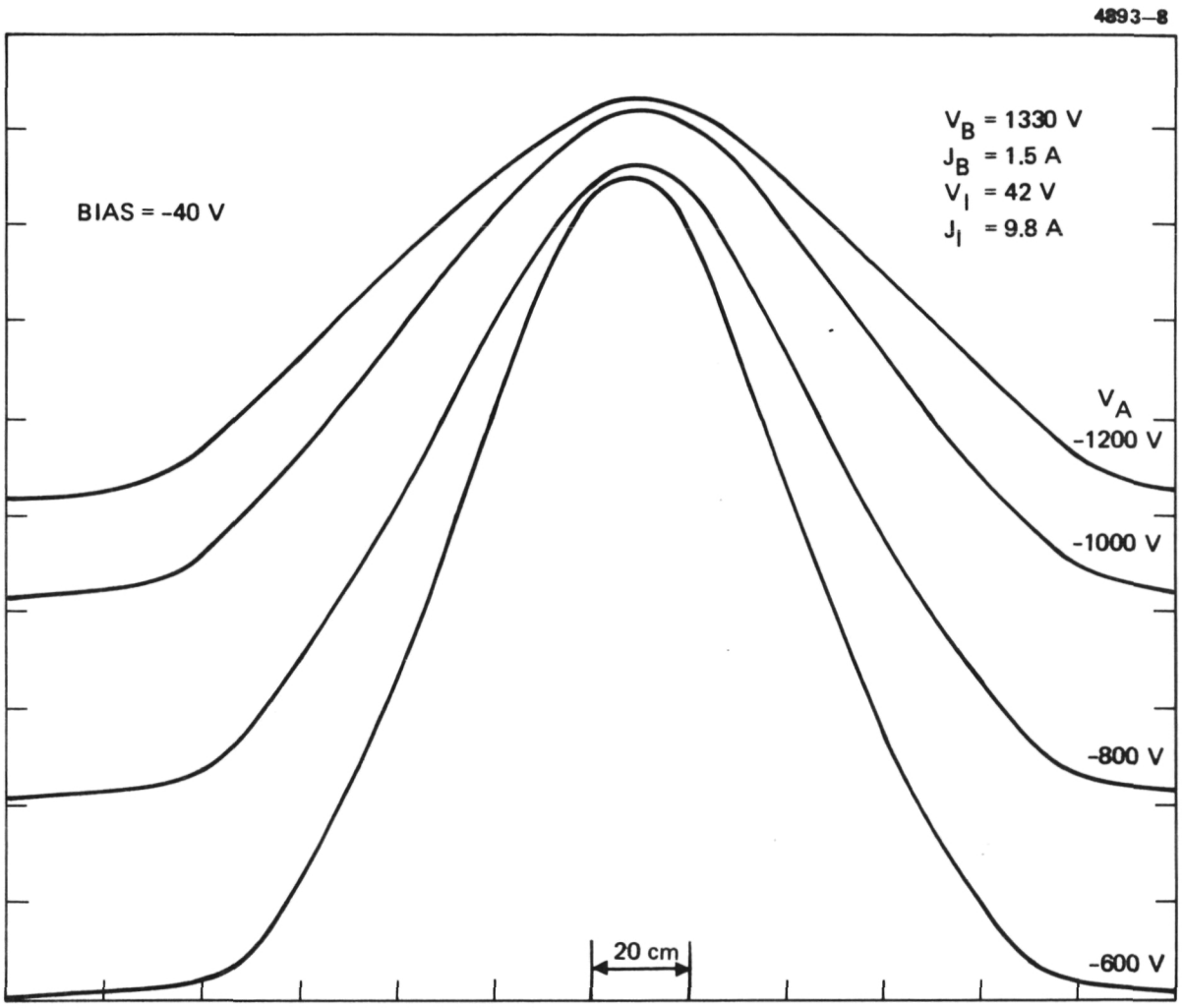

Figure III-1. Beam profiles taken at 4 accel voltages with probe located 2.7 m downstream.

After an initial 72-hour period of manned operation, the remainder of the test was run in the unattended mode that was used during the endurance tests. During this test all of the data measuring and diagnostic features of the facility and test console were exercised. This included automatic data extraction and storage, remote readout at HRL of stored and real time data, taking of beam profiles, photographing of the thruster and frozen mercury collector and visual examination of the thruster with a Questar telescope. The mercury weighing system was used as the principal source of data for calculating mass utilization. Thruster electrical operating data and propellant utilization were automatically recorded once an hour on a teletype printout and punched tape. A continuous record of the chamber pressure was made.

a. Test Results — Thruster start up was performed using the manual mode of the test console. This mode was chosen so the cathode and neutralizer tip heater supplies could be controlled manually in order to determine at what heater current levels the cathode and neutralizer would ignite. The neutralizer ignited at a heater current of 3.25 A and the cathode ignited at a heater current of 4.25 A. Both the neutralizer and cathode vaporizers were between 220 and 230°C at the time of ignition.

During the first 66 hours of the test, thruster performance was measured as the discharge and accel voltages were varied. Based on these results, it was decided to operate at -600 V accel voltage, 39 V discharge voltage and 10.1 A discharge current for the remainder of the test. The results for this period of more than 450 hours, during which the total mass utilization exceeded the contract goal by more than 2%, are presented in Table III-5. A time history of the principal thruster operating parameters plotted at 10-hour intervals throughout the test is shown in Fig. III-2. Of particular interest in these data are the constancy of the cathode keeper voltage and the success of the neutralizer keeper voltage control loop as a means of maintaining the floating potential (and neutralizer flow) at a desirably low level.

Table III-5. Thruster Performance During 500-Hour Test No. 1

Test Hours	Accel Voltage V	Discharge Voltage, V	Discharge Current, V	ϵ_I, eV/ION	$\eta_{m_{DIS}}$, %	$\eta_{m_{TOT}}$, %
0 to 26	800	40	9.8	261	92.1	88.7
26 to 29	700	40	9.8	261	93.0	90.1
29 to 32	600	40	9.8	261	89.1	86.4
32 to 35	600	39	9.8	254	88.0	84.5
36 to 40	600	40	9.8	261	89.7	86.9
41 to 66	700	39	10.1	261	90.0	88.3
66 to 70	600	39	10.1	261	89.0	86.5
72 to 518	600	39	10.1	261	89.7*	87.3*
518 to 522	600	39	10.1	261	89.5	87.3

*Hg flow measured with weighing system.

J_B = 1.51 A

VS = 1330 V

T1850

The test was begun using neutralizer S/N 407. Initial flow measurements indicated the flow was higher than normal for the amount of power being applied to the vaporizer and for the vaporizer temperature measured. By reducing the vaporizer power, turning off the tip heater and lowering the keeper current, it was possible to lower the flow to between 50 and 60 mA equiv. Operating in this manner did not permit closed loop operation at low flow rates so operation was switched over to neutralizer S/N 406. This neutralizer operated in a normal manner for the remainder of the test. Neutralizer 407 was later removed from the thruster, baked out and then tested on a thruster. The neutralizer operated normally leading to the conclusion that the high flow during the 500-hour test must have been caused by wetting of the vaporizer.

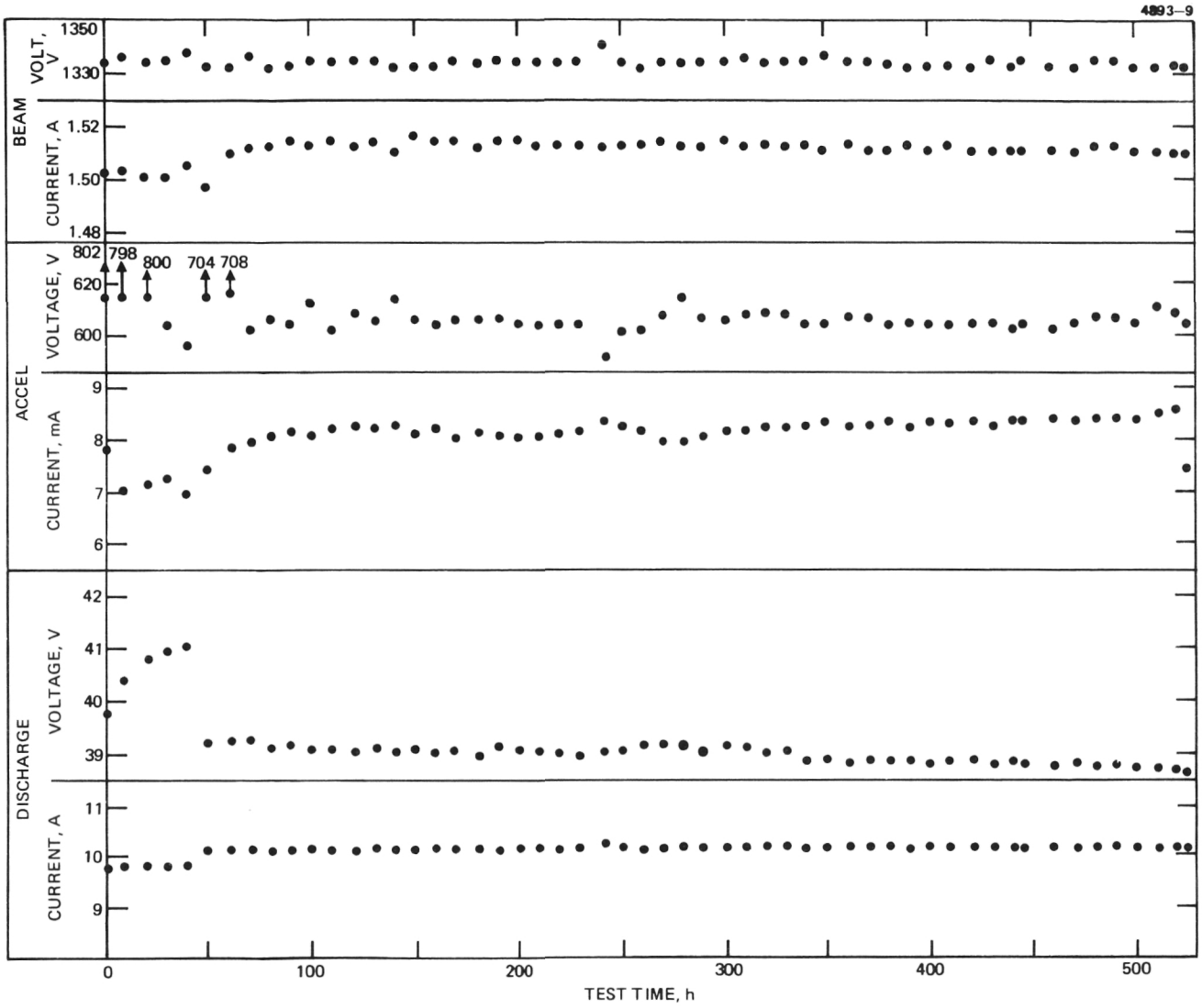

Figure III-2. Time history of principal thruster operating parameters during 500 hour test no. 1.

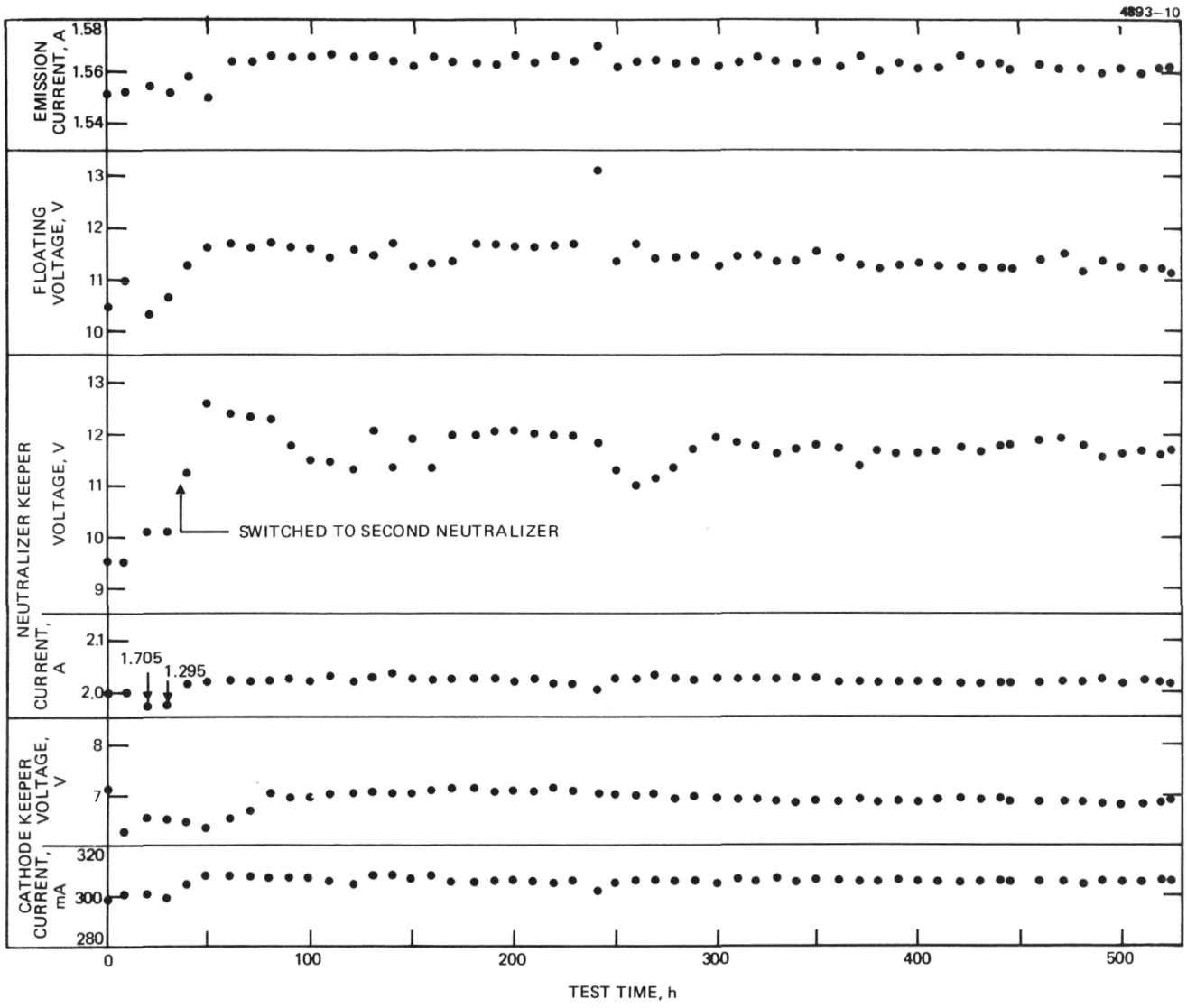

Figure III-2. (Continued).

Cathode isolator leakage was 0.3 μA or less for the first 350 hours of the test. After 350 hours the cathode isolator leakage current began to rise and reached 409 μA by 525 hours when the test was concluded.

At the conclusion of the test, a cold start of the thruster was made. All thruster power was turned off and the thruster allowed to cool off for 5 hours until the vaporizer temperatures ranged from +2°C to -20°C. Thruster turn on was then initiated and full beam operation was reached in one hour.

b. Post Test Analysis — Observation of the optics with a Questar telescope near the end of the 500-hour test had revealed some erosion on the downstream side of the accel electrode near the center cap. Post test examination of the optics confirmed that on the webs adjacent to the center cap there was an abnormal amount of charge exchange erosion (see Fig. III-3). The insulated cap which covered the center support was not eroded. The unblemished condition of the center support cap and the concentration of erosion on the accel around the center cap led to the conclusion that this localized erosion was caused by a distortion in the electric field lines due to the center cap being electrically insulated from the accel.

When the optics were removed from the thruster, another problem associated with the optics center support was observed. The section of the center support which extends into the discharge chamber was eroded due to sputtering. The locking screw from this end of the center support is compared to an unused one in Fig. III-4. While this erosion was not sufficient to weaken the center support, it did provide a source of metal that was deposited on the anode of the discharge chamber. The material deposited on the anode was subjected to spectrographic analysis; the three predominant elements, in order of amount present, were molybdenum, iron and nickel. The optics center support and electrodes are made from molybdenum.

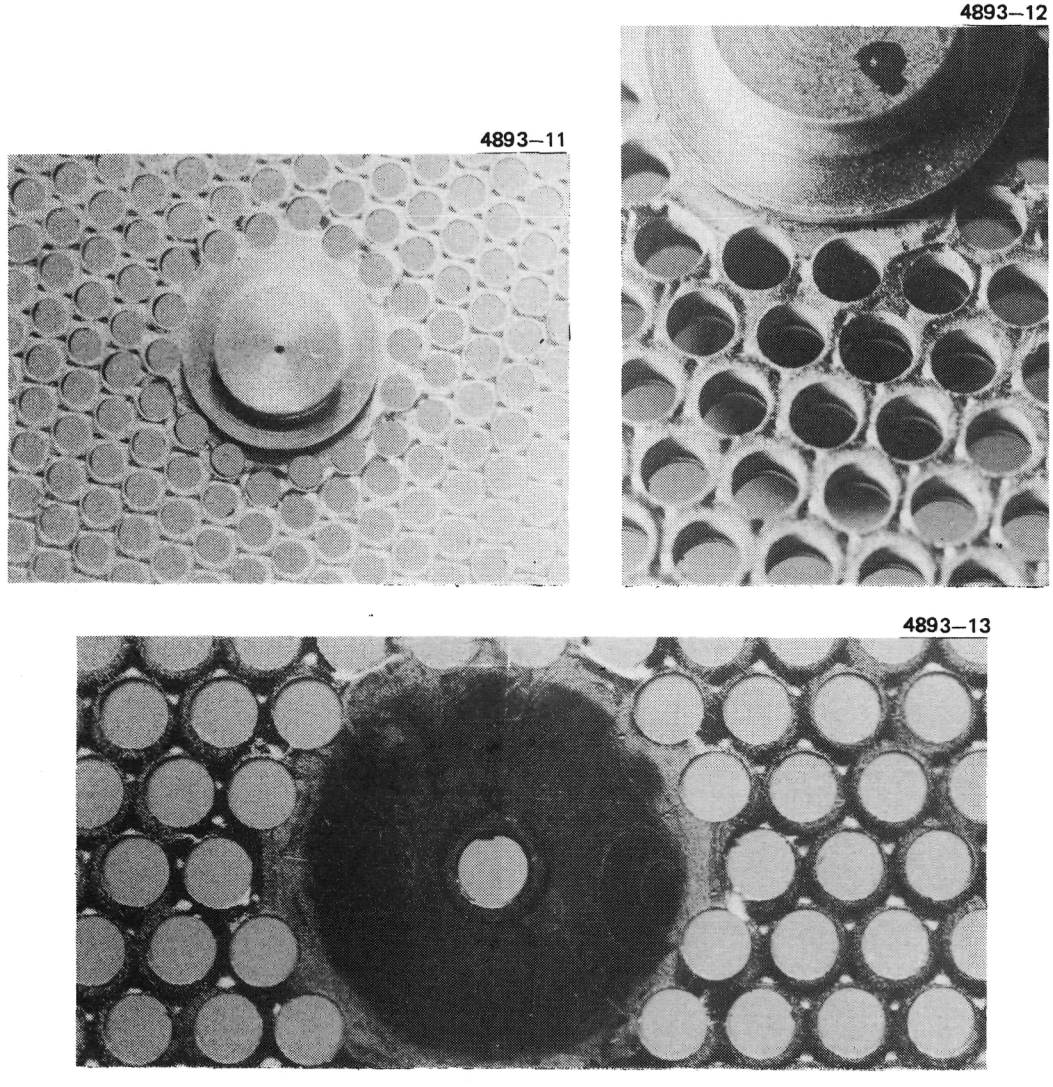

Figure III-3. Center section of accel electrode after 500 hour test No. 1.

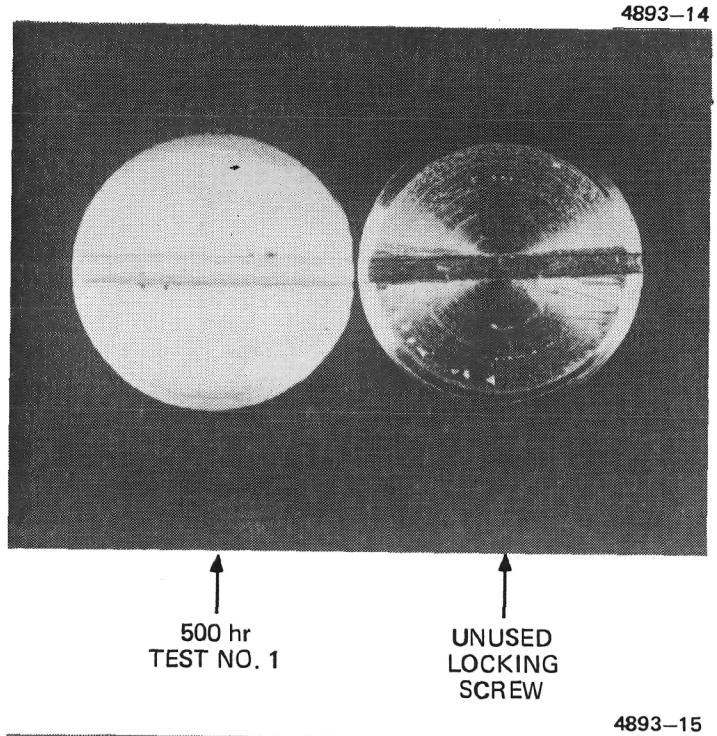

Figure III-4. Locking screw from center support of 500 hour test No. 1 optics and new unused locking screw.

Examination of the cathode-isolator-vaporizer (CIV) showed the gray surface discoloration on the isolator body similar to that observed after the 100-hour test. The CIV was installed in a bell jar and as the isolator was heated the electrical resistance dropped from infinity to 120 MΩ. The exterior surface of the isolator was then lightly sand-blasted and the CIV returned to the bell jar. This time as the isolator was heated the resistance continued to measure infinity on the megger demonstrating that the source of the electrical leakage had been on the exterior surface.

The cathode orifice looked very good following the 500-hour test. There were no signs of erosion on either the chamfered lip or the throat of the orifice. The cathode was separated from the CIV and the insert removed. The tantalum flag was intact, though it showed some signs of embrittlement. A section of the outer layer stuck to the cathode tube and was detached from the flag during removal.

As indicated earlier, both neutralizers were operated during the 500-hour test. S/N 407 was used only for the first 37 hours; S/N 406 was used for the last 488 hours. There was no evidence of erosion, heater failure, or dimensional change in the neutralizer orifices.

The conclusions of the post test evaluation were that with the exception of the two changes described below, the thruster, facility and test console were ready for the endurance test. However, because of the nature of the optics change which was recommended, it was decided to perform a second 500-hour test to evaluate that change. The two changes which were recommended as a result of the first 500-hour test were: (1) substitute dished electrode optics, as developed under Contract NAS 3-16528, in order to eliminate the center support and (2) change the body of the cathode isolator to Wesgo Al 300 alumina and add a high temperature borosilicate glaze to the exterior.

3. 500-Hour Test No. 2

Thruster S/N 402 which was used for the first 500-hour test was also used for the second 500-hour test. The changes incorporated for the second test were (1) substitution of dished electrode optics

without a center support for the flat close spaced optics with center support previously used; (2) a change from McDanel alumina to Wesgo Al 300 alumina for the body of the cathode isolator and the addition of a high temperature borosilicate glaze to the exterior of the isolator; (3) relocation of the two neutralizers to positions 12.7 cm outboard and 6.3 cm downstream of the accel (because of the switch to dished optics) and (4) reduction of the neutralizer tip to keeper spacing to 0.94 mm on S/N 407 and 0.76 mm on S/N 413. The physical characteristics of thruster 402 as assembled for 500-hour test No. 2 are presented in Table III-2.

The procedural format for the second 500-hour test was the same as used for the first 500-hour test. The test was continuously monitored for two days and then left to run unattended, except for periodic checks for the remaining 19 days. The automatic data system built into the test console was used to record data during unattended operation. System performance was periodically monitored at HRL via TTY using the remote interrogation capability of the system. (Real time data were also collected at LeRC in the same manner.) Beam profiles were taken and photos were taken of the thruster and collector during the test.

a. Test Results – The thruster operating point established for the test was screen voltage 1330 V, beam current 1.5 A, accel voltage 500 V, discharge voltage 37 V, discharge current 9.5 A, cathode keeper current 300 mA and neutralizer keeper current 2A. The neutralizer control loop was adjusted to satisfy the dual constraints of flow less than 50 mA equivalent current and coupling voltage of less than 20 V. This set of conditions resulted in an average neutralizer keeper voltage of 15.5 V, an average neutralizer flow of 44 mA and an average coupling voltage of 10.8 V. Neutralizer S/N 413 with a keeper-to-tip spacing of 0.75 mm was used throughout the test. A time history of the principal thruster operating voltages and currents is presented in Fig. III-5.

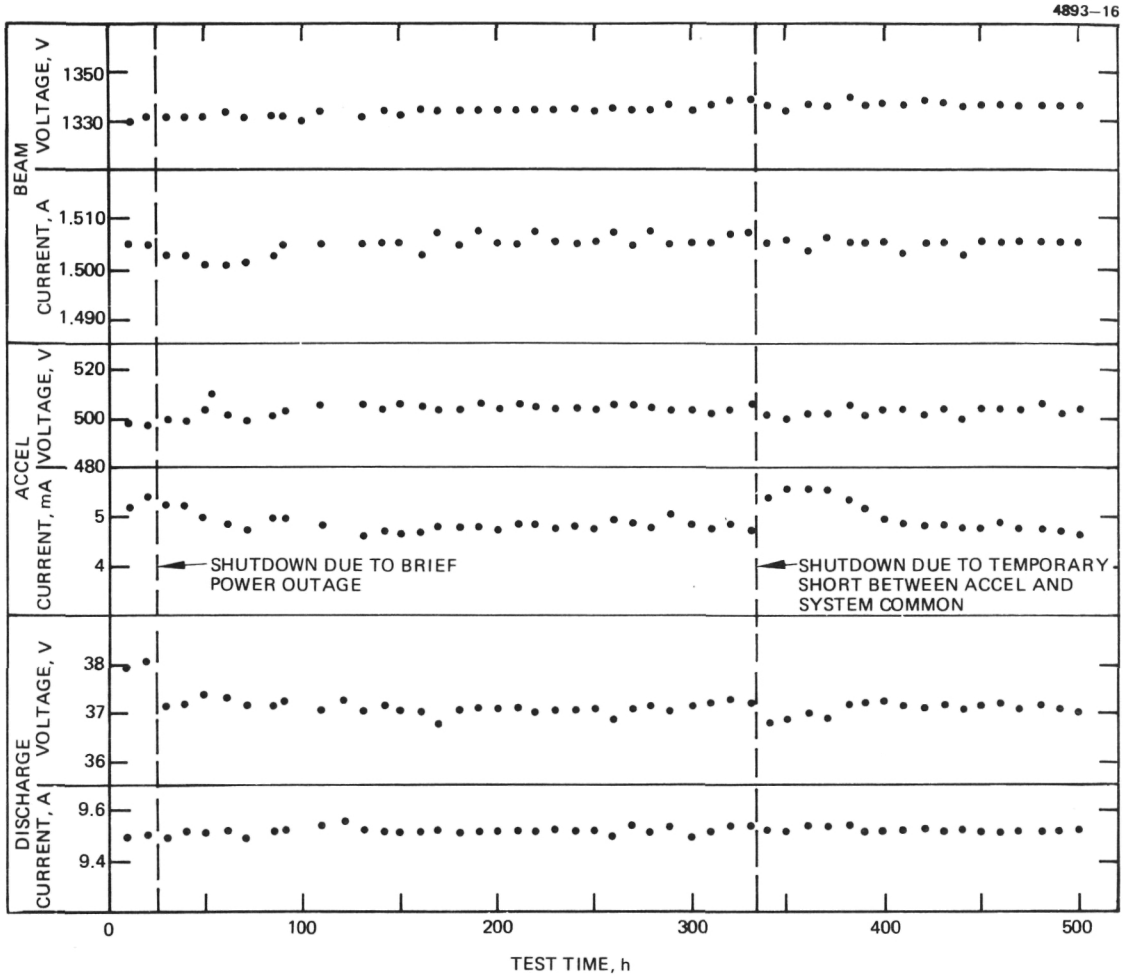

Figure III-5. Time history of the principal thruster operating parameters during 500 hour test no. 2.

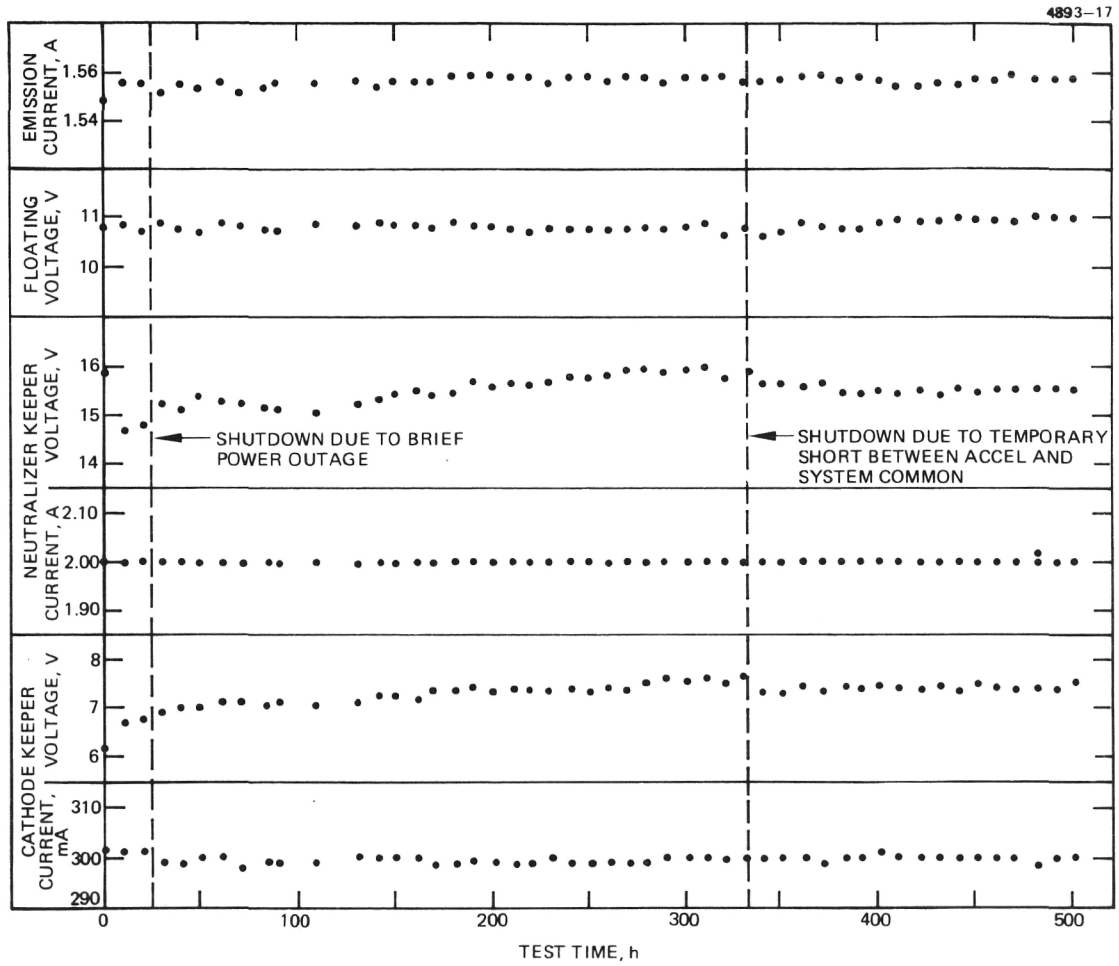

Figure III-5. (Continued)

Isolator leakage was not a problem during this 500-hour test. As noted earlier the cathode isolator body was made from Al 300 and the exterior was coated with a high-temperature borosilicate glaze. At the beginning of the test the leakage current across the cathode isolator, which operated at 350°C, was 1 μA; the leakage across the main isolator, which operated at 275°C, was 0.1 μA. After 7 hours the cathode isolator leakage had decreased to 0.75 μA. This decrease continued until after 42 hours the cathode leakage current reached 0.1 μA. Both the cathode and main isolator leakage currents then remained at 0.1 μA or less throughout the remainder of the test.

The test was begun with the pipette mercury weighing system in operation. After 32 hours the mercury weighing system was substituted for the pipette system and was used until the final 6 hours of the test when the pipette system was used again. For the 462 hours the weighing system was used the mass utilization measured in the discharge was 91.7%. During this period the average neutralizer flow was 44 mA equivalent current making the total mass utilization 89.3%. The mass utilization measurements made with the pipette system agreed within 1% with the mercury weighing system measurements. Electrical efficiency during this test was 82% which when combined with the mass efficiency gave a total efficiency of 73%. The performance of the thruster is summarized in Table III-3.

The total weight of mercury used by the discharge chamber and neutralizer during the last 435 hours of the test was determined by weighing the feed system storage reservoirs at the 66th hour and at the end of the test and subtracting the amounts used for the one restart during the test (see paragraph below) and the cold restart at the end of the test. Using these total weights to calculate mass utilizations resulted in a discharge utilization of 90.6% and a total utilization of 88.3%. These figures are 1% less than the utilizations for the same period calculated from the load cell mercury weighing system data.

There were two interruptions in thruster operation during the 500-hour test. The first occurred after 25 hours when there was a complete loss of power in the Space Simulation Laboratory due to an

electrical storm. The power was off for approximately one minute and the thruster was back on within 2 minutes after power was restored. The second interruption occurred after 332 hours of the test. At that time a short developed between the accel and system common. All power was removed and the thruster was allowed to cool off. The next morning, after the power had been off for approximately 11 hours, the short was gone. The thruster was restarted without difficulty and the remaining 168 hours of the test completed without any further indication of this or any other problem.

Following the conclusion of the 500-hour test, a cold thruster restart test was conducted. All power was removed and the thruster was allowed to cold soak in vacuum until the vaporizer and isolator thermocouples all registered below -10°C. Power was then applied to the thruster in the same sequence as used to initially start the 500-hour test. The thruster restarted without any detectable change in the startup or operating characteristics.

b. Post Test Analysis — Immediately upon removing the thruster from the chamber at the conclusion of the test, a visual inspection was made in an effort to determine the cause of the temporary short which had existed. The only thing observed which might have caused the short was some material deposited on the accel at the periphery where the beam had been striking and eroding the lip of the outer case. This deposited material was located so that if it had flaked off the accel it conceivably could have bridged the space between the accel and the edge of the outer case. The interception of the beam by the lip of the outer case was due to a combination of the wide beam divergence of the dished electrodes, a slight misalignment of the electrodes and a larger than necessary axial spacing between the optics and outer case.

In general, the condition of thruster 402 after 500-hour test No. 2 was very good. The erosion of the accel electrode which had occurred during 500-hour test No. 1 was eliminated by the switch to dished electrode optics and the associated elimination of the center support. Optics S/N 608 which was used for this second 500-hour test

did not show any localized erosion, including the region adjacent to the neutralizer. Charge exchange erosion on the downstream side of the accel was so slight as to be insignificant.

The new position which was selected for the neutralizers as a result of the dished optics evaluation tests proved to be a good choice.* At the conclusion of 500-hour test No. 2 there was no erosion of the neutralizer keeper cover and as mentioned above no accel erosion due to ions from the neutralizer. This neutralizer position was good from an operational standpoint also since the average coupling voltage was 10.8 V at an average neutralizer flow of 44 mA equivalent current.

Disassembly of thruster 402 after the second 500-hour test did reveal a problem which had not been observed after the first 500-hour test. The first evidence of this problem was found when neutralizer assembly S/N 413, which had been used throughout the test, was disassembled. Examination of the neutralizer tip revealed that the sheath on the tip heater had deteriorated so that heater insulation was visible in some spots (see Fig. III-6). The heater electrical integrity had not been impaired as demonstrated by the fact that during the cold restart after the 500-hour test normal startup of the neutralizer had occurred. The second occurrence of the same problem was found when the cathode-isolator-vaporizer assembly was disassembled sufficiently to expose the main cathode tip. The sheath on this heater exhibited a lesser amount of the same deterioration (see Fig. III-6) and in addition the top of the thermal radiator, which is brazed to the tip, was bent, as shown in Fig. III-7. The photo of the cathode radiator from the first 500-hour test, presented in Fig. III-7, illustrates that this problem did not occur during that test.

Both the neutralizer tip and cathode tip were sectioned and examined under high magnification. Figure III-8 shows cross sections of the main cathode tip heater and surrounding braze. From these

*The new neutralizer position was 6.3 cm axially and 12.7 cm radially from the last row of accelerator grid holes.

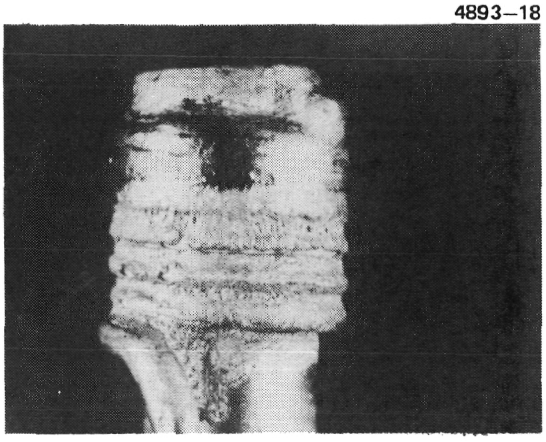

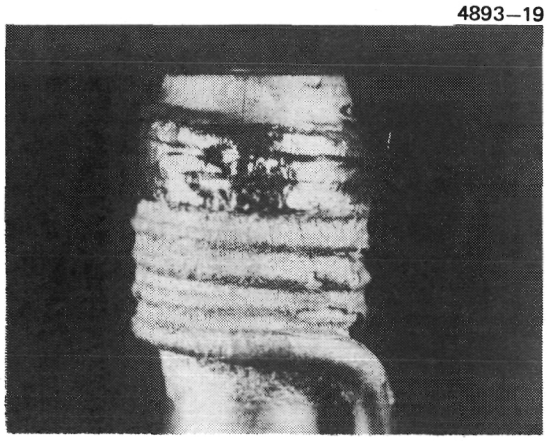

(a) Tip of Neutralizer 413

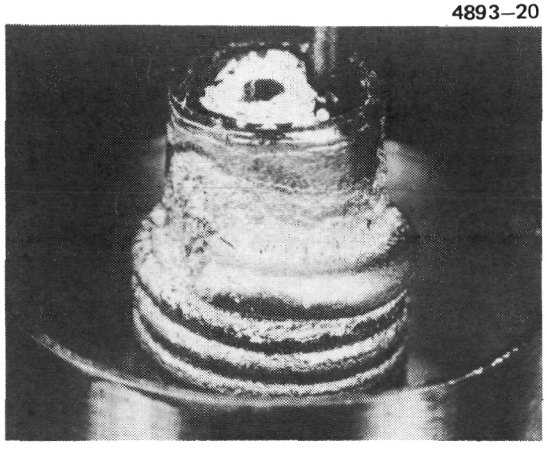

(b) Cathode Heater

Figure III-6. After 500 hour test No. 2.

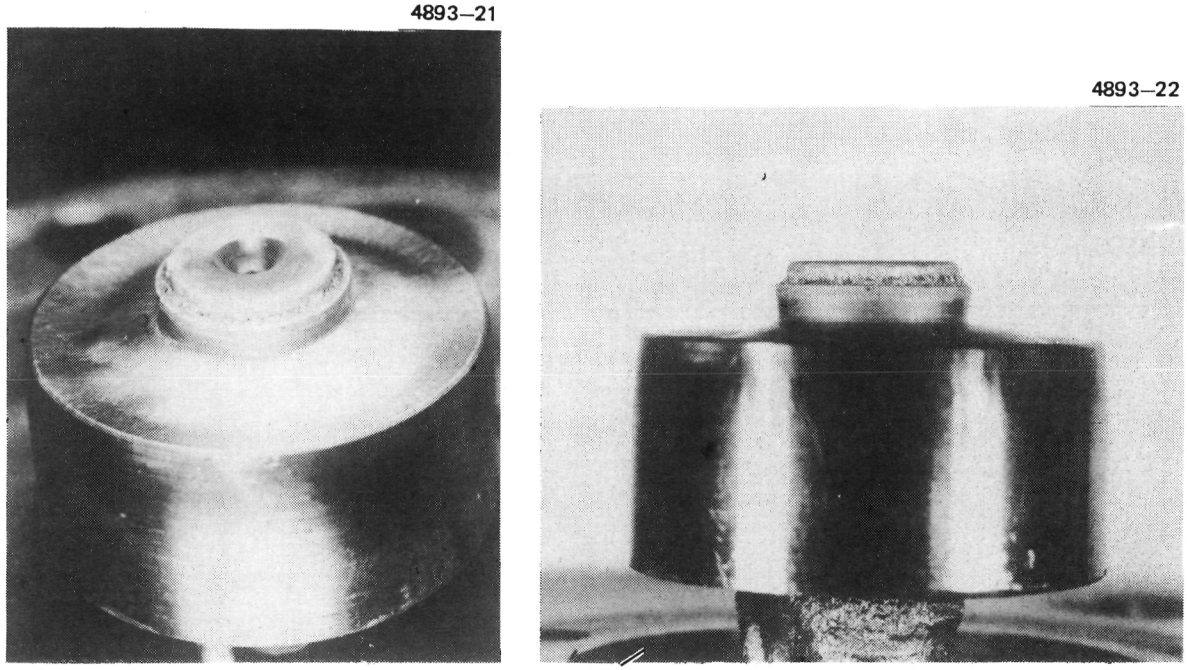

AFTER 500 hr TEST NO. 2

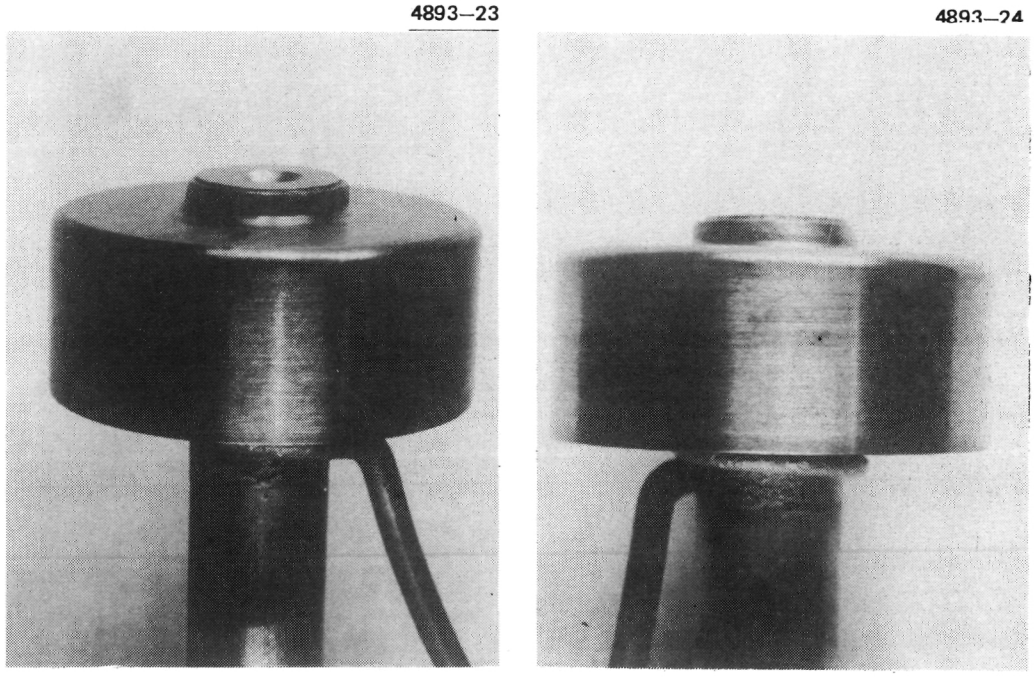

AFTER 500 hr TEST NO. 1

Figure III-7. Cathode thermal radiators after 500 hour tests.

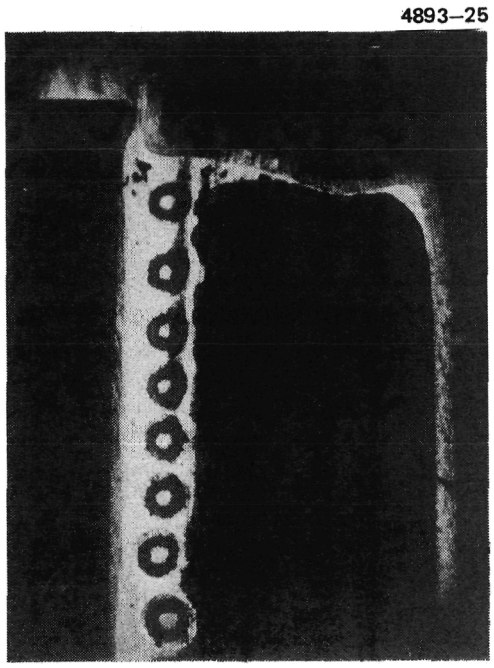

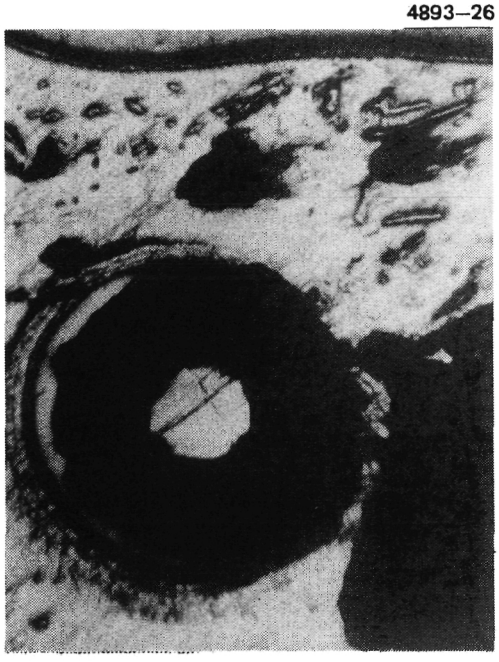

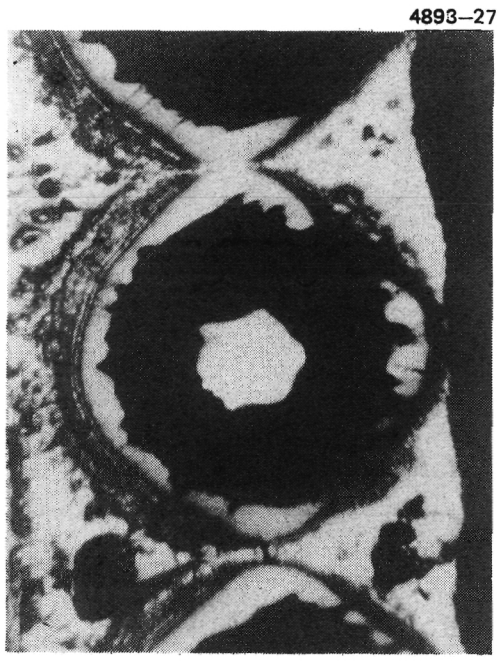

Figure III-8. Cross sections of cathode tip heater and thermal radiator after 500 hour test No. 2.

examinations, it was concluded that an interaction had occurred between the tantalum heater sheath and the NICRO braze used to braze the heater to the cathodes and the radiator to the cathode. An examination of the under side of the main cathode thermal radiator revealed that an excess of braze had been applied. Phase diagrams for tantalum mixed with nickel and boron, which are constituents of NICRO braze, show the existence of an eutectic with a melting temperature of 1090°C if the nickel content is above 59%. Since there was evidence of excess braze on the main cathode, it is believed that the problem was an interaction of the braze and tantalum made possible by the combination of high temperature and excess braze alloy.

The resistance of all eight heaters (2 neutralizers) including the leads from the heaters to the thruster terminals were measured with a precision bridge before and after the test. As shown in Table III-6, the

Table III-6. Pre-Test and Post-Test Heater Resistances for 500 Hour Test No. 2 Thruster

Heater	Resistance		Change
	Before	After	
Cathode Tip	0.582 Ω	0.588 Ω	+1.03%
Neutralizer Tip S/N 407	0.541	0.546	+0.92
Neutralizer Tip S/N 413	0.476	0.621	+30.5
Cathode Vaporizer	2.026	2.070	+2.17
Main Vaporizer	6.057	6.097	+0.66
Neutralizer Vaporizer S/N 407	2.554	2.552	-0.08
Neutralizer Vaporizer S/N 413	1.712	1.719	+0.41
Main Isolator	3.844	3.901	+1.48

T1851

only heater showing a significant change in resistance was the tip heater on neutralizer 413. As discussed earlier, the tip of this component was affected by the tantalum-NICRO braze interaction. The neutralizer did, however, relight satisfactorily during the cold restart test following the 500-hour test.

The conclusions of the post test analysis of the second 500-hour test were that the optics erosion problem had been eliminated. However, the interaction between the NICRO braze and tantalum cathode components was discovered. As a result plasma sprayed heaters of the type used on SERT II were substituted on both the main cathode and neutralizer cathodes for the endurance test.

The three short-term tests conducted prior to initiating the 6000 endurance test proved to be of value in leading to the detection and elimination of the thruster problems described in the preceding sections. The performance of the test console, facility and thruster throughout the short-term tests was very encouraging. The short-term tests served well their intended purpose of providing the desired confidence and knowledge necessary to embark on the endurance test.

B. Endurance Tests

The principal goal of this program was to conduct the endurance test described in this section. Two endurance tests were conducted because the first was aborted after 1108 hours, due to a sudden loss of vacuum in the vacuum test facility. The second endurance test was run for 10,000 hours, a 67% increase in the original contract goal of 6000 hours. The 1100-hour test was run with thruster 402; the 10,000 hour test was run with thruster 701 the first of the engineering model thrusters which were developed under contract NAS 3-16528. Differences between the 400 series and 700 series thrusters are described in references 2 and 3 and summarized in Table III-2.

1. 1100 Hour Endurance Test

Thruster 402 which was used for both 500 hour short term tests was also used for the 1100 hour endurance test. Changes in the thruster since the second 500 hour test were: (1) plasma sprayed heaters

substituted for sheathed heaters in the main discharge cathode and neutralizer cathodes (a second neutralizer for redundancy was included on the thruster during all tests), (2) the number of turns on the magnetic baffle reduced from 3 to 2 and the baffle coil termination brought outside of the discharge chamber, (3) the cathode baffle diameter increased from 5.4 cm to 5.7 cm, and the thickness increased from 0.076 cm to 1.42 cm, (4) the cathode keeper insulators double shielded, (5) the R-500 emissive mix coating on the cathode inserts applied by spraying to a thickness between 0.005 and 0.0013 cm instead of dipping, and (6) the optics electrode dimensions changed as shown in Table III-2.

a. Tests Results — The test procedure for this test was the same as for the earlier 500 hour tests, a short period of attended operation and then unattended operation with periodic filling of the mercury feed system. This test was terminated after 1108 hours due to a vacuum test facility failure. While illuminating the thruster for visual observation, the electrical feedthrough which supplied power to the vacuum chamber internal floodlight ruptured. This rupture caused a rapid loss of vacuum with consequent backstreaming of the diffusion pumps. Examination of the feedthrough indicated that arcing across the feedthrough had caused the glass insulator to melt and the metallic feedthrough to erode until the vacuum integrity of the feedthrough was lost. It is believed that the arcing was precipitated by deposition of sputtered material on the glass insulator. The substitution of uncompensated dished optics for the original flat electrodes widened the thruster ion beam appreciably with a resultant increase of sputtering within the vacuum facility.

Thruster performance for the 1100 hour endurance test is summarized in Table III-3; discharge chamber voltage was 40. In addition to the data presented in Table III-3, time history plots of other important thruster operating parameters are shown in Fig. III-9. Of particular interest is the plot of cathode keeper voltage. As was the case in both the 500 hour tests, after an initial rise the keeper voltage leveled off and even began to decrease as time progressed. The cathode feedline high voltage isolator developed leakage current during this test

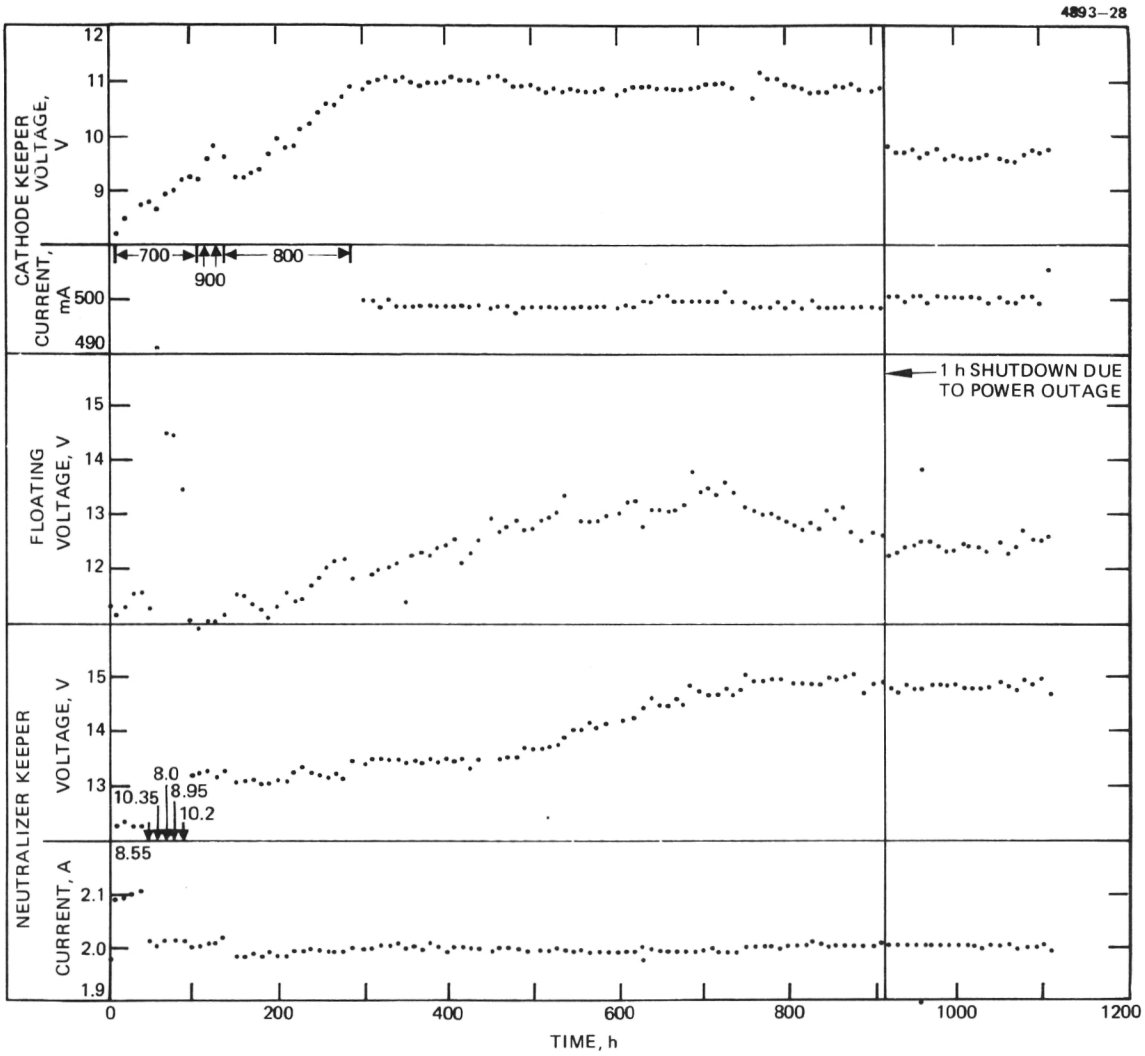

Figure III-9. Time history of selected thruster operating parameters during the 1,100 hour endurance test.

also, reaching 7 mA before the end of the test. After approximately 730 hours the high voltage trip rate began to increase reaching an average of about two trips per hour prior to the vacuum failure. Post test examination showed backsputtered material on the optics mask and inside the discharge chamber. Since the thruster was facing downward, toward the frozen mercury collector, it is believed that the increase in arc rate was caused by backsputtered material within the discharge chamber dislodging and falling onto the optics.

b. Post Test Analysis – Post-test evaluation of the thruster was hampered by the precipitous manner in which the test was terminated. The rapid venting of the vacuum chamber with the thruster at operating temperature coupled with the diffusion pump backstreaming altered the condition of the thruster. However, post-test examination of the thruster did not reveal any signs of unusual erosion or wear. The optics were in very good shape with no evidence of localized erosion in such critical areas as near the neutralizer. The cathode orifices, main and neutralizer, were unaltered in shape or size although both tips were lightly coated with tungsten oxide due to exposure to air while at operating temperature. The external alumina coating on the neutralizer plasma sprayed heater was cracked in several places, but still firmly attached to the tube. When the main cathode assembly was disassembled sufficiently to view the heater, part of the external coat of alumina was missing. It was not possible to tell when the loss of alumina occurred. The remaining alumina overcoat was covered with tungsten oxide as was the inside of the cathode thermal radiator. The tungsten-rhenium heater wire was reduced in diameter in several spots and completely missing near the tip. The evaporation of the heater wire and deposition of tungsten oxide is presumed to have occurred when the cathode heater power was applied for a short time after the loss of vacuum within the chamber. The cathode baffle and keeper were both in good shape. As noted earlier there was backsputtered material on the anode which was flaking off, but there was no indication of any significant erosion inside the discharge chamber. At the time it was believed that the material deposited on the anode had been sputtered from the vacuum facility due

to the wide beam angle of the uncompensated dished electrodes. However, in view of the erosion within the discharge chamber observed after the 10,000 hour test, some of the deposited material in the 1100 hour test thruster may have been caused by thruster erosion.

2. 10,000 Hour Test

The 10,000 hour endurance test was the culmination of the development and test efforts described in the preceding sections of this report. By the time the test was to start, the first of the engineering model 30-cm thrusters (S/N 701) being developed under contract NAS 3-16528 had been assembled and tested. The engineering model thruster development had been occurring in parallel with the earlier tests of the endurance test program. Thus, the thruster changes which had been adopted as solutions to the problems identified by the short term tests and 1100 hour test had been incorporated in thruster 701. The availability of thruster 701 provided an opportunity to endurance test a new thruster that included all the life extending changes.

a. Test Results Thruster Performance — The endurance test as initially contracted was to be run for 6000 hours and at a beam current of 1.5 A. Subsequent contract modifications provided for increasing the beam current in steps to 2 A and extended the test duration to 10,000 hours. The number of hours accumulated and the performance achieved at each beam current level is summarized in Table III-7; the discharge voltage was held at 37 V. When the effects of baffle erosion (described below) became evident while operating at 1.75 A beam current it was decided to limit the maximum current to 1.75 A.

Results of this test indicate that the three thruster modifications incorporated as a result of the earlier short term tests were all successful. In contrast to the previous tests the cathode feedline high voltage isolator did not develop any leakage current. The test system wiring was configured so that the cathode and main feedline isolators were continuously stressed with the 1100 V screen voltage. Periodically a microammeter was inserted in series with each of the high voltage

Table III-7. Summary of Thruster Performance During 10,000 Hour Test

Test Period, Hours	Beam Current, A	Accel Current, A	High Voltage Trip/Rate, No./Hour	eV/Ion	Total Power, kW	Propellant Efficiency, (Meter Value), %	Electrical Efficiency, (Meter Value), %	Total Efficiency (Corrected), [a] %	Effective Specific Impulse, [a] sec	Thrust (Corrected), [a] N	Remarks
100 to 2110	1.50	0.0030	0.14	185	2.03	88.0	83.3	65.7	2800	0.098	
2110 to 2750	1.61	0.0033	0.19	185	2.17	89.8	83.6	67.0	2850	0.104	
2750 to 3000	1.71	0.0034	0.36	185	2.30	92.3	83.6	68.6	2920	0.111	
3000 to 6050	1.75	0.0038	0.21	185	2.36	93.3	83.5	69.2	2950	0.113	Flakes on optics at hour 4530. Hole in baffle at hour 5845.
6050 to 7300	1.51	0.0029	1.21	214	2.08	93.1	81.3	67.8	2960	0.098	Baffle edge erosion at hour 6845. Cryoshroud LN_2 leak at hour 7197.
7300 to 7500	1.00	0.0017	0.42	278	1.47	87.3	76.7	61.0	2800	0.066	
7500 to 8130	1.00	0.0025	1.35	240	1.43	90.4	78.5	64.8	2900	0.066	Chamber pressure on 10^{-5} Torr scale until LN_2 leak eliminated at hour 8036.
8130 to 8380	1.01	0.0018	0.29	253	1.46	85.7	78.2	61.2	2750	0.066	
8380 to 9000	1.01	0.0018	1.24	278	1.48	85.7	76.9	60.0	2750	0.066	
9000 to 9300	1.01	0.0020	2.00	296	1.50	83.9	76.0	58.8	2690	0.066	
9300 to 10000	0.51	0.0010	0.41	370	0.82	70.5	69.8	46.6	2300	0.034	

a. Correction factors for doubly-charged ions and beam divergence were developed from beam probe measurements made under Contract NAS 3-17831. Correction factors used were for 185 ev/ion operation.

T1852

Table III-8A. Performance Summary of 10,000 Hr Test Thruster 701

Time Period	J_S, A	J_A, mA	V_I, V	V_{CK}, V	V_{NK}, V	V_G, V	$\dot{m}_M$, eq. A	$\dot{m}_C$, eq. A	$\dot{m}_N$, eq. A	η_{m_D}, %	η_{m_T}, %	Arcs per Hour
100 to 250	1.503	2.90	37.55	7.47	14.19	11.88	1.580	0.108	0.029	88.9	87.4	0.14
200 to 300	1.503	2.94	37.55	7.62	14.43	12.44	1.580	0.110	0.034	88.8	87.0	0.14
300 to 400	1.505	3.04	37.55	7.73	14.78	12.58	1.591	0.111	0.033	88.2	86.6	0.16
400 to 500	1.499	3.06	37.38	7.60	14.32	12.58	1.570	0.109	0.038	89.1	87.1	0.08
500 to 600	1.497	3.09	37.15	7.44	14.36	12.56	1.568	0.108	0.036	89.1	87.3	0.11
600 to 700	1.495	3.11	37.09	7.40	14.52	12.58	1.561	0.103	0.037	89.7	87.7	0.12
700 to 800	1.484	3.12	37.03	7.30	14.25	12.61	1.553	0.108	0.037	89.2	87.2	0.22
800 to 870	1.475	3.08	36.92	7.19	14.18	12.60	1.523	0.105	0.037	90.4	89.4	0.22
870 to 1000	1.498	2.95	36.97	7.51	14.90	12.79	1.584	0.106	0.036	88.5	86.6	0.27
1000 to 1100	1.495	3.16	36.90	7.35	13.72	13.20	1.556	0.106	0.046	89.8	87.4	0.14
1100 to 1240	1.504	3.19	36.90	7.34	14.10	12.86	1.570	0.106	0.038	89.6	87.6	0.10
1250 to 1300	1.502	3.05	37.15	7.31	13.97	12.70	1.560	0.095	0.035	90.6	88.7	0.15
1340 to 1400	1.496	2.99	37.35	7.25	13.88	12.78	1.547	0.096	0.038	90.9	88.8	0.11
1540 to 1600	1.508	2.79	37.25	7.63	14.01	13.00	1.583	0.099	0.054	89.5	86.7	0.09
1600 to 1700	1.508	3.01	37.23	7.44	14.51	13.01	1.542	0.100	0.035	91.7	89.7	0.07
1700 to 1800	1.508	3.05	37.08	7.39	14.54	13.11	1.554	0.098	0.035	91.1	89.2	0.12
1800 to 1910	1.508	3.05	37.02	7.33	14.51	13.16	1.556	0.097	0.036	91.0	89.1	0.06
1930 to 2000	1.508	3.05	36.96	7.31	14.51	13.21	1.559	0.095	0.036	91.0	89.0	0.10
2000 to 2110	1.509	3.04	37.05	7.36	14.51	13.25	1.541	0.097	0.037	91.9	89.9	0.15
100 to 2110	1.500	3.03	37.16	7.41	14.30	12.79	1.562	0.103	0.037	89.9	88.0	0.14
2130 to 2200	1.609	3.30	36.55	7.38	15.69	14.46	1.670	0.095	0.036	91.0	89.2	0.10
2200 to 2270	1.608	3.37	36.55	7123	15.52	13.60	1.667	0.096	0.029	91.0	89.6	0.13
2280 to 2400	1.612	3.26	36.46	7.40	14.52	13.10	1.680	0.093	0.032	90.8	89.1	0.14
2130 to 2400	1.610	3.31	36.51	7.34	15.15	13.60	1.674	0.094	0.032	90.9	89.3	0.13
2400 to 2500	1.613	3.42	36.49	7.25	14.49	13.20	1.678	0.094	0.034	90.8	89.1	0.22
2500 to 2600	1.618	3.35	37.07	7.17	14.44	13.23	1.654	0.091	0.033	92.6	90.8	0.17
2600 to 2700	1.617	3.34	37.04	7.15	14.42	13.54	1.653	0.090	0.036	92.6	90.7	0.28
2700 to 2750	1.614	3.20	37.11	7.56	15.29	13.66	1.655	0.093	0.038	92.1	90.2	0.28
2130 to 2750	1.613	3.33	36.73	7.29	14.82	13.47	1.666	0.093	0.034	91.5	89.8	0.19
2750 to 2800	1.708	3.41	36.94	6.68	15.42	14.20	1.719	0.092	0.033	94.1	92.4	0.42
2800 to 2900	1.707	3.42	37.06	6.66	15.45	14.32	1.712	0.091	0.037	94.5	92.6	0.21
2900 to 3000	1.714	3.50	37.16	6.81	15.42	14.42	1.730	0.087	0.041	94.1	92.1	0.49
2750 to 3000	1.710	3.45	37.08	6.72	15.43	14.34	1.721	0.090	0.038	94.3	92.3	0.36
3000 to 3100	1.761	3.69	37.06	6.62	15.88	15.04	1.778	0.086	0.044	94.2	92.1	0.24
3100 to 3200	1.760	3.66	37.34	6.56	16.30	15.42	1.768	0.087	0.049	94.7	92.2	0.37
3200 to 3300	1.760	3.68	37.28	6.54	16.47	15.36	1.756	0.088	0.058	95.3	92.4	0.18
3300 to 3400	1.760	3.66	37.26	6.52	17.92	14.38	1.772	0.087	0.026	94.5	93.2	0.18
3400 to 3500	1.759	3.68	37.30	6.50	17.94	14.65	1.768	0.086	0.027	94.6	93.3	0.19
3500 to 3600	1.761	3.69	37.27	6.48	17.96	15.16	1.770	0.087	0.032	94.6	93.1	0.19
3600 to 3700	1.762	3.69	37.26	6.45	17.96	14.97	1.764	0.086	0.030	95.0	93.5	0.14
3700 to 3800	1.763	3.66	37.31	6.44	17.84	14.32	1.761	0.086	0.031	95.2	93.7	0.19
3800 to 3900	1.756	3.69	37.22	6.55	17.82	14.86	1.759	0.086	0.031	95.0	93.4	0.27
3900 to 4000	1.752	3.66	37.14	6.46	17.78	14.35	1.755	0.085	0.028	95.0	93.6	0.18
4000 to 4100	1.749	3.70	37.14	6.64	15.68	12.32	1.742	0.086	0.027	95.4	94.1	0.25
4100 to 4200	1.749	3.68	37.10	6.72	15.64	12.50	1.763	0.086	0.028	94.3	92.9	0.12
4200 to 4300	1.747	3.64	37.02	6.58	15.54	12.60	1.760	0.084	0.028	94.5	93.0	0.41
4300 to 4400	1.744	3.60	37.10	6.48	15.44	12.80	1.748	0.083	0.030	95.0	93.5	0.25
4400 to 4500	1.750	3.62	37.02	6.36	15.44	13.16	1.756	0.083	0.031	94.9	93.4	0.21
4500 to 4600	1.750	3.65	①	6.36	15.42	13.88	1.759	0.082	0.035	94.9	93.1	0.32
4600 to 4700	1.748	3.98	37.21	6.40	17.22	14.64	1.758	0.080	0.035	94.9	93.1	0.21
4700 to 4800	1.753	4.06	37.22	6.42	16.87	15.52	1.744	0.084	0.040	95.7	93.6	0.17
4800 to 4900	1.755	4.14	37.06	6.32	17.86	17.06	1.750	0.080	0.069	95.7	92.2	0.16
4900 to 5000	1.752	4.12	37.16	6.28	17.48	15.20	1.754	0.081	0.048	95.3	92.8	0.27
5000 to 5100	1.753	4.16	37.36	6.28	17.16	15.44	1.751	0.080	0.035	95.5	93.7	0.15
5100 to 5200	1.754	4.14	37.10	6.29	17.19	15.54	1.751	0.079	0.036	95.6	93.8	0.11
5200 to 5300	1.752	4.16	②	6.27	17.10	15.36	1.754	0.077	0.035	95.5	93.7	0.02
5300 to 5400	1.751	4.16		6.27	17.10	15.18	1.756	0.076	0.034	95.4	93.6	0.04
5400 to 5500	1.751	4.12		6.22	17.44	16.31	1.750	0.076	0.048	95.7	93.2	0.15
5500 to 5600	1.748	4.10		6.23	17.78	14.70	1.759	0.075	0.028	95.1	93.7	0.04

① Data channel failure at hour 4504.8.

② Data channel failure at hour 5161, V_i is periodically checked at the bulkhead.

T1912

Table III-8A. Performance Summary of 10,000 Hr Test Thruster 701

Time Period	J_S, A	J_A, mA	V_I, V	V_{CK}, V	V_{NK}, V	V_G, V	$\dot{m}_M$, eq. A	$\dot{m}_C$, eq. A	$\dot{m}_N$, eq. A	η_{m_D}, %	η_{m_T}, %	Arcs per Hour
5600 to 5700	1.744	4.10		6.26	17.83	14.76	1.753	0.076	0.029	95.1	93.6	0.11
5700 to 5800	1.752	4.10		6.37	20.15	20.86	1.734	0.084	0.029	96.1	94.6	0.16
5800 to 5900	1.752	4.08		6.59	15.73	13.69	1.743	0.083	0.031	95.7	94.1	0.04
5900 to 6000	1.753	3.54		6.60	15.70	13.97	1.755	0.083	0.032	95.2	93.5	0.35
6000 to 6050	1.756	3.61		6.59	15.34	13.47	1.642	0.092	0.042	--	--	≥11.1
③ 6050 to 6200	1.510	3.01		6.37	16.82	13.60	1.479	0.081	0.032	96.6	94.7	1.20
6200 to 6300	1.514	3.30		7.29	14.84	12.01	1.532	0.085	0.034	93.4	91.5	0.31
6300 to 6400	1.525	3.14		7.57	14.87	12.10	1.534	0.084	0.034	94.1	92.1	0.20
6400 to 6500	1.524	3.02		7.62	14.90	12.20	1.530	0.081	0.034	94.4	92.5	0.34
6500 to 6600	1.521	3.00		7.77	14.88	12.32	1.528	0.081	0.035	94.3	92.3	0.56
6600 to 6700	1.503	2.87		8.66	14.71	12.56	1.488	0.084	0.038	95.4	93.2	0.34
6700 to 6800	1.502	2.81		8.62	14.79	12.63	1.499	0.080	0.037	94.9	92.8	0.18
6800 to 6900	1.497	2.77		8.68	14.81	12.76	1.486	0.080	0.038	95.4	93.1	0.25
6900 to 7000	1.498	2.79		8.92	14.82	13.09	1.478	0.081	0.040	95.9	93.5	0.20
7000 to 7100	1.499	2.78		9.44	14.80	13.39	1.489	0.083	0.046	95.2	92.3	0.28
7100 to 7200	1.506	2.77		9.25	14.87	13.83	1.473	0.084	0.049	96.5	93.8	0.10
7200 to 7300	1.509	2.63		8.93	15.49	13.97	1.465	0.080	0.041	97.5	95.0	≥0.59
④ 7300 to 7400	1.005	1.68		10.48	16.84	12.70	0.995	0.118	0.039	90.1	87.1	--
7400 to 7500	1.003	1.67		10.28	16.82	12.84	0.980	0.124	0.040	90.7	87.5	--
⑤ 7500 to 7600	1.005	2.04		10.86	17.14	14.26	0.979	0.117	0.040	91.5	88.3	--
7600 to 7700	1.008	2.01		10.87	17.53	14.02	0.940	0.119	0.044	95.0	91.2	--
7700 to 7800	1.009	2.54		10.19	17.45	13.60	0.920	0.120	0.042	96.7	93.0	--
7800 to 7900	1.008	2.70		10.09	17.48	13.79	0.915	0.121	0.042	97.0	93.2	--
7900 to 8000	1.008	2.89		11.26	17.50	13.99	0.900	0.122	0.048	98.3	93.9	--
8000 to 8120	1.007	2.49		10.28	16.46	11.36	1.101	0.070	0.039	85.7	83.0	0.29
⑥ 8130 to 8200	1.008	1.79		10.34	16.05	11.63	1.004	0.112	0.039	90.1	87.1	0.10
8200 to 8300	1.008	1.74		10.75	16.03	11.67	1.020	0.109	0.039	89.1	86.1	0.27
8300 to 8380	1.008	1.94		9.41	16.04	11.73	1.087	0.072	0.039	86.8	84.0	0.07
⑦ 8390 to 8500	1.008	1.77		10.30	16.08	12.04	0.996	0.113	0.041	90.7	87.5	0.31
8500 to 8600	1.008	1.76		10.18	16.02	11.98	1.007	0.112	0.041	89.9	86.7	0.37
8600 to 8700	1.008	1.78		9.94	16.01	12.17	1.011	0.109	0.043	89.8	86.5	0.88
8700 to 8800	1.009	1.84		9.45	16.45	12.69	1.062	0.095	0.043	87.0	83.9	0.70
8800 to 8900	1.010	1.78		9.76	16.61	12.35	1.028	0.108	0.040	88.7	85.7	0.74
8900 to 9000	1.009	1.93		9.50	16.67	13.09	1.075	0.080	0.045	87.2	83.9	0.84
⑧ 9000 to 9100	1.011	1.98		8.22	16.82	13.64	1.111	0.066	0.048	85.7	82.4	0.81
9100 to 9200	1.010	2.03		8.20	16.99	12.72	1.110	0.060	0.040	86.2	83.3	0.73
9200 to 9300	1.012	2.13		8.10	17.05	12.86	1.079	0.053	0.041	89.2	86.1	0.70
⑨ 9300 to 9400	0.511	1.18		9.82	17.30	12.02	0.595	0.065	0.050	77.3	71.8	0.08
9400 to 9500	0.511	1.14		9.92	17.27	12.22	0.603	0.064	0.052	76.5	70.9	0.07
9500 to 9600	0.508	1.10		9.86	18.26	13.36	0.601	0.064	0.053	76.2	70.6	0.14
9600 to 9700	0.509	1.12		9.88	18.48	13.90	0.596	0.065	0.058	76.9	70.7	0.11
9700 to 9800	0.509	1.12		9.89	18.22	13.65	0.599	0.064	0.062	76.8	70.2	0.07
9800 to 9900	0.510	1.14		9.94	17.86	13.44	0.600	0.065	0.062	76.5	70.0	0.10
9900 to 10,000	0.510	1.16		9.92	18.14	13.92	0.601	0.063	0.068	76.7	69.5	0.29

③ eV/ion increased to 216 from 185 (increased J_I, V_I still at 37 V)

④ eV/ion increased to 278 (increased J_I)

⑤ eV/ion decreased to 240

⑥ eV/ion increased to 259 (J_I increased to prevent "low mode")

⑦ eV/ion increased to 278 (J_I increased to prevent "low mode")

⑧ eV/ion increased to 296 (J_I increased to prevent low mode)

⑨ eV/ion set at 370

T1912

Table III-8B. Performance Summary of 10,000 Hr. Test Thruster 701

Time Period	Main Vap		Cath Vap		Neut Vap		Neut Cath		Main Cath		Isolators	
	V	A	V	A	V	A	V	A	V	A	V	A
2400 to 2500	5.99	0.97	4.10	1.31	3.20	0.99	0.68	0.24	1.45	0.41	1.18	0.43
2500 to 2600	5.94	0.96	4.07	1.29	3.18	0.99	0.71	0.24	1.44	0.40	1.17	0.42
2600 to 2700	5.93	0.96	4.05	1.29	3.20	1.02	0.69	0.24	1.40	0.40	1.16	0.42
2700 to 2750	5.96	0.96	4.07	1.29	3.17	0.98	0.68	0.24	1.42	0.41	1.17	0.42
2750 to 2800	5.85	0.94	3.96	1.25	3.05	0.94	0.70	0.24	1.40	0.39	1.18	0.42
2800 to 2900	5.89	0.94	3.95	1.25	3.20	1.00	0.67	0.24	1.49	0.41	1.18	0.42
2900 to 3000	5.96	0.95	3.96	1.25	3.17	0.99	0.64	0.23	1.35	0.39	1.16	0.42
2750 to 3000	5.91	0.94	3.96	1.25	3.15	0.98	0.67	0.24	1.42	0.40	1.17	0.42
3000 to 3100	6.00	0.96	3.94	1.25	3.16	0.99	0.62	0.23	1.35	0.39	1.16	0.42
3100 to 3200	6.09	0.99	4.01	1.27	3.21	1.02	0.67	0.23	1.30	0.39	1.16	0.42
3200 to 3300	6.10	0.98	4.01	1.27	3.39	1.04	0.68	0.23	1.31	0.38	1.16	0.42
3300 to 3400	6.11	0.98	4.04	1.28	2.62	0.83	0.66	0.24	1.25	0.39	1.14	0.42
3400 to 3500	6.06	0.98	4.04	1.28	2.64	0.83	0.58	0.23	1.29	0.38	1.14	0.43
3500 to 3600	6.08	0.98	4.04	1.28	2.68	0.86	0.63	0.23	1.32	0.39	1.15	0.42
3600 to 3700	6.12	1.02	4.04	1.28	2.71	0.85	0.70	0.23	1.30	0.38	1.15	0.42
3700 to 3800	6.12	1.04	4.05	1.28	2.59	0.81	0.77	0.24	1.38	0.39	1.15	0.42
3800 to 3900	6.12	1.05	4.04	1.28	2.62	0.82	0.78	0.24	1.36	0.38	1.16	0.43
3900 to 4000	6.10	1.03	4.03	1.28	2.57	0.85	0.80	0.25	1.34	0.39	1.16	0.43
4000 to 4100	6.08	1.03	4.03	1.28	2.84	0.94	0.85	0.25	1.30	0.39	1.16	0.42
4100 to 4200	6.09	1.05	4.02	1.28	2.85	0.91	0.86	0.25	1.29	0.39	1.15	0.42
4200 to 4300	6.05	1.05	4.02	1.27	2.93	0.91	0.78	0.25	1.28	0.40	1.15	0.43
4300 to 4400	6.12	1.04	4.01	1.27	2.90	0.96	0.74	0.26	1.30	0.41	1.16	0.43
4400 to 4500	6.16	1.05	4.00	1.27	2.93	0.94	0.75	0.26	1.31	0.41	1.15	0.43
4500 to 4600	5.99	1.02	4.01	1.27	2.92	0.96	0.78	0.26	1.31	0.41	1.16	0.43
4600 to 4700	6.04	1.04	3.98	1.26	2.84	0.90	0.73	0.25	1.29	0.41	1.15	0.42
4700 to 4800	6.05	1.04	3.98	1.26	2.93	0.94	0.81	0.26	1.32	0.41	1.16	0.43
4800 to 4900	6.01	1.05	3.96	1.25	3.00	0.94	0.78	0.26	1.33	0.41	1.16	0.42
4900 to 5000	6.07	1.04	3.98	1.26	2.78	0.87	0.76	0.25	1.33	0.41	1.15	0.42
5000 to 5100	6.10	1.05	3.97	1.25	2.68	0.85	0.79	0.26	1.32	0.42	1.15	0.42
5100 to 5200	6.10	1.05	3.95	1.25	2.71	0.86	0.77	0.25	1.29	0.41	1.14	0.42
5200 to 5300	6.10	1.04	3.93	1.24	2.71	0.86	0.75	0.25	1.29	0.42	1.14	0.42
5300 to 5400	6.08	1.04	3.93	1.24	2.71	0.86	0.78	0.26	1.29	0.41	1.13	0.42
5400 to 5500	6.06	1.04	3.92	1.24	2.97	0.95	0.82	0.25	1.42	0.42	1.15	0.42
5500 to 5600	5.97	1.03	3.79	1.24	2.56	0.85	0.78	0.25	1.34	0.42	1.13	0.42
5600 to 5700	5.82	0.98	3.90	1.25	2.67	0.86	0.76	0.25	1.33	0.41	1.13	0.42
5700 to 5800	6.14	1.07	4.01	1.27	2.73	0.89	0.84	0.29	1.51	0.48	1.21	0.44
5800 to 5900	6.13	1.05	4.01	1.27	2.62	0.88	0.81	0.25	1.41	0.41	1.16	0.42
5900 to 6000	5.99	1.03	4.01	1.27	2.87	0.96	0.81	0.26	2.32	0.55	1.16	0.44
6000 to 6050	6.00	1.03	3.96	1.30	2.81	0.97	0.84	0.26	2.44	0.57	1.12	0.43
(3) 6050 to 6200	5.66	0.98	3.86	1.22	2.86	0.92	0.84	0.26	2.06	0.51	1.18	0.46
6200 to 6300	5.85	1.02	4.10	1.30	3.05	1.01	0.83	0.26	2.42	0.56	1.18	0.45
6300 to 6400	5.82	1.01	4.08	1.30	2.97	0.98	0.85	0.25	2.49	0.56	1.18	0.45
6400 to 6500	5.83	1.03	4.06	1.29	3.04	0.98	0.90	0.25	2.49	0.56	1.17	0.44
6500 to 6600	5.90	1.02	4.06	1.29	3.02	0.99	0.93	0.25	2.48	0.56	1.17	0.45
6600 to 6700	5.96	1.02	4.06	1.30	2.96	1.01	1.07	0.26	3.85	(10) 1.00	1.16	0.44

(3) eV/ion increased to 216 from 185 (increased J_I, V_I still at 37 V)

(10) New mag amplifier installed at hour 6666.

T1914

Table III-8B. Performance Summary of 10,000 Hr. Test Thruster 701

	Time Period	Main V	Main A	Vap Cath V	Vap Cath A	Vap Neut V	Vap Neut A	Neut Cath V	Neut Cath A	Main Cath V	Main Cath A	Isolators V	Isolators A
	6700 to 6800	5.82	1.00	4.01	1.27	3.10	0.99	1.11	0.26	3.84	1.00	1.10	0.47
	6800 to 6900	5.80	1.00	4.01	1.28	3.06	0.99	1.16	0.27	4.27	1.19	1.07	0.46
	6900 to 7000	5.84	1.01	4.01	1.28	3.16	1.01	1.15	0.27	4.26	1.18	1.07	0.46
	7000 to 7100	5.77	1.00	4.01	1.27	3.20	1.05	1.17	0.27	4.22	1.15	0.93	0.53
	7100 to 7200	5.81	1.00	4.03	1.28	3.09	1.05	1.17	0.27	4.14	1.14	0.92	0.53
	7200 to 7300	5.84	0.99	3.99	1.26	3.20	1.01	1.15	0.26	4.08	1.12	0.91	0.52
(4)	7300 to 7400	5.38	0.92	4.37	1.43	3.30	1.09	1.22	0.28	4.01	1.09	0.89	0.51
	7400 to 7500	5.36	0.93	4.42	1.45	3.12	1.09	1.24	0.28	4.02	1.10	0.88	0.51
(5)	7500 to 7600	5.44	0.94	4.46	1.46	3.37	1.10	1.26	0.29	3.85	0.98	0.91	0.52
	7600 to 7700	5.50	0.95	4.47	1.46	3.27	1.07	1.25	0.28	3.99	1.09	0.89	0.52
	7700 to 7800	5.43	0.94	4.52	1.48	3.18	1.03	1.26	0.29	3.85	1.07	0.89	0.51
	7800 to 7900	5.52	0.95	4.50	1.47	3.22	1.06	1.26	0.29	3.81	1.04	0.89	0.51
	7900 to 8000	5.46	0.93	4.51	1.47	3.24	1.07	1.23	0.29	3.77	1.02	0.89	0.52
	8000 to 8120	5.67	0.97	4.34	1.41	3.20	1.04	1.14	0.28	3.76	1.03	0.83	0.50
(6)	8130 to 8200	5.54	0.95	4.27	1.38	3.28	1.14	1.12	0.27	3.78	1.03	0.84	0.50
	8200 to 8300	5.48	0.94	4.40	1.43	3.31	1.08	1.17	0.27	3.71	0.99	0.85	0.49
(7)	8300 to 8380	5.65	0.96	4.02	1.27	3.36	1.10	1.09	0.26	3.75	1.00	0.84	0.50
	8390 to 8500	5.41	0.92	4.39	1.42	3.32	1.08	1.12	0.27	3.77	1.01	0.82	0.49
	8500 to 8600	5.42	0.92	4.38	1.42	3.28	1.07	1.14	0.27	3.77	1.01	0.83	0.49
	8600 to 8700	5.45	0.93	4.38	1.42	3.34	1.05	1.12	0.26	3.79	1.00	0.83	0.49
	8700 to 8800	5.49	0.93	4.25	1.37	3.29	1.08	1.10	0.26	3.80	1.03	0.84	0.50
	8800 to 8900	5.47	0.92	4.36	1.41	3.34	1.09	1.15	0.27	3.78	1.01	0.84	0.50
	8900 to 9000	5.49	0.95	4.49	1.30	3.40	1.12	1.10	0.26	3.79	1.02	0.84	0.50
(8)	9000 to 9100	5.56	0.94	3.88	1.23	3.34	1.10	1.19	0.25	3.78	1.01	0.85	0.50
	9100 to 9200	5.46	0.92	3.83	1.15	3.24	1.10	1.09	0.25	3.76	0.99	0.86	0.51
	9200 to 9300	5.34	0.89	3.68	1.15	3.14	1.05	1.11	0.24	3.81	0.99	0.86	0.51
(9)	9300 to 9400	5.22	0.88	4.27	1.39	3.51	1.16	1.15	0.25	3.62	0.97	0.83	0.50
	9400 to 9500	5.23	0.88	4.28	1.39	3.77	1.17	1.16	0.26	3.64	0.97	0.83	0.50
	9500 to 9600	5.21	0.88	4.26	1.39	3.76	1.13	1.21	0.25	3.70	0.98	0.85	0.50
	9600 to 9700	5.21	0.88	4.27	1.39	3.80	1.15	1.22	0.26	3.69	0.98	0.85	0.50
	9700 to 9800	5.20	0.89	4.27	1.39	3.72	1.16	1.24	0.25	3.66	0.99	0.84	0.50
	9800 to 9900	5.22	0.89	4.27	1.39	3.71	1.13	1.22	0.26	3.69	0.99	0.84	0.50
	9900 to 10,000	5.22	0.88	4.26	1.39	3.75	1.13	1.24	0.26	3.67	1.01	0.83	0.50

(4) eV/ion increased to 278 (increased J_I)

(5) eV/ion decreased to 240

(6) eV/ion increased to 259 (J_I increased to prevent "low mode")

(7) eV/ion increased to 278 (J_I increased to prevent "low mode")

(8) eV/ion increased to 296 (J_I increased to prevent low mode)

(9) eV/ion set at 370

T1914

isolators, and throughout the test neither isolator showed any measurable leakage current.

The discharge chamber erosion, vacuum chamber problems and test console repairs described below made some thruster restarts necessary during the more than one year the test continued. Although not planned, these thruster restarts provided data on the reliability of the plasma sprayed heaters which were substituted for the original sheathed heaters on the main cathode and neutralizer cathode. The cathode heaters are used only when starting the thruster; during normal operation self heating maintains the cathodes at the temperature necessary for electron emission. All thruster restarts were uneventful and made with the same heater power supply settings as used for the initial thruster turn on. The longest thruster off time was for 70 hours at test hour 8036 when a cryoshroud LN_2 leak made it necessary to turn the discharge off.

Final evaluation of the third modification, compensated dished electrodes in place of the original flat optics with center support, was made when the test was concluded and the optics were available for close inspection. However, the performance of the thruster (i.e., low accel drain current, and low arc rate), and the appearance of the optics when viewed in situ through a questar telescope indicated that this modification had also been successful. (Localized erosion due to the flakes described below was visible on the accel electrode). This conclusion was confirmed during the post-test analysis of the optics.

A thruster problem was encountered immediately after test initiation. It was found that liquid mercury had penetrated both the main and cathode vaporizers. The vaporizers were baked out in situ. The vaporizers then held back liquid mercury and their performance was normal for the remainder of the test. Two thruster problems were identified during the course of the test. These problems were: (1) a variation in the neutralizer operating characteristics, and (2) discharge chamber erosion. The first of these problems necessitated a system adjustment at test hour 3310; the neutralizer keeper voltage setpoint was raised and the neutralizer keeper current was increased to 1.5 A from 1.3 A. These changes were made to compensate for a shift in the

neutralizer operating characteristics. One of the three system control loops implemented in the test console adjusts the neutralizer vaporizer flowrate to maintain the neutralizer keeper voltage at a selected value. At this point in the test the neutralizer mercury flowrate increased above the desired maximum level of 50 mA equivalent flow (0.375 gms/hour). This increase in flowrate indicated that the keeper voltage was trying to rise but was being constrained by the vaporizer control loop. A mapping of the neutralizer was performed by measuring the keeper voltage range and neutralizer vaporizer temperature range over which the control loop would control as the keeper current was varied. The neutralizer control range is bounded at one extreme by the neutralizer "decoupling"; i.e., the electron emission decreases to the point where the beam is insufficiently neutralized to maintain an acceptable voltage to ground. The other boundary of the neutralizer control range is identified by vaporizer "runaway" when a setpoint below the minimum achievable keeper voltage is selected.

From the neutralizer mapping it was determined that the neutralizer keeper voltage versus vaporizer flowrate characteristic had shifted upward. Also, at 1.3 A keeper current the usable keeper voltage range was only 1.3 V; at 1.5 A the keeper voltage control range was 3.5 V. Therefore, both the keeper voltage and keeper current were adjusted to provide a satisfactory combination of keeper voltage and flowrates (at hour 6048 the keeper current was raised to 1.6 A).

After the initial shift in neutralizer keeper voltage there were several other shifts down to a lower keeper voltage mode and back up to a higher voltage regime. The shift to a lower mode typically followed a thruster restart and may have been caused by the cathode (and insert) heating associated with a thruster restart. The shift to the higher keeper voltage operation happened during thruster operation and was characterized by a gradual increase in flowrate caused by the control loop trying to maintain the selected keeper voltage.

The first evidence of thruster discharge chamber erosion was the observation at test hour 4530 of flakes lying on the upstream side of the screen grid (the thruster was mounted in the vertical vacuum chamber pointing down at a frozen mercury collector).

After the first observation of flakes the number and size of flakes varied as the test continued. Figure III-10 illustrates the quantity and size of flakes in existence at test hours 8600 and 10,000. Some of the erosion of the accelerator electrode apertures caused by the flakes is shown in Fig. III-11. The uneroded apertures adjacent to eroded apertures in Fig. III-11 demonstrate the localized nature of the erosion. The source of flakes on the screen electrode was presumed to be spalling of the material which had been sputter eroded from within the discharge chamber and deposited on other discharge chamber surfaces. Substantiation of this theory was provided when at test hour 5845 a small hole was observed in the center of the cathode baffle. The baffle is cold rolled steel and originally was 0.075 cm thick. The maximum dimension of this hole when first observed was approximately 0.4 cm. Additional erosion of the cathode baffle than appeared at two locations on the edge (see Fig. III-10). The two regions of edge erosion began diametrically opposite each other and appeared to be coincident with the axis of the cathode keeper which is mounted 1.7 cm upstream from the baffle. The condition of the baffle at the conclusion of the 10,000 hour test is shown in Fig. III-10.

Thruster performance did not seem to be affected by the presence of the flakes on the optics until 1450 hours after they were first detected. In fact, the lowest 100 hour average high voltage trip rate of the test occurred after the flakes were first observed. However, at test hour 5980 while operating at 1.75 A beam, a period of high and erratic trip rate did begin. At hour 6050 it was decided to lower the beam current back to the original starting level of 1.5 A. The discharge current was left at 8.75 A, thereby increasing the electron volts per ion from 185 to 214. The high trip rate was attributed to penetration of the 0.06 cm interelectrode gap by the flakes on the screen electrode. This assumption seemed justified when at test hour 6610 a short developed between the accelerator electrode and the screen electrode. The short was eliminated by discharging a 1 μF capacitor, charged to 600 V, between the accelerator electrode and the screen electrode. After clearing the short the beam was re-established and the test continued.

M10333

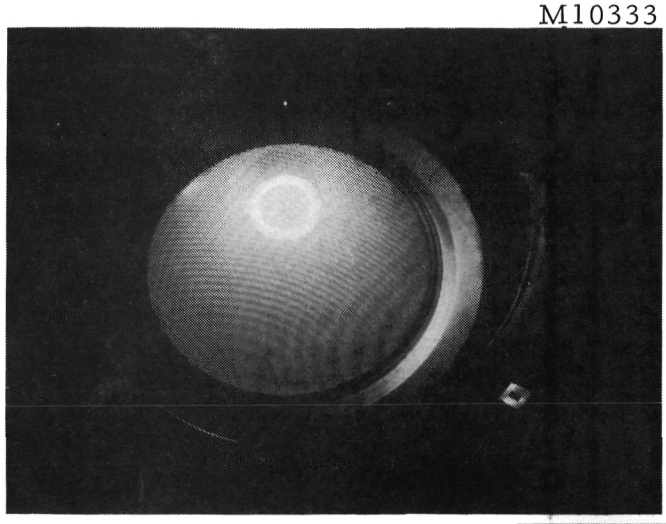

1800 hours

M10882

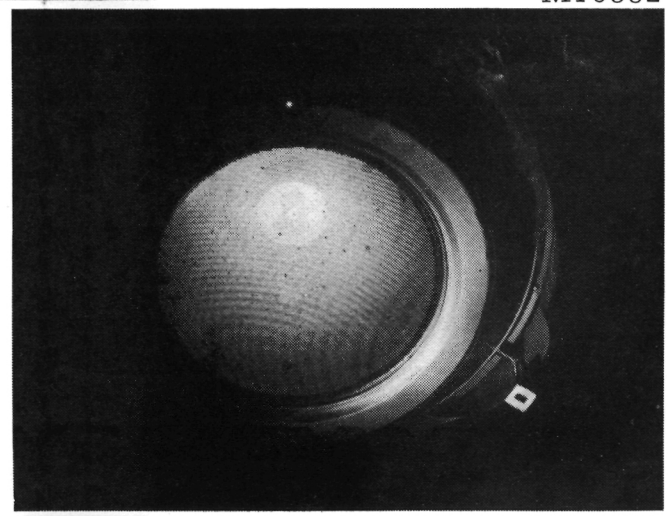

8600 hours

M11009

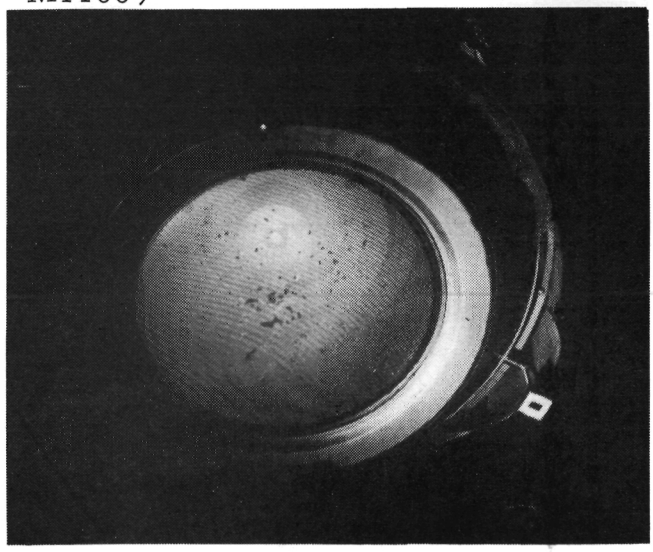

10,000 hours

Figure III-10. Thruster at test hours 1800, 8600, and 10,000 showing flakes on optics and eroded baffle.

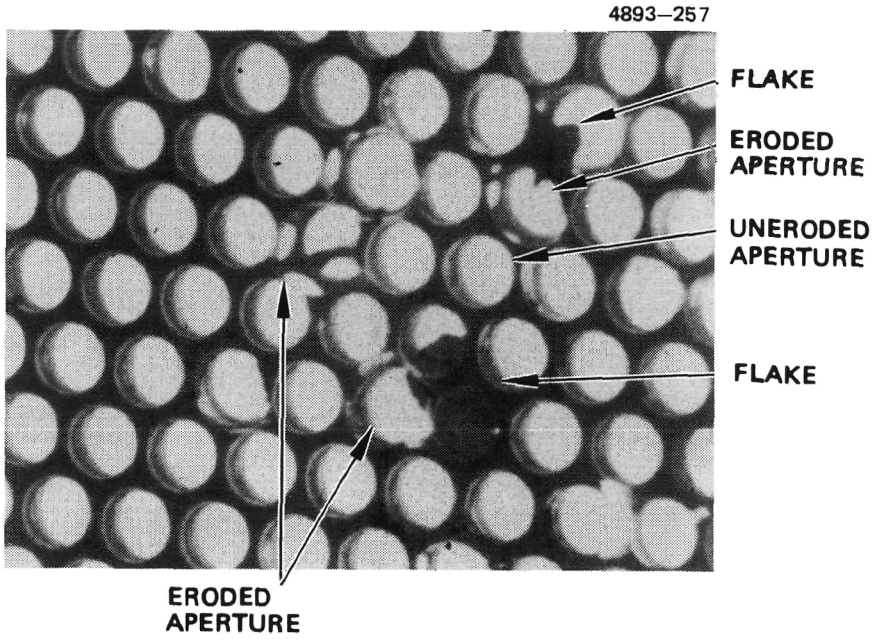

Figure III-11. Photograph of optics showing flakes on screen electrode and localized erosion of accelerator electrode apertures caused by flakes. (Accelerator aperture diameter is 0.15 cm.)

Following the success of the grid clearing experiment the system wiring was modified to add a grid clearing circuit which was used when an excessive trip rate indicates a flake had penetrated the interelectrode gap. The circuit consisted of a 1 μF capacitor which was connected between the shell and system common so that it was charged to the screen voltage (nominally 1100 V). A switch was incorporated so that when operated the charged capacitor was connected between the shell and the accelerator electrode.

Discharge chamber erosion and the consequent creation of flakes is also presumed to have been the cause of a cathode keeper to shell short which developed at test hour 7255. This problem was eliminated by discharging a 1 μF capacitor, charged first to 400 V and then to 600 V, between the cathode keeper and shell. The cathode keeper to shell short occurred only the one time.

The final effect attributed to discharge chamber erosion, in general and specifically to cathode baffle erosion, was a change in discharge operating parameters at 7100 hours. Presumably because of reduced cathode baffle area the discharge began to shift into the "low" mode at beam currents above 1 A and discharge currents below 7.5 A. The "low" discharge mode was characterized by a low cathode flowrate, low discharge voltage, a high main flowrate and a loss of up to 10% in total mass utilization efficiency. Raising the magnetic baffle current did not ensure operation in the normal discharge mode, so the beam was lowered to 1 A. After 9300 hours the beam current was lowered to 0.5 A. Figure III-12 shows the beam current profile for the entire test.

Before removing the thruster at the end of the 10,000-hour test, two brief tests of interest were conducted. The redundant neutralizer was operated and a cold restart of the thruster was made. Neutralizer S/N 415 had not been operated during the more than 14 months the thruster had been in the endurance test vacuum chamber. The last time it had been operated was during the thruster checkout at HRL prior to the endurance test. When the thruster was shut down at the conclusion of the 10,000-hour test, the system wiring was switched so that the appropriate test console supplies were connected to neutralizer 415. Starting power was applied to the tip heater, vaporizer and keeper. The neutralizer ignited without difficulty and control of the keeper voltage was normal.

Power was left off the thruster for 5.7 hours until all three vaporizer thermocouplers read below $0^{o}C$. The automatic startup sequence of the test console was then used to restart the thruster. Startup through discharge ignition was normal. When the high voltages were applied, the flakes lying on the optics caused 42 high voltage recycles to occur before the beam was established.

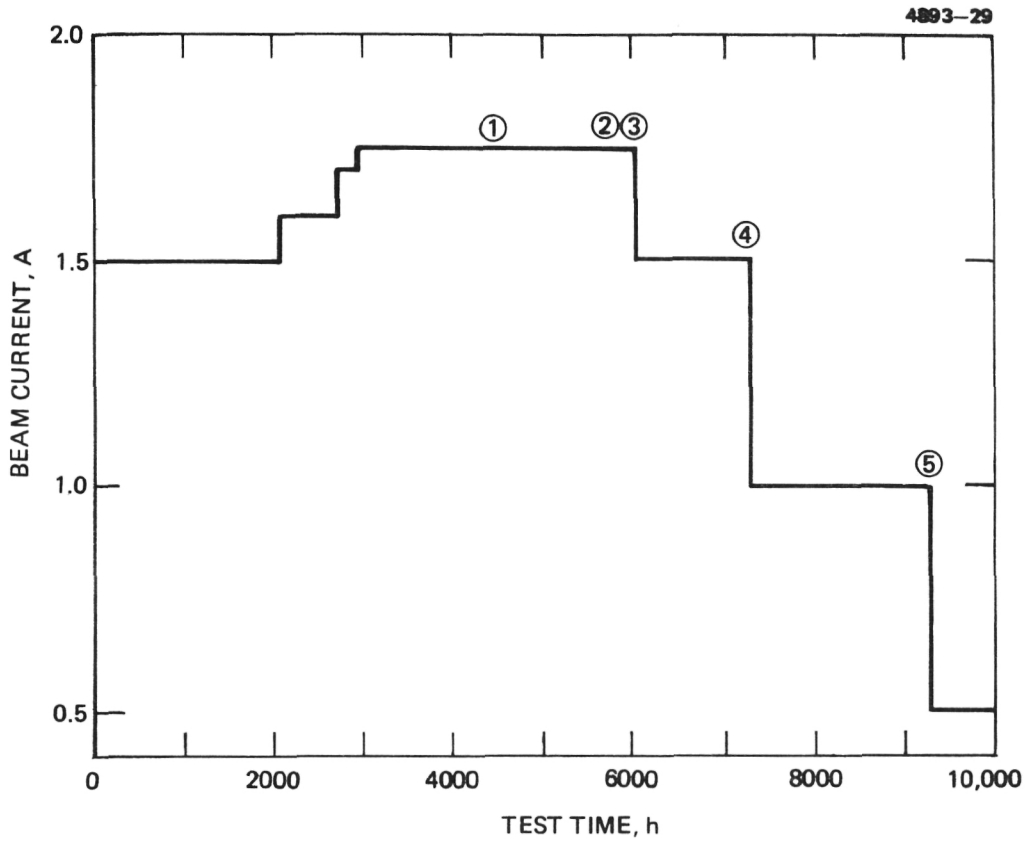

1 FLAKES ON OPTICS AT HOUR 4530

2 HOLE IN BAFFLE AT HOUR 5845

3 HIGH TRIP RATE DUE TO FLAKES

4 LOW DISCHARGE VOLTAGE MODE DUE TO ERODED BAFFLE

5 HIGH TRIP RATE DUE TO FLAKES AND ERODED BAFFLE

Figure III-12. Beam current time history profile for 10,000 hour test.

b. Test Console Performance – The portion of the test console of most interest in terms of performance and reliability is the transistorized power processor which is the predecessor to the thermal vacuum breadboard (TVBB) system developed under Contract NAS 3-17223. Operation of the power processor unit (PPU) was relatively trouble free. It should be mentioned that this test console had accumulated several thousands of operating hours during the tests which preceded this endurance test. Only two repairs were made to the power supplies during this test. At hour 4668 it was noted on the data printout that the screen voltage was 890 V instead of 1100 V. A check of the screen supply revealed that the 250 V line fuse was open in two of the 8 inverter modules. Replacing the fuses restored the supply to normal operation. It is possible that one of the fuses may have been open prior to observing the low voltage since the screen supply regulator could compensate for the loss of one module. The second power processor failure was a magnetic amplifier in the cathode heater supply which had to be replaced at hour 6667. It is significant that none of the inverter transistors failed during normal operation even though the PPU was subjected to thousands of high voltage trips and recycle sequences. (A pair of transistors was lost due to human error while troubleshooting the failed cathode heater magnetic amplifier in the middle of the night.)

The integrated circuits in the test console controller and data system were not as immune to the adverse transient environment generated by an ion thruster high voltage arc as the components in the PPU. On several occasions integrated circuits had to be replaced. When the combination of flakes on the optics and high chamber pressure described below caused numerous high voltage trips, some of the unessential thruster alarms were disabled to eliminate false alarms. The test console controller contains significantly more logic circuitry than the TVBB in order to provide the functions of automatic startup, automatic shutdown, and alarm generation.

c. Vacuum Test System Performance – The basic performance of the vacuum system was good. The nominal chamber pressure with the thruster beam bombarding the frozen mercury collector was less than 2×10^{-6} Torr at all beam current levels. The difficulties experienced with the vacuum system can be divided into two categories: problems with the vacuum system components themselves and interruptions in the utility services to the vacuum system.

The most serious of the vacuum system component problems was a leak that developed in the lower of the two LN_2 cryoshrouds inside the vacuum chamber (see Fig. III-17). This leak caused the chamber pressure to rise to the 10^{-4} Torr scale, making it necessary to shut down the thruster for 70 hours at the 8036th hour. The external piping of the LN_2 system was rerouted to bypass the leaking cryoshroud. With the defective cryoshroud isolated and evacuated the chamber pressure returned to less than 2×10^{-6} Torr and the test was resumed. The only other problems with vacuum system components were two incidents of burned out wires to one of the two 32 in. diffusion pumps and an intermittent flow switch in the diffusion pump cooling water line. None of these latter problems caused more than a brief interruption in system operation.

As might be expected in a test lasting more than a year, several unanticipated events occurred which caused interruption in system utilities. There were two building circuit breaker failures; a transfer to an emergency generator and back to electric company power when the incoming power lines required preventive maintenance and interruptions in the building cooling water supply due to a leak and also when a new annex was added to the Space Simulation Laboratory. Although none of these problems seemed beneficial at the time, the interruptions they caused did provide opportunities to demonstrate the excellent restart capability of the thruster and the value of the automatic startup sequence built into the test console controller.

d. Feed System Performance – The laboratory feed system built for this program performed faultlessly throughout all of the tests which were conducted. The only attention required was periodic filling of the reservoirs with mercury during the test, cleaning of the reservoirs between tests, and calibration of the load cells.

Post Test Analysis – At the conclusion of the 10,000-hour endurance test, a thorough post test examination and analysis of thruster 701 was performed. The full details of that analysis are presented in Appendix A and only the significant findings are summarized in this section.

Analysis of thruster SN 701 emphasized careful and nondestructive disassembly of the thruster to preserve all possible observable characteristics. The analysis began with an extensive visual inspection and photographic documentation of the thruster to identify both the damaged and undamaged components. This type of inspection and documentation continued while carefully removing the thruster outer coverings, the entire upstream boundary with all its subassemblies in place, and finally the removal and disassembly of each subassembly.

Most of the thruster components showed little or no evidence of the long test duration. These undamaged components included the main and cathode propellant isolator-vaporizer assemblies, all structural elements, main standoff insulator and most of the wiring. Components which had been damaged extensively were the accelerator grid (from direct impingement by defocussed ions due to flakes on screen grid), the cathode pole piece assembly (includes baffle and baffle support), two of six anode standoff insulators, and the keeper cover of the neutralizer which was operated throughout the test. Components which showed wear but still had considerable useful lifetime included the main and neutralizer cathodes (slight orifice wear), accelerator grid (where not damaged by interception), screen grid (upstream side eroded), thruster anode, and both cathode and neutralizer keepers.

Erosion of the baffle and cathode pole piece by ion sputtering were concluded to be the major problem areas. All major damage could be related to either the removal or deposition of material which results from this process. Precise assessment of erosion sites and erosion rates was not possible because of the almost complete destruction of the baffle, which exposed the cathode and baffle support members to high energy discharge ions. Definite erosion sites included the baffle, the cathode pole piece (downstream of the plane of the cathode) and probably the baffle support structure, to some extent. Deposition sites included the anode, all thruster boundaries in the plane of or upstream of the cathode and the cathode keeper. Discharge chamber surfaces which were not obviously eroded or coated included the downstream surface of the propellant distributor and the screen pole piece.

A number of dimensional and weight measurements were made for comparison with the pre-test measurements. Some significant findings included the following:

- There was no significant enlargement of screen or accel grid apertures in areas which were not damaged by beamlet defocussing (from flakes masking parts of the apertures).
- Cathode orifice dimensions were not significantly changed ($\sim$0.001).
- Cathode keeper deposits increased the keeper weight by $\sim$10%.
- Edges of cathode pole and remaining baffle had been thinned to knife edge.
- Cathode heaters on both main and neutralizer cathodes showed cracking of flame sprayed insulation but none of the insulating coating had been lost.
- Main cathode and neutralizer inserts could be removed and unrolled without destruction, and appeared to still have coating over most of the insert surface.
- There was no evidence of excess charge exchange erosion associated with the neutralizer.
- Charge exchange ion erosion of the accelerator grid is a secondary factor in life limitation.

Page intentionally left blank

Page intentionally left blank

IV. CONCLUSIONS

The 10,000 hour test of thruster SN 701 has served to identify either the major wearout mechanism or confirm the long lifetime capability of thruster components and subassemblies. On the basis of the results of this test, the following components or subassemblies could provide operating lifetime in excess of 10,000 hours without any design changes.

- All structural components
- Main and cathode isolator-vaporizer assemblies (C-IV, MIV)
- Discharge and Neutralizer cathodes
- All shadow-shielded insulators
- Ion optics assembly.

The major wear mechanism has been identified as erosion of discharge chamber components by ion sputtering. This process also causes secondary damage because the deposits of back-sputtered material either short out insulators or spall and form large flakes of conducting material. To provide longer thruster lifetime, a number of design modifications are recommended as follows.

A. Insulators

All insulators should be better shadow shielded to prevent deposition of back-sputtered material. Wiring should be routed and/or protected to prevent deposition on wiring insulation that could form current leakage paths. Specific instances of insulators requiring attention are:

- Anode insulators
- Keeper insulators
- Neutralizer support insulators
- Neutralizer isolator insulator
- Neutralizer wiring insulation.

Re-entrant shielding should be used where space permits and/or isolation requirements demand minimum leakage current. It is thought that damage to insulators, such as observed in the case of the anode insulators, will be eliminated by protection from conductive coatings.

B. Eroded Components

Three types of erosion were noted in this test; erosion by low energy discharge chamber ions, erosion by high energy beam ions, and erosion by high energy charge exchange ions. Erosion of discharge chamber components by low energy ions is a strong function of the ratio of multiply charged ions to singly charged ions. Therefore, any modification which reduces the doubly charged ion density or the discharge voltage is recommended as the preferred method of eliminating component erosion of this type. Care must be exercised in that a substantial reduction of true propellant efficiency does not accompany any design modification that is incorporated to reduce double ionization, thereby causing more severe charge exchange erosion of the accelerator grid. In lieu of eliminating double ionization in the discharge chamber, some of the vulnerable surfaces could be protected with lower sputtering yield materials. If possible, the design of components observed to be heavily eroded ought to be modified so that dimensional changes caused by the expected erosion will not critically affect thruster operational characteristics. Components that could be easily protected are the cathode pole piece, the baffle, and the baffle support. The screen grid electrode of the ion optics assembly is also eroded by discharge ions but cannot be protected without appreciable loss of performance. Therefore, extension of its lifetime must rely on reduction in double charged ion density and/or energy.

Direct erosion by high energy beam ions occurred on the accel electrode and the neutralizer cover. Erosion of the accel electrode in this test was a consequence of beam deflection that is caused by flakes of spalled, backsputtered material. This phenomena may be reduced

by reducing discharge chamber sputtering, but can be eliminated only by controlling the formation of metallic flakes. Flake control has been demonstrated by NASA LeRC with 5 cm and 8 cm thrusters through use of either grit blasting the surfaces where flakes form, or by use of wire mesh to cover these surfaces. Surfaces where such treatment has been shown to be necessary by the results of this test are:

- The entire upstream discharge chamber boundary
- The discharge anode
- The keeper electrode and insulator shields.

The neutralizer cover intercepts a small but significant number of ions that emerge from the outermost apertures of the ion optics assembly. The preferred modification would be one that eliminates these trajectories, however the erosion rate is sufficiently low that an adequate thickness of material can be provided to accept this direct interception and consequent erosion and still prevent penetration of the neutralizer housing. The choice of material for this erosion site should take into consideration the possible sites where the sputtered material will be deposited.

Finally, erosion of the accelerator electrode by charge exchange ions remains a concern, but is not the major life limiting factor as determined here. The main recommendations at this point are:

- Reduce accelerator operating voltage, if possible
- Disallow modifications to the thruster design that appreciably reduce effective propellant utilization.

Charge exchange erosion as measured in a vacuum chamber is probably more severe than would be experienced in the vacuum of space and until other wear mechanisms have been reduced, it is of secondary importance to discharge chamber (screen electrode) erosion.

The recommendations for design modifications mentioned above are based on the observations and their interpretations as described in Appendix A. Modifications to other assemblies have been implemented

to alleviate fabrication, quality control, operational control or structural problems. Design modifications to provide extended thruster lifetime have already been incorporated into a 900 series thruster under Contract NAS 3-17803. A second endurance test, with special documentation of these modifications, is being performed.

APPENDIX A

POST TEST ANALYSIS OF 10,000 HOURS ENDURANCE TEST THRUSTER

I. INTRODUCTION

This appendix contains a complete description of the post test examination of thruster serial number 701 (SN 701) after 10,000 hours of testing. Disassembly and documentation procedures are described, and all data and observations considered noteworthy are included. Wherever possible, an attempt has been made to interpret the observed data.

To establish a common basis for discussing the post-test condition of thruster SN 701, the thruster design, its initial assembly, and the test conditions are described as follows. Thruster SN 701 is the first thruster built to meet the "Engineering Model" (EM) thruster design specifications on structural strength, overall efficiency, and total weight. Some features of the EMT design have since been changed to correct structural deficiencies determined by vibration tests or to facilitate fabrication but these modifications have not significantly changed the operating characteristics of the thruster and S/N 701 can be considered representative of the 800 series thruster design (Ref. 2). As the first thruster module built to the EMT design specifications, S/N 701 was not designated as the endurance test thruster until after construction and initial testing had been successfully completed. Consequently, documentation of the detailed history of the thruster components is not as complete as one would desire to perform a detailed quantitative analysis of the effects of long term testing. Future tests should benefit from improvement in the documentation and assembly procedures that have recently been established for EMT construction. The conduct of the test has been described in Section III of this report and will only be outlined briefly here. Initially, the thruster was operated at 1.5 A beam current because contractual agreements had originally specified this value and the peripheral test equipment had to be modified to permit

operation at the nominal EMT level of 2 A. After 2000 hours of operation at 1.5 A beam current, the beam current was increased to 1.75 A in several steps. After about 4500 hours of testing "flakes" were noted on the ion acceleration optics screen grid. These "flakes" are formed by the deposition and spalling of material that is sputtered from cathode potential surfaces by ion bombardment. This sputter erosion and its consequences have been identified as the major wearout mechanism of the 30 cm thruster used in this 10,000 hour test. The consequences of these metallic flakes resting on the screen grid is twofold. The first may be considered specific to the mounting of the thruster in the endurance test such that the beam is directed vertically downward. Consequently, the flakes which spall from anode or other surfaces fall onto the screen grid under the force of gravity and either remain there or fall through the screen apertures. The larger flakes block, or partially block, the screen grid apertures and distort the ion trajectories through these apertures. This results in direct interception of high energy ions on the accelerator grid and machines away relatively large segments of this grid in short periods of time. The accelerator grid sustained considerable damage from this "flake initiated" mechanism. The second consequence of "flake" formation could occur equally well in a gravity free environment. If a flake is small enough to pass through a grid aperture, it can short circuit the ion optics grids. This may result in a brief arc as the flake is vaporized by the power available from the power processor but at least produces a high voltage overload and recycle sequence. If the flake is substantial enough, a more or less permanent short circuit results, and thruster operation can only be restored by using extraordinary means to burn out the flake. A number of these latter types of short circuits between the screen and accelerator grid were removed during the course of the 10,000 hour test by capacitive discharge. It is not known whether any of the observed thruster wear can be attributed to the repeated overload recycling or short removal associated with the atypical operation (due to the flakes) of the ion optics electrodes.

After about 5800 hours of testing, the major consequence of sputtering erosion was evidenced by the appearance of a hole in the baffle (which isolates the cathode plasma from the main discharge plasma). From this point in time until the end of the test, the isolation of the cathode and discharge plasma decreased as the baffle continued to decrease in size. A consequence of this modification to the baffle was a more or less continuous change in thruster control characteristics which had to be compensated by varying the controlled parameters. Eventually this resulted in reducing beam current and operating at increased discharge to beam current ratio. Thus, the 10,000 hours of testing was logged at beam currents that varied between 1.75 A and 0.5 A with a weighted average of 1.4 A. The effect of this variation in beam current and/or discharge conditions to compensate for baffle erosion also represents an unknown factor in considering the wear on thruster SN 701 described in this report.

After completion of the test, considerable care was taken in removing the thruster from the test facility and documenting the condition of the thruster. The documentation procedure followed a sequence of visual inspection, photographing, disassembly and measurement for each major assembly, subassembly, and finally component by component with some components being dissected and more carefully analyzed. The details of this post-test analysis procedure are described in the next section. The discussion of results is then presented and organized according to the major sub-assemblies and describes the notable observations at all levels of complexity used in the analysis.

Page intentionally left blank

Page intentionally left blank

II. POST TEST EXAMINATION AND DOCUMENTATION PROCEDURES

After removal from the test facility, thruster SN 701 was carefully inspected and photographed on the test stand. Flake samples were collected from a number of locations and electrical measurements were made at the vacuum interface terminals. The thruster was then removed from its test facility mounting and carefully inspected, photographed, disassembled and measured on a step by step basis. One goal of this procedure was to gain as much information as possible with minimum alteration of the thruster condition. Initially, the only disassembly performed was the removal of the outer casings, the neutralizer assemblies and the ion optics assembly. In this phase of the thruster examination the following measurements and documentations were performed:

- Electrical resistance measurements at thruster terminals
- Close-up photographs of the interior and exterior discharge chamber assembly
- Mapping of the magnetic field strength distribution
- Dimensional checks of critical discharge chamber, ion optics assembly and neutralizer assembly parameters
- Collection of additional flake and deposition samples
- Close-up photographs of neutralizer and ion optics subassemblies.

During these measurements, the thruster discharge chamber assembly was mounted through one gimbal mount, on a portable stand that facilitated both visual inspection, photography and handling without disturbing or altering the condition of the thruster. Further disassembly and documentation was delayed until all photographs were developed and examined to permit retakes if necessary.

The next phase of the examination involved the complete mechanical disassembly of the thruster and subassemblies. Before removal of any subassembly or component, visual observations were noted and photographs were taken where indicated. Notes were made during the disassembly and the separated subassemblies were photographed, weighed or otherwise measured. The order of disassembly was as follows:

- The entire upstream boundary (backplate) including the structural braces, isolators and cathode pole piece assemblies was removed from the discharge chamber body.
- Damaged anode insulators were examined and removed.
- All components and subassemblies were removed from the upstream boundary (backplate). This includes the propellant distribution plenum, the main and cathode isolators, the support structures and the cathode pole assembly.
- Subassemblies were disassembled. This includes the neutralizers, the ion optics electrodes and mounting, the cathode pole assembly and the discharge chamber. During the disassembly, special attention was paid to component orientation, erosion of, or depositions on surfaces and the presence of discoloration or other markings.

Having completed the mechanical disassembly, the next phase of the examination called for dissecting selected components. This action was again delayed until the results of the disassembly documentation were assured. Selection of components to be sectioned for further analysis was restricted to those components that showed evidence of erosion or wear which could not be adequately measured in other ways. (Dental molding techniques were attempted but proved to be unsuccessful because the molding would not release from the eroded surfaces.) Such components included the baffle support mount, the thruster and neutralizer cathodes, the accelerator and screen grids, anode insulators, and the main keeper electrode. Sectioned parts were examined by microscope and microphotographs and in some cases by scanning electron

microscope. The latter procedure provides a detailed analysis of the materials present as well as their distributions in deposited layers.

The most meaningful procedure available in this post test examination of thruster S/N 701 was visual examination using microscope and magnified photographs of thruster components. Dimensional and weight measurements rely on comparison with pre-test data if meaningful interpretations are to be offered. Without an "a priori" knowledge of what is expected to occur in an endurance test such as this, the initial documentation of the proper parameters to appropriate accuracy is more a question of chance than careful planning. In describing the results of this test in the sections which follow, an interpretation of thruster wear must be based on certain assumptions (which will be stated), since the preparation for and conduct of the test, although carefully planned, were performed without rigid control over many of the conditions that could appreciably affect interpretation of results.

Page intentionally left blank

Page intentionally left blank

III. POST TEST EXAMINATION OF THRUSTER SN 701 RESULTS AND INTERPRETATIONS

A. Total Thruster Assembly

This section presents the documentation and observations that relate primarily to the complete thruster assembly. Component wear is noted, however the detailed discussion of such wear is deferred to later sections. A photograph of the thruster taken during the final hours of testing is shown as Fig. A-1. On the ion optics assembly can be seen the damage to the accelerator grid and also the "flakes" of material that partially block screen grid holes causing the deflection of the ion trajectories to cause this damage. Erosion of the baffle is also visible and a "severed" portion of the baffle is identified by a circle where it lies on the screen grid. The comparable portion of the opposite side of the baffle has not yet been severed, and is identified by an arrow. The operating neutralizer (SN 701) is seen nearer the top of the figure. In Figs. A-2 and A-3, the thruster is seen as it appeared upon removal from the test facility. The most noteable observances on the thruster exterior are the coatings on the downstream surfaces of the thruster's outer case and unused neutralizer, SN 415 (see Figs. A-2(c) and A-3(a) and (b)), the machining of the outer case of neutralizer SN 701 (operating neutralizer throughout the test (see Fig. A-2(d)), and the machining of the accelerator grid (see Fig. A-3(d)). Samples of this flake material taken from the locations shown in Fig. A-4 were analyzed to yield the elemental composition listed in Table A-1. Note that the flakes from locations I and II are composed predominantly of iron and also have a high cromium content. These deposits are considered to be constituents of stainless steel sputtered by the ion beam from either the collector during preliminary thruster testing at HRL or the cryowall during the endurance test at SSL. Note that the sample from location III, though similarly located to I and II, is composed predominantly of molybdenum. Location III has a reduced view factor for the cryowall, since it is in the shadow of neutralizer SN 415. Because the view factor for the beam target would be essentially equivalent for locations I, II, and III, it is

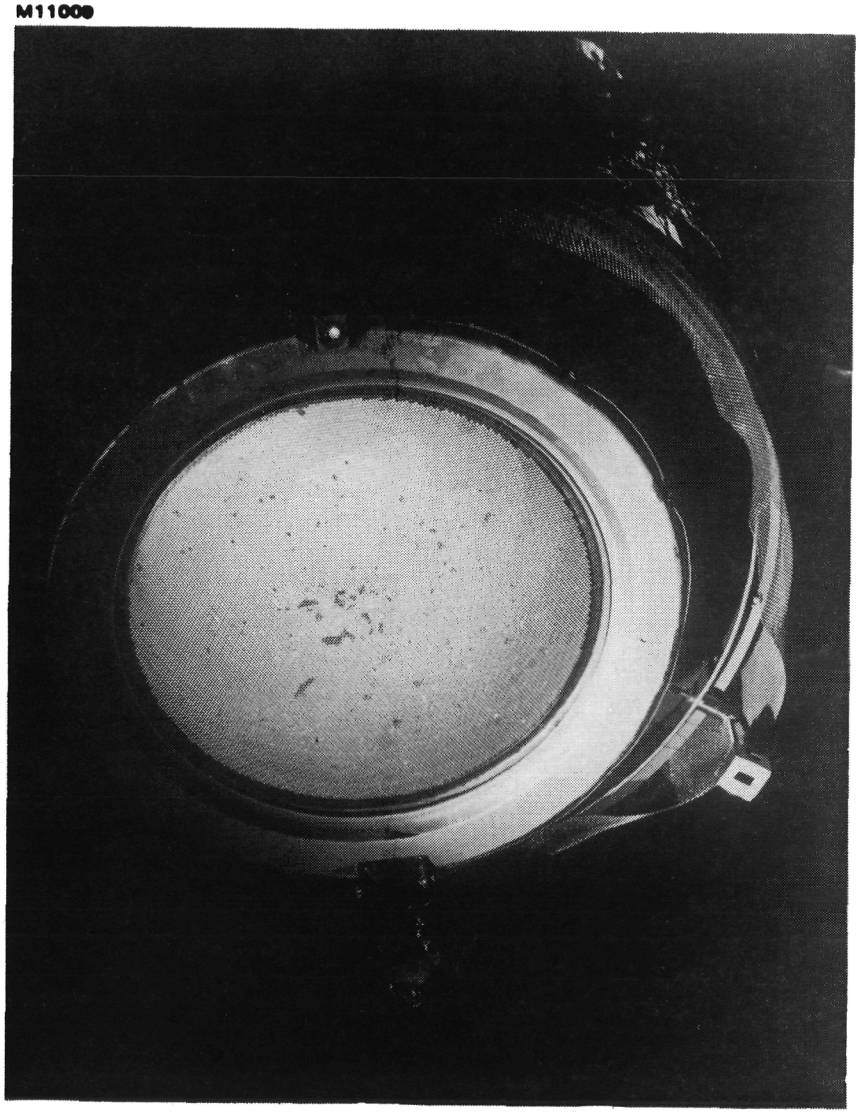

Figure A-1. Thruster during final hours of 10,000 hr. test.

4893–38

(a) THRUSTER SN701 BEING REMOVED FROM ENDURANCE TEST FACILITY

4893–39

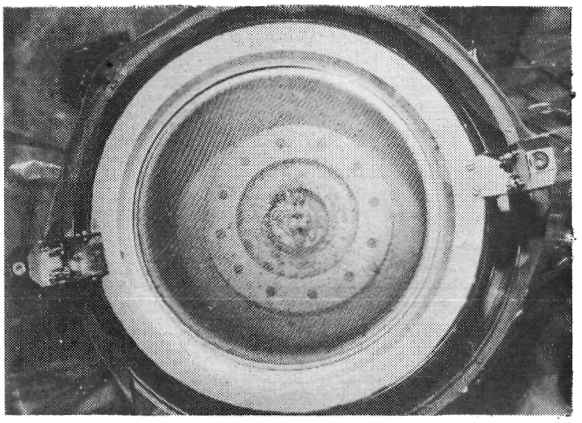

(b) DOWNSTREAM VIEW

4893–40

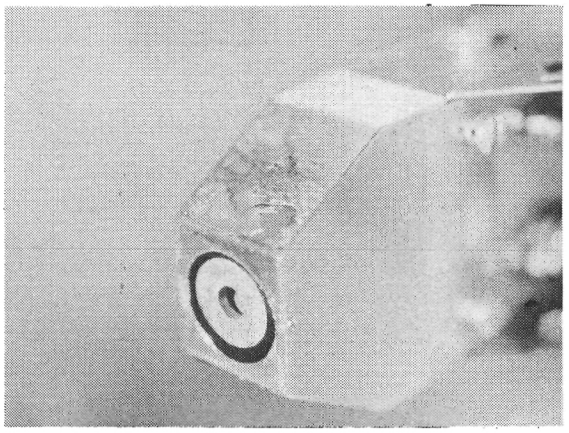

(c) NEUTRALIZER SN415

4893–41

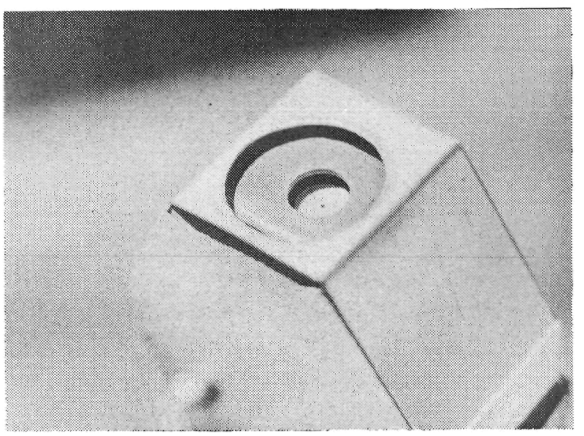

(d) NEUTRALIZER SN701

Figure A-2. a. Thruster SN 701 being removed from endurance test facility.
b. Downstream view.
c. Neutralizer SN 415.
d. Neutralizer SN 701

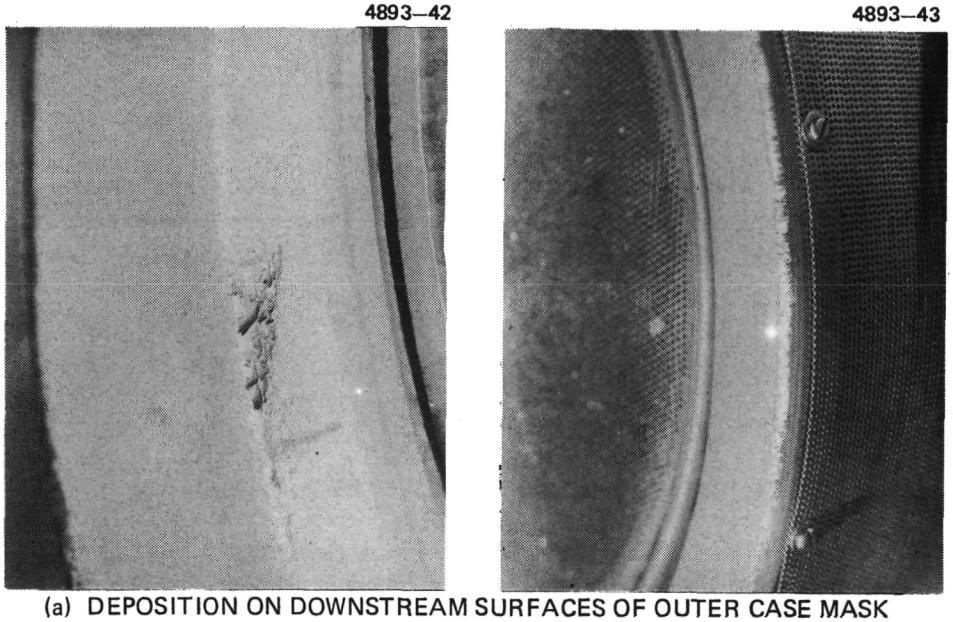

(a) DEPOSITION ON DOWNSTREAM SURFACES OF OUTER CASE MASK

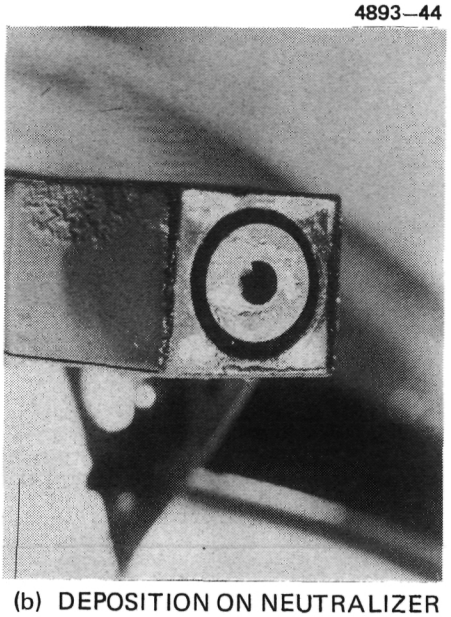

(b) DEPOSITION ON NEUTRALIZER SN 415

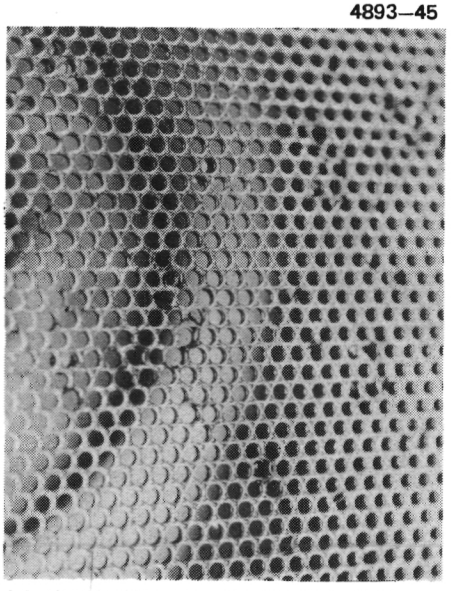

(c) DAMAGE TO ACCELERATOR APERTURES

Figure A-3. a. Deposition on downstream surfaces of outer case mask.
b. Deposition on neutralizer SN 415.
c. Damage to accelerator apertures.

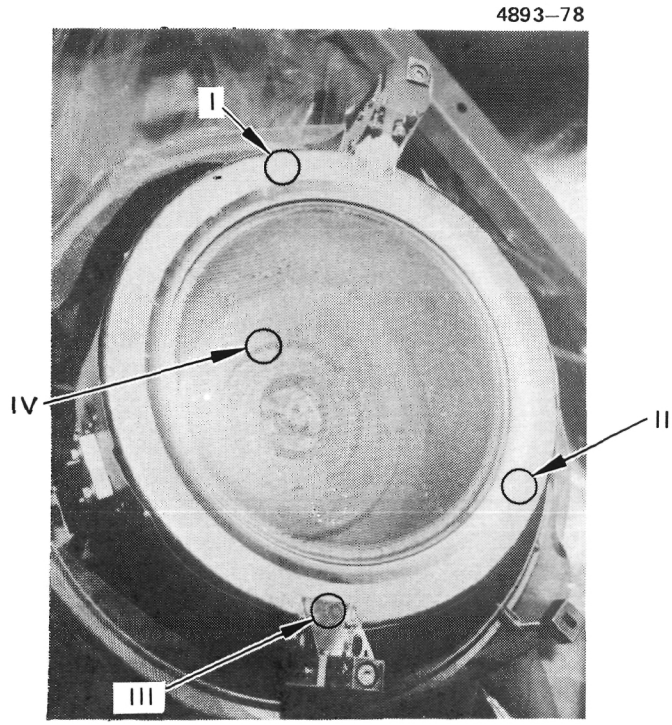

Figure A-4. Location of flake sampler.

Table A-1. Semiquantitative Analysis of Flake Samples

	COMPOSITION			
SAMPLE LOCATION	I	II	III	IV
ELEMENTS				
Fe-	REM	REM	18 %	4.8 %
Cr-	11 %	26 %	5.8	0.14
Ni-	13	12	7.5	0.44
Ti-	12	0.70	4.9	0.21
Mo-	4.3	6.1	REM	REM
Si-	4.3	1.6	4.9	0.040
Mn-	2.8	1.1	0.27	TR < 0.010
Mg-	0.19	0.078	0.080	TR < 0.003
Al-	2.4	0.25	1.3	0.14
Ag-	ND < 0.010	0.0085	0.016	ND < 0.002
Hg-	9.8	0.78	8.4	2.8
Pb-	TR < 0.50	ND < 0.05	ND < 0.50	ND < 0.05
Cu-	0.27	0.22	0.053	0.0051
Co-	TR < 0.10	0.28	ND < 0.10	ND < 0.01
Ca-	0.32	0.092	0.17	ND < 0.002
Sr-	ND < 0.05	ND < 0.005	ND < 0.05	ND < 0.005
Ba-	ND < 5.0	ND < 0.50	ND < 5.0	ND < 0.50
Ta-	ND < 3.0	ND < 0.30	ND < 3.0	ND < 0.30
W-	ND < 4.0	ND < 0.40	ND < 4.0	ND < 0.40
Au-	ND < 0.06	ND < 0.006	ND < 0.06	ND < 0.006
OTHER ELEMENTS	NIL	NIL	NIL	NIL

REM = remainder

concluded that the deposits of stainless steel constituents found on the downstream surfaces of the thruster case are caused primarily by ion beam sputtering of the cryowall. Sample IV was a single flake that was lodged in a grid aperture and is seen to be predominantly molybdenum. The molybdenum found in all these samples is presumed to originate from the electrodes of the ion optics assembly. Three forms of erosion of grid material can be observed; a thinning of the screen grid electrode by discharge chamber ions, machining of the accelerator electrode by direct interception, and charge exchange erosion on the accelerator electrode. No technique has been devised, as yet, to determine how much each of these processes contributes to the deposition. The ion optics electrode wear will be discussed in more detail in a later section.

Measurement of electrical resistance (or insulation) was performed and recorded when the thruster was installed in the endurance test facility (2-21-74), after completion of 10,000 hours of testing (5-14-75) and again after the thruster was removed from its test mount. The resistances were measured with a Leeds & Northrup Model 5305 resistance, bridge (HAC ID No. 37381) which is calibrated against a primary standard. The values measured have been corrected for test lead resistance and are shown in Table A-2. Although some differences can be seen, the percentage of change is small, and in some cases is greater for the two measurements made after the test was completed than for the measurements before and after the test. Consequently, it is concluded that the change in resistance of the thruster heaters during the 10,000 hour test was not significant. Leakage resistance across insulators was measured using a high voltage ohmeter ("Megger" insulation tester, James G. Biddle Co.) that applies 1000 V to the terminals in question. Table A-3 gives values of leakage resistance measured before and after the test. The low value of the insulation between the ion optics electrodes (discharge chamber shell to accel electrode) is attributed to "flakes" between the electrodes. The leakage resistance between the thruster outer case and ground represents conductive coatings on mounting insulators (which could be condensed Mercury) and reflects on test facility design, rather than thruster design.

Table A-2. Resistance Measurements

Heater	Value Before Test	Value After Test		Δ_{21}[a]	Δ_{31}	Δ_{32}
	2-21-74 ① ohms	5-14-75 ② ohms	6-3-75 ③ ohms	%	%	%
Cathode Tip	1.216	1.163	1.209	-4.4	-0.6	4.0
Main Isolator	4.060	4.158	4.162	2.4	2.5	0.1
Cathode Isolator	3.835	3.867	3.877	0.8	1.1	0.3
Main Vaporizer	5.563	5.553	5.570	-0.2	0.1	0.3
Cathode Vaporizer	2.528	2.562	2.559	1.3	1.2	-0.1
Neutralizer (701)[b]						
Tip	1.167	1.122	1.190	-3.9	2.0	6.1
Vaporizer	2.507	2.492	2.682	-0.6	7.0	7.6
Neutralizer (415)[c]						
Tip	0.526	0.490	0.563	-6.9	7.0	14.9
Vaporizer	2.160	2.149	2.178	-0.5	0.8	1.3

a. $\Delta_{\alpha\beta} = (\alpha/\beta - 1) \times 100$

b. Neutralizer SN 701 was operated over entire 10,000 hours

c. Neutralizer SN 415 was not operated during the 10,000 hour test

T1853

Table A-3. Insulation Leakage Measurement

Terminals	Leakage	Resistance
	2-21-75	5-14-75
Discharge Chamber Shell-Accelerator	∞	-20 Ω (erratic)
Discharge Chamber Shell-Outer Cover	∞	∞
Discharge Chamber Shell-Cathode Keeper	∞	∞
Discharge Chamber Shell-Anode	∞	5 kΩ
Discharge Chamber Shell-Main Propellant Line (MIV)	∞	∞
Discharge Chamber Shell-Cathode Propellant Line (C-IV)	∞	∞
Outer Cover - Ground	1000 MΩ	260 MΩ
Accelerator - Ground	∞	∞
Accelerator - Outer Cover	∞	∞
Neutralizer Cathode (SN 701) - Neutralizer Propellant Line (NIV)	2 MΩ	130 MΩ
Outer Cover - Neutralizer Keeper (SN 701)	∞	1 MΩ
Outer Cover - Neutralizer Keeper (SN 415)	∞	1.2 MΩ
Outer Cover - Neutralizer Cathode (SN 701)	250 MΩ	9 MΩ
Neutralizer Keeper - Neutralizer Cathode (SN 701)	∞	1.1 MΩ

T1854

Thruster insulators or wiring which show deterioration are the neutralizer and thruster cathode keeper electrodes, the neutralizer isolator and mounting insulators (SN 701), and the thruster anode. The source of of this leakage will be discussed in later sections. It is noteworthy, that the propellant isolators, the C-IV and the MIV, show no measurable loss of insulation properties (leakage current during operation also remained at a satisfactorily low value throughout the test).

Views of the thruster assembly taken during initial disassembly are shown in Figs. A-5 through A-12. In Fig. A-5, the major wear of the thruster baffle and cathode pole is visible as well as its consequence, the deposition of the sputtered material on the thruster backplate and anode. This wear and its consequences will be discussed in detail in the following sections covering the discharge chamber assembly and the cathode pole/baffle assembly.

Figure A-6 is a side view of the thruster and two observations are noteworthy. First, it can be seen that two of the insulators used to support the outer case have the "shadow shields" removed, exposing the ceramic surfaces. These insulators showed no electrical leakage and the ceramic surfaces are clean and free of any discoloration. Second, on the discharge chamber shell adjacent to the anode terminal seen in the center of the photograph (arrow) a "bright" region can be seen on the metal where the insulator makes contact, surrounded by a darker region. The anode insulator leakage resistance mentioned earlier was a consequence of damage to this and one other anode support insulator. This damage will be discussed in detail in the discharge chamber section with reference made to the coloration noted here. Figure A-7 shows the opposite side of the thruster. The fracture seen in the cover on neutralizer SN 701 is considered a weakness of the prototype cover and support design and a design change has already been incorporated in thruster SN 702A.

M11050 4893–270

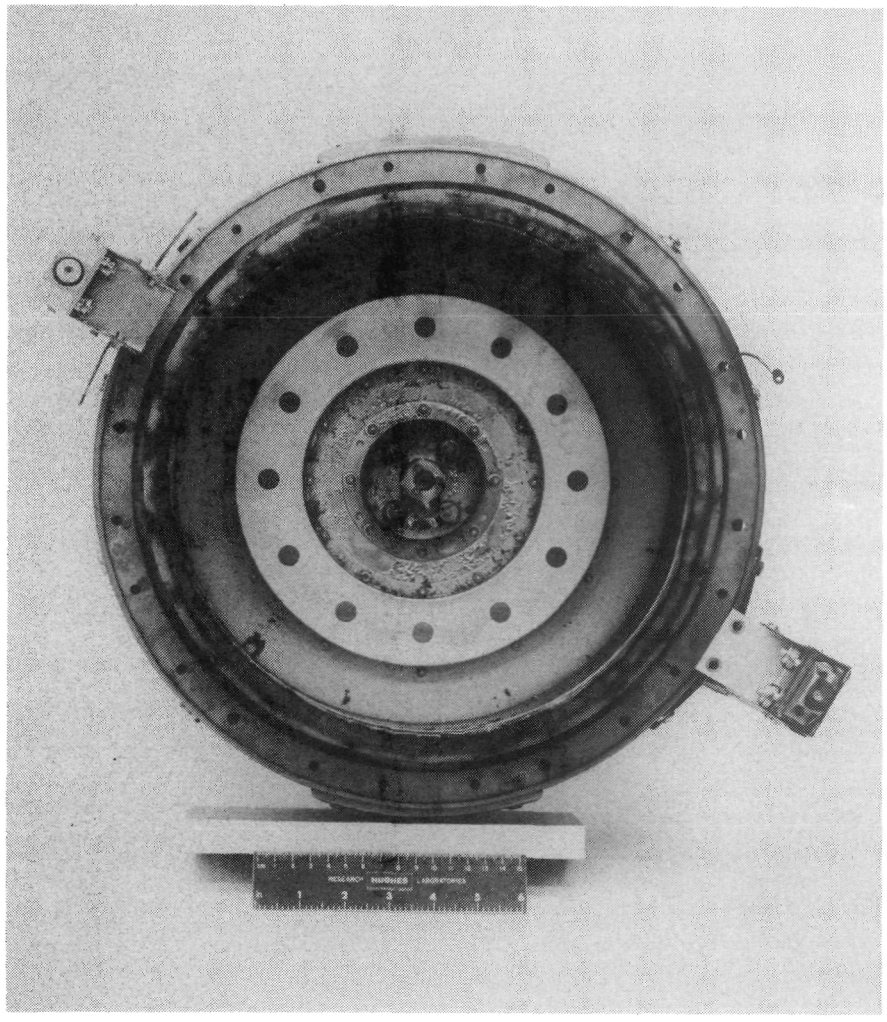

Figure A-5. Thruster 701 - front view with optics removed.

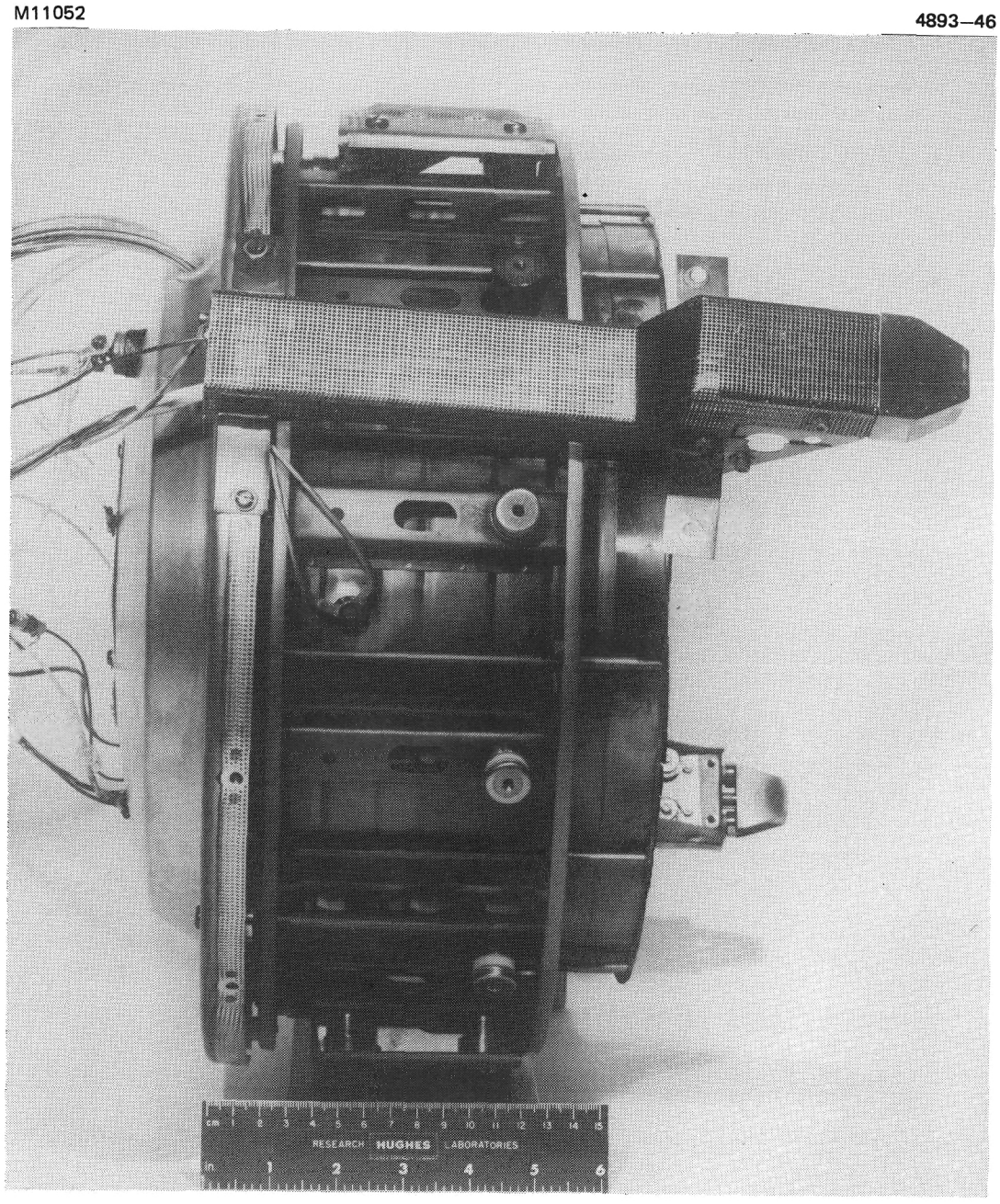

Figure A-6. Thruster 701 - side view with ground screen removed.

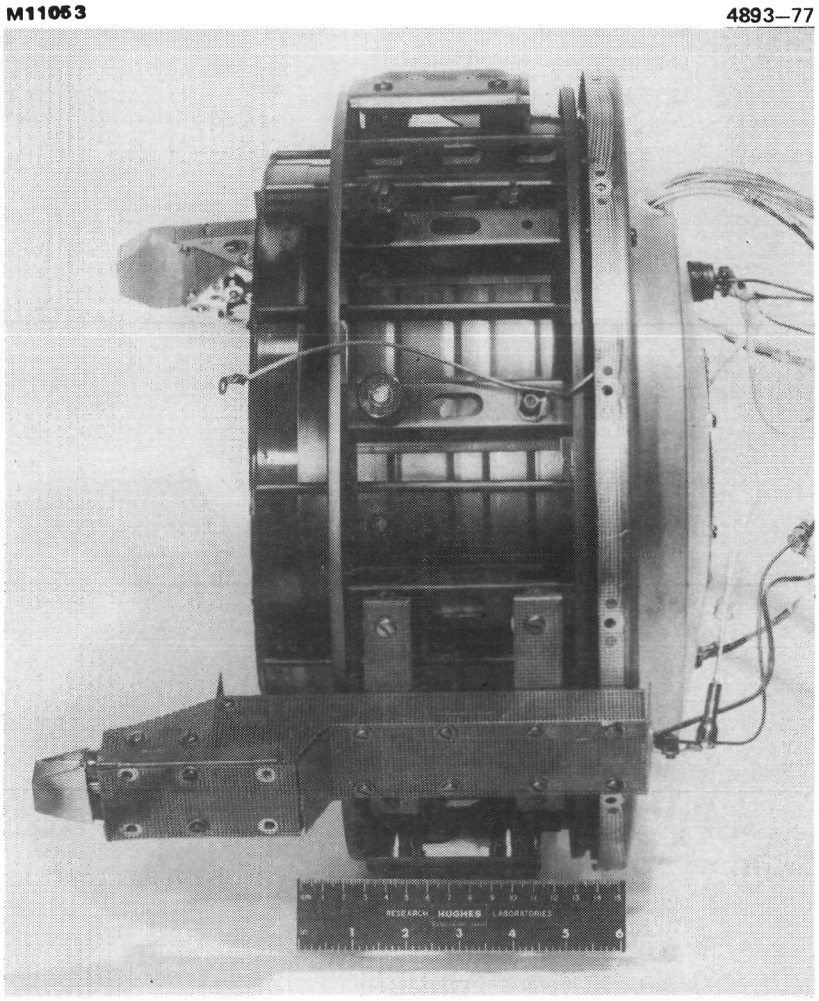

Figure A-7. Thruster 701 - side view with ground screen removed.

M11051

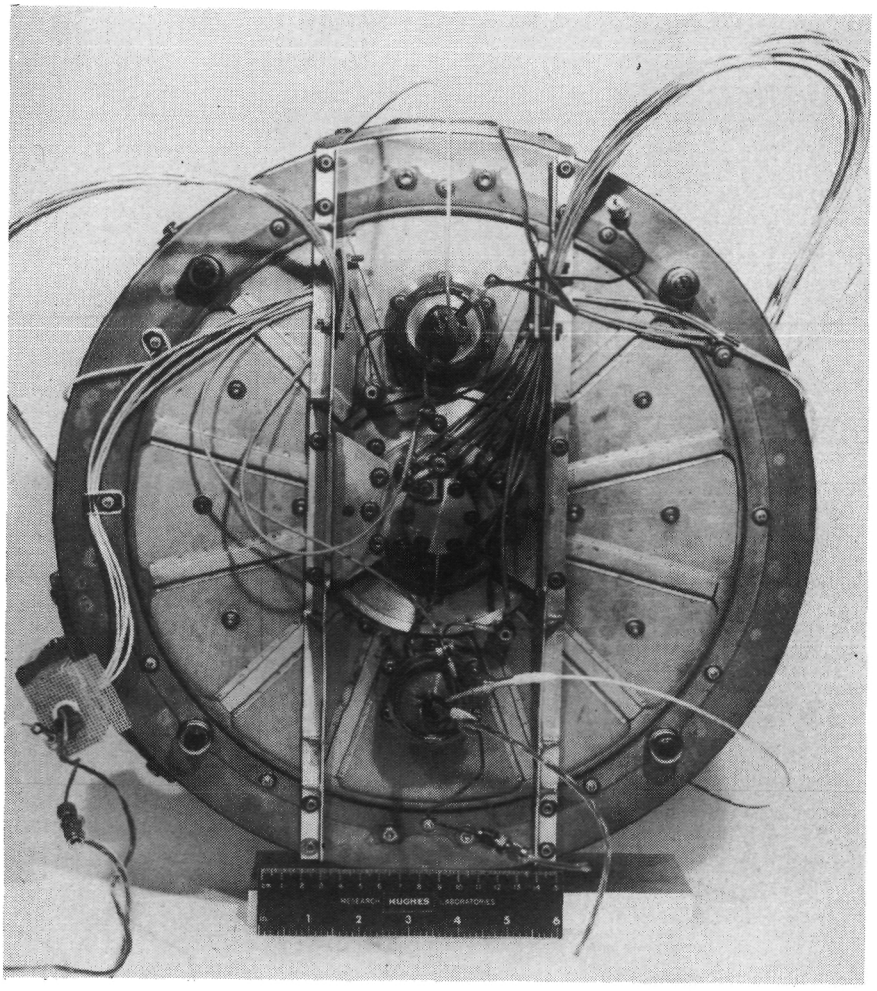

Figure A-9. Thruster 701 - rear view with rear cover removed.

M11054

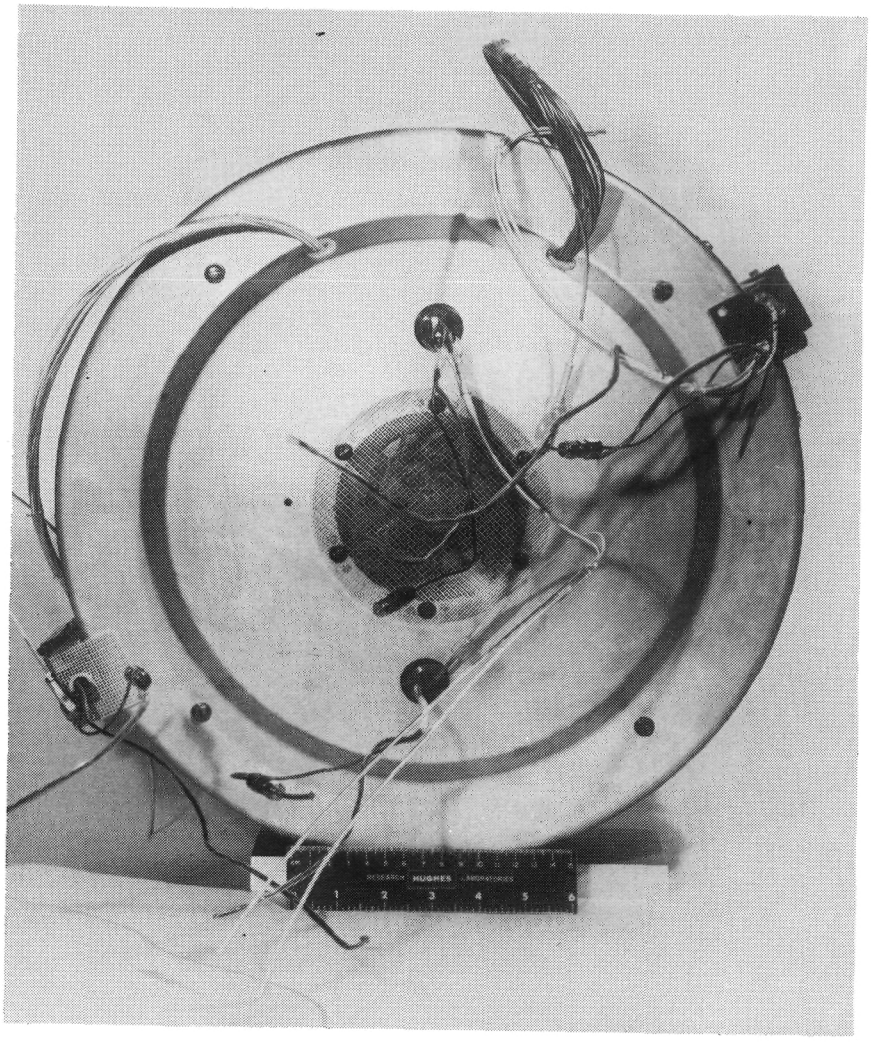

Figure A-8. Thruster 701 - rear view.

M11055 4893–47

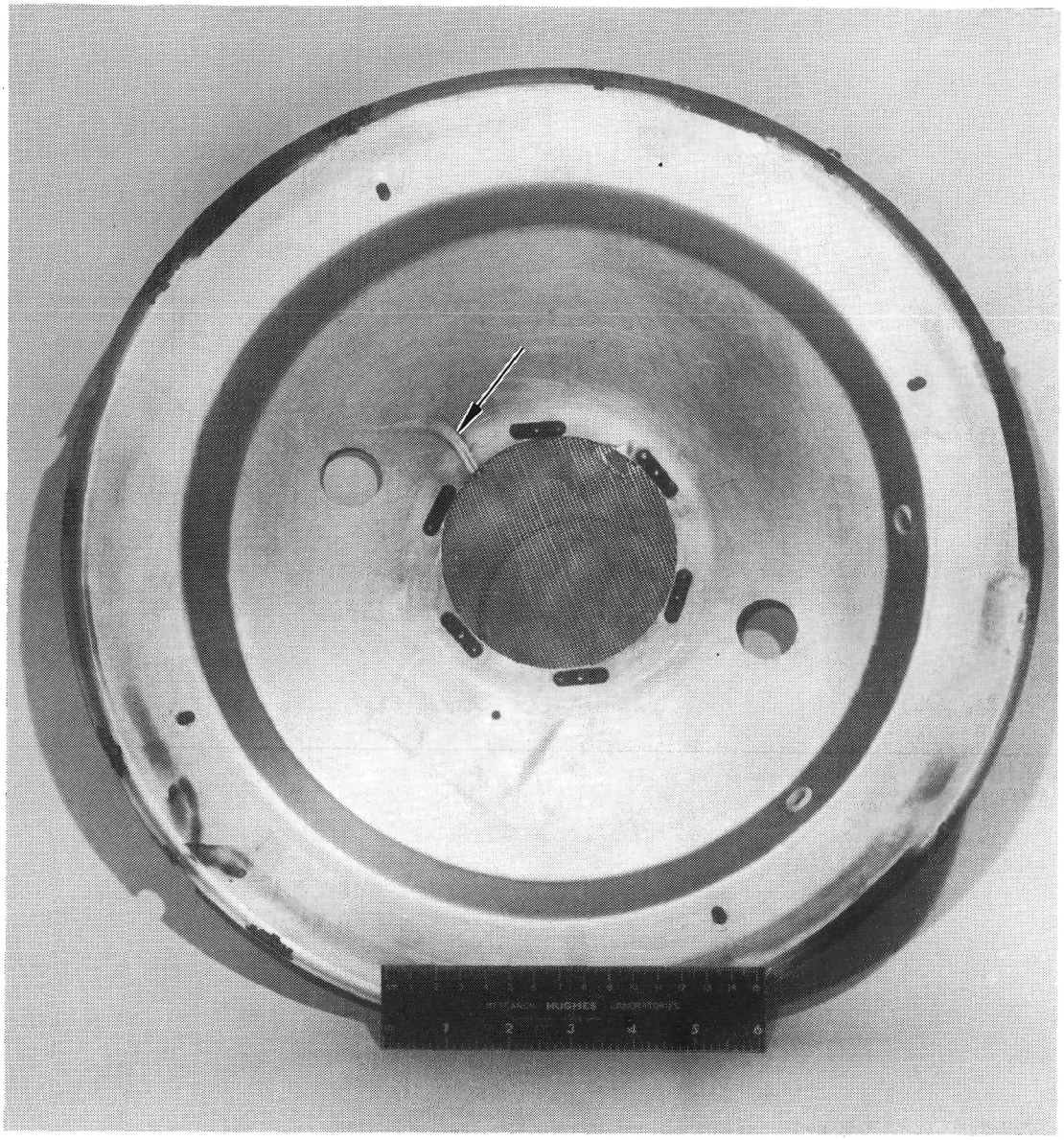

Figure A-10. Inside of rear cover.

M11078

4893–79

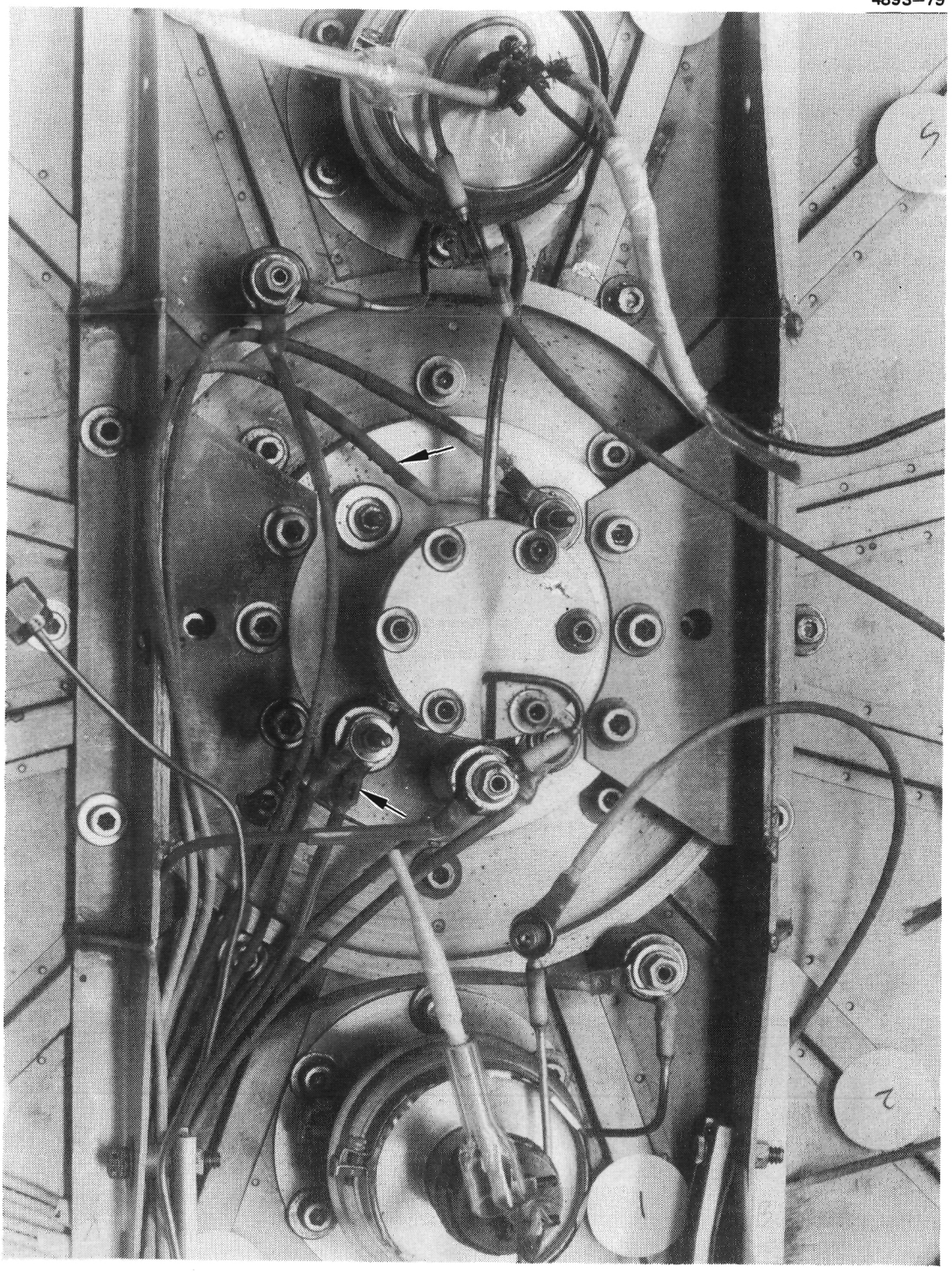

Figure A-11. Closeup of wiring in center region of backplate.

M11010

4893-48

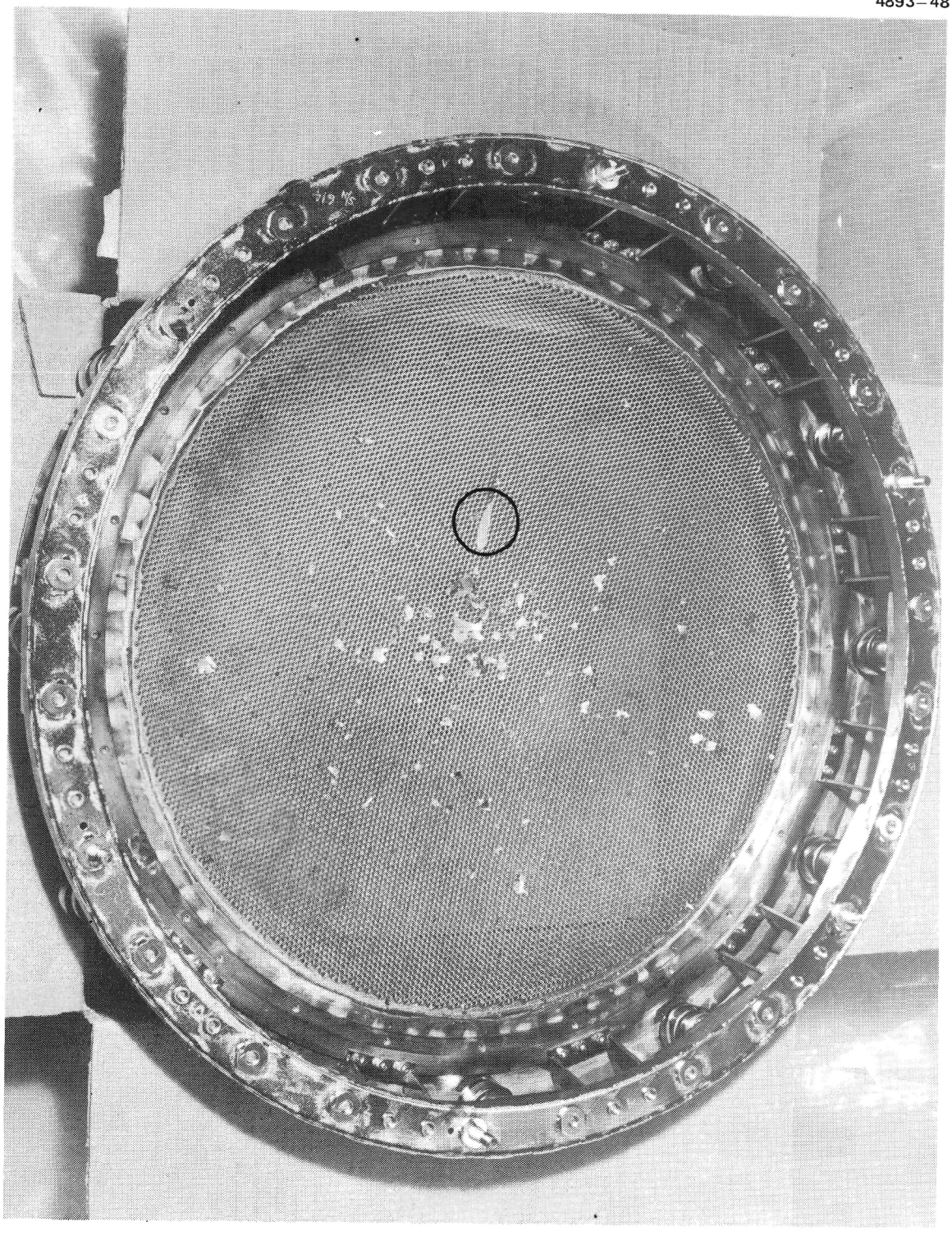

Figure A-12. Optics with flakes on upstream side of screen electrode. Encircled flake is piece of baffle.

Figures A-8 and A-9 show the thruster as viewed from an upstream location, with and without the back outer case. On the basis of what can be seen from these photographs, it would be impossible to estimate how long the thruster has been operated. The slight discolorations seen on the vaporizer and central access plate of the back cover are considered to be a consequence of wiring insulation deterioration. Other evidence of this deterioration is seen in Figs. A-10 and A-11. The wires affected are attached to or are routed very close to components that operate at relatively high temperature (~300°C). Notice also, the relatively large number of mercury droplets seen on the thruster surface in Fig. A-11. This mercury is thought to be a consequence of the vacuum chamber venting and thruster dismounting procedures rather than deposits which have condensed during the test.

Figure A-12 shows the upstream view of the ion optics assembly after careful removal to preserve the orientation of the "flakes" resting on the screen grid. The circled "flake" is a portion of the baffle, comparable to the remaining portion seen in Fig. A-5. The markings around the edge of the screen grid are a consequence of the tantalum "gasket" used to cover the gap between the screen grid and screen pole piece. This assembly will be discussed in detail in a separate section.

Before proceeding to the detailed discussion of the thruster subassemblies, it is considered appropriate to point out that a relatively large number of the thruster components show no significant wear or damage and have thereby demonstrated the durability of a number of the component designs. The sections which follow will concentrate on the discussion of damage and wear and although this damage may represent the result of relatively few processes and affect only a relatively small number of parts, the volume of discussion on damage far exceeds that on success.

B. Discharge Chamber Assembly

The discharge chamber assembly is comprised of the following components and subassemblies:

- discharge chamber shell
- anode
- propellant distributor plenum
- magnets and pole pieces (magnetic circuit)
- cathode pole-baffle subassembly.

All of these elements, except the last will be discussed in detail in this section. The cathode pole-baffle subassembly sustained the greatest wear and its elements will be described in detail in another section. Figures A-13 and A-14 show the extent of this wear. (For comparison, a photograph of a new subassembly is shown as Fig. A-15.) The baffle is eroded almost completely away, exposing the internal components of the subassembly to ion bombardment. Similarly, the pole piece is seen to be thinned to a "knife-edge" at the downstream edge. The material removed from these components is re-deposited on the internal surfaces of the discharge chamber and as the coating builds in thickness, the deposited material spalls and forms "flakes". These deposits are evident in Figs. A-13, A-14, A-16 and A-17 primarily on the upstream discharge chamber boundary or backplate and the anode. Samples of these deposits were taken at the locations marked on the photographs in Figs. A-13 and A-16 and analyzed to provide the results listed in Table A-4. Except for the deposit taken from the outboard location on the backplate (L) the samples were comprised predominantly of iron. The sources of this iron are the baffle and the cathode pole which are fabricated from cold rolled electrolytic steel. The other constituents and impurities anticipated to be present in steel are also in evidence.

M11013

4893–49

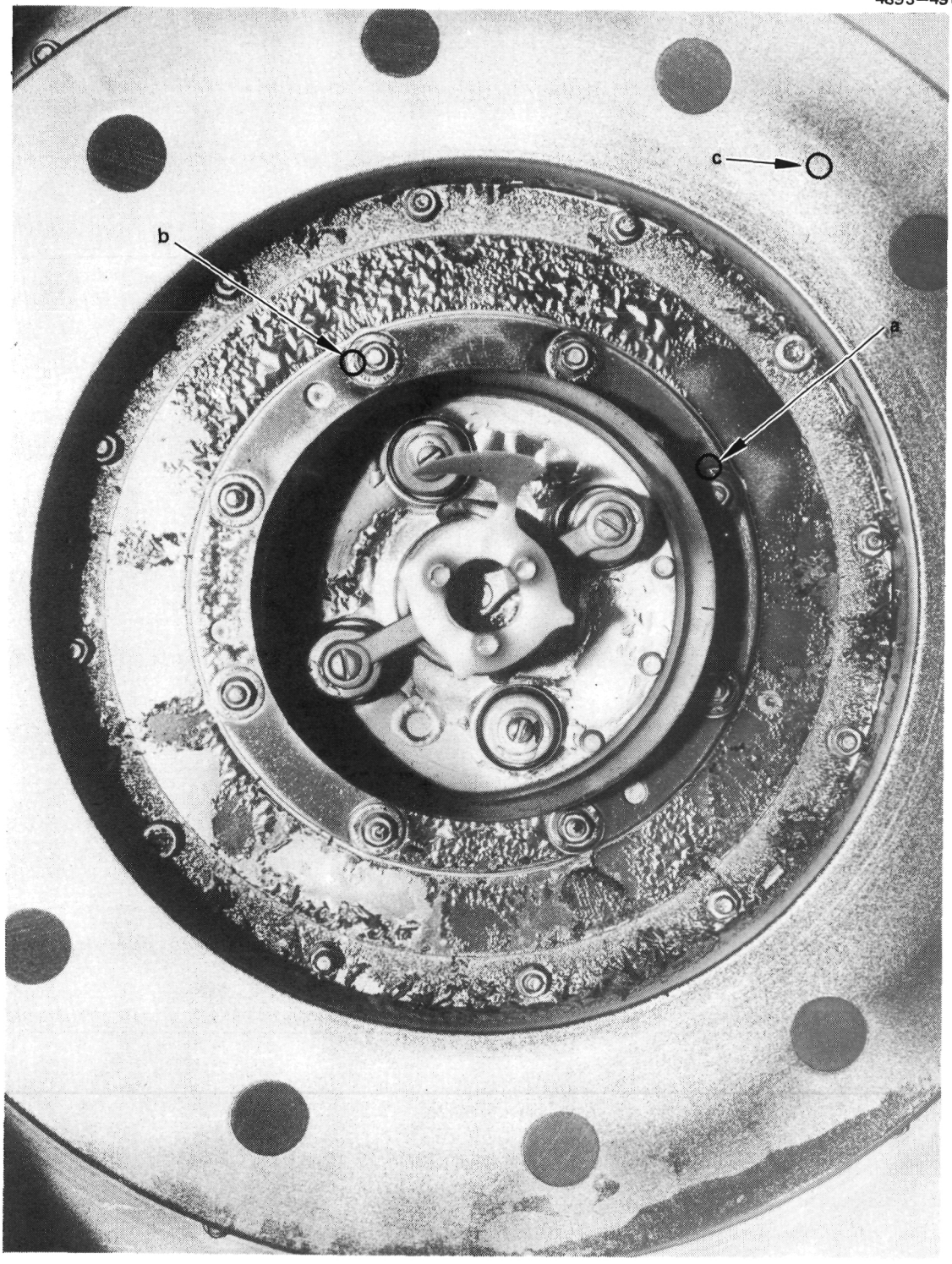

Figure A-13. Cathode pole-baffle region.

M11014 4893–258

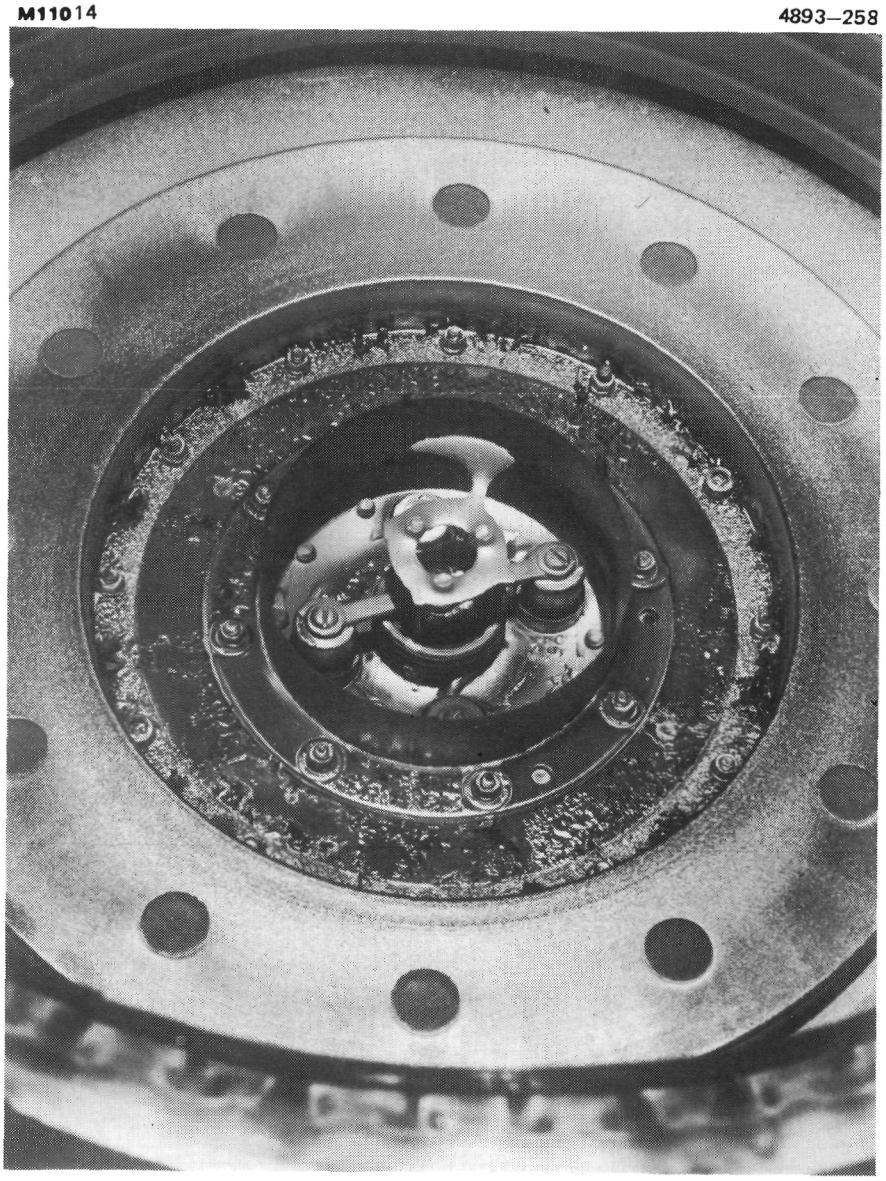

Figure A-14. Cathode pole-baffle region.

M110128 4893–259

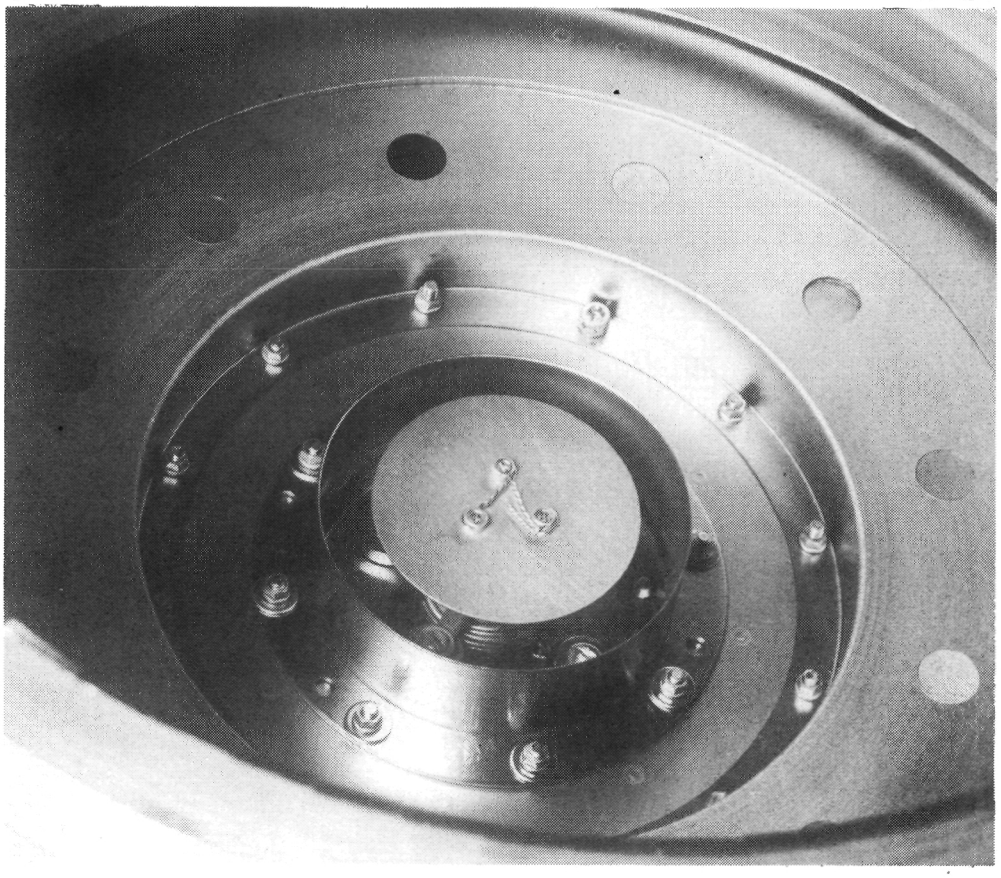

Figure A-15. Cathode pole-baffle region of a new 700 series thruster.

Figure A-16. Sputter deposition on anode.

M11011

Figure A-17. Sputter deposition on anode.

Table A-4. Semiquantitative Analysis of Discharge Chamber Flake Samples

Sample Location	Composition					
	A	B	E	F	G	L
Elements						
Fe-	Rem.	Rem.	Rem.	Rem.	Rem.	6.8%
Cr-	0.27%	0.52%	0.61%	0.57%	0.61%	1.4
Ni-	11.	22.	4.1	4.4	3.9	6.2
Ti-	0.17	0.61	0.56	0.48	0.66	2.8
Mo-	27.	7.4	25.	16.	16.	Rem.
Si-	ND<0.020	TR<0.020	0.22	0.32	0.15	1.2
Mn-	0.061	0.24	0.46	0.61	0.35	TR<0.020
Mg-	0.0048	0.013	0.025	0.025	0.034	0.12
Al-	0.061	0.048	0.24	0.22	0.18	ND<0.10
Ag-	0.0059	0.018	0.051	0.040	0.032	ND<0.010
Hg-	0.043	0.087	0.92	0.15	0.76	8.4
Pb-	ND<0.05	—	—	—	—	ND<0.50
Cu-	0.019	0.041	0.11	0.11	0.076	0.047
Co-	0.093	0.33	0.087	0.070	0.056	ND<0.10
Ca-	ND<0.002	—	—	—	—	0.13
Sr-	ND<0.005	—	—	—	—	—
Ba-	ND<0.50	—	—	—	—	—
Ta-	ND<0.30	—	—	—	—	—
W-	ND<0.40	—	—	—	—	—
Au-	ND<0.006	—	—	—	—	—
Other Elements	nil					

T1855

Higher concentrations of Ni were found in locations A and B. Locations A and B are near mild steel components which were originally nickel plated. Note that the percentage of molybdenum found in the anode samples decreases with distance from the screen grids. The only molybdenum components are the screen and accelerator electrodes and the keeper electrode. The molybdenum present in the deposit samples is thought to be from the screen electrode. The erosion of this electrode was significant, as will be described in the ion optics assembly section. The locations noted as C, D, and H did not yield any measurable deposit although several attempts were made to dislodge deposits in these locations by thermal shock and also by scraping the surface while observing it under a microscope. These locations do not appear to be erosion sites either. Note also that there is very little titanium in evidence in these samples and therefore it is concluded that there is little or no ion erosion of the propellant distribution plenum or other cathode potential surfaces of the discharge chamber shell.

In the 700 series thruster design, a small gap exists between the screen electrode of the ion optics assembly and the screen pole piece. If left uncovered, this gap allows ions to be accelerated radially outward to impinge on the outer case. Although the number of these ions is small, the outer case and elements of the ion optics support can be detectably sputtered. Consequently, the 700 series discharge chamber design included a thin tantalum gasket that is spotwelded to the screen pole piece and makes slight contact with the screen electrode (see Fig. A-5). No appreciable erosion or deposition could be detected on this tantalum gasket (measured thickness with micrometer).

Consequently, the erosion sites in the discharge chamber are:

- the cathode pole piece
- the baffle
- the screen electrode.

Deposition sites in the discharge chamber are:

- the thruster backplate and innermost wall of the propellant distribution plenum
- the central 3-in. (7.6 cm) of the anode

- the upstream boundaries of the interior and exterior surfaces of the cathode pole-baffle subassembly.

Locations in the discharge chamber which are not appreciably eroded or covered with deposits are:

- the downstream surface of the plenum
- the upstream and downstream edges of the anode (about 0.5 to 0.8 in.; 1.3 to 2 cm)
- the screen pole piece.

The erosion and deposition sites on the cathode pole-baffle subassembly will be discussed in more detail in a later section.

The radical modification of the baffle and baffle support by sputtering erosion was expected to have modified the magnetic field distribution in the thruster. The axial and radial magnetic field components were measured using a Hall effect probe gaussmeter and probe positioning mechanism that automatically plots field strength versus probe movement on an x-y plot. These measurements are made by moving the probe axially at constant radius from upstream to downstream discharge chamber boundaries. Field distributions of this type were not available from the pre-test data, however the second 700 series thruster built, SN 702 was measured in this manner. Figures A-18 and A-19 compare the axial and radial field strengths for thrusters SN 701 and SN 702. It is apparent that the field strength in the vicinity of the damaged cathode pole is reduced by about 25% at some radii and less as one moves away from the damaged polepiece-baffle subassembly. The radial magnets were removed and measured in the fixture which has been established as the standard for calibrating and documenting new magnets used in thruster fabrication. Although this type of documentation was not performed in the fabrication of thruster SN 701, the procedure used in magnetizing thruster SN 701's permanent magnets is thought to be the same as that used now, and it is reasonable to assume that these magnets originally had the same strength as those being magnetized and measured recently. The standard field strength required for each of the radial magnets is 4.8 to 5.0 gauss, as measured in the calibrating

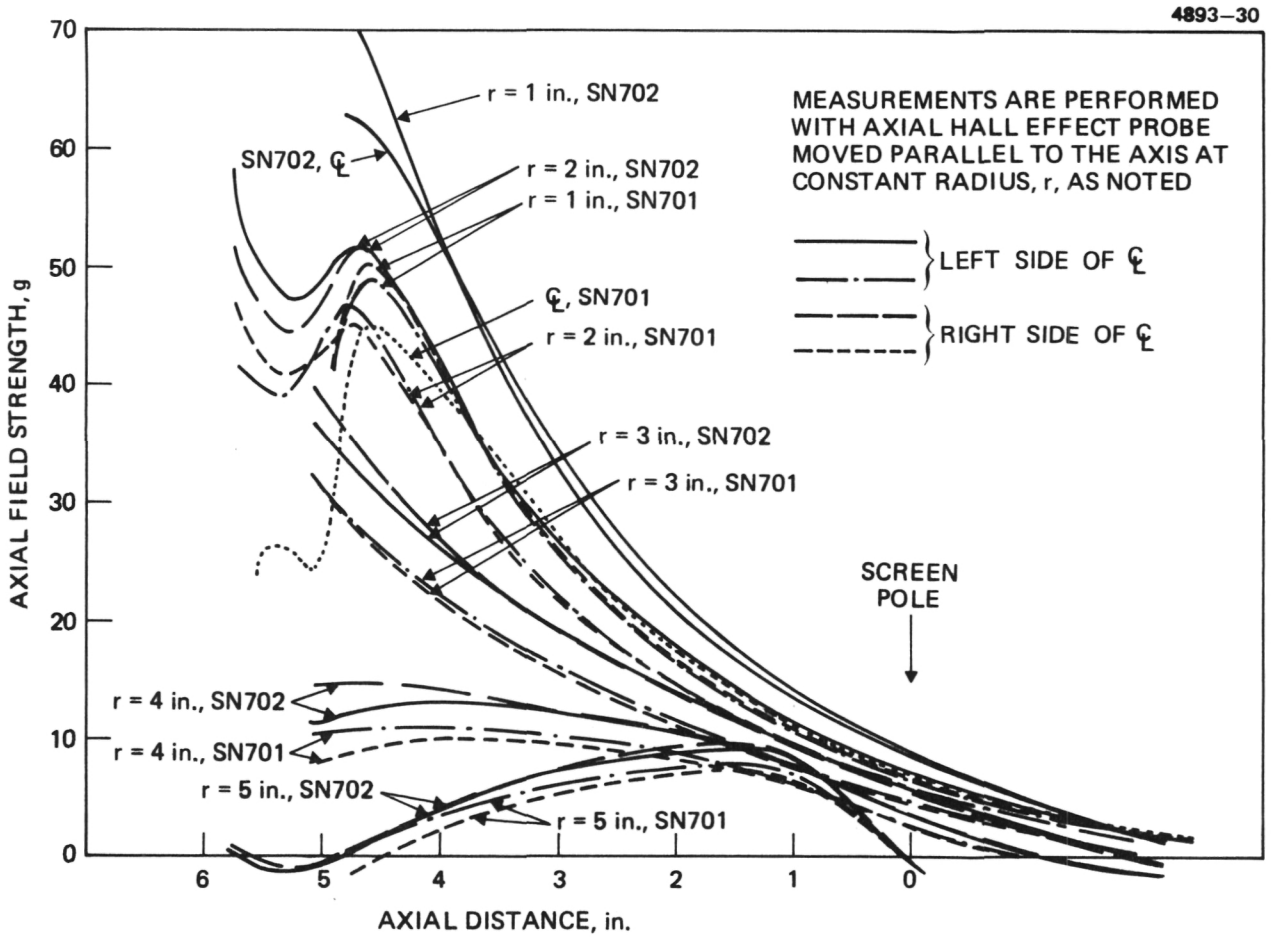

Figure A-18. Comparison of axial magnetic field components of thruster SN 701 after 10,000 hour test with those of thruster SN 702.

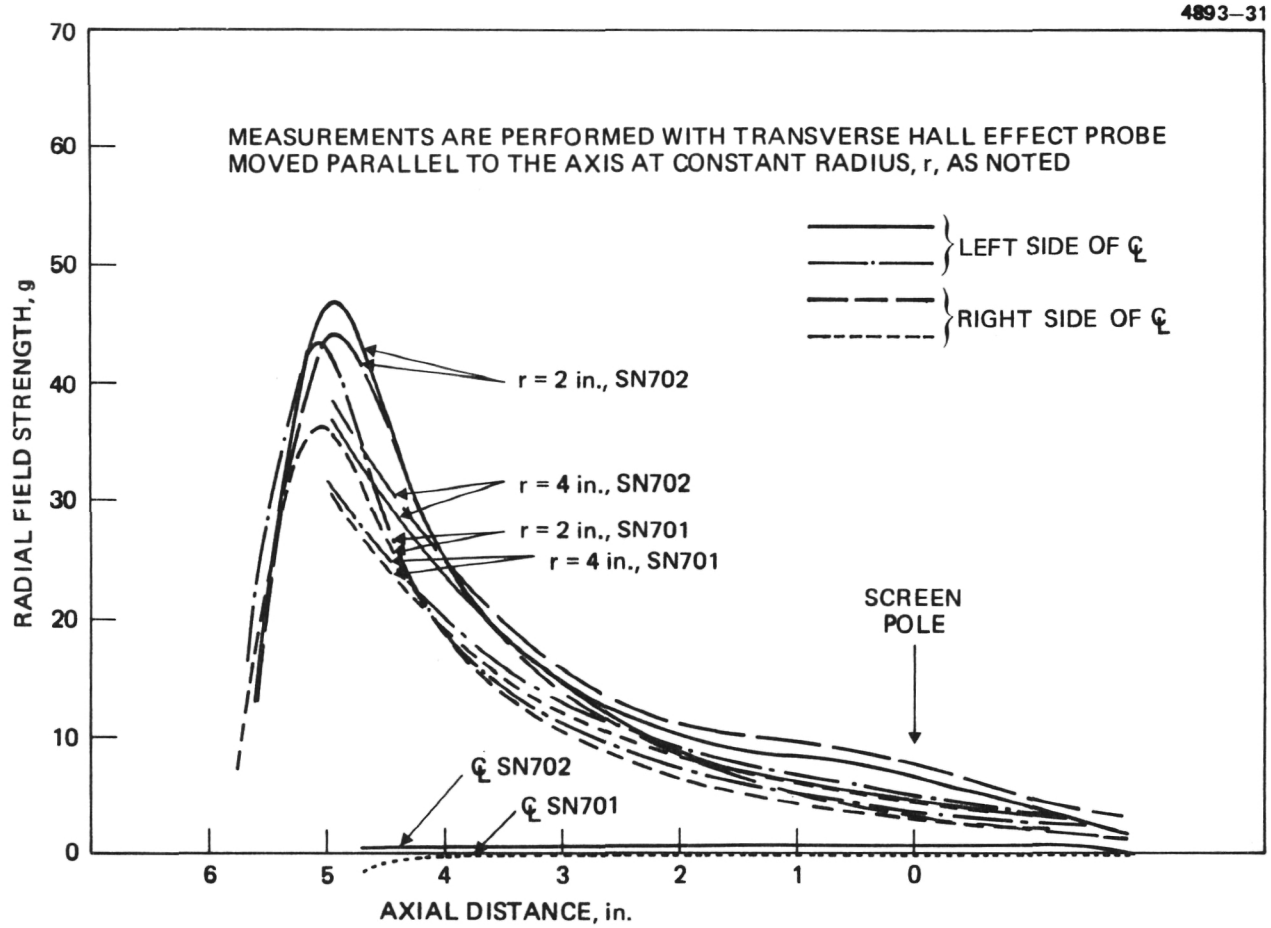

Figure A-19. Comparison of radial magnetic field components of thruster SN 701 after 10,000 hours test with those of thruster SN 702.

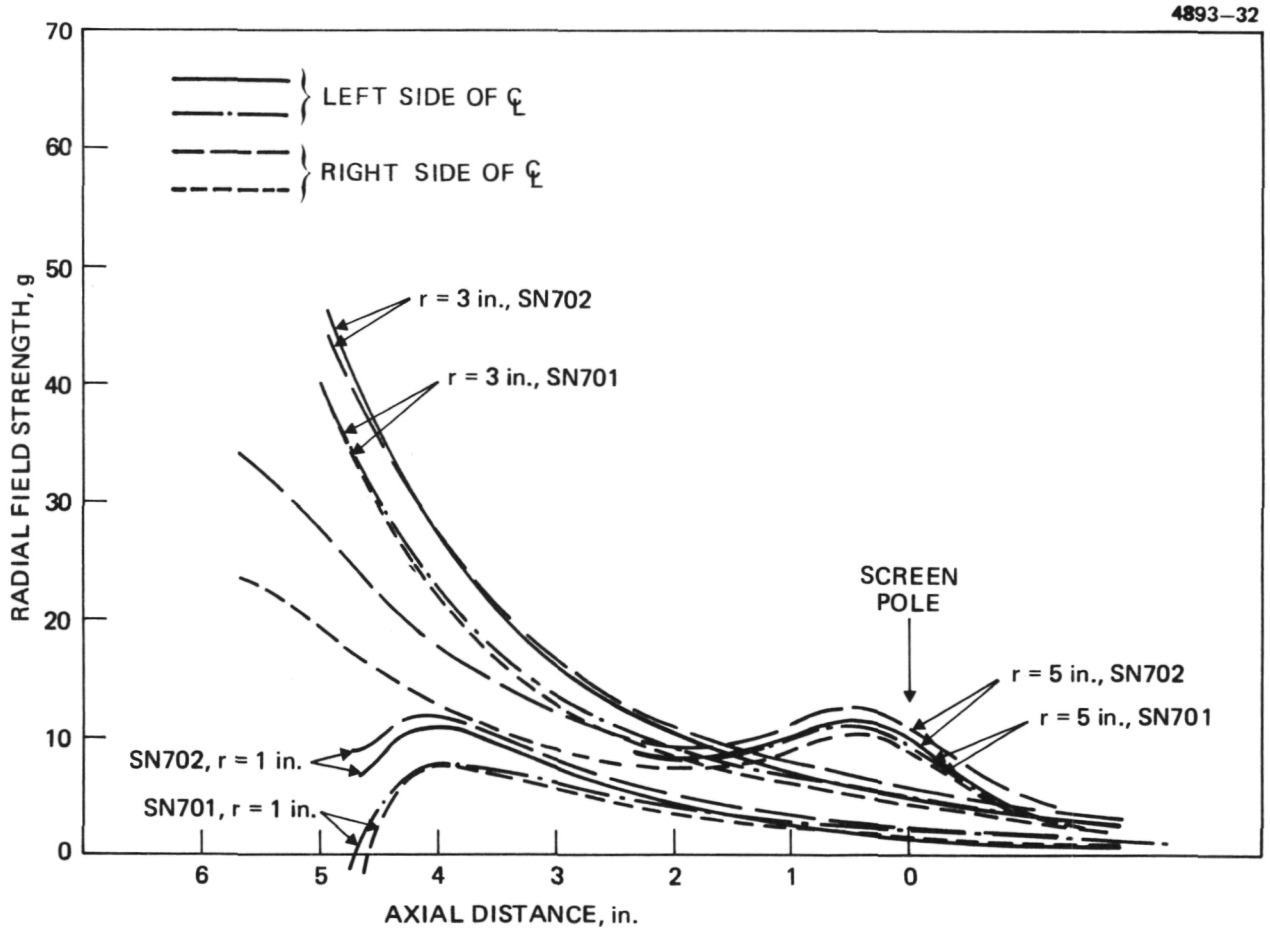

Figure A-19. (Continued)

calibrating fixture. The measured values of the radial magnets from thruster SN 701 vary in strength between 4.35 and 4.9 with an average value of 4.5. Thus, assuming that these magnets were originally the same as those being used now, the magnetization appears to have decreased by at least 6% below the value considered to be minimum in new thruster fabrication. This decrease in magnetization can account for at least a part of the generally lower magnetic field components of thruster SN 701 as compared to thruster SN 702 in Figs. A-18 and A-19.

As mentioned earlier, the anode to discharge chamber shell insulation appeared to degrade between removal of the thruster from the test facility mounting and the first measurements taken before beginning disassembly (from 5000 Ω to 350 Ω). The reason for this decrease became evident after removing the discharge chamber backplate, and is shown in Fig. A-20. A flake of magnetic material was held between the screen polepiece and the anode by the thruster magnetic field (see arrow) and was responsible for the low resistance measurement. When the flake was removed, the anode to discharge chamber shell resistance increased to 5000 Ω again.

Another observation that can be seen in Fig. A-20 is the distortion in the downstream edge of the anode. A possible explanation of this distortion is that current surges from shorting by flakes, such as the one seen bridging the gap between the screen pole piece and the anode, caused local heating of the anode, thereby causing the observed distortion. Although the localized current may not be caused by flakes, it is probable that some form of localized heating is responsible for the anode distortion seen in Fig. A-20.

An interaction between the anode and the anode fasteners can be seen on two of the six fasteners which hold the anode in place. The anode supports numbered 1, 3, and 5 were nearer the downstream end of the discharge chamber, while numbers 2, 4, and 6 were located nearer the upstream end. Enlarged photographs of these two fasteners are shown in Figs. A-21 and A-22 (which will be referred to as anode support numbers 6 and 2, respectively). The stainless steel screw of anode support number 2 is the only anode current path and carries the

M11079 4893—80

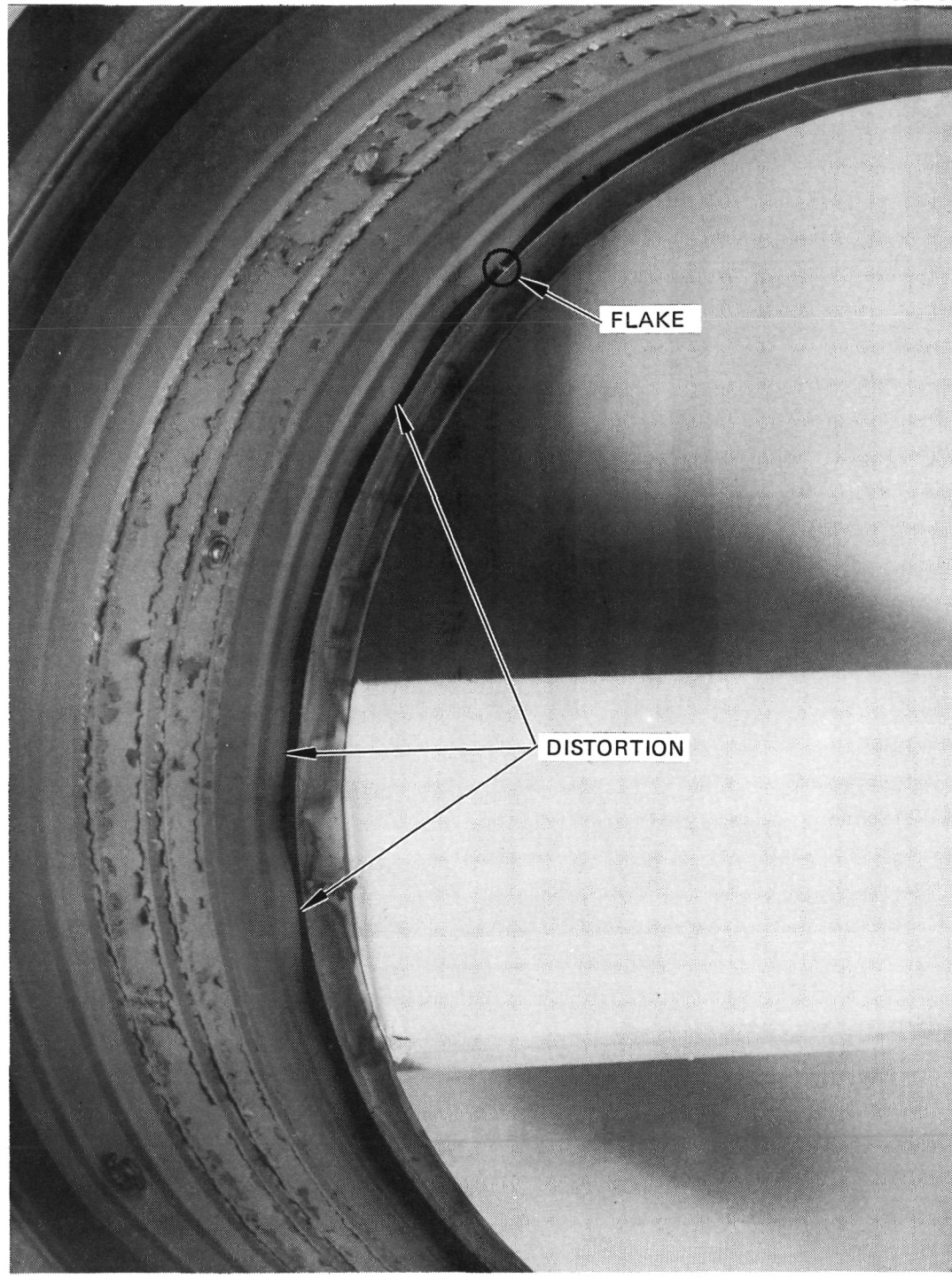

Figure A-20. Part of anode showing distortion and flake.

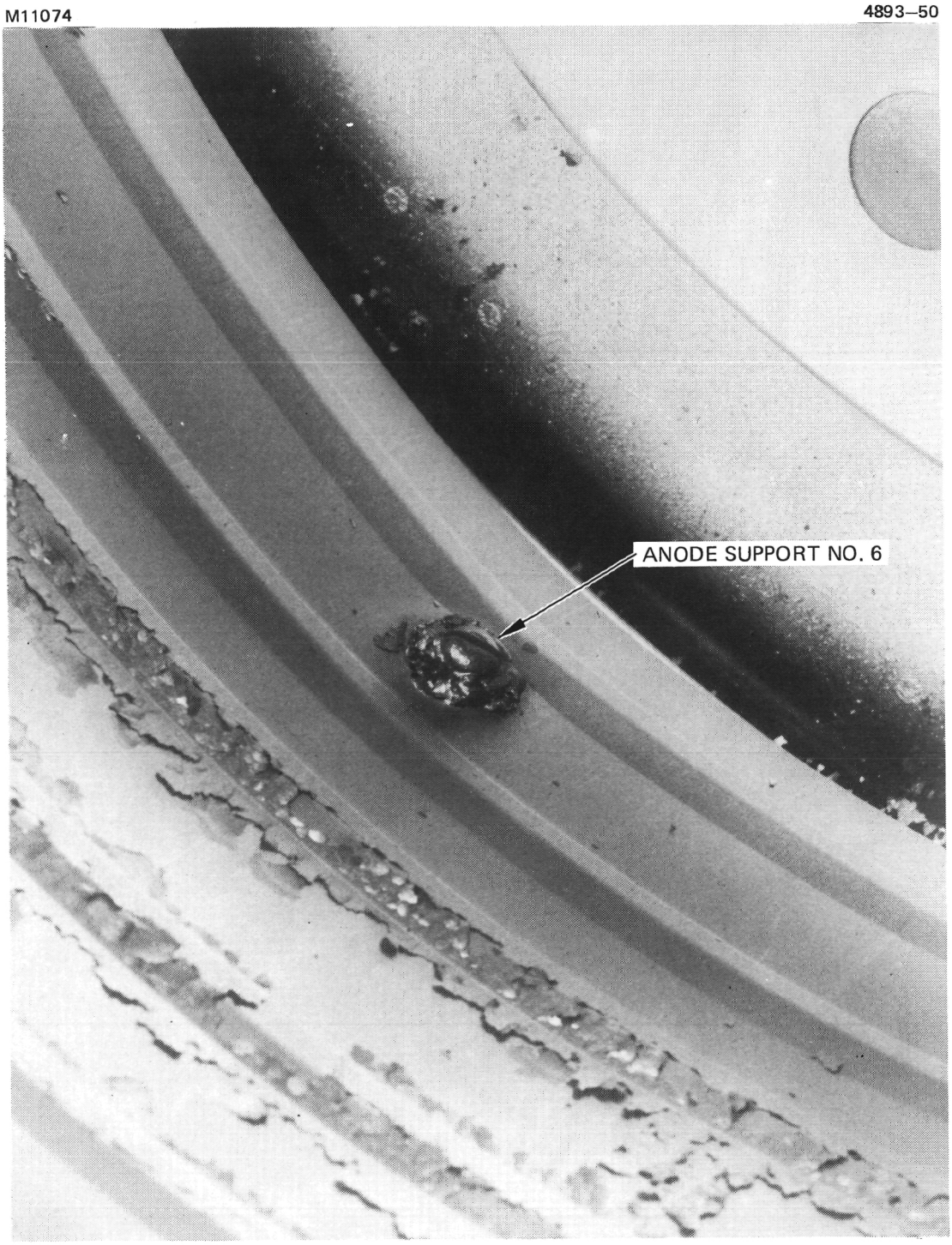

Figure A-21. Part of anode showing damaged anode support No. 6.

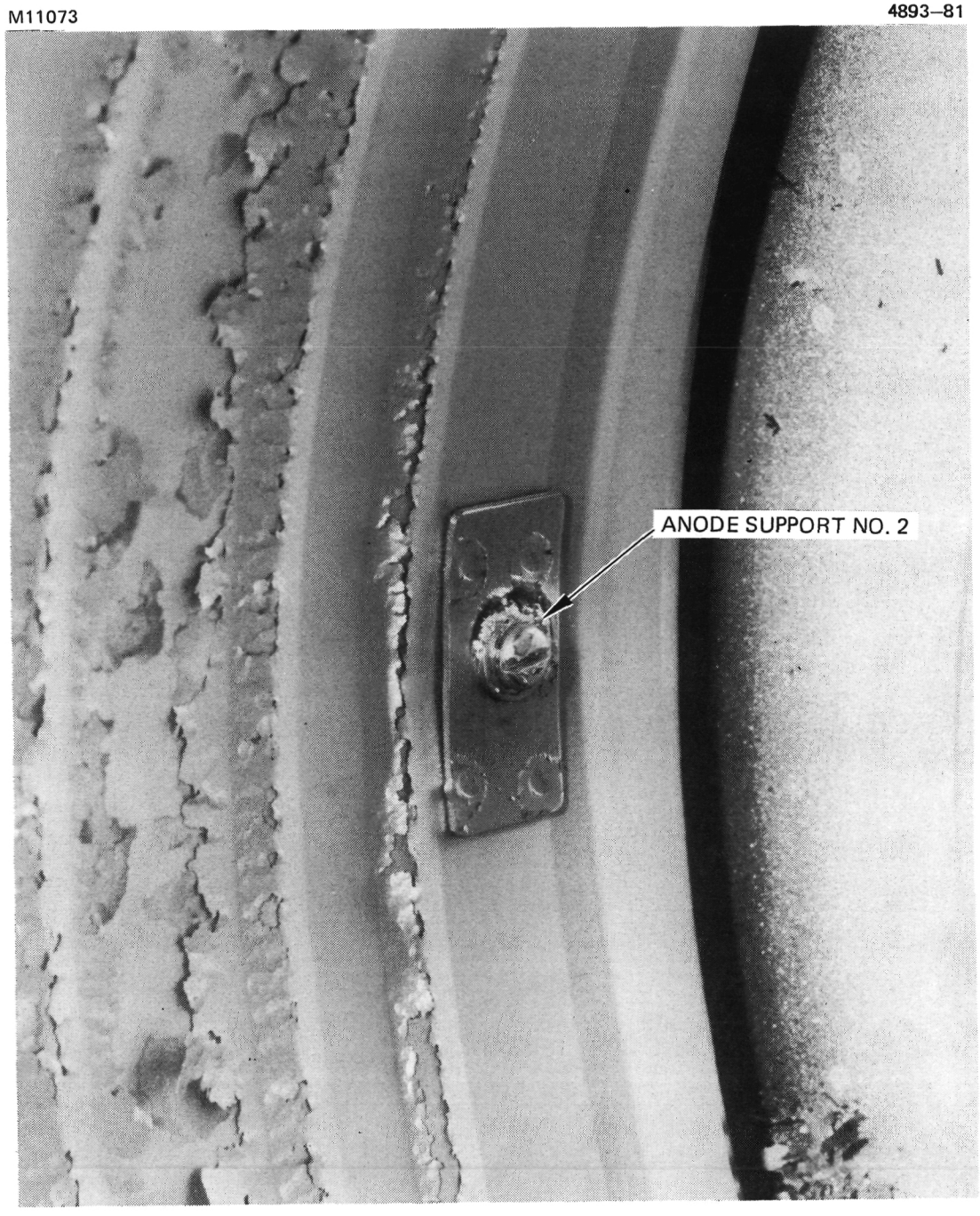

Figure A-22. Part of anode showing damaged anode support No. 2.

combined beam and discharge currents. After removing all the anode wiring, the leakage resistance measured between the anode and the discharge chamber shell was still only 5000 ohms, and these two fasteners and their anode support insulators then became the most probable source of this relatively low leakage resistance.

The thruster backplate was removed to expose these support insulators and upon inspection the ceramics were seen to have sustained damage, as shown in Figs. A-23 and A-24. The damaged insulators were removed intact by cutting the anode and discharge chamber shell with a high speed abrasive wheel. Removal of anode support number 2 (current connection) resulted in an increase in the leakage resistance, as measured with the "megger" 1 kV ohmmeter, to 10 kΩ. The megger measurement was seen to fluctuate to readings as high as 25 kΩ. Removal of the other damaged support, number 6, did not appreciably change the leakage resistance. Figures A-25 and A-26 show all sides of the damaged anode supports after removal from the discharge chamber. The leakage resistance measured across these insulators was approximately 10 kΩ. Removal of the third upstream anode support, number 4, by normal disassembly increased the leakage resistance to a value fluctuating between 30 and 200 kΩ and sparking was seen around the downstream insulators. The remaining anode supports were removed with care taken to preserve a record of their orientation. The ceramic insulators removed are shown in Fig. A-27.

The ceramic parts shown in Fig. A-27(a) are the portion of the anode support insulators which are located on the exterior side of the discharge chamber shell, while those shown in Fig. A-27(b) are located between the anode and the shell. The exterior insulators have a shield and are only slightly coated on the downstream surface (arrows seen on insulator tags indicate beam direction). The interior insulators are not shielded, except by means of their location between anode and shell, and are coated more or less uniformly with no indication of the orientation of the source of the deposited material. The nature of this coating will be discussed later. Figure A-27(c) and (d) show the opposite views

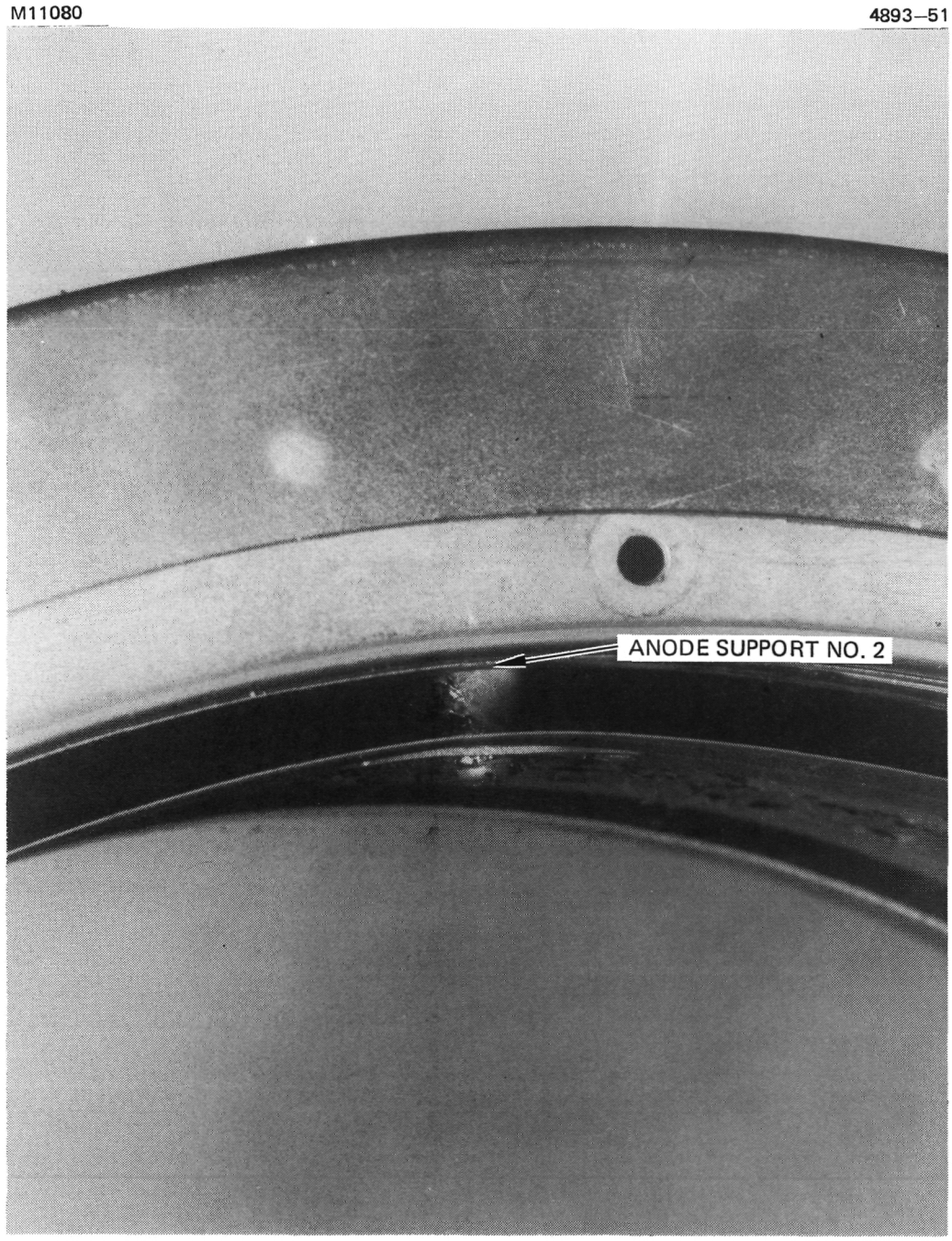

Figure A-23. Anode support No. 2 in place.

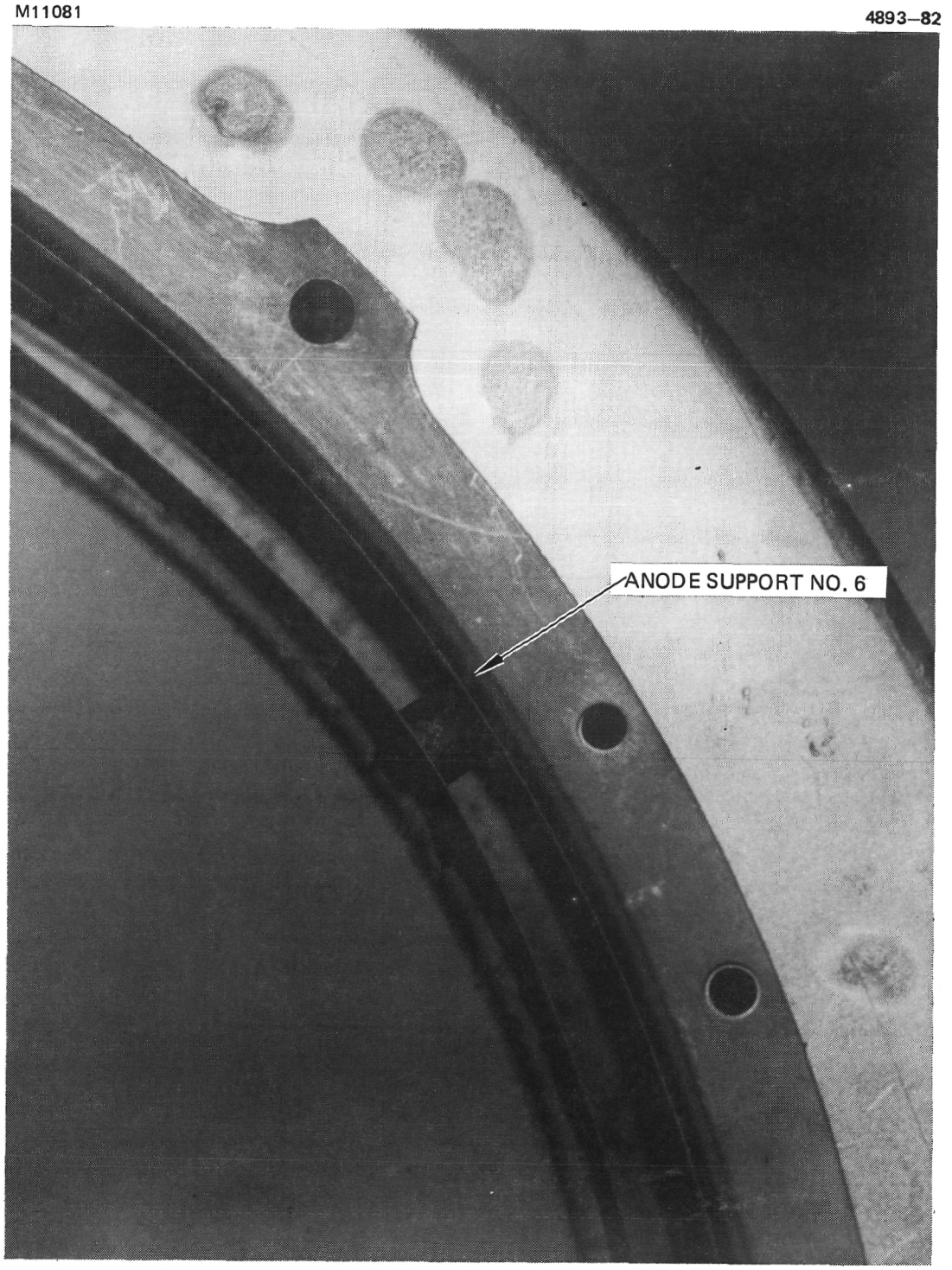

Figure A-24. Anode support No. 6 in place.

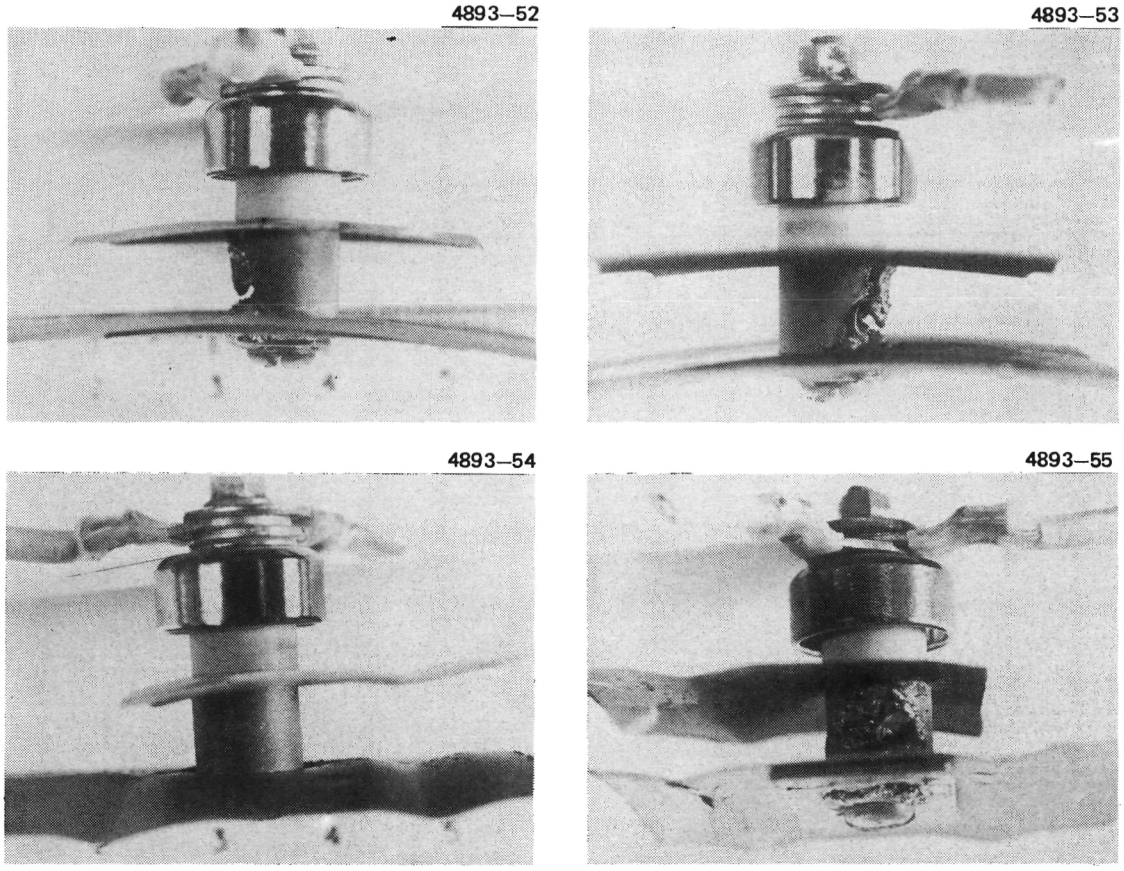

Figure A-25. Damaged anode support No. 2.

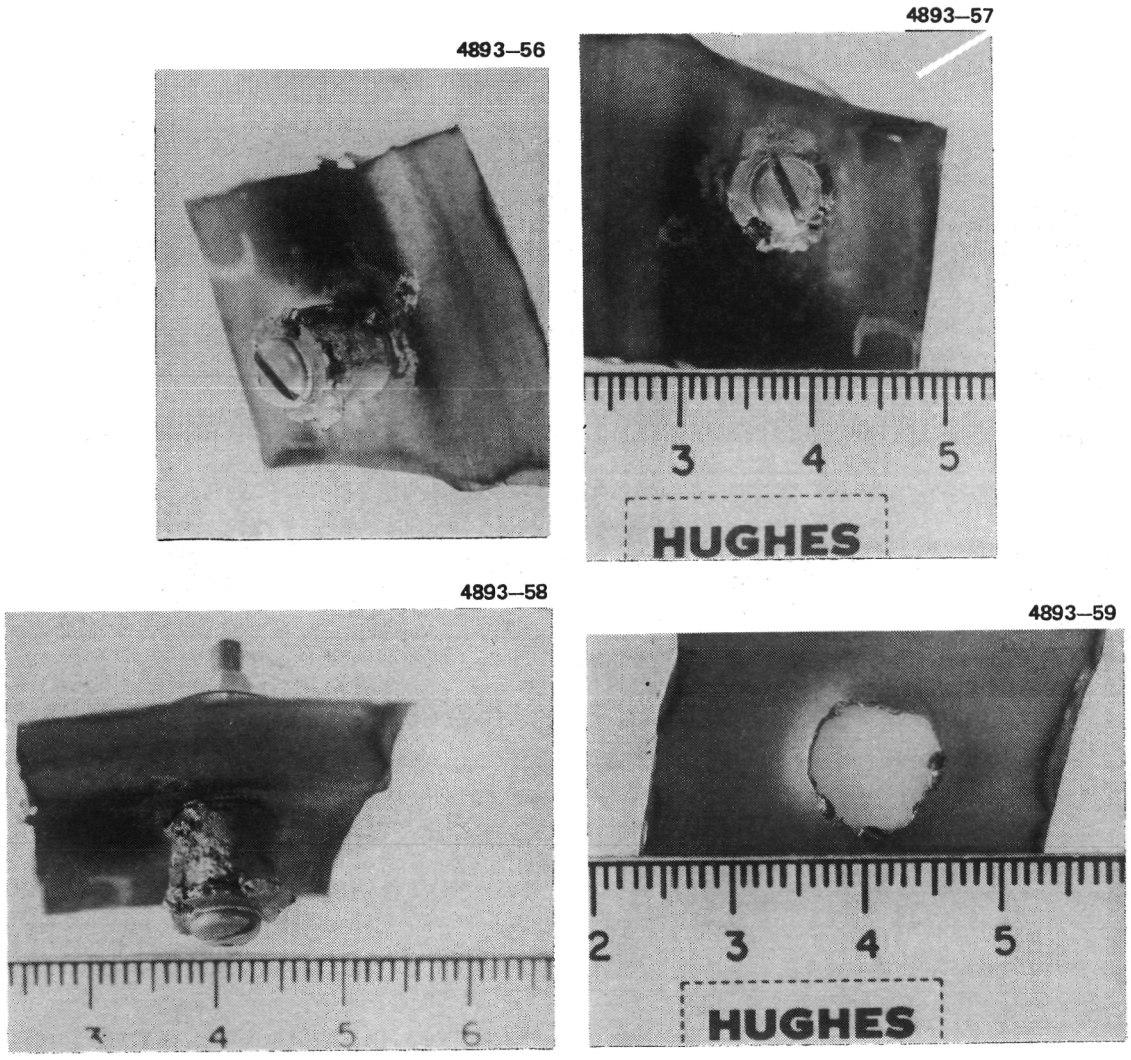

Figure A-26. Damaged anode support No. 6.

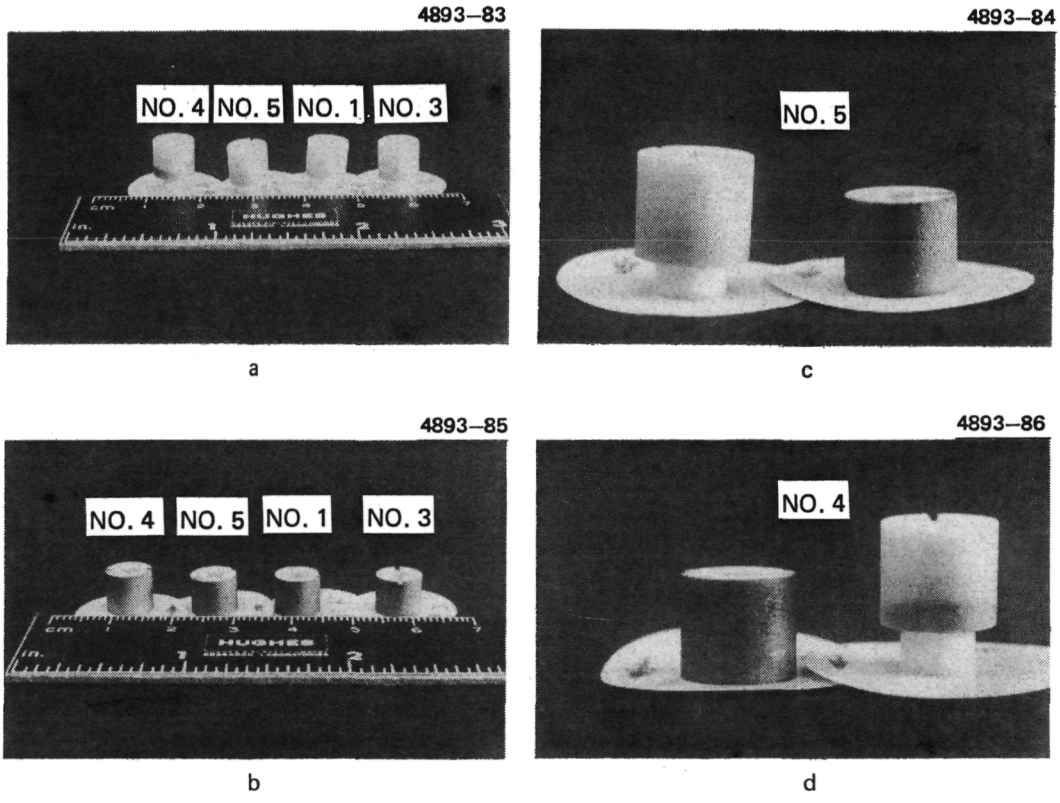

Figure A-27. Cermaic insulators from anode supports Nos. 1, 3, 4 and 5.

(downstream) of insulators No. 5 and No. 4. Note that there is no apparent difference between the coating on the upstream (No. 4) interior insulator and the downstream (No. 5) interior insulator in spite of the fact that both of the damaged anode supports occupied the upstream location (No. 2, No. 6).

Comparison of the upstream and downstream anode support locations on the interior of the discharge chamber shell and the anode reveals evidence of arc formation around the upstream insulators but not around the downstream insulators. Figures A-26, A-28, A-29, and A-30 show photographs in support of this statement. In Figs. A-26, and A-28, "arc tracks" can be seen on the discharge chamber shell around anode support locations No. 6 and No. 4, respectively. Note that in Fig. A-29, there is no evidence of arcing in the vicinity of the downstream anode support location, even though some "arc tracks" are present near the upstream anode boundary, away from the anode support. The view of the exterior surface of the anode shown in Fig. A-30 displays the difference seen in the coloration around the upstream (No. 4) and downstream (No. 3) anode support locations. Around anode support No. 3, the coloration is uniform and shows no variation around the periphery of the anode. There is a definite localized coloration in the vicinity of anode support No. 4, however, and this could be an indication of localized heating.

On the basis of the examination discussed above, it was impossible to discern what caused the damage to anode supports No. 2 and No. 6. Consequently, one of the failed insulators, No. 6, and the surviving insulator, No. 4, were encapsulated and cross-sectioned as shown in Figs. A-31 and A-32 with the areas of interest identified. Magnification of Area 1 is shown in Fig. A-33(a). The screw head and washer are composed of stainless steel and the melted region contains Fe, Ni, Cr, Ti, Mn, Si, Co, and C in decreasing order of proportion as determined by S. E. M. microprobe. It is apparent that the portion of the anode which was held between the stainless steel washer and the ceramic has been completely absorbed in the alloy melt seen. An S. E. M. reproduction and K_α x-ray analysis of the spatial distribution of some of these elements is included in Fig. A-34.

Figure A-28. Part of anode showing "arc tracks" around location of anode support.

M11132

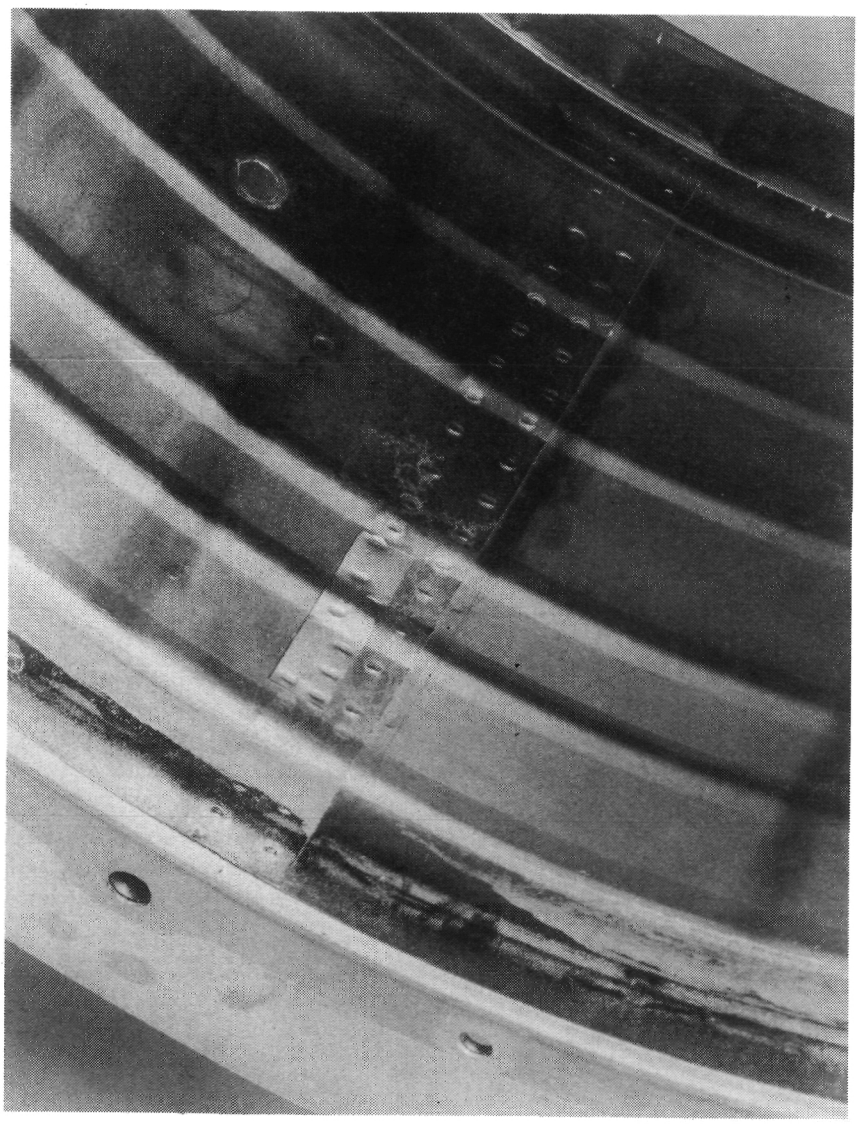

Figure A-29. Part of anode showing support location without "arc tracks".

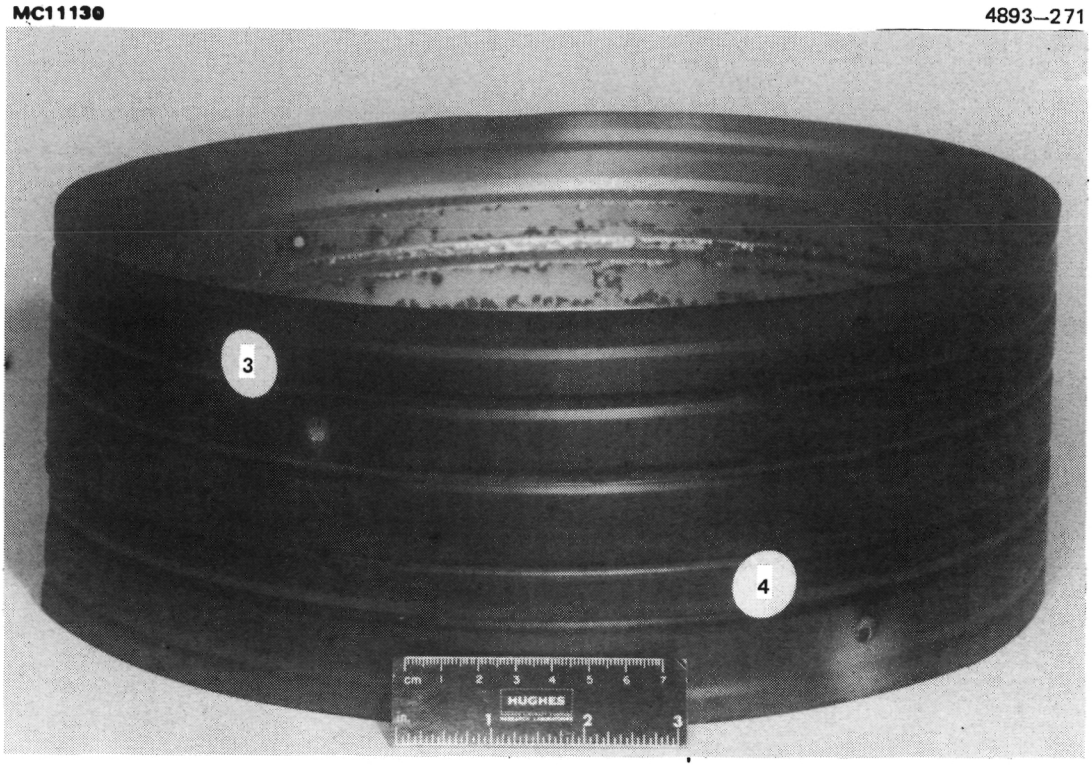

Figure A-30. Exterior surface of anode showing difference in coloration around upstream and downstream support locations.

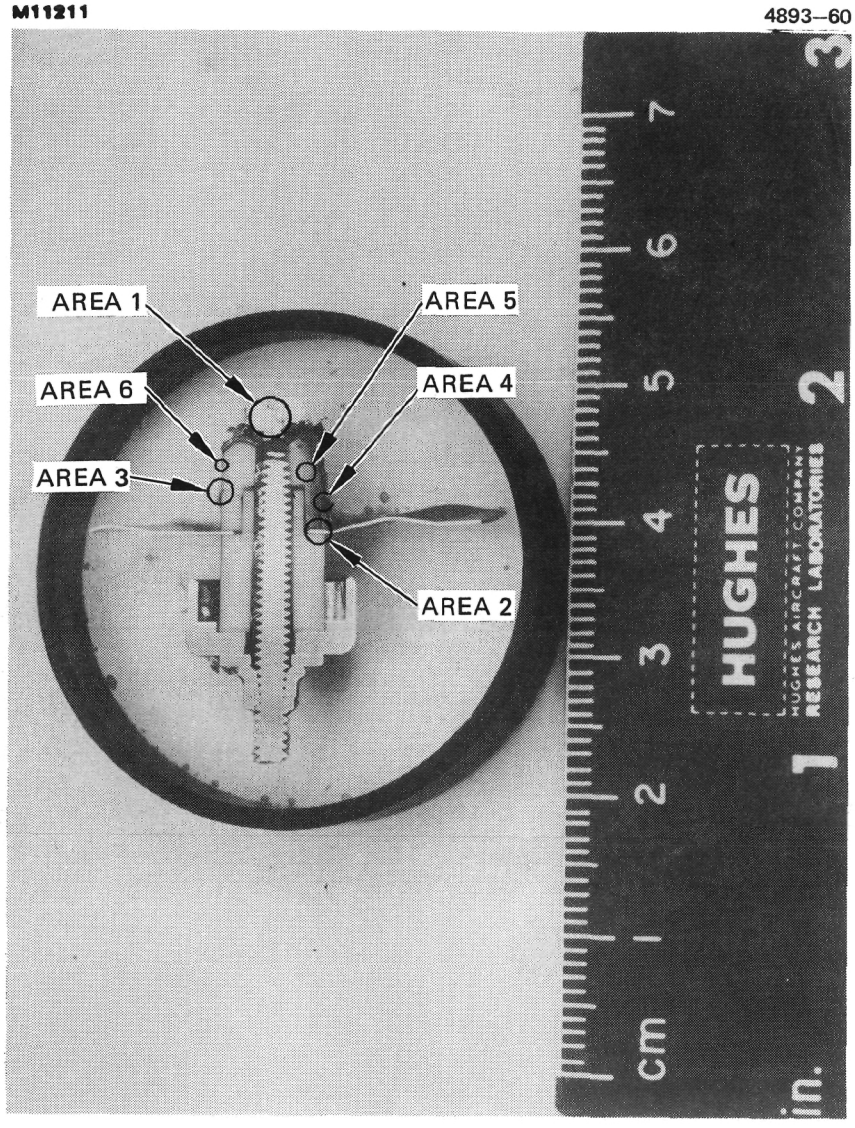

Figure A-31. Cross-section of damaged anode support.

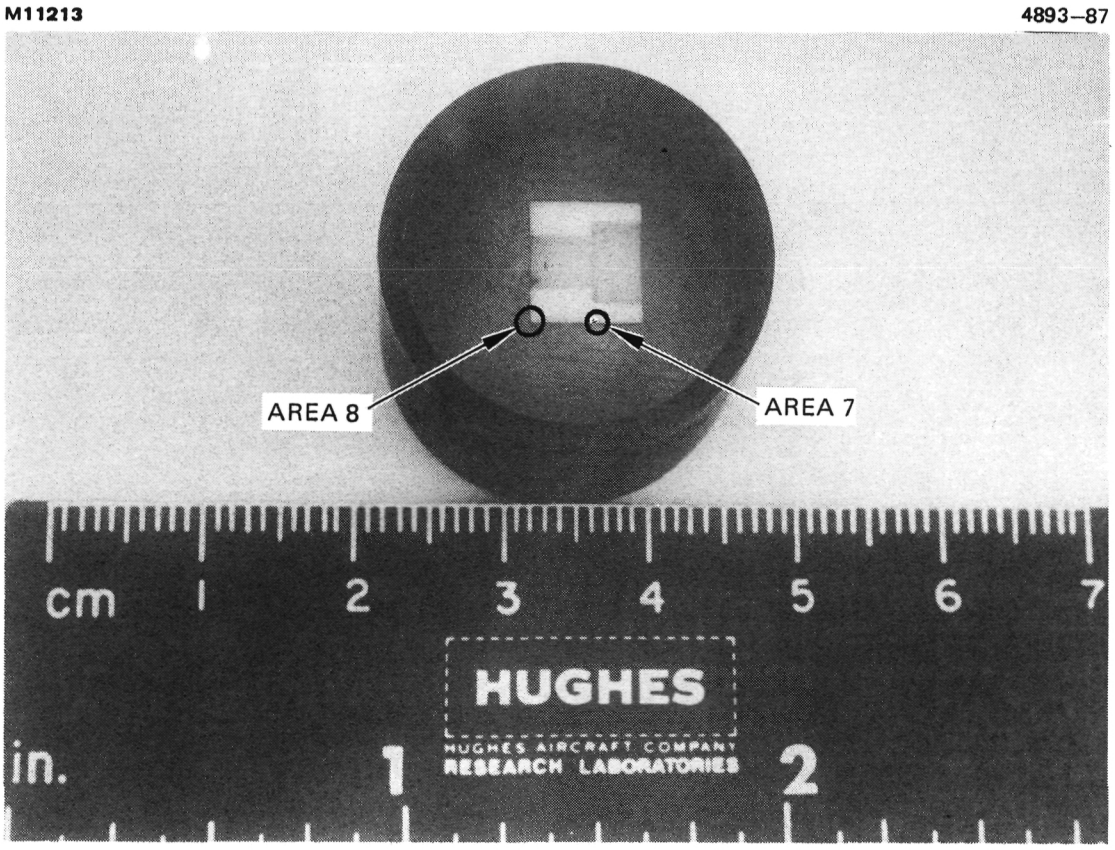

Figure A-32. Cross-section of anode support insulator.

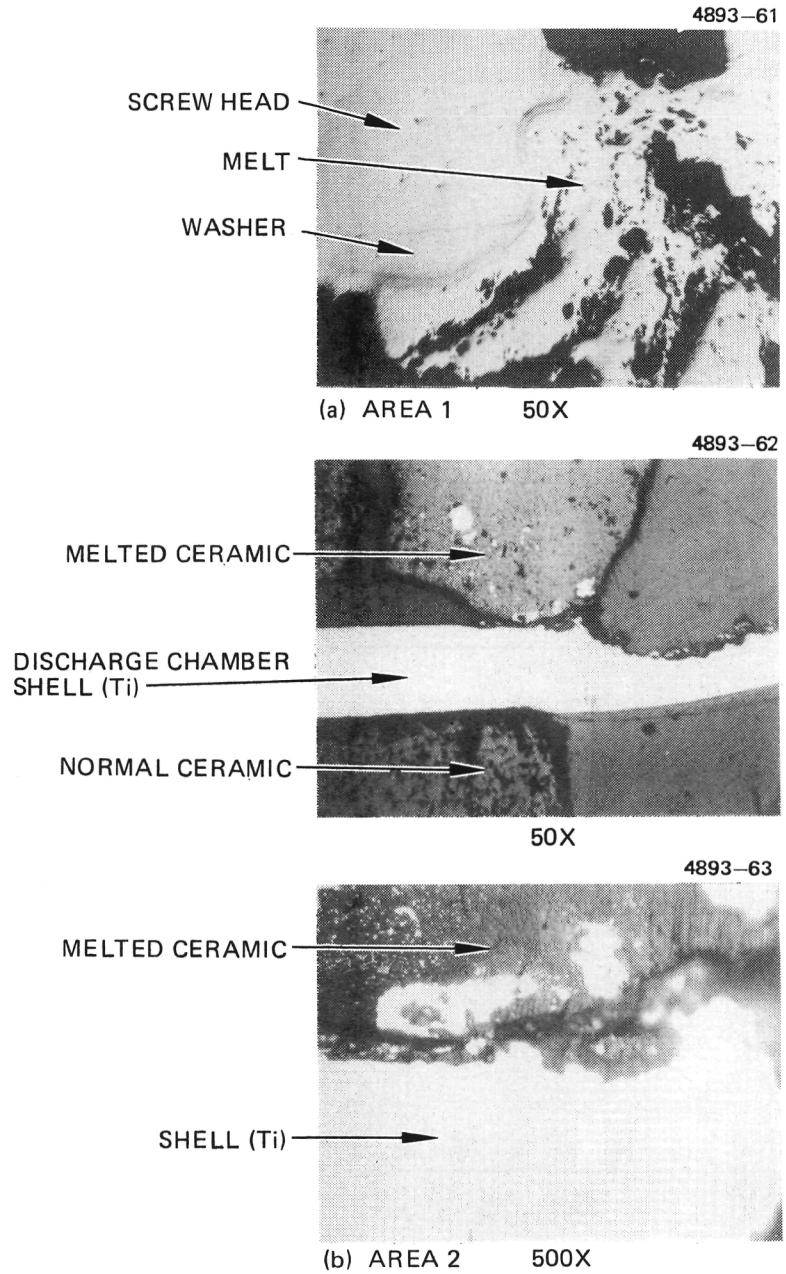

Figure A-33. Magnified view of damaged areas of anode support.

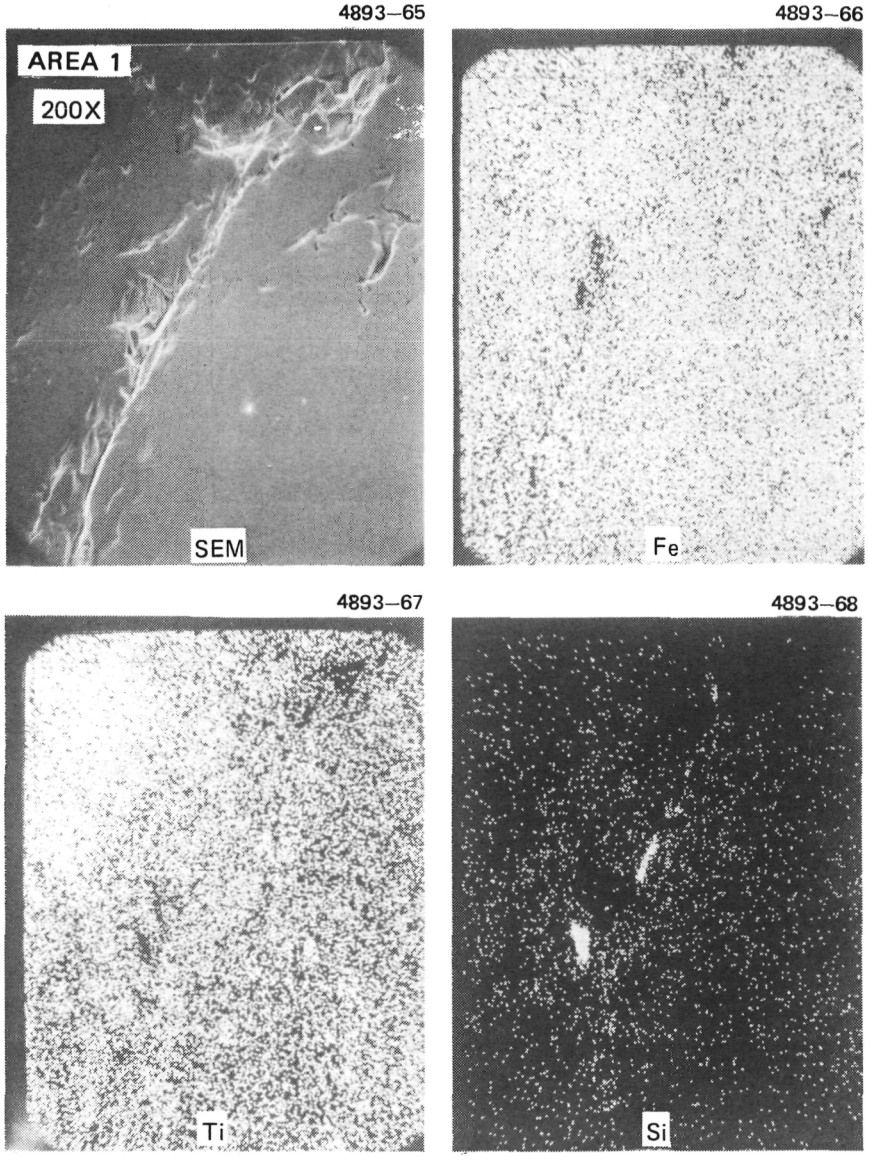

Figure A-34. Scanning electron microscope photo and K_α X-ray analysis of area 1 of anode support.

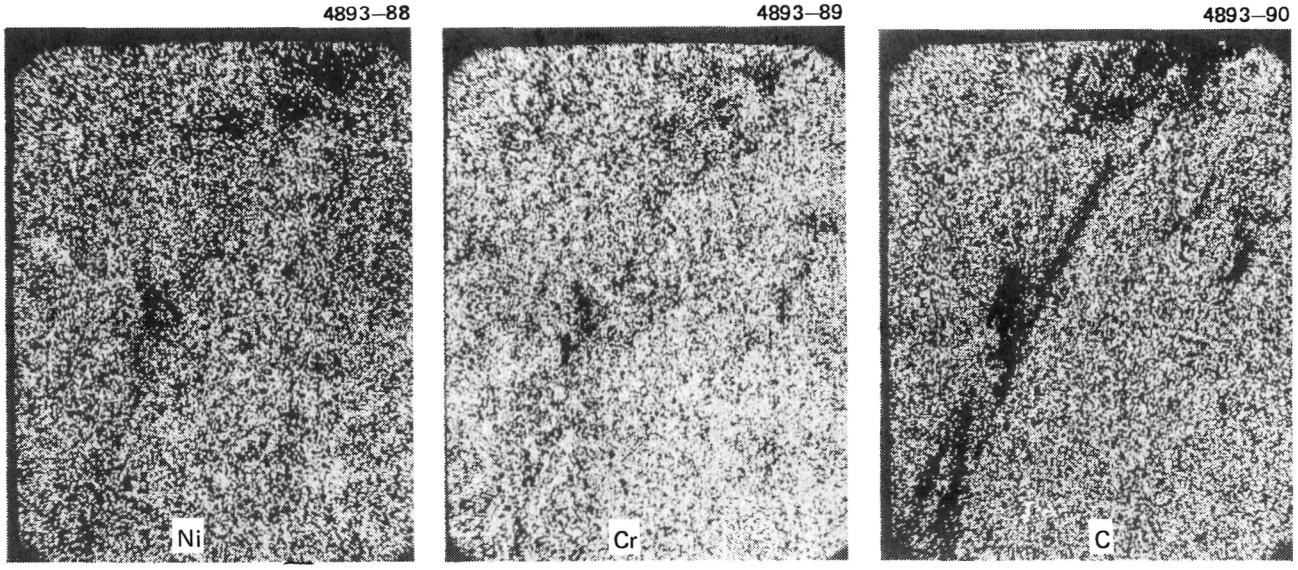

Figure A-34. (Continued).

Microscopic examination of Area 2 shows that the titanium discharge chamber shell is eroded on the interior surface adjacent to the point of contact with the ceramic anode support insulator and that this ceramic has been melted in the vicinity of this point of contact (see Fig. A-33(b), 50X and 500X). Melting of the ceramic is indicated by the dendritic structure of the cross-sectioned ceramic. Titanium appears to be distributed throughout this melted region of the insulator which would imply some sort of "wicking" or melting. This latter observation was substantiated by the S. E. M. x-ray scan shown in Figs. A-35(a) and (b). The elements contained in this area are in decreasing order of concentration Al, C, O, Ti, Si, Ca (the high percentage of C may be a consequence of the carbon coating necessary to prevent the sample from charging up in the S. E. M.). Thus it appears that the interaction seen between the anode and the anode support elements is a consequence of melting. Considering the elements involved, the lowest melting point eutectic that could occur would be for Al and Ni at 640°C. All other binary combinations yield higher melting points. This temperature is well above ambient for any part of the discharge chamber (excluding the cathode tip). Although the presence of mercury might have some influence on the metallurgical behavior, it is considered more probable that intense heating occurs during some form of transient occurrence such as a vacuum arc across the insulator surface.

On the supposition that some form of insulator deterioration might have contributed to initiation of the phenomena that resulted in melting of the anode support insulator, the ceramic material was examined further in the areas shown as 3 through 8 in Figs. A-31 and A-32. The magnified photograph of Area 3, shown in Fig. A-36(a), seems to show a coating of about 4 μm thickness. An attempt to scan the coating in this area with the S. E. M. microprobe showed only the elements C, Al, O, Ca, Si and Cl. A second attempt in Area 6 produced Ti and Fe as well (S. E. M. and the Al K_α x-ray scan are shown as Fig. A-37). Area 4 is in the damaged area, and it was thought that if the ceramic, which is predominantly Al_2O_3, was reduced to produce elemental Al, it would be possible to detect this by comparing the

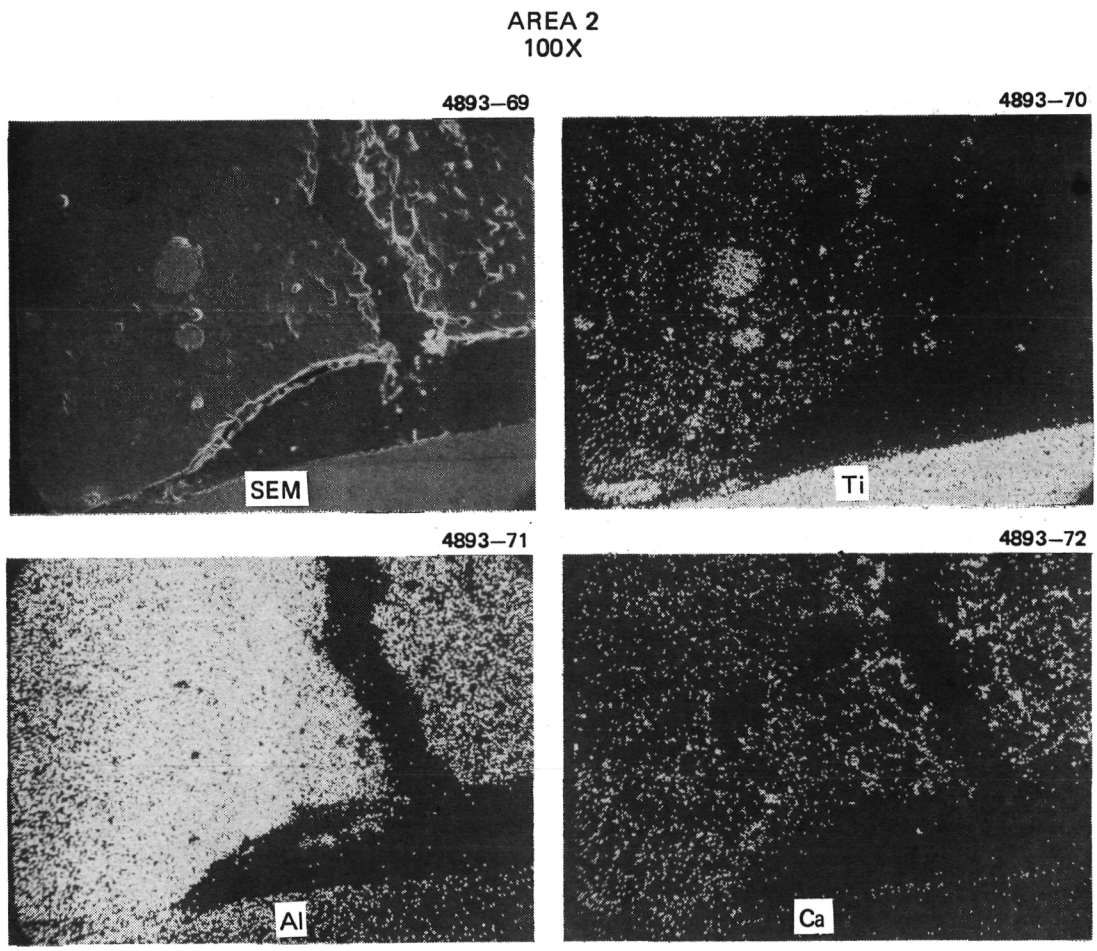

Figure A-35. Scanning electron microscope photo and K_α X-ray analysis of area 2 of damaged anode support.

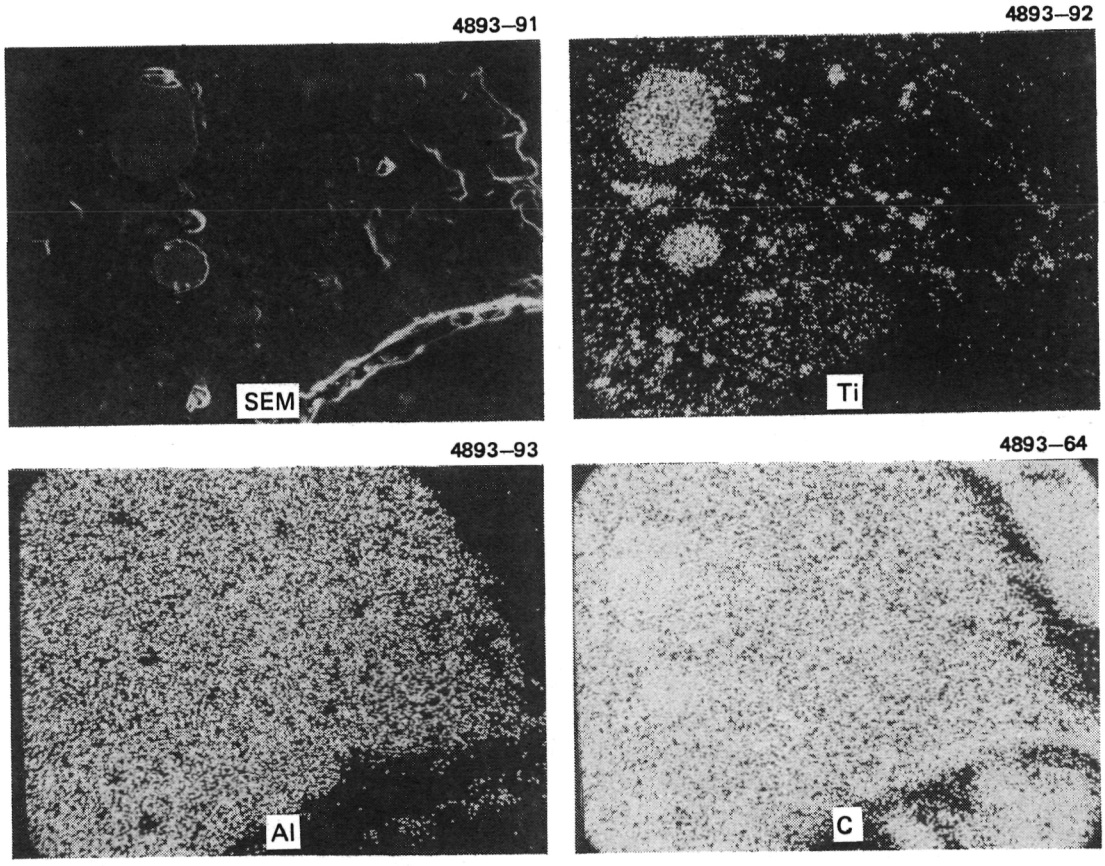

Figure A-35. (Continued).

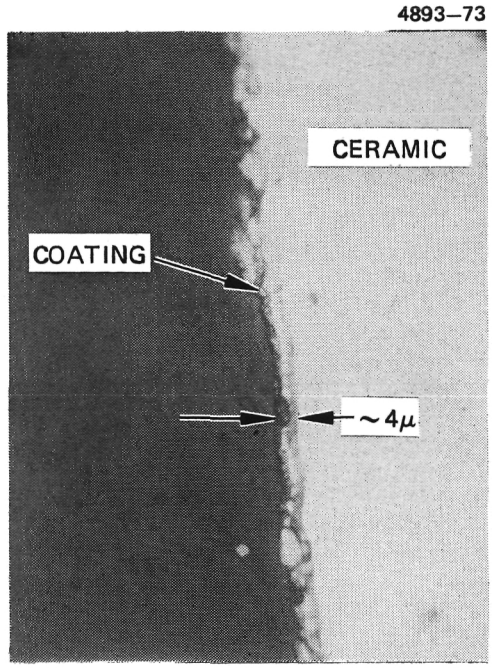

1000X

(a) AREA 3

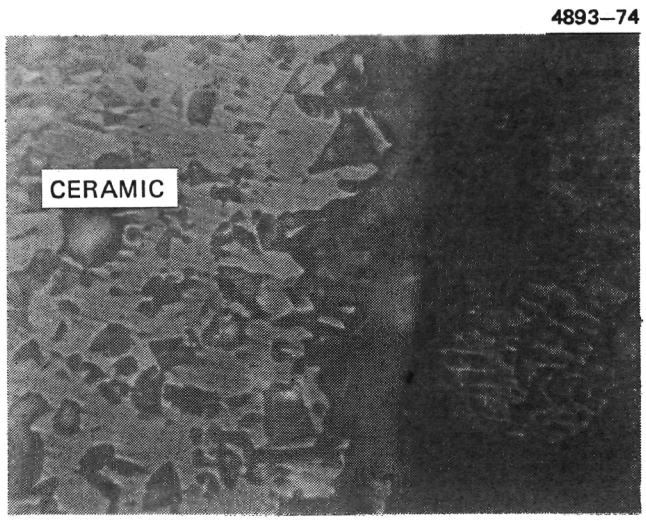

500X

(b) AREA 7

Figure A-36. Magnified view of regions 3, 7 and 8 of anode support No. 6.

4893–94

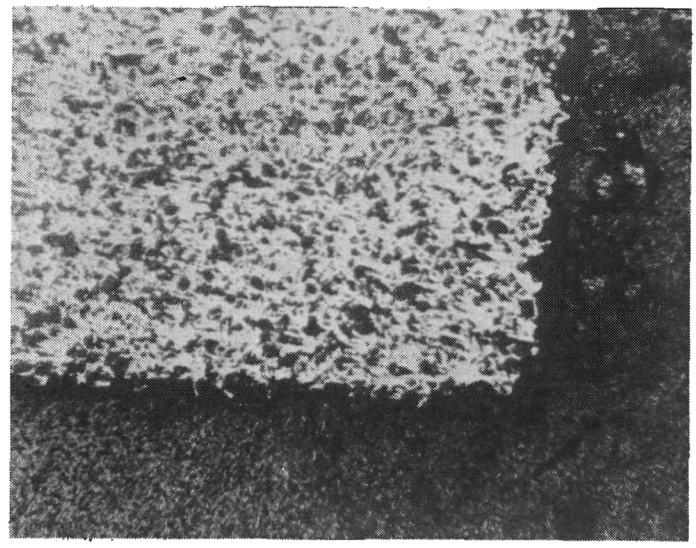

100X

4893–95

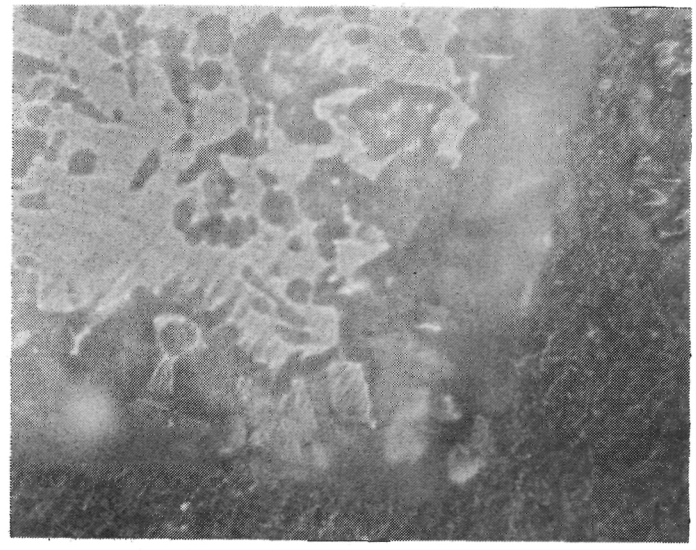

500X

(c) AREA 8

Figure A-36. (Continued).

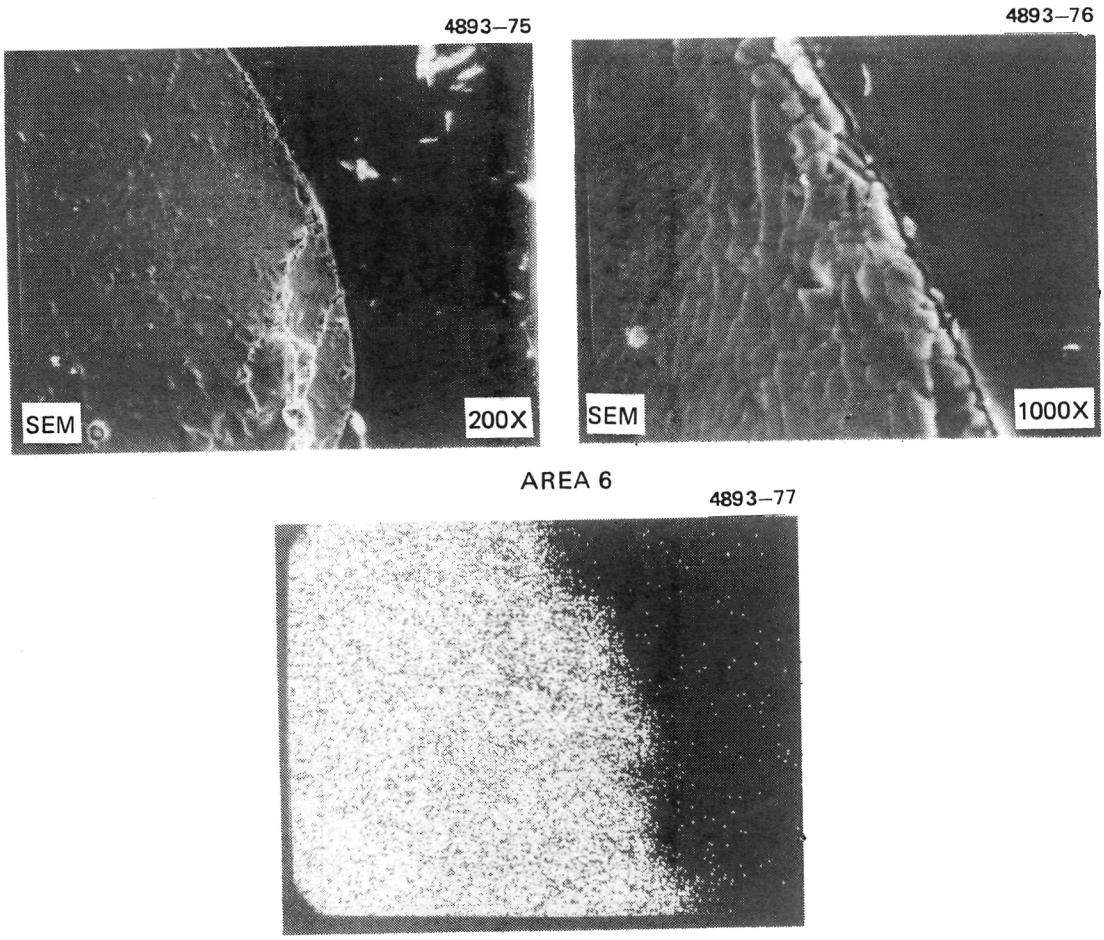

Figure A-37. S.E.M. photo and K_α X-ray analysis of area 6 of anode support No. 6.

relative concentrations of Al and O in the damaged and undamaged areas. Figure A-38 shows an attempt to compare the Al signals from the S. E. M. microprobe. Although it appears that the damaged area (left side of the void) has a greater concentration of Al in Fig. A-38, this is not necessarily the case, as shown by Fig. A-38 where the scan field has been shifted slightly. Thus, the apparent gradation in the concentration of Al depends more on the scan location than on the location in the material. Area 5, which is located in what is thought to be undamaged material shows no real variation in concentration of Al, no titanium, and the remaining impurities, Si and Ca, seen in Fig. A-39, are probably remnants of the polishing compound, trapped in the normal voids of the Al_2O_3. Areas 7 and 8 appear identical to area 5 under the microscope and no coating was discernable on the insulator surface. Consequently, these areas were not examined further with the S. E. M. microprobe.

The damage to the anode support insulators is concluded to be a melting or fusion of the Al_2O_3 insulator, the Ti anode, and the stainless steel machine screw. On the basis of the observable evidence, the only logical explanation of this melting is that local high temperature produces some alloying of the Ti and Al to form a moderately low temperature eutectic ($\sim 600^{\circ}$ to 800°C). On the basis of the "arc tracks" visible on the thruster shell, formation of a vacuum arc breakdown in the vicinity of the insulator seems to be the best explanation which can be offered for generation of these temperatures. Except for the coating seen on the insulator surface, there does not appear to be any deterioration of the bulk material. Because of the relatively low voltage applied to the anode, formation of an arc by the discharge supply might be considered unlikely, unless the applied voltage appears across a very small gap. This condition could be established if a conductive coating covered the entire anode support insulator except for a small gap between the anode and the insulator as shown in Fig. A-40. The coating and gap are shown on an exaggerated scale to illustrate the conjecture being developed here. The insulator surface would most probably charge to thruster shell potential because the thruster shell is clamped firmly between two mating

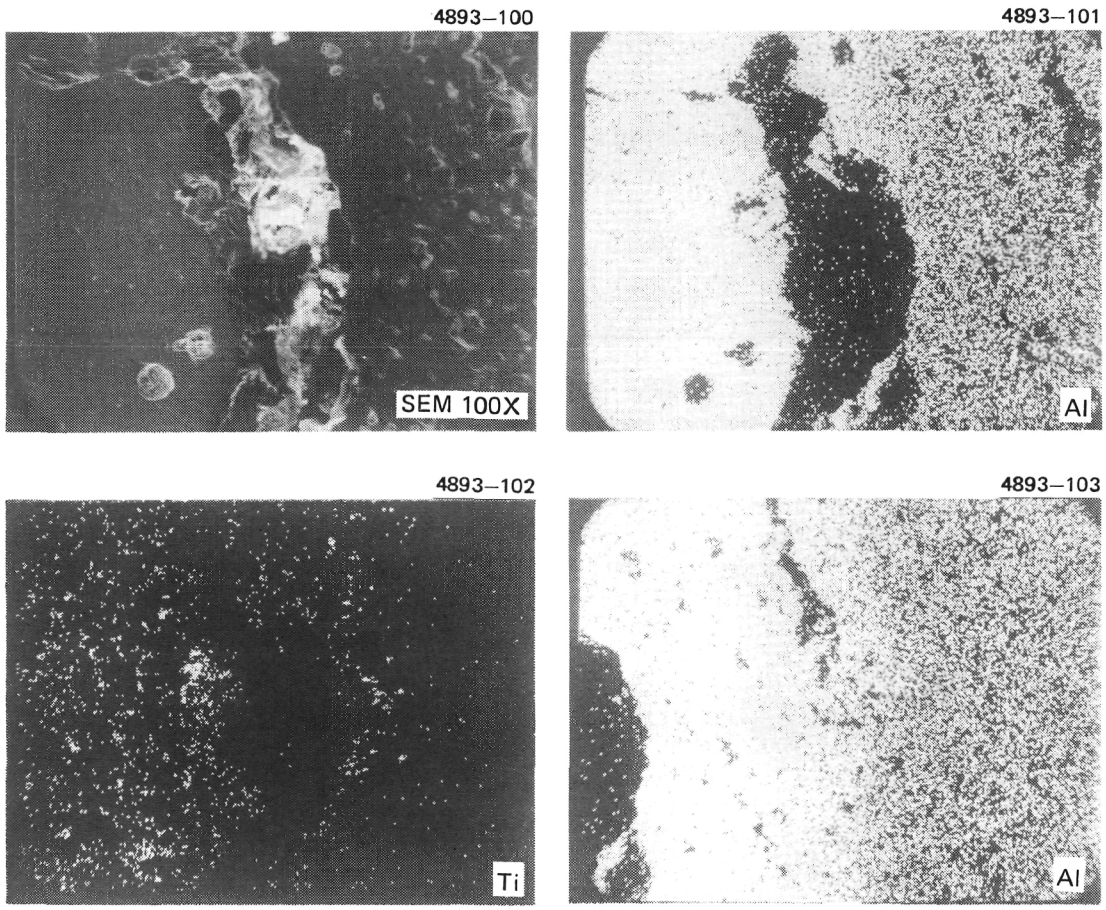

Figure A-38. S. E. M. photo and K_α X-ray analysis of area 4 of anode support No. 6.

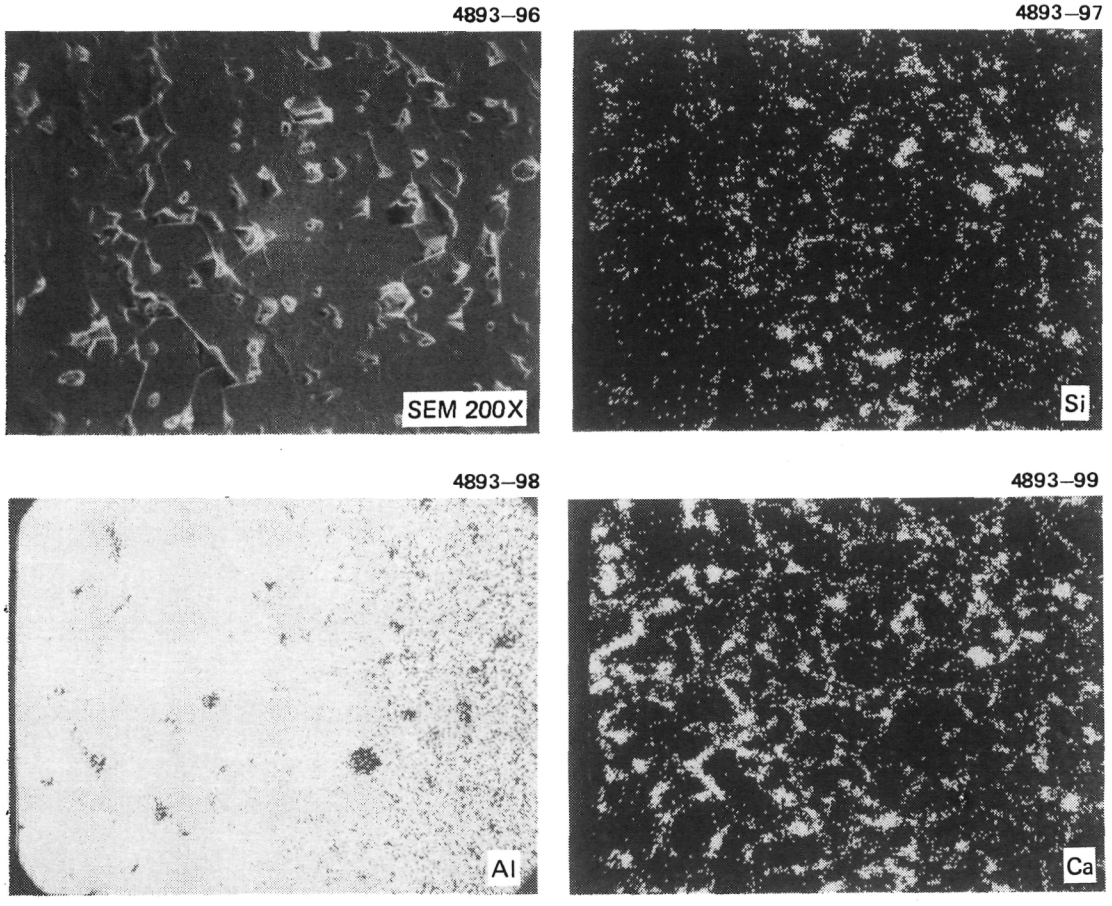

Figure A-39. S. E. M. photo and K_a X-ray analysis of area 5 of anode support No. 6.

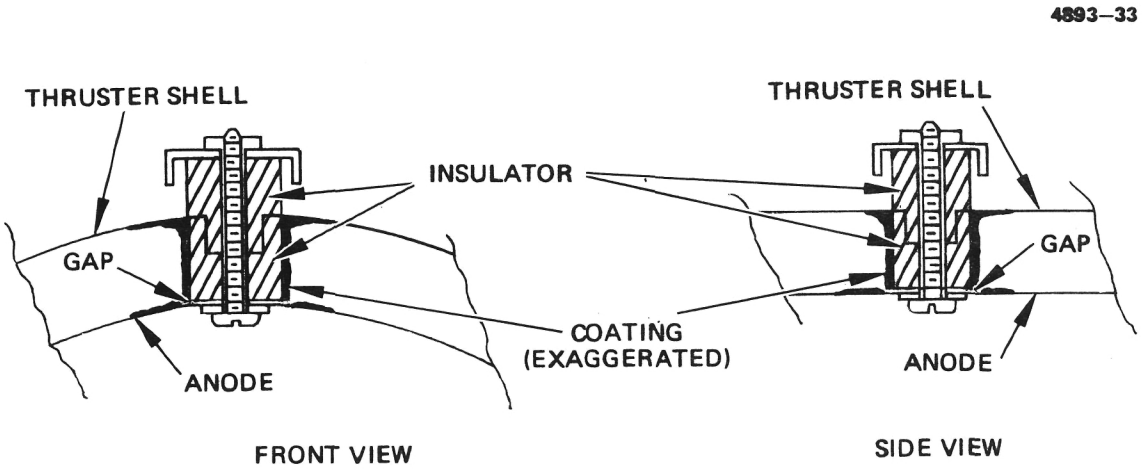

Figure A-40. Drawing illustrating possible explanation of cause of anode support damage.

ceramic parts, one being the coated insulator. The anode, on the other hand is backed by a washer, smaller in diameter than the ceramic, and this does not assure positive contact between the anode and the insulator at the edges. Moreover, the anode support insulator has a "pumpout slot" ground into the surface that mates with the anode. Consequently, a coating on the insulator would tend to form a "spark gap" as shown instead of merely providing a resistive path from shell to anode. The downstream anode supports cannot quite satisfy this condition because one of the anode stiffening ribs interferes with the insulators, requiring special grinding on the insulator. This probably improves the anode-insulator contact such that the insulator coating makes contact with the anode and no arcing occurs, (see Fig. A-29). Insulator Number 4, the upstream insulator which showed no damage could have also benefitted from improved anode contact because of the orientation of the "pumpout slot" with respect to the anode curvature (see Fig. A-30). While this explanation is highly speculative, it is the only one available that fits all the observations.

Thus, it has been concluded, that the observed damage to the anode insulators is a direct result of the deposition on the insulators, and that damage of the type sustained by insulators number 2 and 6 may be avoided by shadow shielding the insulators to prevent deposition from reducing the insulator length.

The propellant distribution plenum is the final component to be discussed in this section. Figure A-41 shows views of the discharge and propellant sides of the plenum after its removal from the backplate, enlargements of the screen covering the plenum ports, and the discharge chamber backplate with the plenum removed. Careful examination and measurement of the plenum revealed no evidence of deposit or erosion on either the downstream surface or the screens covering the ports (compare Figs. A-41(c) and (e)). Neither was it possible to obtain a measurable coating sample from the discolored areas seen on the back-plate in Fig. A-41(d), (where the plenum is normally situated). Deposits were found on the plenum's inner mounting plate and inner wall (Fig. A-41(a)). Although these deposits were not analyzed, they are assumed to have the same constituents as samples A and B listed in Table A-4.

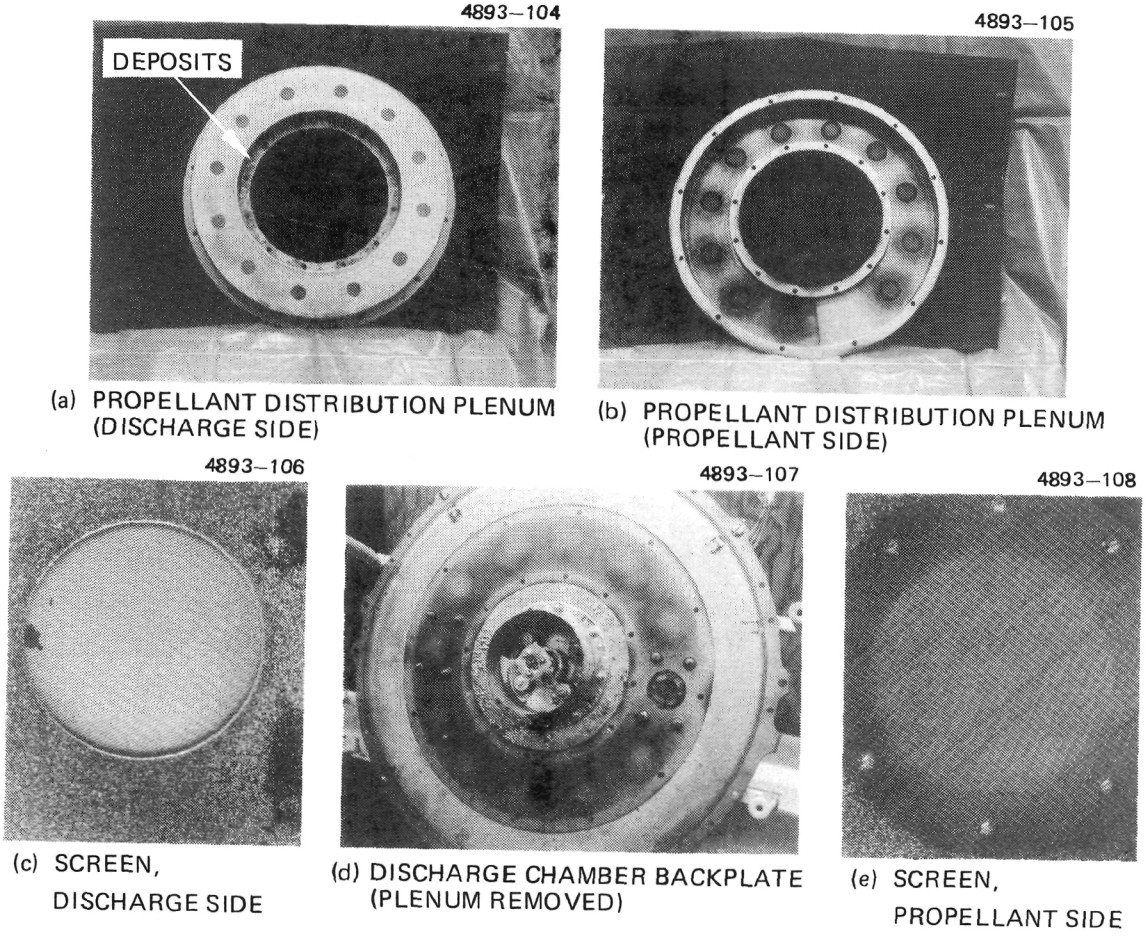

(a) PROPELLANT DISTRIBUTION PLENUM (DISCHARGE SIDE)

(b) PROPELLANT DISTRIBUTION PLENUM (PROPELLANT SIDE)

(c) SCREEN, DISCHARGE SIDE

(d) DISCHARGE CHAMBER BACKPLATE (PLENUM REMOVED)

(e) SCREEN, PROPELLANT SIDE

Figure A-41. Discharge and propellant sides of plenum and spreen which covered plenum ports.

Although some concern has been expressed by Hughes and NASA metallurgists with respect to embrittlement of titanium by Mercury, there was no evidence of embrittlement in the plenum or other discharge chamber components after 10,000 hours of exposure to mercury vapor. This is to say that no titanium part cracked in the manipulation which was necessary to disassemble the thruster components and the sheet metal parts (such as the plenum and anode) seemed as flexible as new parts. No tests were made to determine hardness or yield strength since these quantities are not considered of primary importance to thruster operation after a thrust system achieves orbit.

C. Cathode Pole Piece/Magnetic Baffle Assembly

The principal components of the cathode pole piece/magnetic baffle assembly are the following:

- Cathode pole and mounting flange
- Baffle
- Baffle control coil and its terminal insulators
- Keeper electrode and its support insulators
- Cathode subassembly.

This assembly and some of its components are the most severely worn of the thruster parts and exhibit radical modification of component dimensions, as indicated earlier in comparing Figs. A-14 and A-15. The extensive wear seen on these components is considered to be a consequence of ion sputtering, presumably dominated by doubly charged ions. Close-up photographs of this assembly illustrating the damage are presented in Figs. A-42 to A-45. By referring back to Fig. A-15, most of the component damage is obvious in these photographs. Some of the less obvious wear or damage is pointed out specifically in Figs. A-44 and A-45. One point of interest to be noted here is that the baffle coil sheath and the cathode radiator are eroded while the keeper electrode and most of the other cathode potential surfaces in their vicinity are

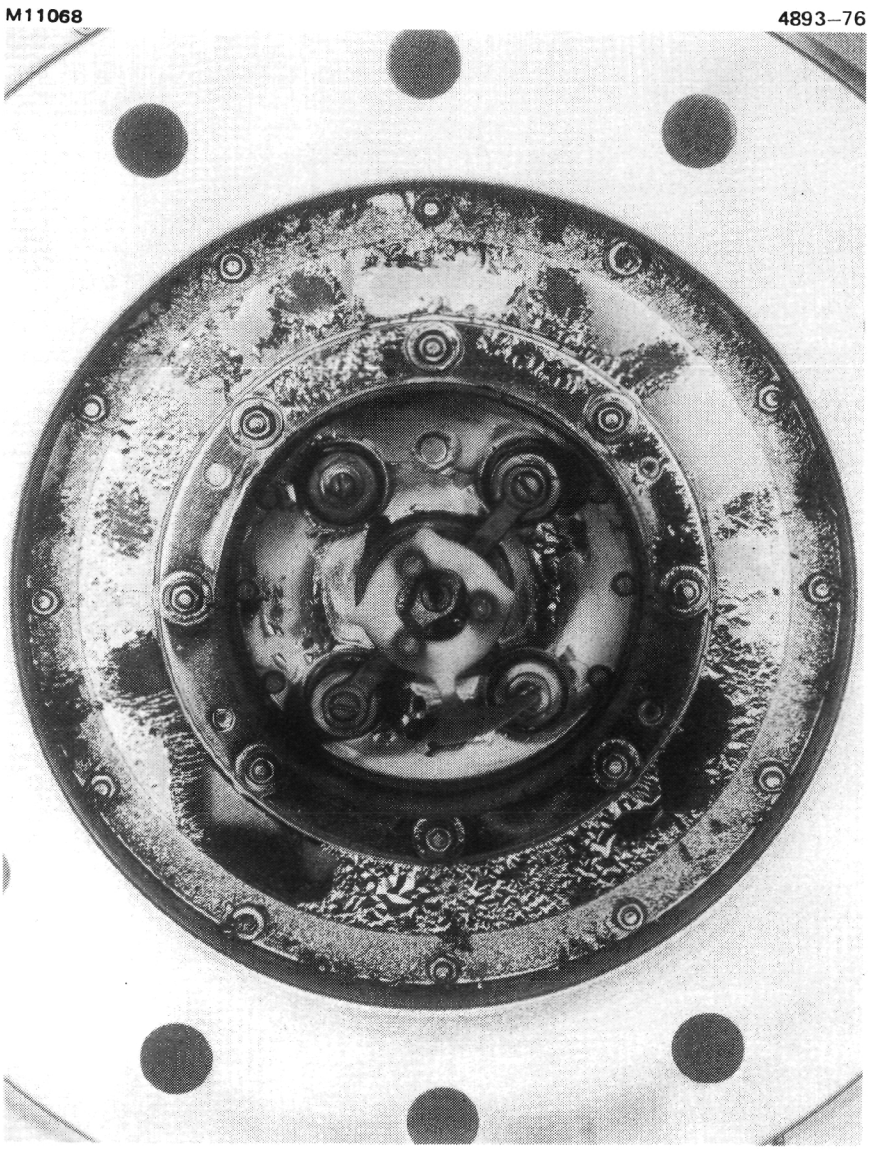

Figure A-42. Cathode pole piece/magnetic baffle assembly.

M11066

Figure A-43. Cathode pole piece/magnetic baffle assembly.

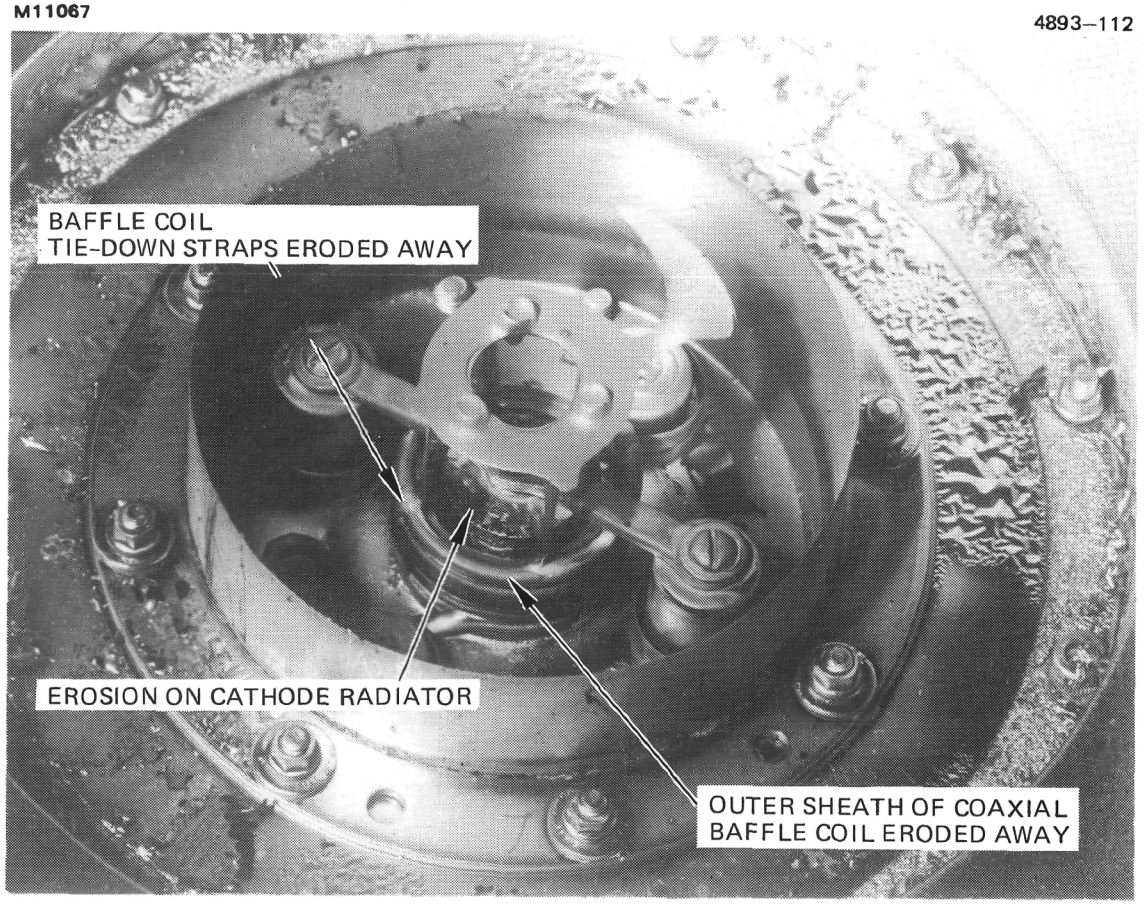

Figure A-44. Cathode pole piece/magnetic baffle assembly.

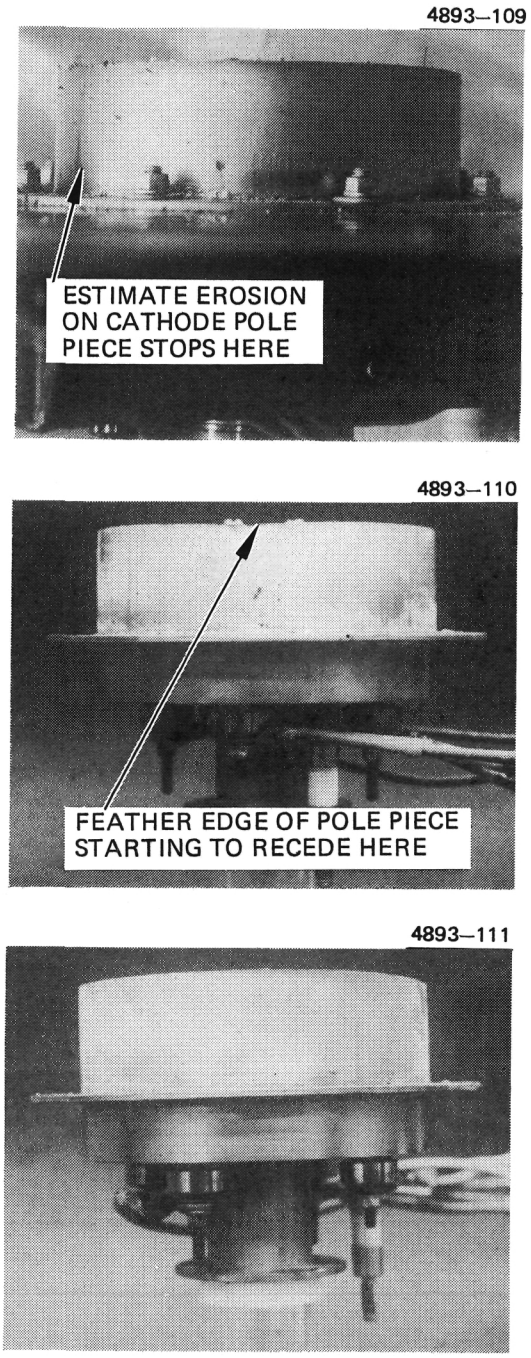

Figure A-45. Cathode pole piece/magnetic baffle assembly.

heavily deposited. The erosion patterns have an imperfect symmetry that seems related to the orientation of the baffle coil terminations. The outer conductor of the coaxial baffle coil is seen to be eroded away in Fig. A-44, exposing the insulator over a relatively large area, while the counterpart of the coil seen in Fig. A-43 shows penetration of the coils outer sheath over a relatively smaller area. Similarly, a remnant of the baffle coil tie-down strap can be seen on the downstream side of the coil in Fig. A-43, whereas the counterpart strap is seen in Fig. A-44 to be completely eroded away on the downstream end and barely visible on the upstream end. It has not been possible to formulate a cohesive explanation for the erosion seen on the baffle coil and cathode radiator. The generally accepted model of the discharge chamber plasma potential distribution would place the plasma potential within the cathode pole piece at approximately the keeper voltage. Thus, no doubly charged ions should be formed in the region and singly charged ions should not be capable of causing damage. It is possible that this erosion is entirely a consequence of exposure to high energy ions from the discharge chamber after the baffle was eroded away. However taking note of the pattern of baffle wear in these photographs, it is apparent that remnants of the baffle show a "spoke-like" configuration and these remaining elements are aligned with the four baffle support members. This could be interpreted as a shielding of the baffle from ions originating within the support structure or as a magnetic field effect. No conclusive evidence exists to determine whether the erosion pointed out in Fig. A-44 is "typical" or a consequence of operation without the baffle.

Similarly, in examining the erosion of the baffle and cathode pole piece, it has not been possible to determine where the eroding particles originate. The cylindrical pole piece is worn to a "feather" edge on the downstream side and as shown in Fig. A-45(b), this wear has begun to reduce the pole piece length. The erosion seems to end upstream of the region indicated in Fig. A-45(a).

Closer examination of the keeper electrode disclosed heavy deposition on the upstream surface, light deposition on the downstream side, and slight erosion around the keeper orifice on the downstream side. Illustrations of this deposition and erosion are seen in Figs. A-46 through A-48. The deposition seen increased the weight of the keeper by 0.545g (about 12% of the keeper weight) and the keeper thickness by 0.02 in. (0.05 cm). The coating is very adherent and shows no tendency to form "flakes" although protrusions that have the appearance of "flakes or chips" embedded in the coating can be seen in Fig. A-46. Erosion of the keeper aperture is apparent in Fig. A-46(b) also. The keeper aperture diameter measured before the test was 0.184 in. (0.467 cm) and the asymmetric increase in diameter noted is considered inconsequential to thruster operation. Consequently, the keeper electrode is considered to have been relatively unaffected by the 10,000 hours of testing.

It was thought that a detailed analysis of the keeper deposits might offer some explanation of the erosion process or history and the sectioned keeper was analyzed using the electron beam microprobe. The "layered appearance of the upstream coating seen in Fig. A-48(a) can also be seen in the S.E.M. photograph and to some extent in the elemental analysis scans of Fig. A-49. The elements found were Fe, Ta, Ni, Cr, and K. The distribution was more or less uniform throughout the coating hence it was not possible to establish a time history based on an abrupt appearance of one of the elements. The Fe, Ni, and Cr are thought to originate in the stainless steel baffle coil sheath and tie-down straps while the Ta originates in the cathode radiator. Next, an attempt was made to relate the layer thickness to test events as indicated in Table A-5, starting the layer formation at either the start of the test, or at the appearance of the hole in the baffle. Changes in thruster beam current were selected as the test events for correlation. As shown in Table A-5, there is no significant relationship between the selected test events and the layer structure (thickness).

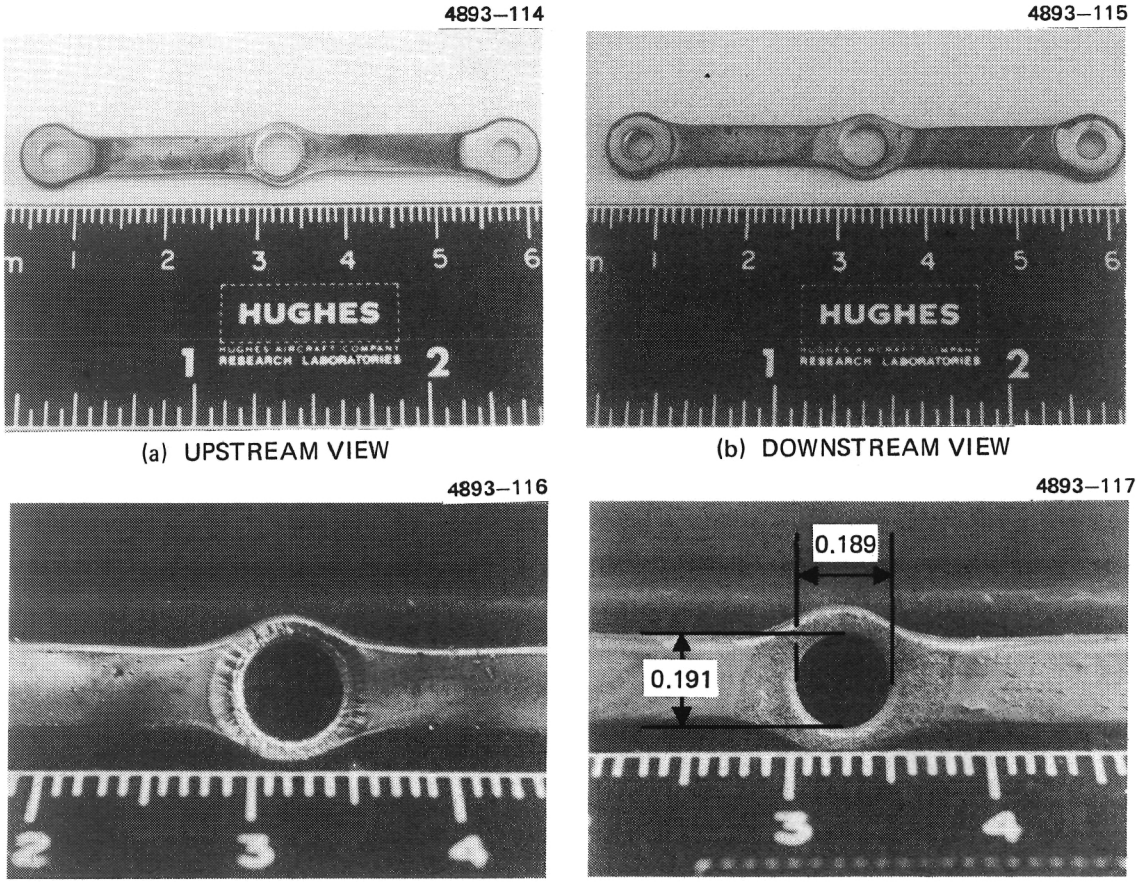

Figure A-46. Cathode keeper.

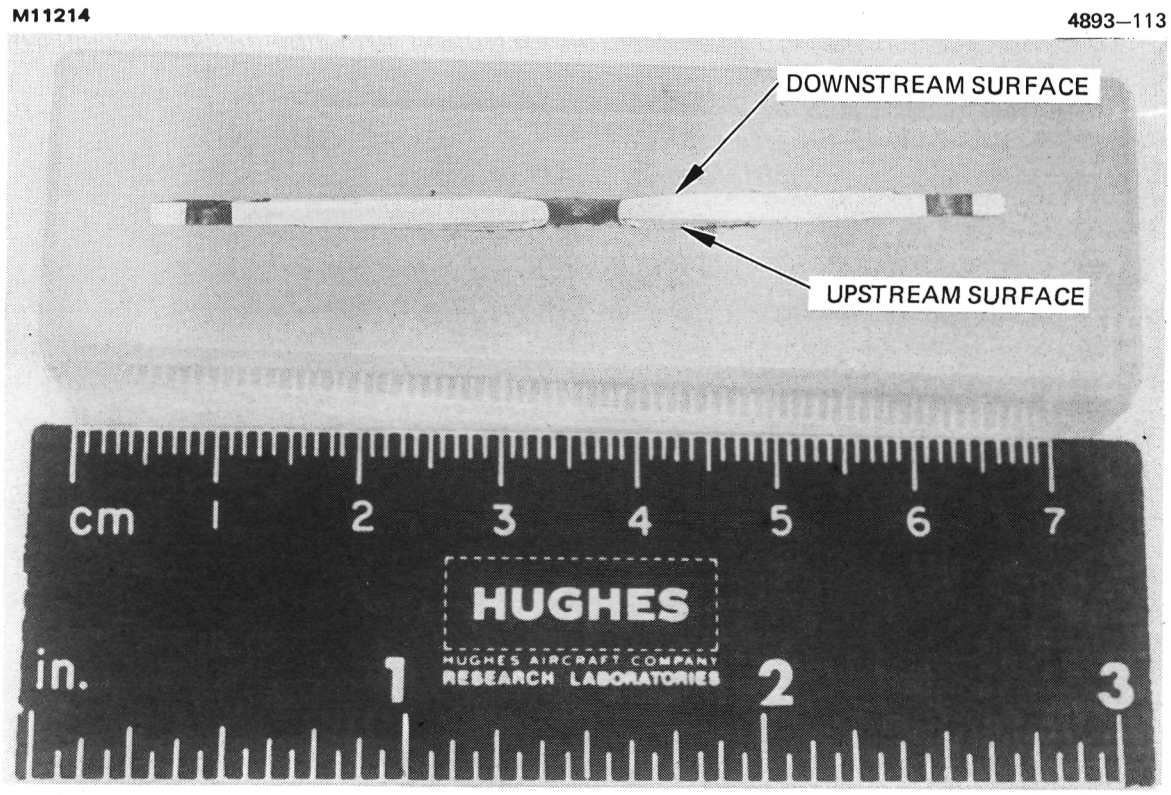

Figure A-47. Cathode keeper.

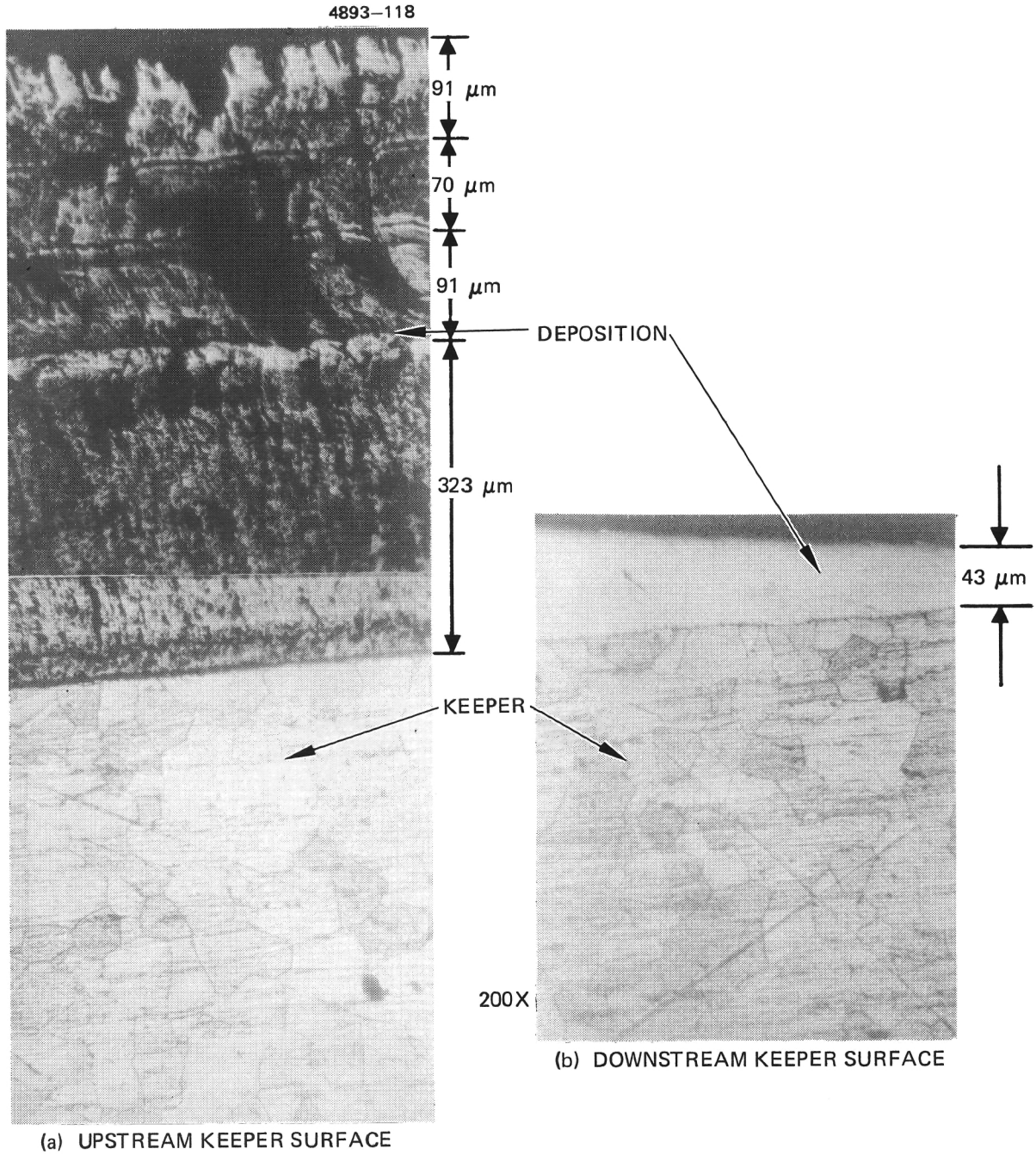

Figure A-48. Magnified views of cathode keeper.

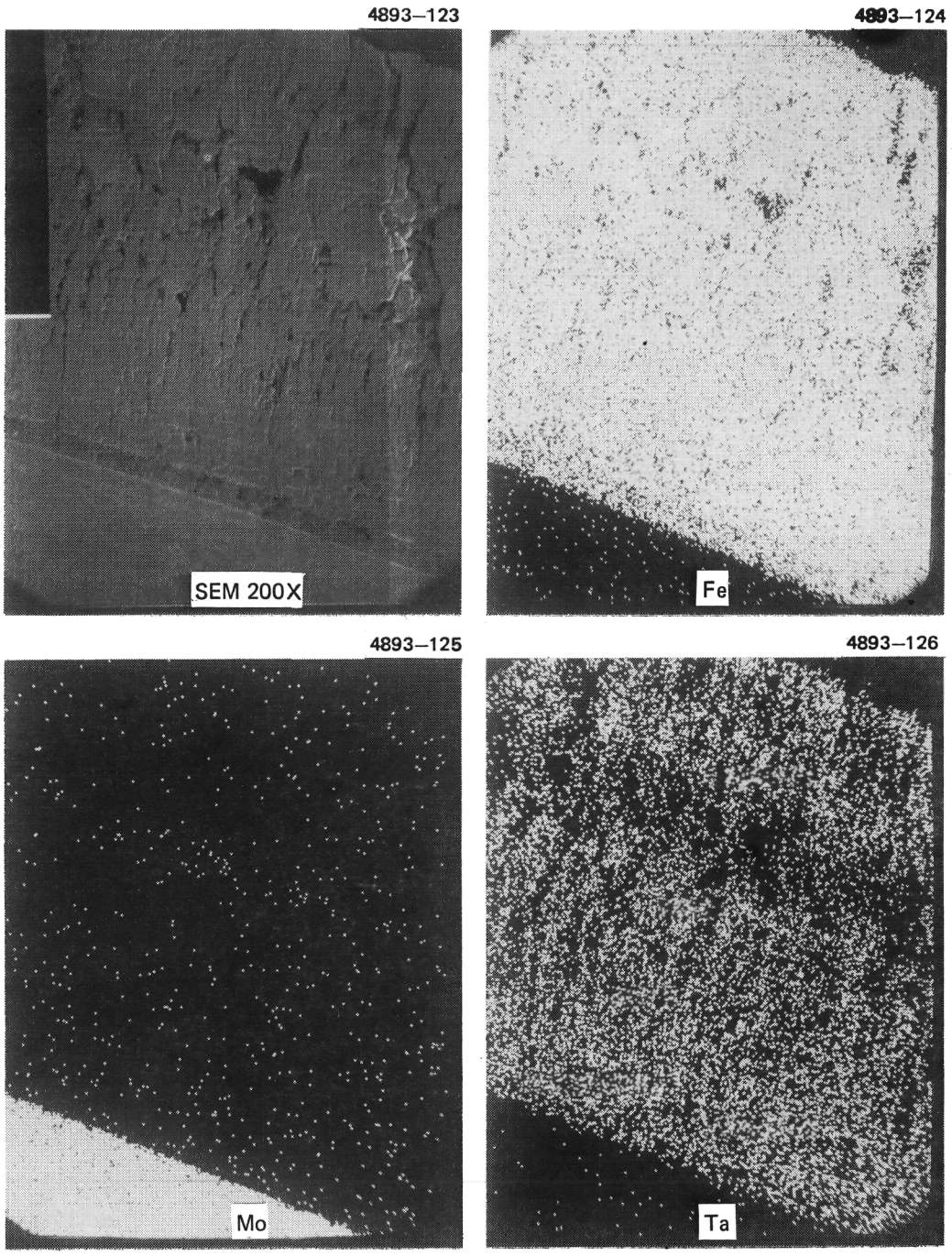

Figure A-49. S.E.M. photo and K_α X-ray analysis of upstream keeper coating.

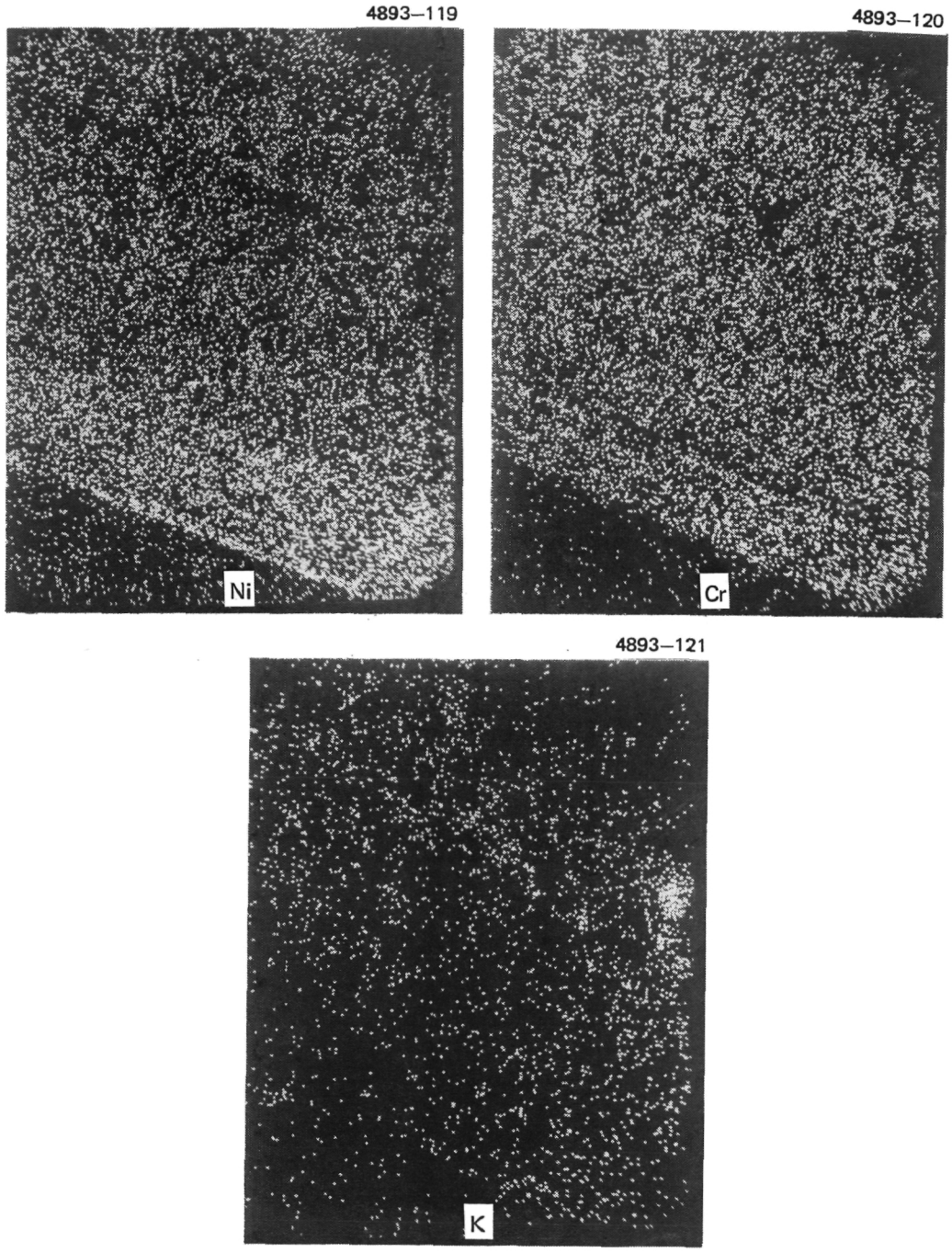

Figure A-49. (Continued).

Table A-5. Comparison of Endurance Test Events and Hypothetical Events Based on Keeper Deposit Layers

Endurance Test Events		Layer Thickness Assumed Linearly Proportional to Hours or Ampere-Hours			
Test Hour	Test Ampere-Hour	Hours	Ampere-Hour	Hours	Ampere-Hours
0	0	0	0		
2,100	3,150				
2,800	4,270				
3,000	4,610				
		5,617	7,912		
5,845 (A)	9,589 (A)			5,845(0)	9,589(0)
6,100	10,035				
			10,141		
7,200	11,685	7,200			
			11,856	8,179	
		8,761			12,114
				8,836	12,826
9,300				9,300	13,376
	13,685				
10,000	14,085	10,000	14,085	10,000	14,085

All test events correspond to beam current changes except (A) which is the test time that the hole in the baffle was noted.

T1856

The coating on the downstream surface of the keeper does not have the same sort of layer structure and the composition of the deposit is slightly different. This coating is predominantly iron, presumably from the baffle support, with some Ta and Cr. There seems to be one thin line in the electron beam scan for Mo (see Fig. A-50) that appears to be richer in Mo. Except for this unexplainable observation the coating on the downstream surface of the keeper provides little or no new information.

It is apparent in Figs. A-43 and A-44 that removal of the machine screws which secure the baffle to its support is a questionable operation because of the erosion of the baffle supports, which weakens the structure, and because the heads of the screws are eroded to the extent that they cannot be gripped by any tool. After several unsuccessful attempts at removing these screws, the entire support was removed with a high speed abrasive wheel. Several photographs showing the structure as it was removed in several views and variations in focus are included in Fig. A-51. Note that the erosion on the baffle fastening screws is predominantly on the inner side. It is also of interest to note that a thin lip of the baffle remains extending beyond the outer diameter of the baffle support, as if the baffle had been shielded from internally generated ions by the baffle support, (further evidence to support concept of erosion by ions from the cathode plasma). The wear on this structure is documented and recorded in Fig. A-52 by dimensional measurements at the locations indicated. The most wear occurred on Member C, in agreement with the asymmetry in wear seen on the baffle itself and the pole piece.

Having documented the support structure in this manner, a second attempt at removing the baffle fastening screws proved successful but the baffle still could not be removed, and was found to be securely "welded" in place. The assembly was then sectioned as shown in Fig. A-53 and the "welded" region was identified as a nickel "braze" by means of the electron beam microprobe analysis shown in Fig. A-54. It is thought that the nickel coating placed on the mild steel parts to prevent oxidation is responsible for the "welding" of these parts. It is

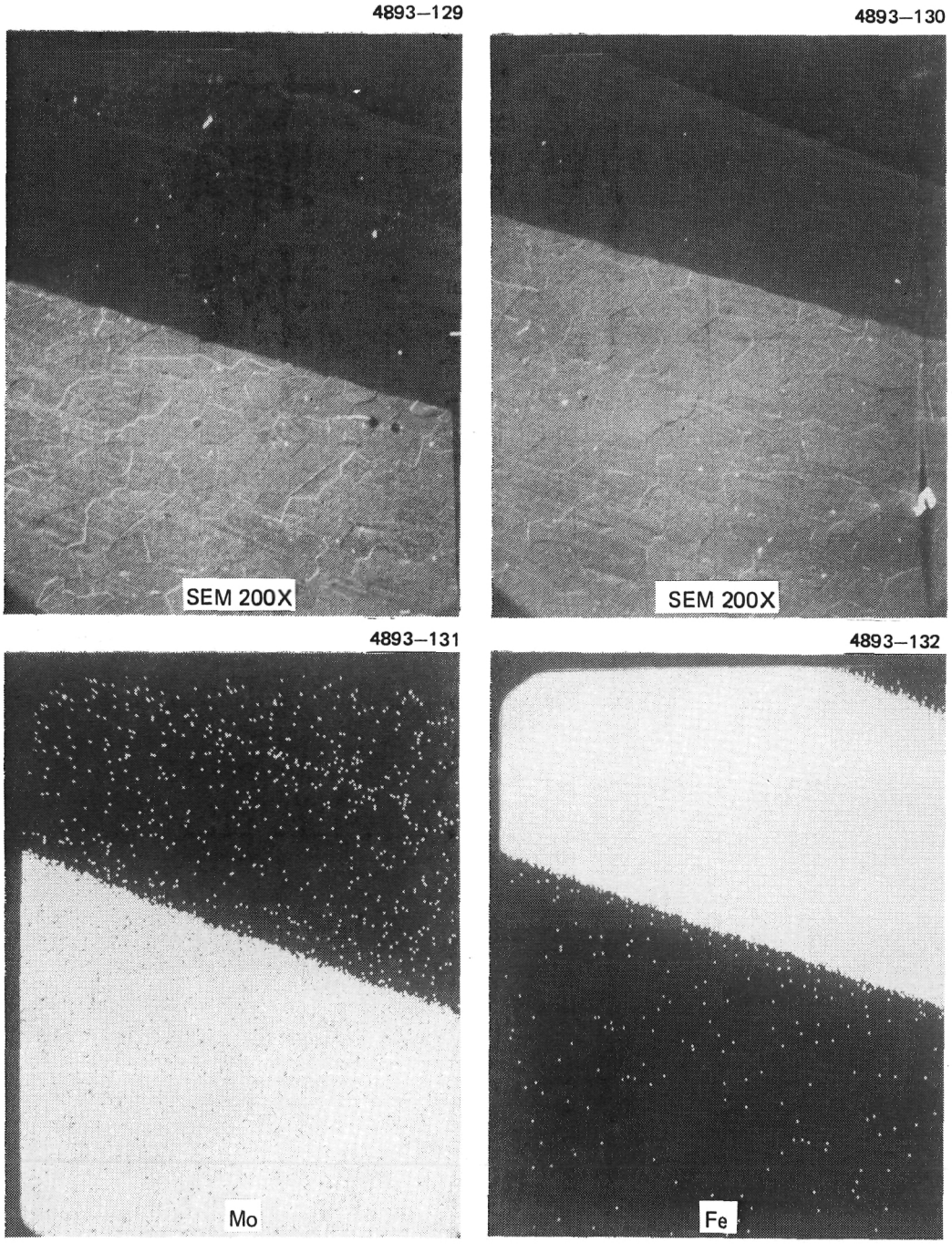

Figure A-50. S. E. M. photo and K_α X-ray analysis of downstream keeper coating.

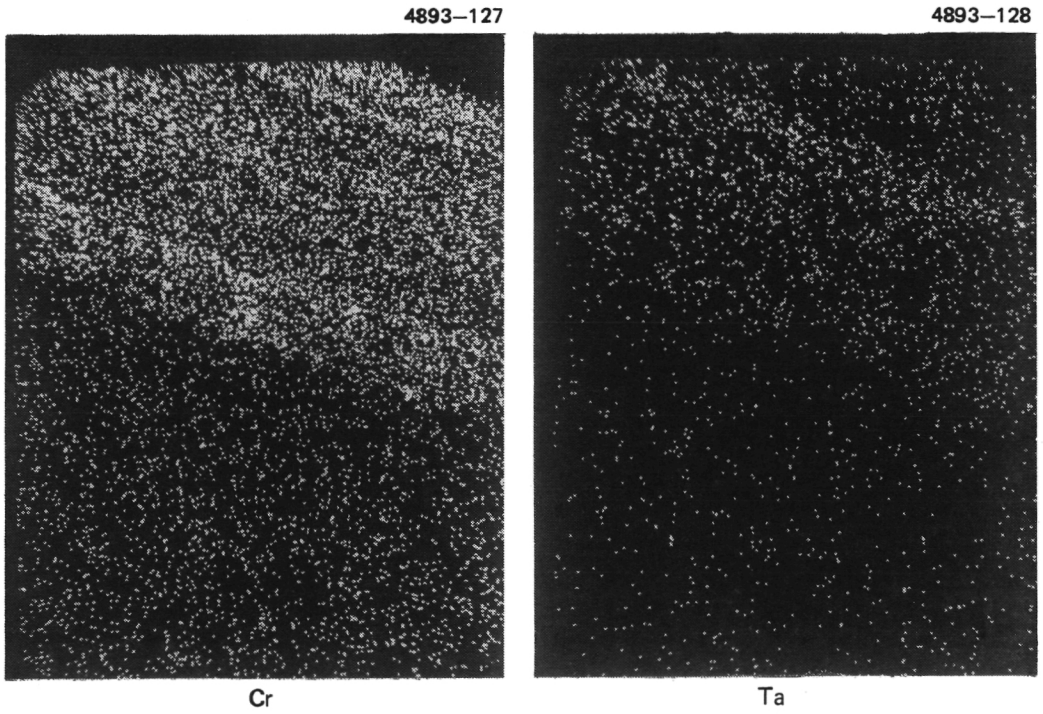

Figure A-50. (Continued).

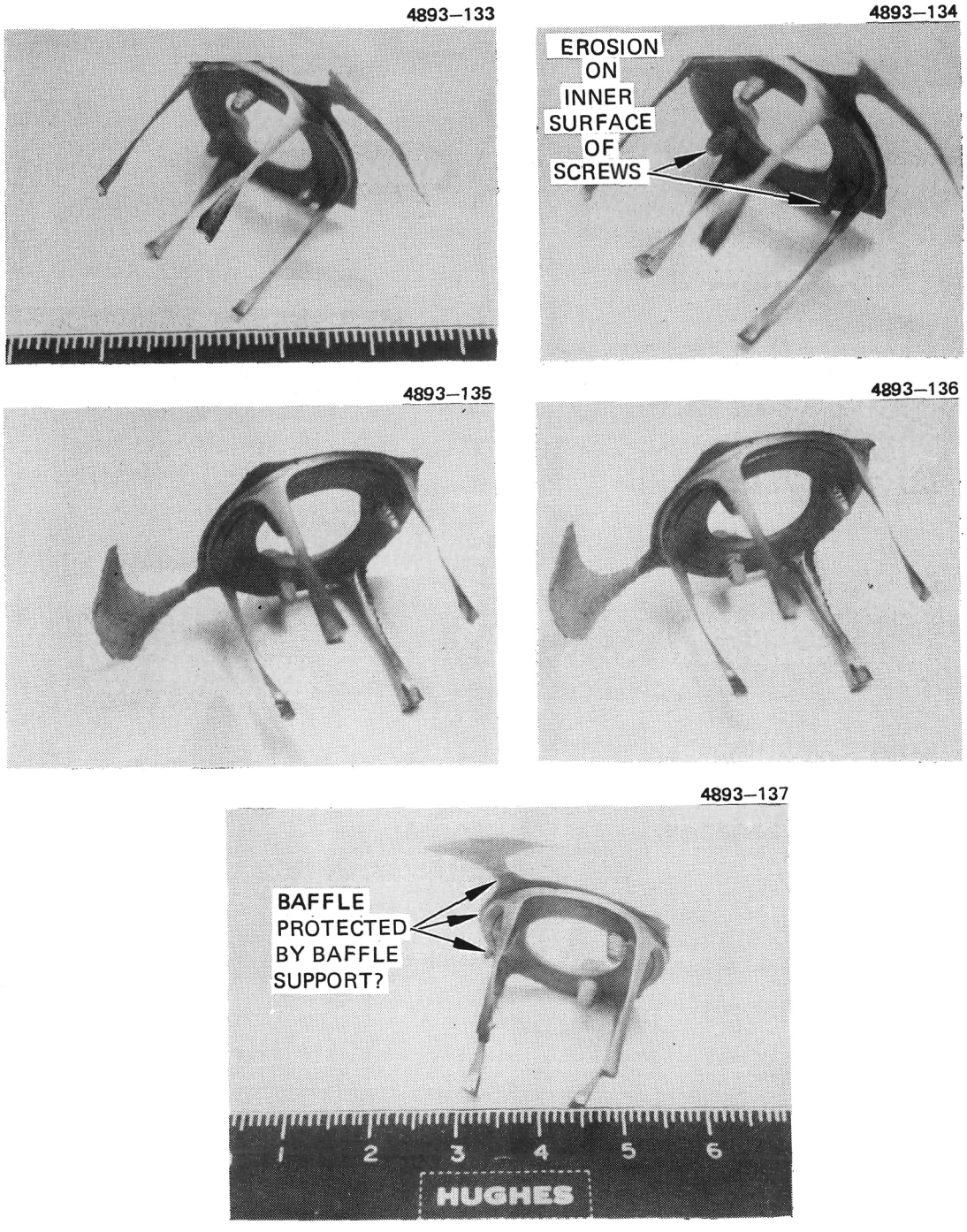

Figure A-51. Baffle support.

4893–34

ENDURANCE TEST BAFFLE
SUPPORT DIMENSIONS

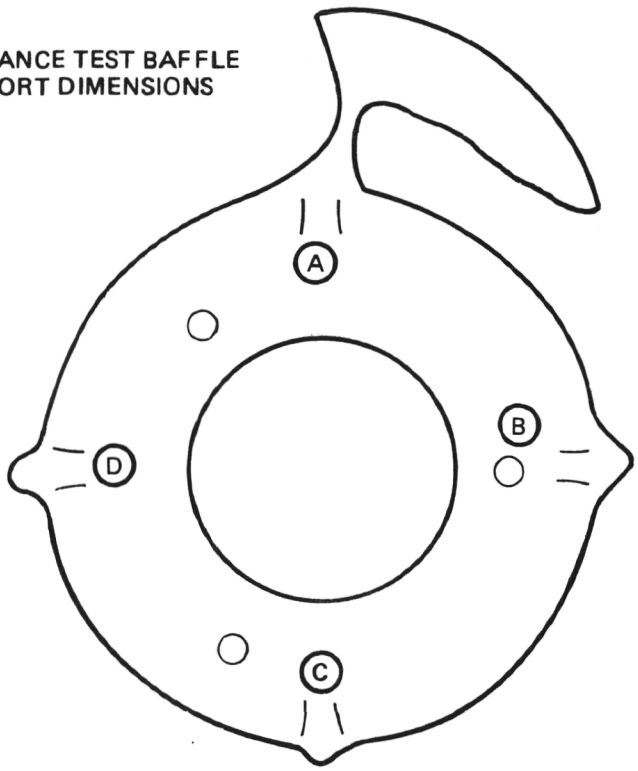

UPSTREAM VIEW

	A	A′	B	B′	C	C′	D	D′
1	0.135	0.053	0.132	0.057	0.131	0.052	0.134	0.054
2	0.082	0.047	0.084	0.048	0.081	0.037	0.090	0.043
3	0.080	0.029	0.062	0.030	0.052	0.021	0.070	0.030
4	0.030	0.008	0.055	0.020	0.019	0.003	0.052	0.017
5	0.057	0.021	0.072	0.030	0.037	0.020	0.068	0.027
6	0.086	0.047	0.090	0.047	0.077	0.045	0.089	0.045
7	0.102	0.050	0.106	0.051	0.102	0.049	0.108	0.045

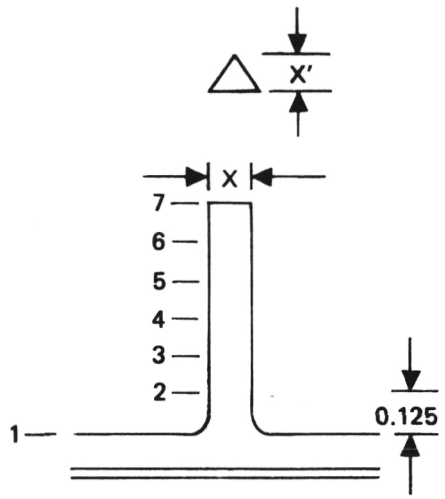

Figure A-52. Endurance test baffle support dimensions.

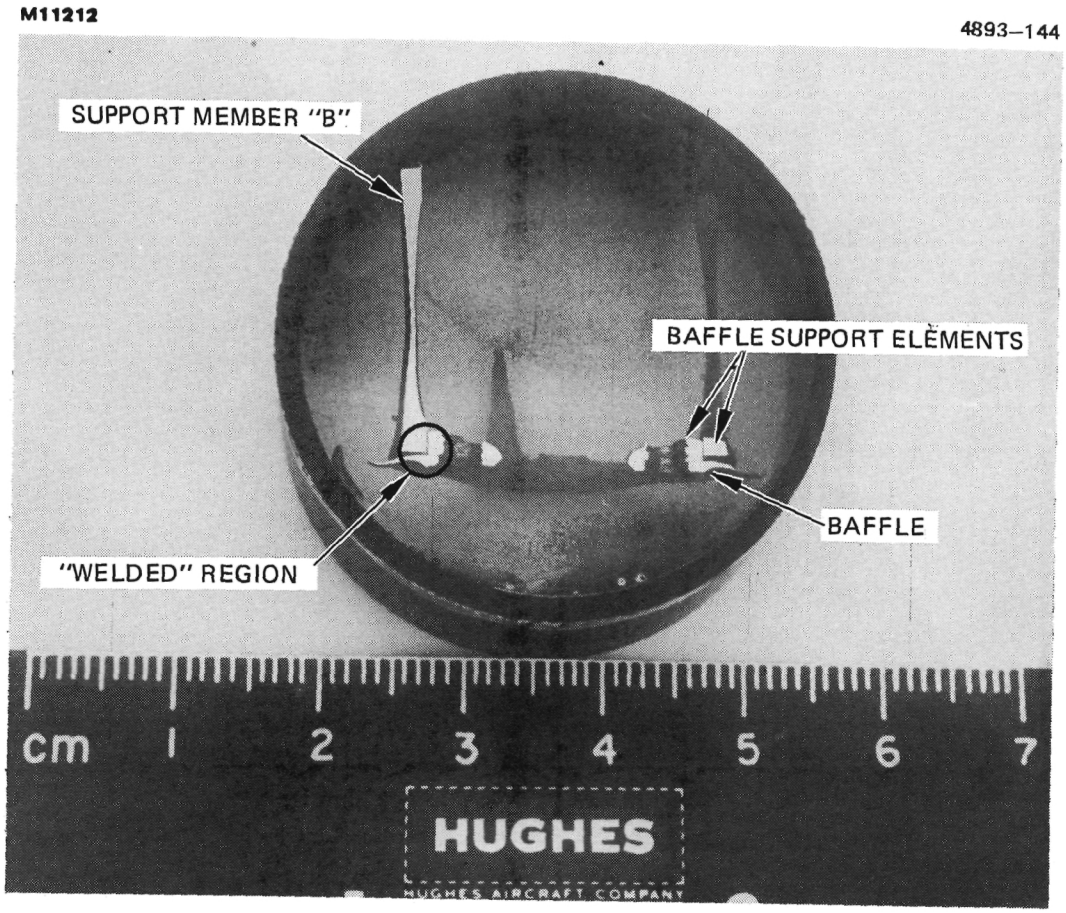

Figure A-53. Magnified view of baffle support cross-section.

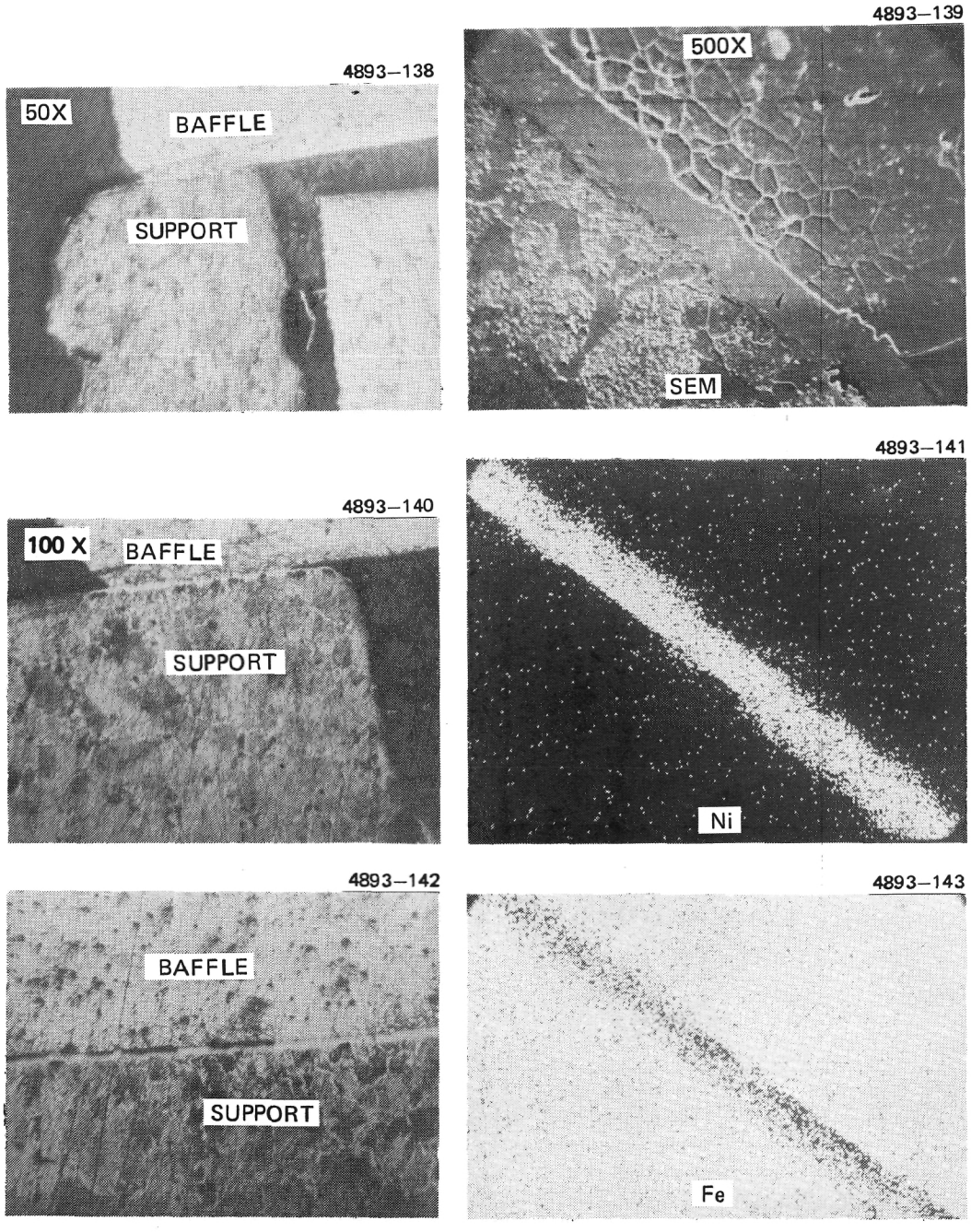

Figure A-54. S. E. M. photo and electron beam microprobe analysis of "welded" region of baffle support.

not known whether the fusion of these nickel coatings occurred by cold flow under the pressure of the fastening screws, or whether it was aided by an abnormally high temperature. Thus, the one part of the thruster that was extensively documented prior to the test — the baffle — could not be similarly analyzed in the post-test examination.

Other observations that were made in examining this assembly are documented in Figs. A-55 and A-56. Deposition on the keeper support insulator and shield, and the baffle coil termination insulators and shield is shown in Fig. A-55. This deposition did not cause any problems in the test, but suggests a need for double shielding of the insulators and surface treatment on the shields to prevent formation of sizeable "flakes". Baffle coil termination will be made outside the discharge chamber in subsequent thrusters. A portion of the flake removed from the keeper insulator (Fig. A-55(b) was 0.0015 in. thick (0.004 cm) and would be extremely hazardous to thruster operability if it lodged between the ion optics grid. Figure A-56 shows the cathode subassembly as it appeared after removal (the threaded rods seen were used to facilitate handling). The discussion of cathode condition is deferred to a later section; however, the erosion on the cathode radiator that was visible in Figs. A-43 and A-44 can be seen more readily here. This damage is considered of little importance to either the operation or lifetime of the cathode.

In summary, the major wear to the cathode pole piece/baffle assembly was sustained by the cylindrical pole piece, the baffle, and the baffle support members. These components are considered near end of life after 10,000 hours (14,000 ampere-hours) of testing. The wearout process is thought to be ion sputtering but it has not been possible to determine the details of the process by examination of the eroded parts. The maximum erosion rate, by whatever the process, is derived from the penetration time (5845 hours) of the baffle (0.029 thick) and is 9.4 μin. per hour (0.12 μm/hour). This quantity can be expressed in terms of ampere hours as 3.02 μin. per ampere-hour (0.08 μm/amp-hr). To achieve long thruster lifetime, this erosion rate must either be reduced appreciably or these eroded components must be

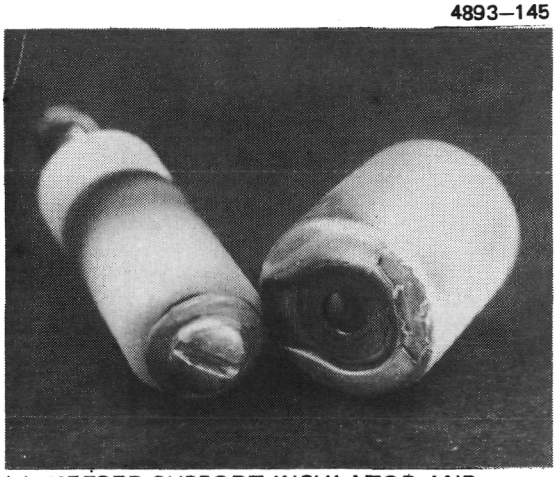

(a) KEEPER SUPPORT INSULATOR AND SHIELD

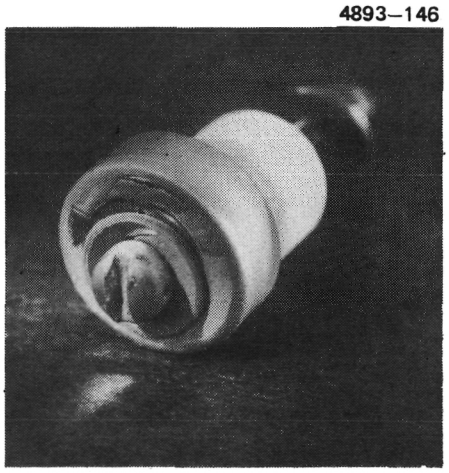

(c) BAFFLE TERMINAL INSULATOR AND SHIELD

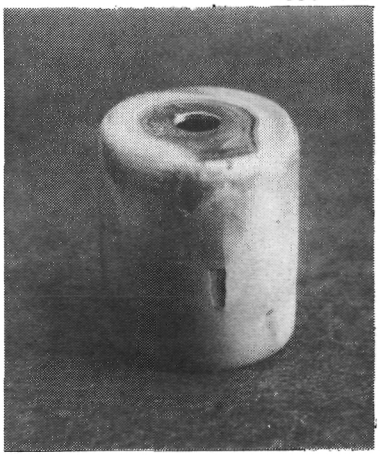

(b) KEEPER INSULATOR SHIELD

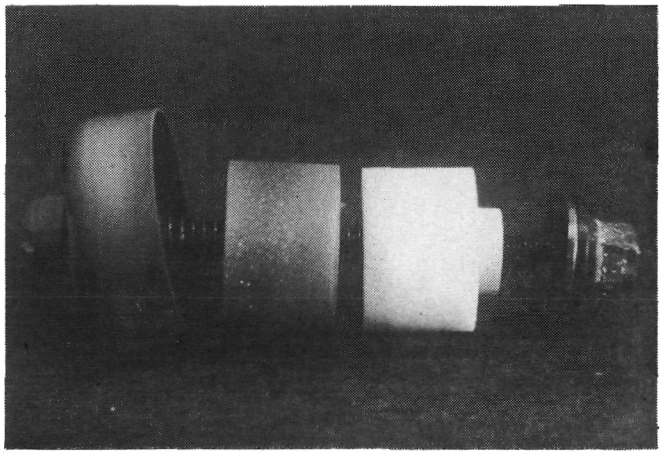

(d) BAFFLE TERMINAL INSULATOR AND SHIELD

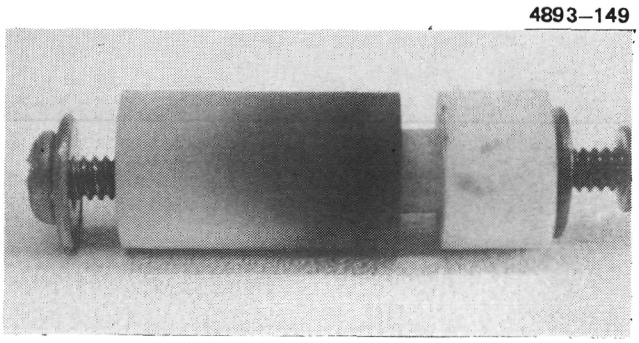

(e) KEEPER SUPPORT INSULATOR

Figure A-55. Cathode keeper supports and baffle terminal supports.

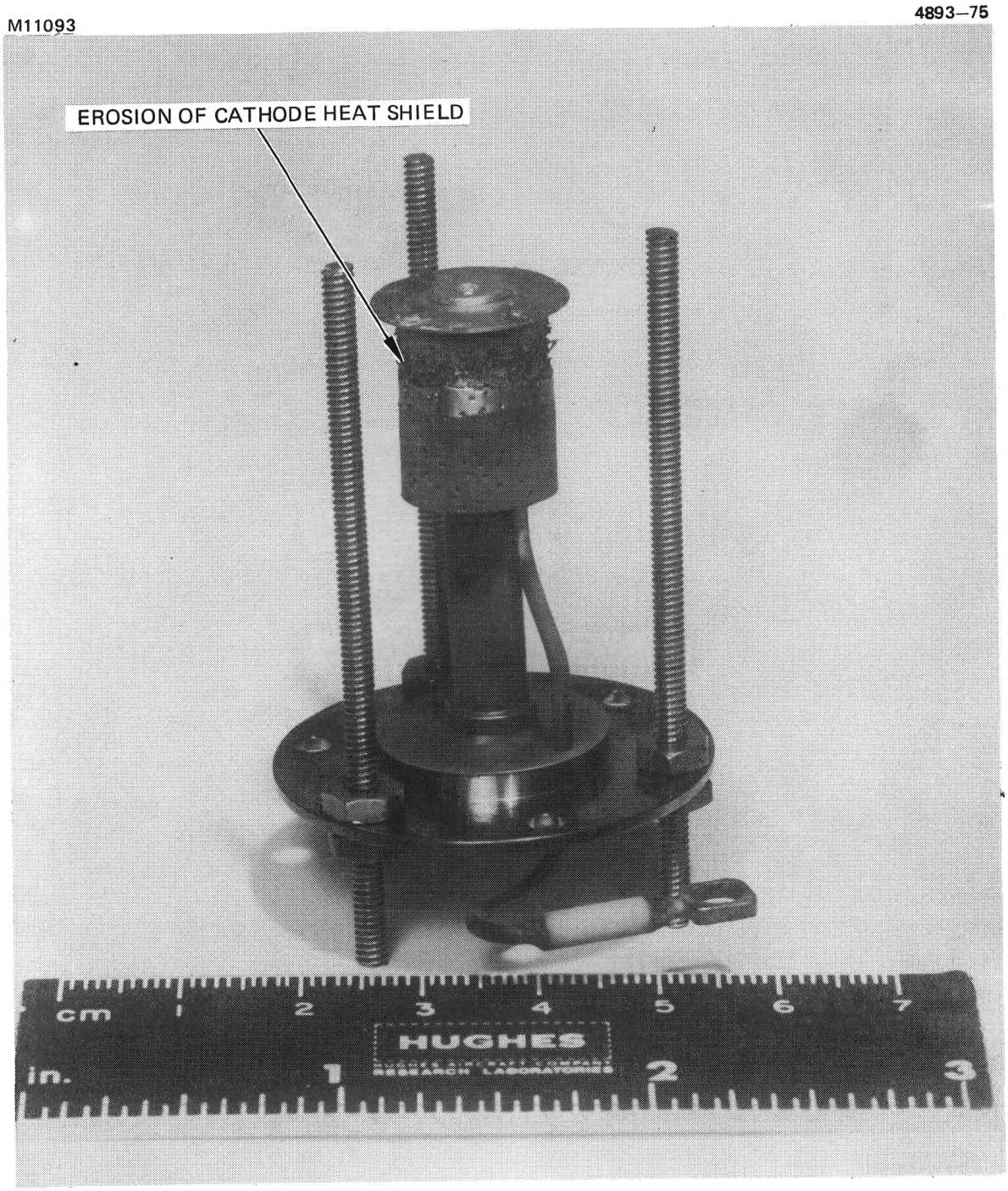

Figure A-56. Thruster cathode.

adequately protected. Diagnostic work in the area of discharge chamber sputter erosion and deposition has also been reported in references 4 and 5.

D. Ion Optics Assembly

The ion optics assembly is perhaps the most important single subassembly to the operational characteristics of the ion thruster. Its principal components as discussed here are:

- The accelerator electrode
- The screen grid electrode
- The electrode support assembly.

Before discussing the component parts individually, several measurements and observations concerning the complete assembly will be presented. After completion of the 10,000 hours of testing, the ion optics assembly was removed from the life test thruster, photographed, and measured to determine whether the inter-electrode grid spacing had changed. Tables A-6 and A-7 give the electrode specifications and spacing measurements recorded before and after testing. There appears to be a tendency for the spacings to be somewhat smaller in Table A-7 but the change is considered relatively insignificant. The grids were next cleaned as carefully as possible (to remove the flakes) and mounted on thruster SN 301B, which is the laboratory prototype version of the 700 series design. Thruster operation with the optics assembly was normal except for an extremely high arc rate. The grid set was capable of operation at ever increasing arc rate up to 1 A of beam current but the arc rate was too high to obtain any meaningful performance or optics perveance data. It is not known whether this condition was a consequence of flake material which had not been adequately removed from the grids or whether there is a loss of the electrodes structural stability because of wear.

Wearout of the accelerator electrode by charge exchange ion erosion has in the past been considered a critical, if not the major factor in determining thruster lifetime. This type of wear was not the major factor in this test. The most severe damage to the accelerator

Table A-6.

30 cm OPTICS ASSEMBLY RECORD
SCREEN ACCELERATOR SPACING CHART

DATE: 2/19/74
TECH: Brian J. Reeves

MOUNTING RING ASSEMBLY S/N 648
ACCELERATOR ELECTRODES S/N 648
NOTES:

SCREEN ELECTRODES S/N 648
NOTES:

TYPE	Dished .830
DRAWING NO.	D1026138-92
APERTURE dia	.060
SPACING CTR/CTR	.087
THICKNESS	.020
DRAWING NO.	D1026137-93
APERTURE dia	.075
SPACING CTR/CTR	.087
THICKNESS	.015
REDUCTION (%)	

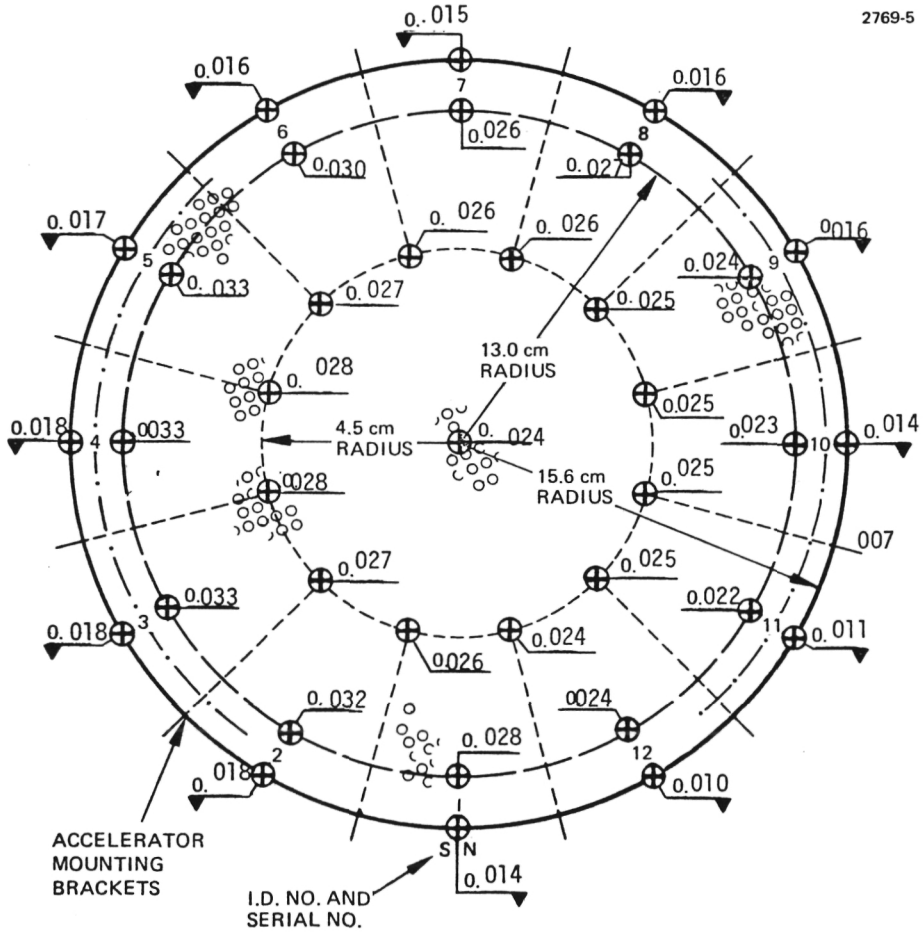

Table A-7.

30 cm OPTICS ASSEMBLY RECORD
SCREEN ACCELERATOR SPACING CHART

DATE: 6/4/75
TECH: H.T.

MOUNTING RING ASSEMBLY S/N 648
ACCELERATOR ELECTRODES S/N 648
NOTES:

SCREEN ELECTRODES S/N 648
NOTES:

TYPE	.830 Dished
DRAWING NO.	D1026138-92
APERTURE dia	.060
SPACING CTR/CTR	.087
THICKNESS	.020
DRAWING NO.	D1026137-93
APERTURE dia	0.075
SPACING CTR/CTR	0.087
THICKNESS	0.015
REDUCTION (%)	0.4%

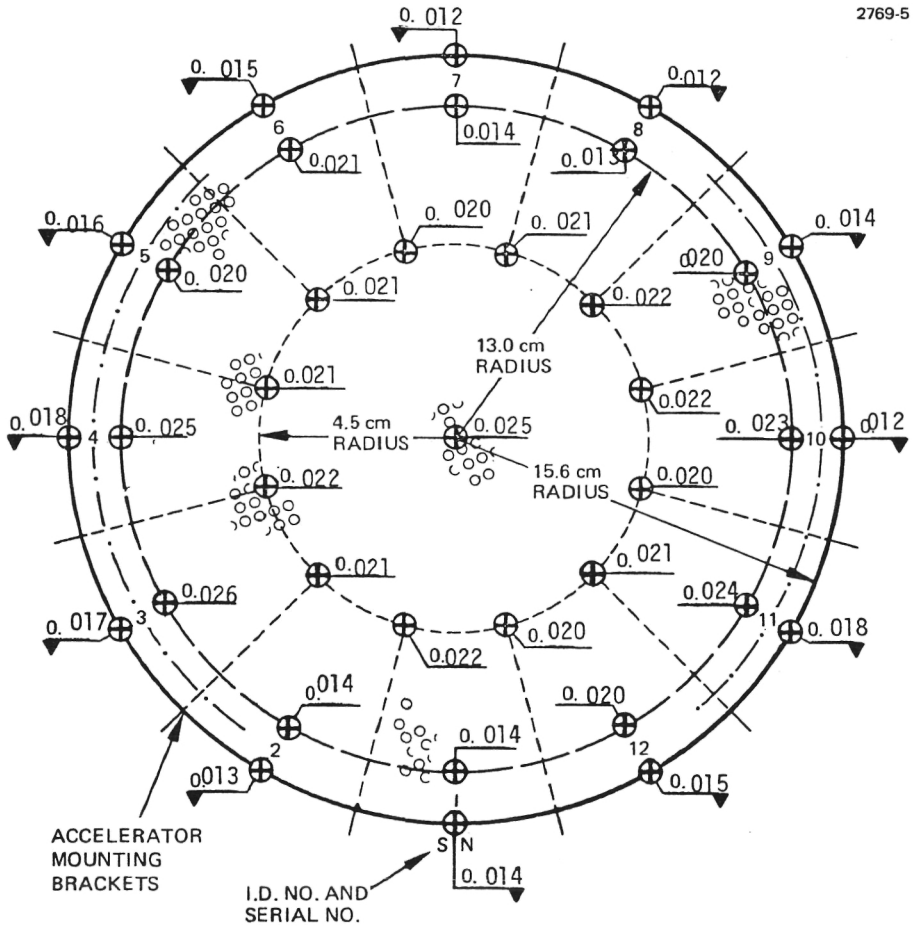

electrode was caused by direct interception of high energy ions which were deflected or defocused by flakes of material partially covering screen grid apertures (as seen earlier in Figs. A-1 and A-12). Several examples of damage of this type are pointed out in Fig. A-57. The typical pattern of "pits" and grooves caused by charge exchange ions is also seen. Photographs comparing the downstream side of the accelerator electrode before and after testing are shown in Figs. A-58 through A-67. By careful examination of these photographs (or the actual electrodes under a microscope) it is seen that the ion machining damage is randomly distributed and irregular in form. The erosion caused by charge exchange ions, on the other hand, is quite uniformly distributed and exhibits a well defined pattern. This pattern is oriented to the hexagonal aperture array but does not show any region of accelerated wear that would indicate the neutralizer location. Thus, the major difficulty observed in the SERT II tests is not at all in evidence here.

Some selected areas of damage are shown magnified in Fig. A-68. Note that in the views shown as (b) and (f), some webs of material between the apertures have been cut through completely by beam ions. View (e) shows a flake lodged in the electrodes and the resultant damage. Views (a), (b), and (c) illustrate the change in orientation of the charge exchange erosion patterns that can be seen as a function of thruster radius. The orientation of these photographs places the center of the electrode at the top of the page and view (a) is nearest the center, while view (c) is nearest the edge. It is apparent that the erosion is deepest near the electrode center, view (a), and that the erosion pattern is centered on and symmetric with the aperture pattern. Nearer the edge, as in Fig. A-68(c), the erosion is less and the pattern is shifted towards the grid center. This offset in the erosion pattern occurs because the beamlets formed at the edge apertures are by grid design deflected radially inward to counteract the divergent effect introduced by grid curvature and therefore the charge exchange ions are also focused towards the grid center.

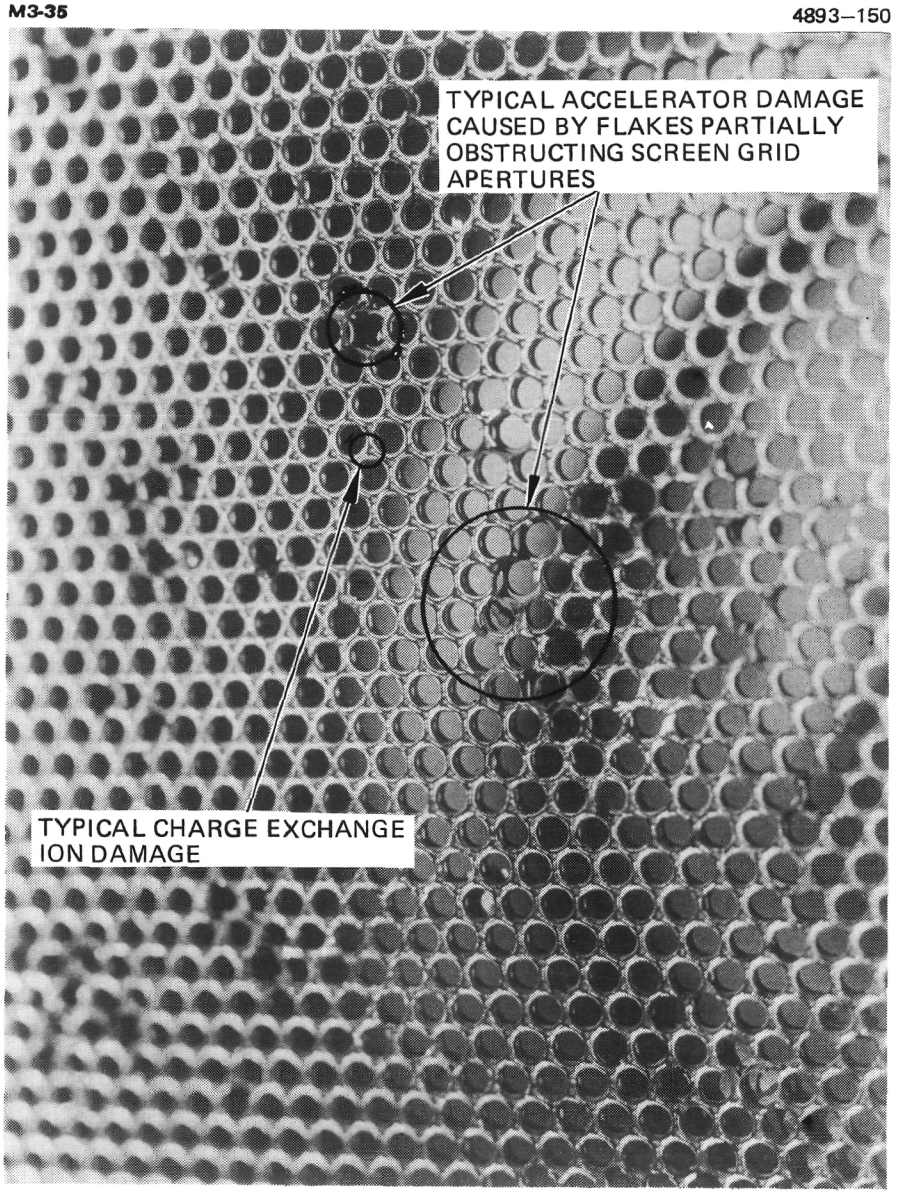

Figure A-57. Accelerator electrode, downstream view.

M10067 4893–260

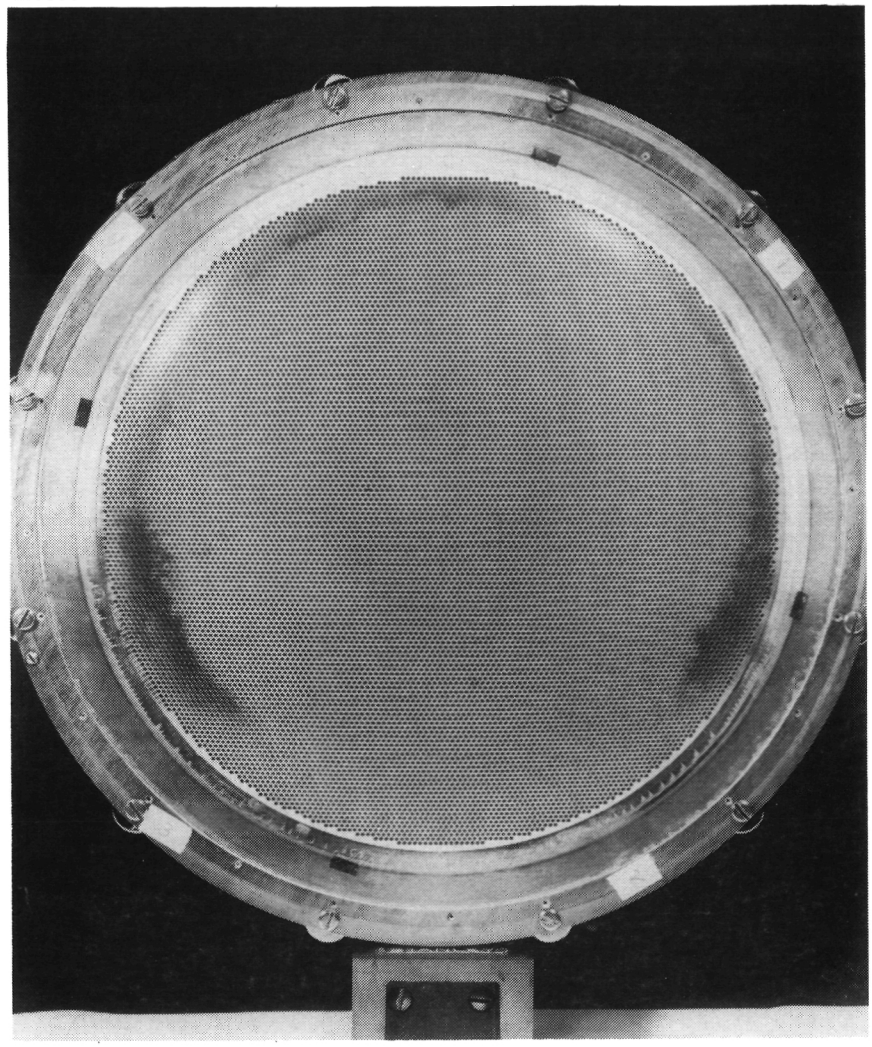

Figure A-58. Ion optics assembly SN648 downstream view before test.

M11056

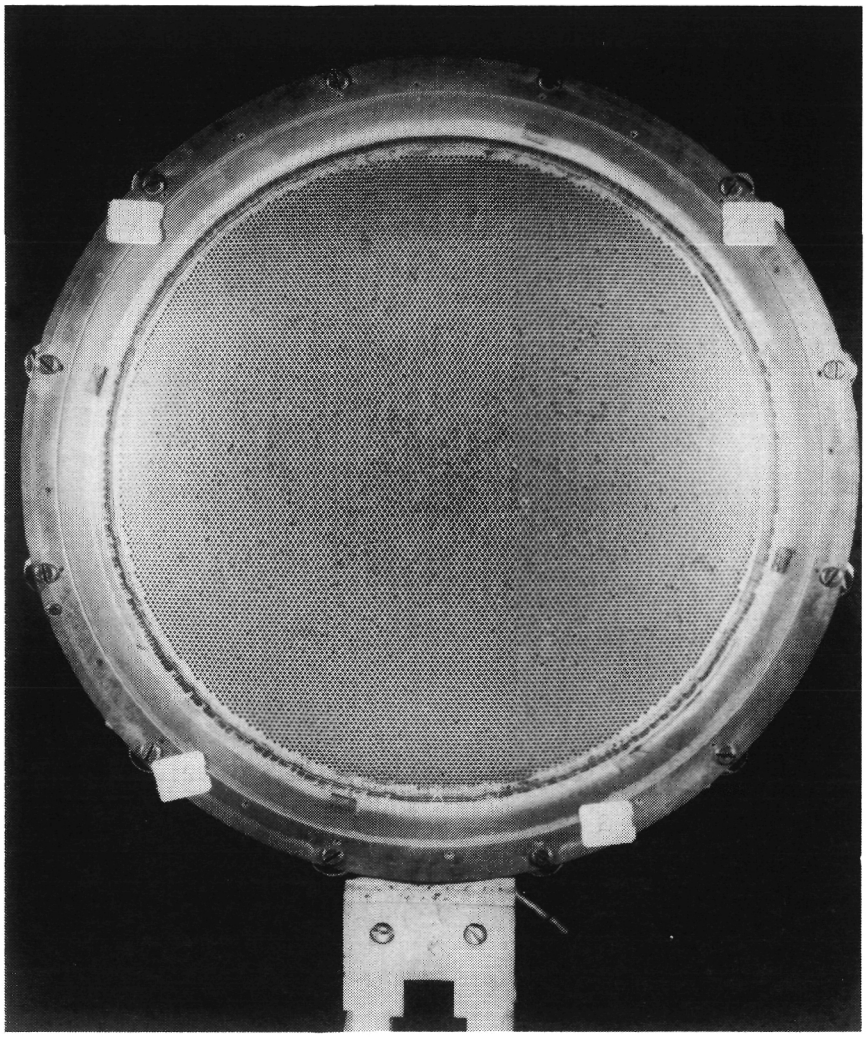

Figure A-59. Ion optics assembly SN648 downstream view after test.

M10068

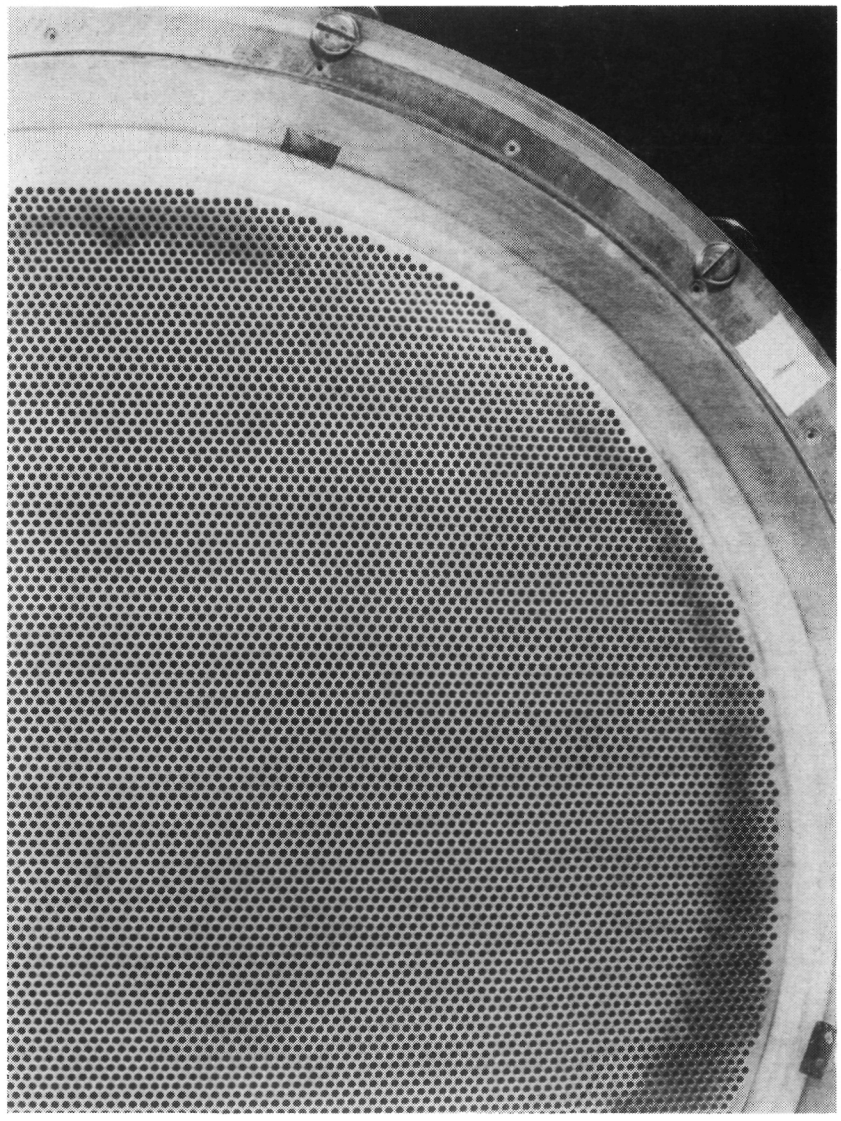

Figure A-60. Accel before test.

M11060 4893–151

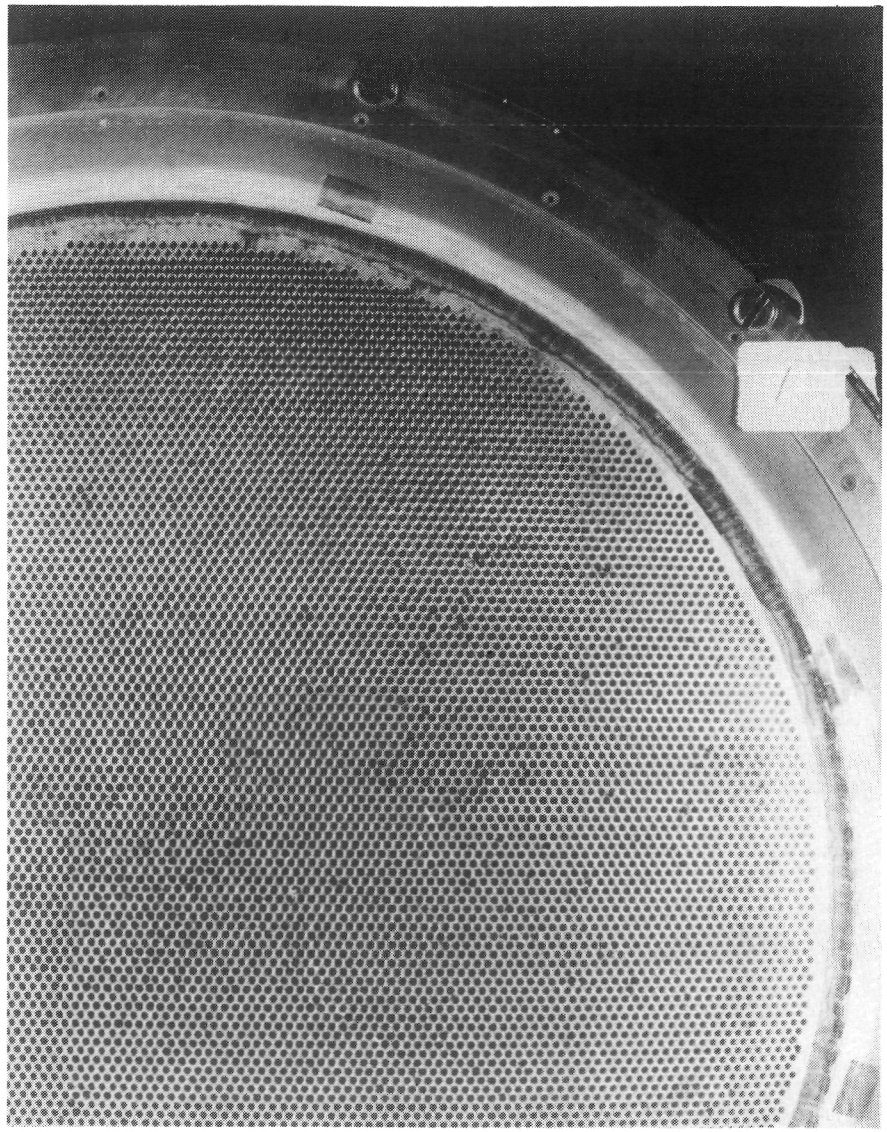

Figure A-61. Accel after test.

M10069 4893–173

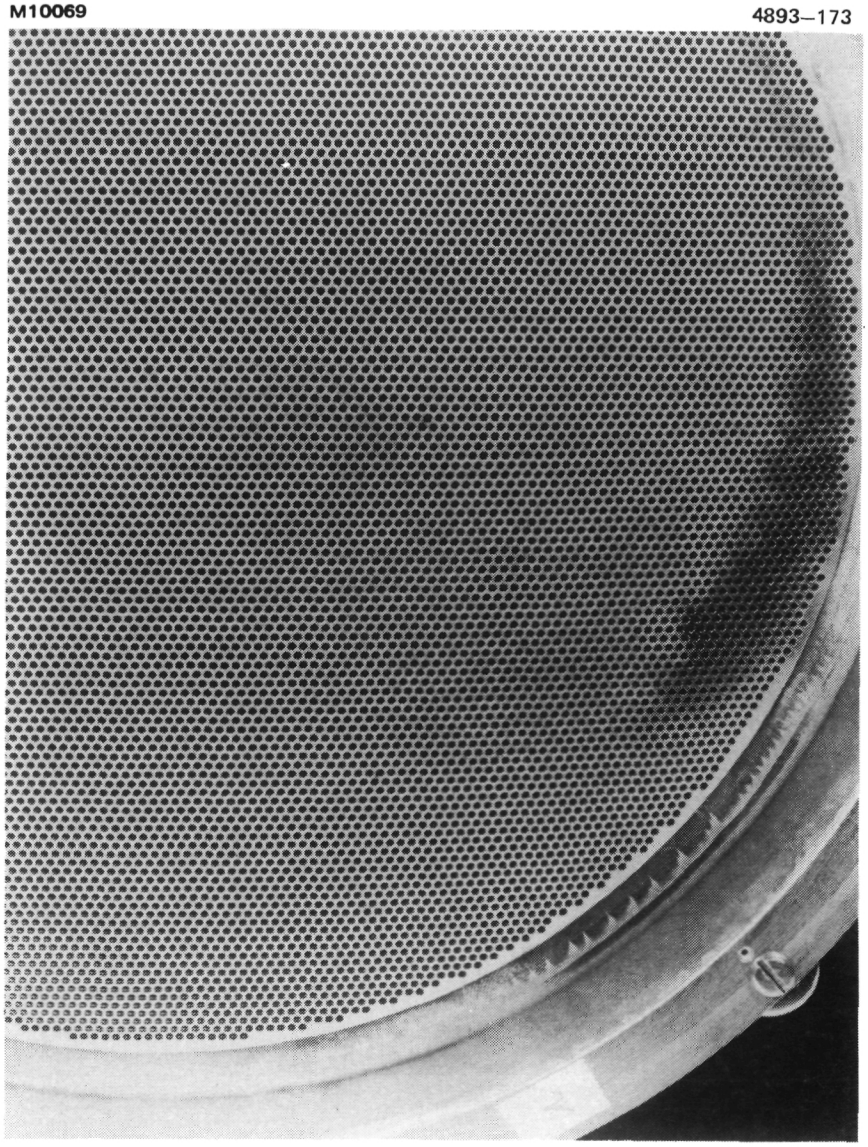

Figure A-62. Accel before test.

M11059

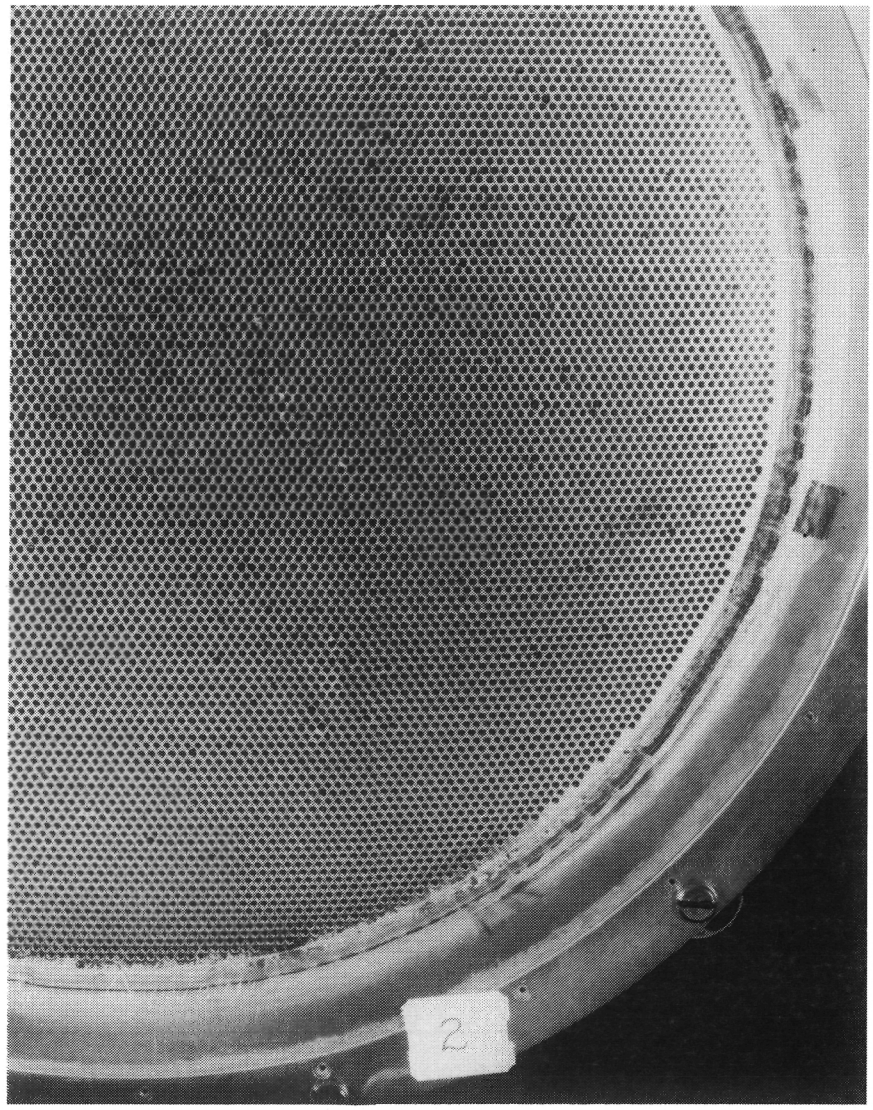

Figure A-63. Accel after test.

M10070

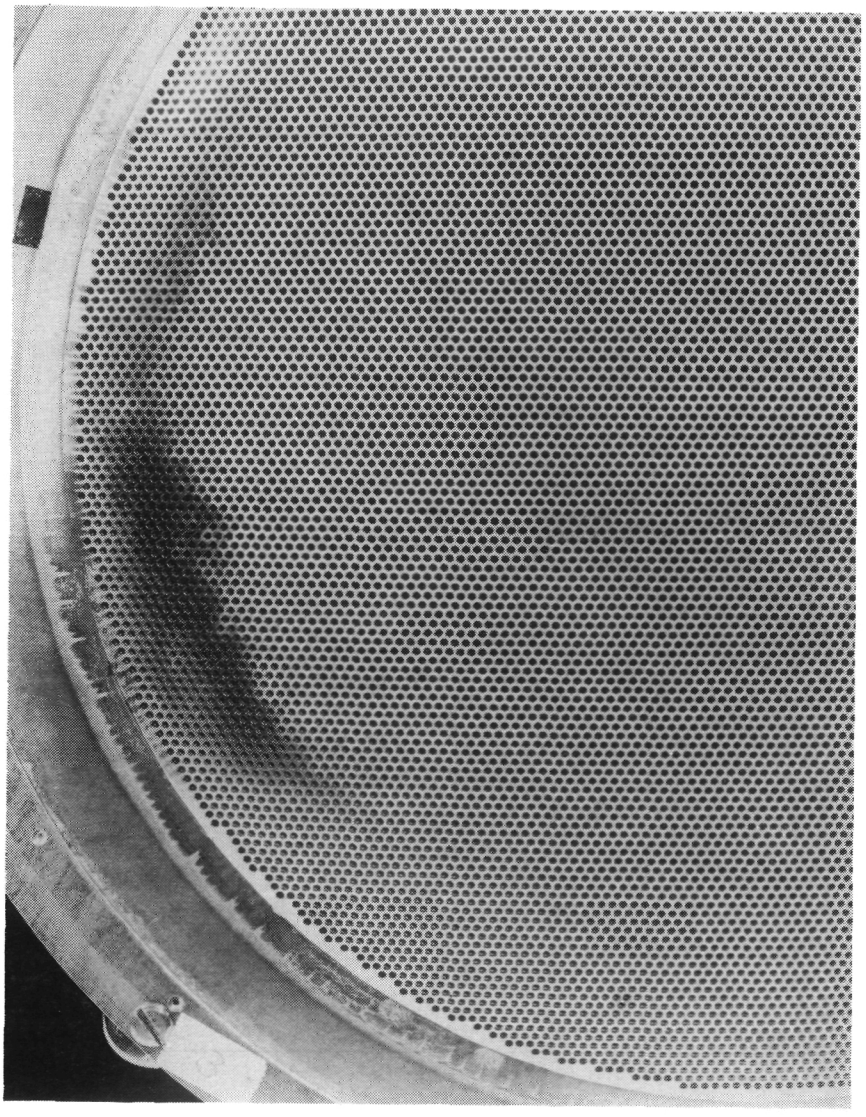

Figure A-64. Accel before test.

M11058

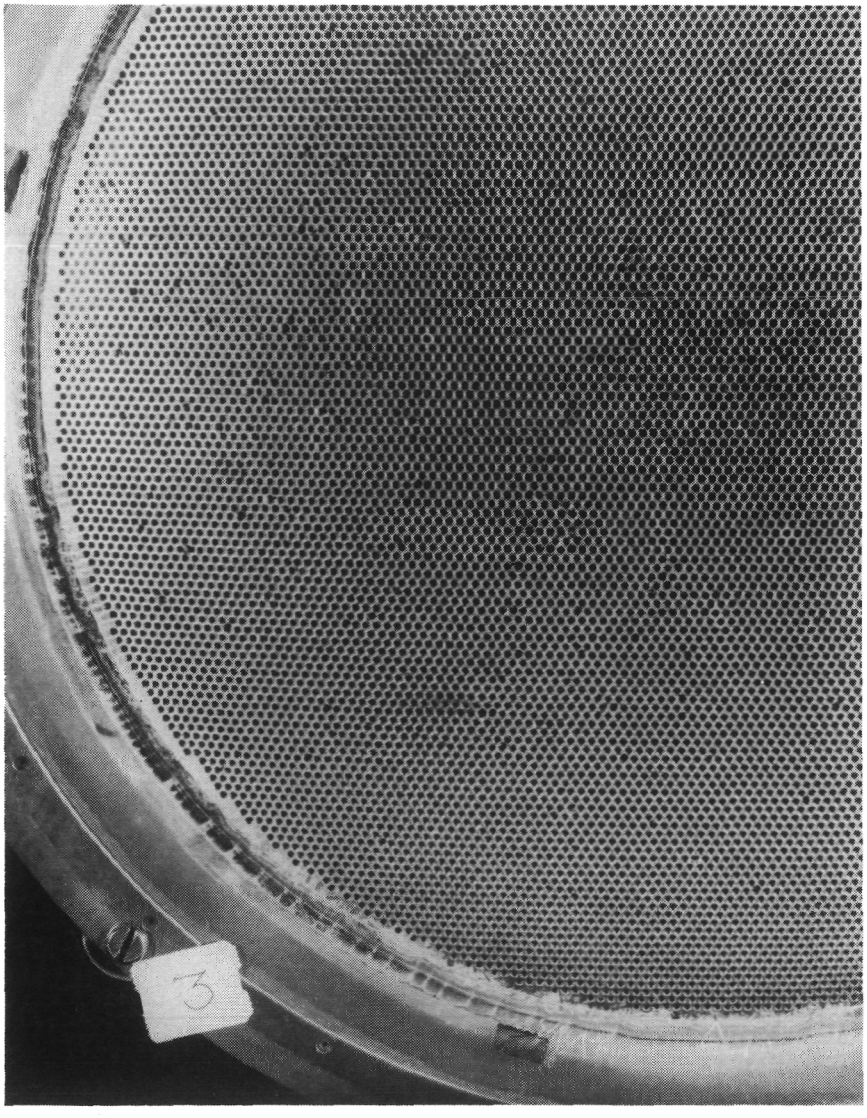

Figure A-65. Accel after test.

M10071

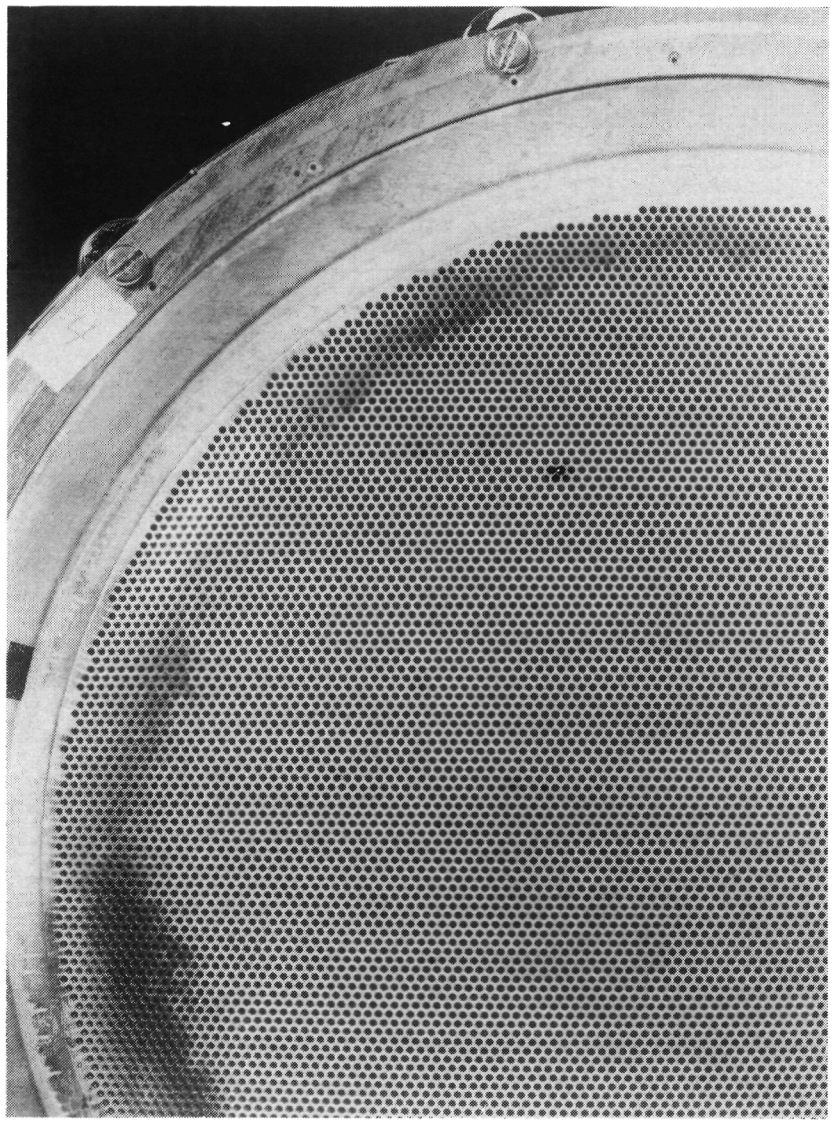

Figure A-66. Accel before test.

M11061 4893-262

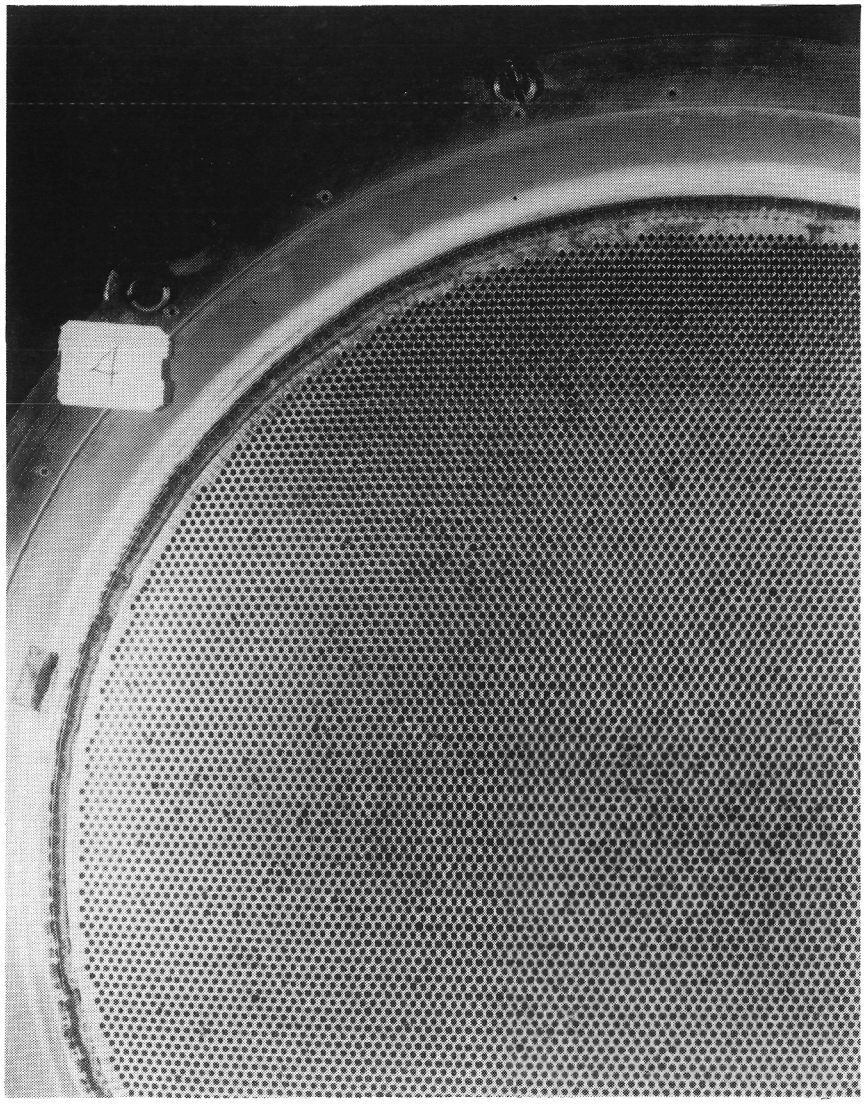

Figure A-67. Accel after test.

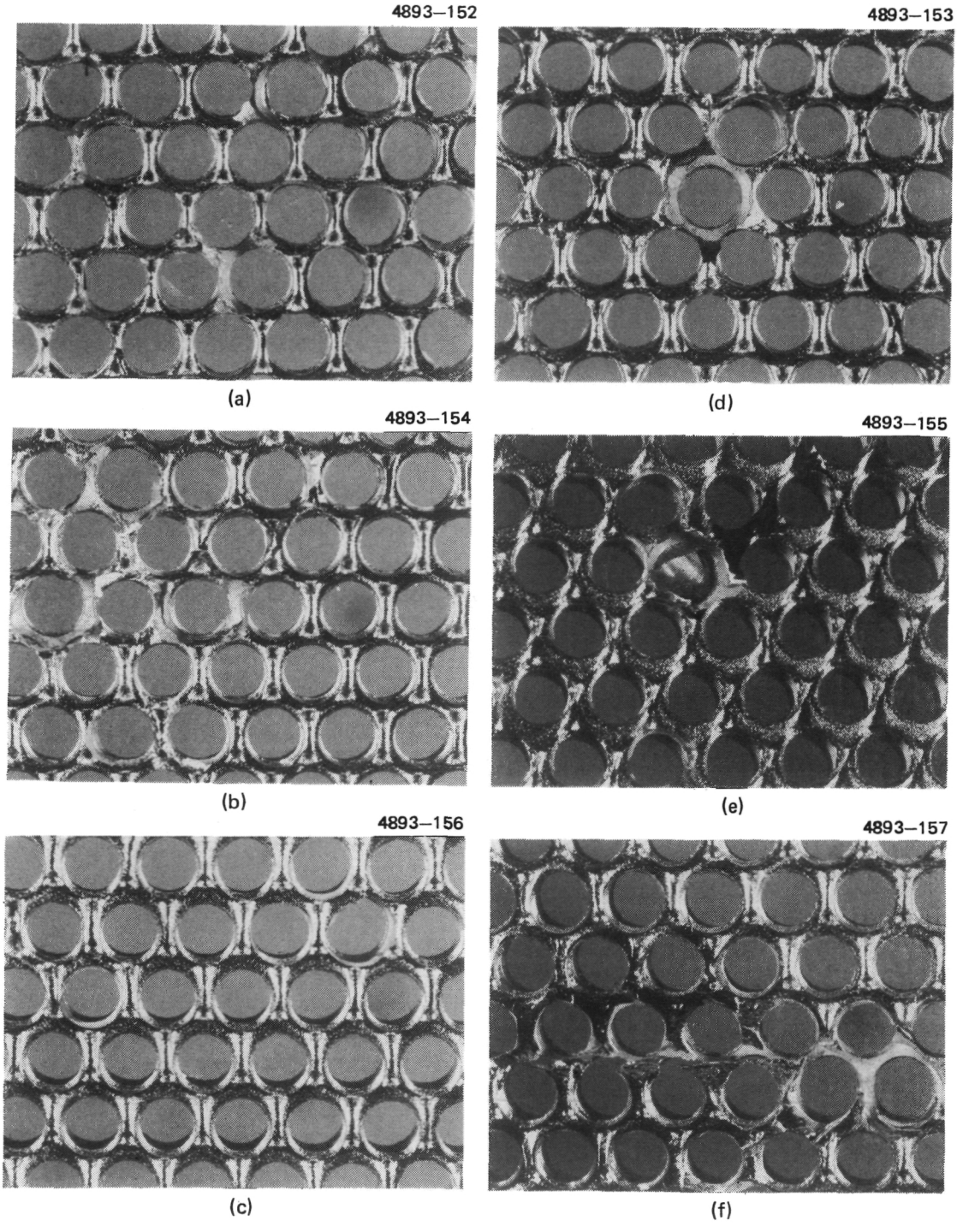

Figure A-68. Selected areas of downstream surface of accel electrode.

The depth of the charge exchange erosion was investigated carefully, both by microscopic examination and by cross-sectioning segments of the electrode taken from the center and the edge of the grid. The "pits" are seen as triangles (Fig. A-68) in the center of the web of material common to any three apertures. These pits vary but are usually almost conical in shape with a very small cross-section at the deepest point. They vary in depth from a maximum of 0.013 in. (0.033 cm) near the center to being immeasurable near the edge. The pits are connected by grooves, which are a maximum of 0.006 in. (0.015 cm) deep at the mid-point between pits. The depth and shape of the pits and grooves eroded by charge exchange ions appears to also be influenced by their proximity to defocused beam ion damage. In areas where there is extensive ion machining damage, the pits and grooves are shallower and broader. Figure A-69 shows some selected cross-sections of the accelerator electrode near the center and the edge. The difference in the views shown reflects the location and angle of the cut through the material. The views shown as Fig. A-69(a) and (b) represent a cut along the groove and through the pits, the depth of the pit shown being approximately 0.012 in. (0.030 cm). It is thought that the sample in (b) has been polished to nearly pass through the center of the pit. A survey of pit depth was made using a microscope at high magnification (1000X) and measuring the travel required to focus on the bottom of the pit as compared to focusing on the undamaged edge. A plot of representative pit depth variation is shown in Fig. A-70.

To illustrate that there is no uniform erosion or thinning of the accelerator grid, Table A-8 shows electrode thickness measurements as measured with a micrometer for the endurance test electrode and for a new electrode. Note that there is some variation in thickness over the electrode but this variation does not appear to be systematic. The only explanation that can be offered for the thickness variation is that either the original material was not uniform or the electropolish was uneven. Accelerator aperture wear, except for damaged apertures, appears only slightly related to thruster radius. A comparison of the endurance test accelerator aperture measurements is made with those of a new accelerator grid in Table A-9. The relatively small changes in accelerator

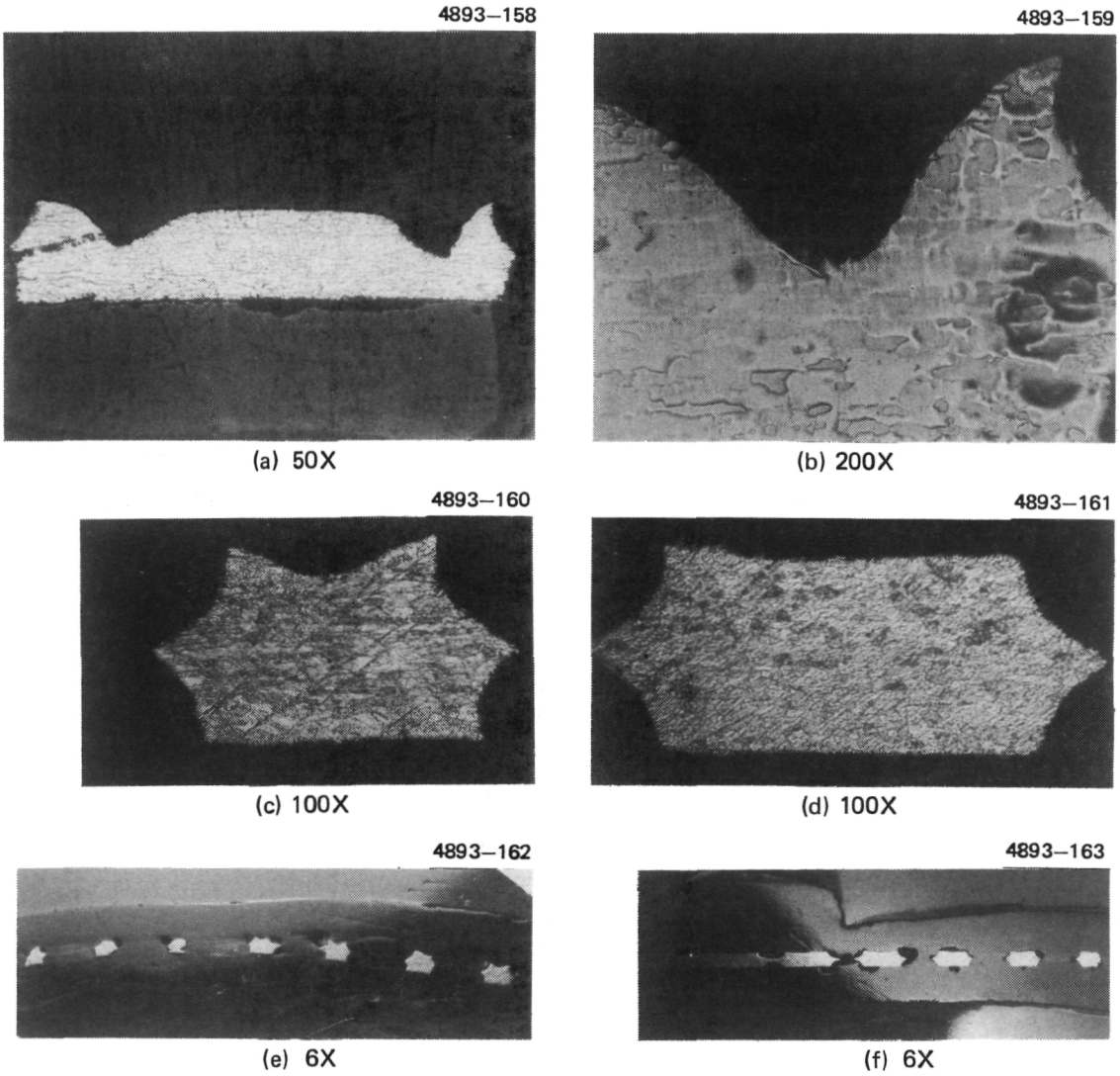

Figure A-69. Selected cross-sections of accel electrode.

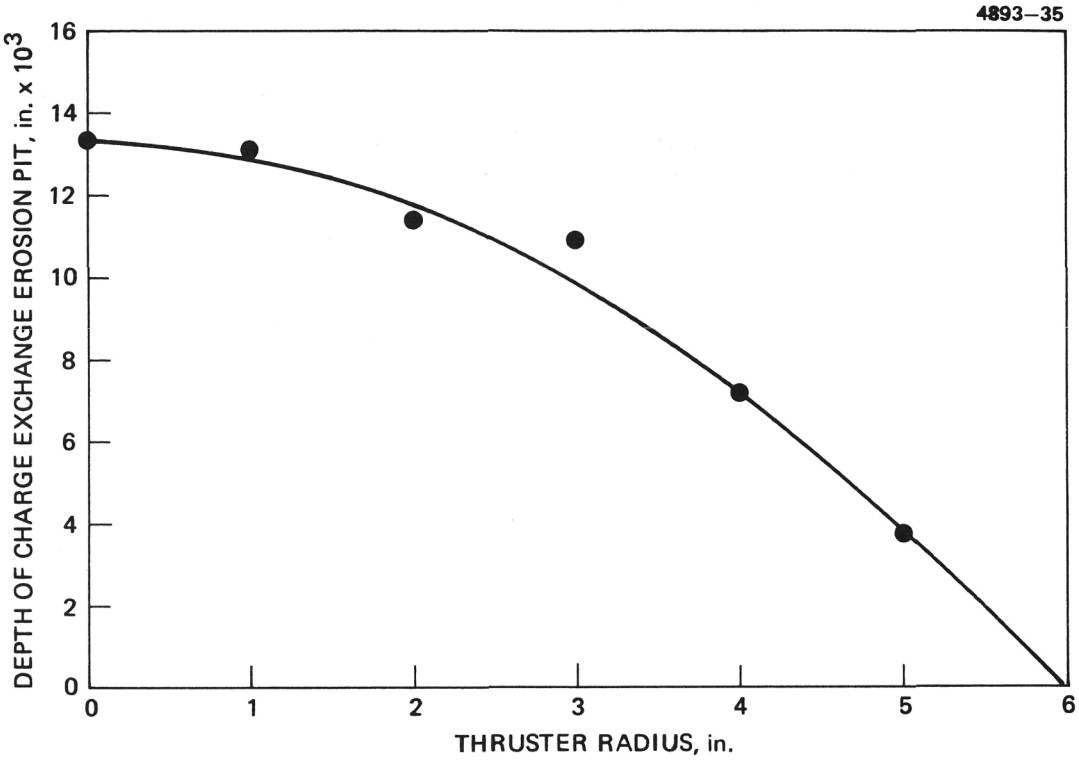

Figure A-70. Depth of charge exchange ion erosion pits as a function of thruster radius on accelerator grid SN648 after 10,000 hour endurance test.

Table A-8.

Comparison of Electrode Thickness Versus Radius for Endurance Test Accelerator Electrode (SN 648) and New Electrode (SN 803) Measured Along a Different Radii								
Radius in.	Electrode Thickness							
	SN 648 in. x 10^3				SN 803 in. x 10^3			
0	18.7 Ⓐ	19.2	19.2	19.2	19.5	19.5	19.5	19.5
1	19.9	19.5	18.7	17.7	19.5	19.4	19.2	19.4
2	17.5	16	18	17.5	18.9	18.9	18.7	18.8
3	19.9	19.2	17	16.5	18.3	18.2	17.6	17.5
4	18.3	17.2	17.2	16.5	18.5	18.4	17.8	17.9
5	18	17.2	17	17.0	18.6	18.5	18.1	17.8
Ⓐ Entries in this column measured with microscope								

T1857

Table A-9.

Comparison of Accelerator Electrode Aperture Diameter Versus Radius for the Endurance Test Electrode (SN 648) and a New Electrode (SN 653) Measured Along Different Radii						
Radius in.	Electrode Thickness					
	SN 648 in. x 10^3				SN 653 in. x 10^3	
0	63	63	62.5	63	60	60
1	62	62	60	52	60	59
2	61	61	60	61	60	59
3	61	61	60	61	59	59
4	60	60	58	60	59	59
5	59	60	58	59	59	59

T1858

electrode thickness and aperture diameter as indicated in Tables A-8 and A-9 are not considered significant to thruster lifetime or operation.

Photographs of the upstream surface of the accelerator are shown in Figs. A-71 through A-75. Careful examination of these pictures reveals several features that have been magnified and included in Fig. A-76. View (a) shows an area that is relatively undamaged but has a "matte" finish that may be the result of low energy ion erosion. Figure A-76(b) shows a typical area in which deflected beam ion erosion has occurred causing "scythe" shaped markings on the grids. This type of damage is rather widespread and in areas where flakes remained on the screen grid for long time periods, the damage progresses as shown in view (d). View (c) is rather unusual in that the small triangular areas seen in the location that is usually occupied by charge exchange ion erosion pits on the downstream surface is actually a deposition here on the upstream surface. In addition, the edges of the apertures seen in view (c) appear rounded in a chamfered fashion, which is not typical of most other areas on the electrode. No explanation can be offered for the wear seen in view (c). In considering the relatively large number of high voltage overload recycles which occurred during the test, it was thought that arc damage might be distinctly visible on the upstream surface of the accelerator electrode. It has not been possible to identify any damage seen on this electrode with the appearance of damage that is seen when grids are purposely short circuited and the shorting material is then removed by capacitive discharge. This statement does not imply that such damage did not occur, but only that it cannot be conclusively identified.

The screen grid electrode has not in the past been of great concern as a factor limiting thruster lifetime. It will be seen in the following paragraphs that appreciable concern is justified. Proceeding in the same manner as above for the accelerator electrode, Figs. A-77 through A-86 compare photographs of the upstream surface of the screen grid before and after testing. It is difficult to detect any differences in the appearance of the screen grid. There appears to be a slight rounding of the aperture edges as seen in views (a) and (b) of the magnified photographs shown in Fig. A-87. These views are representative of the appearance of the center of the electrode while view (e) shows that such

M11158

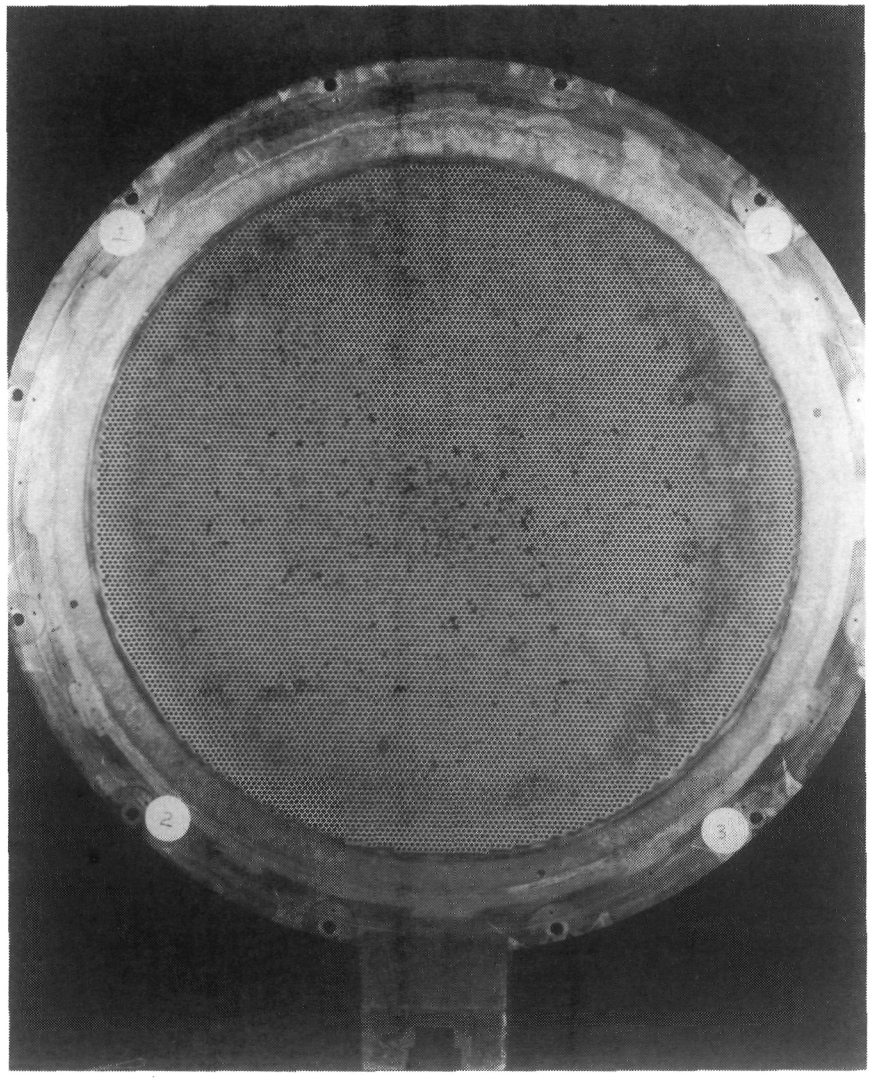

Figure A-71. Accel after test, upstream side.

M11161

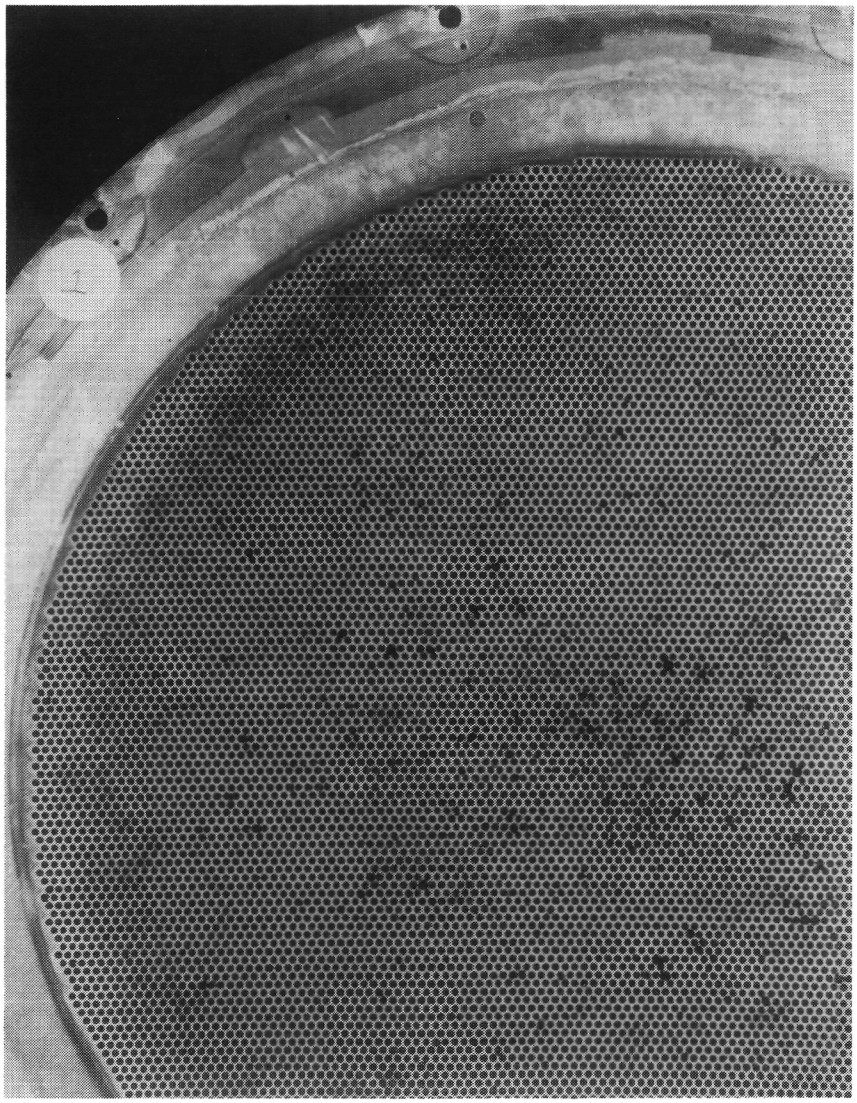

Figure A-72. Accel after test, upstream side.

M11160

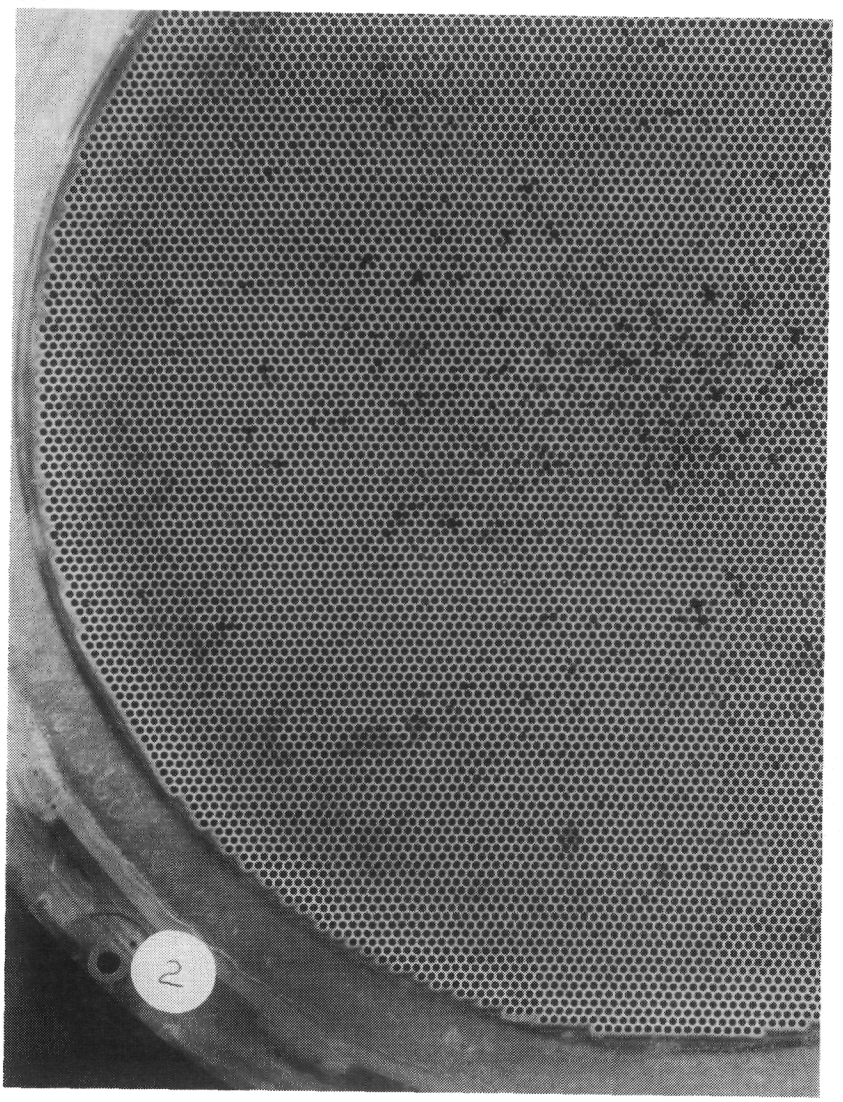

Figure A-73. Accel after test, upstream side.

M11156

Figure A-74. Accel after test, upstream side.

M11159 4893-261

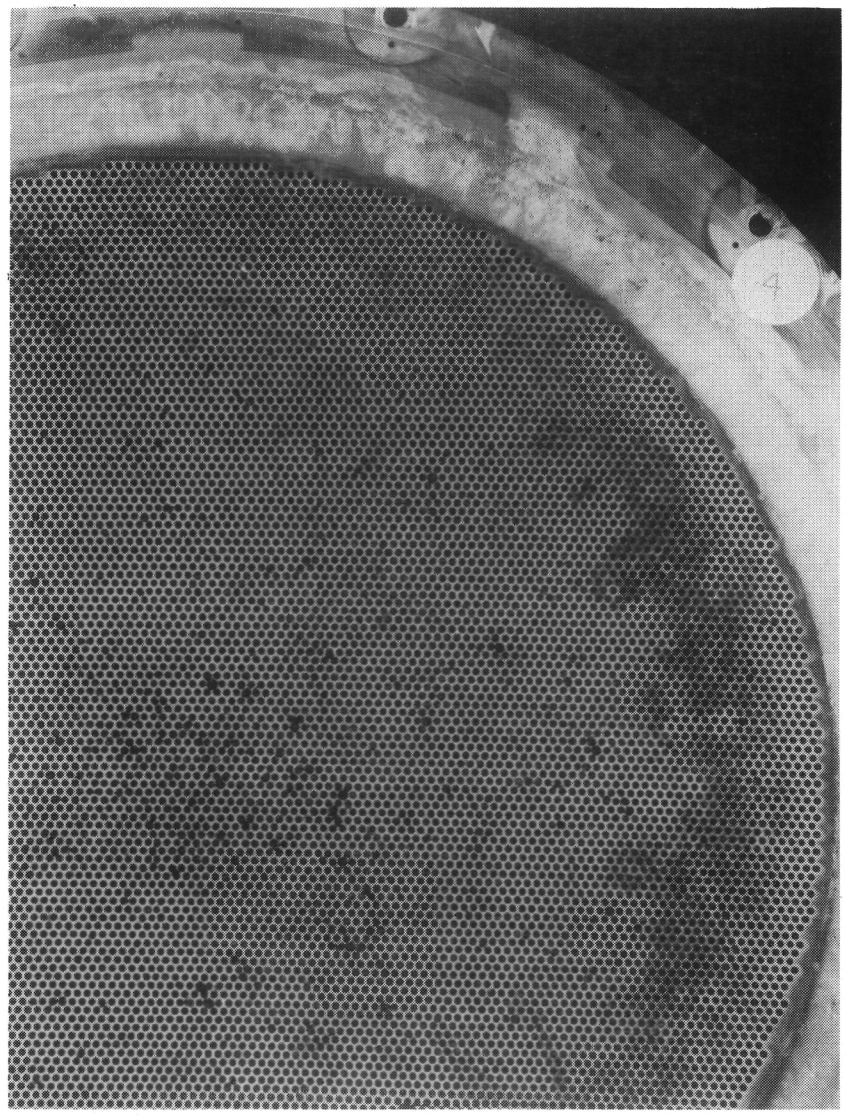

Figure A-75. Accel after test, upstream side.

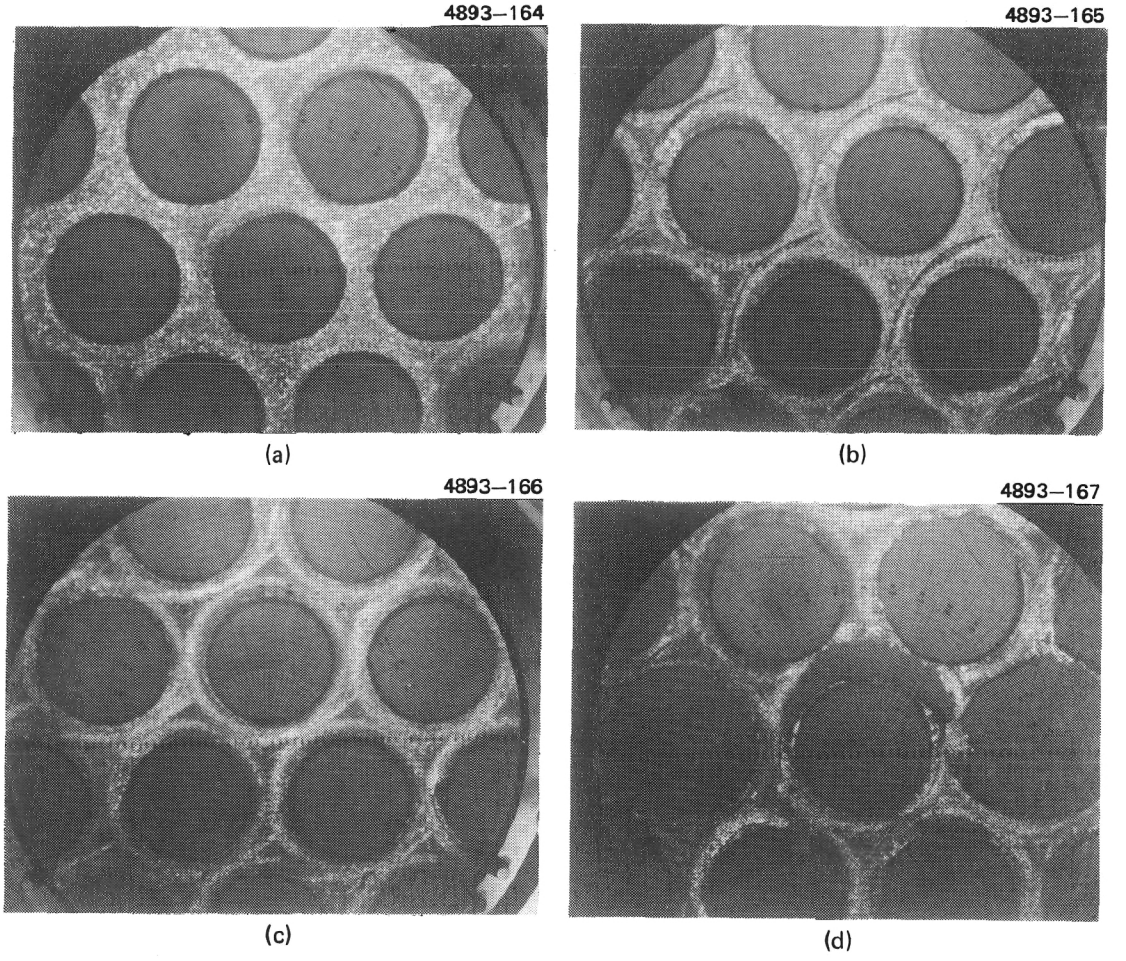

Figure A-76. Magnified view of selected areas of upstream surface of accel electrode.

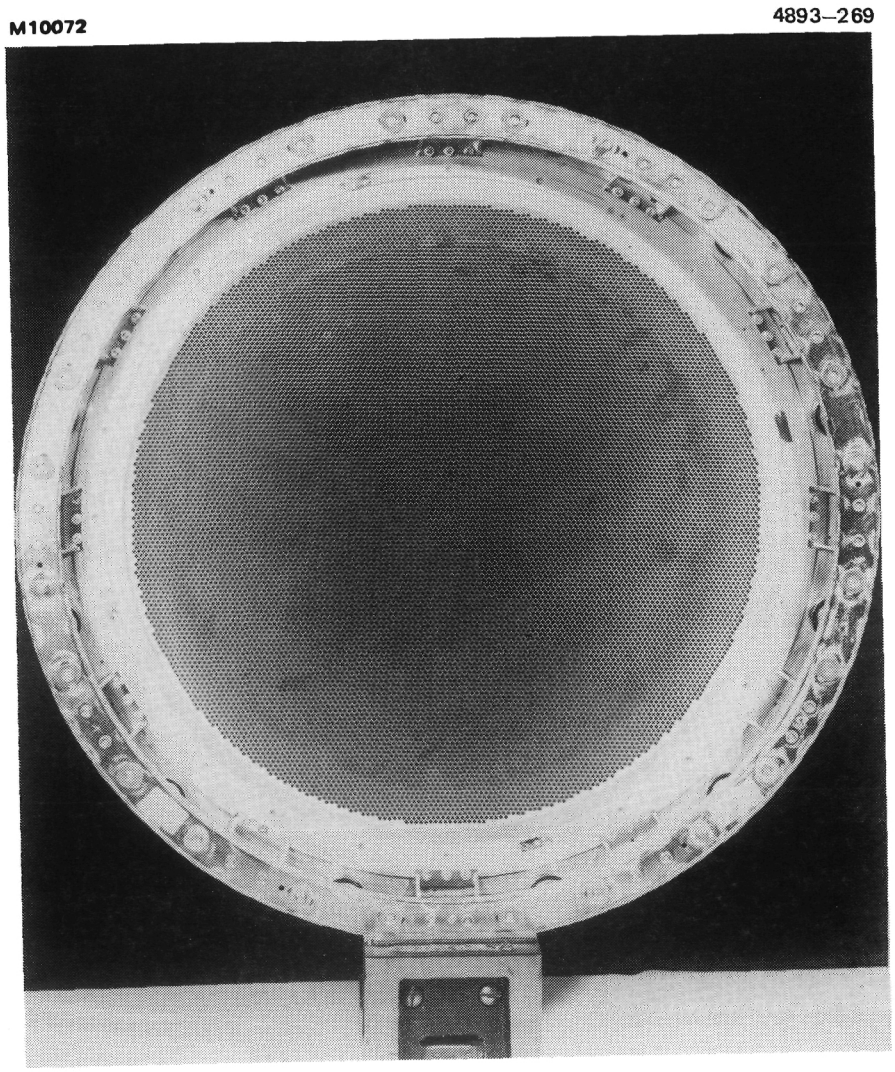

Figure A-77. Screen electrode, before test.

M11057

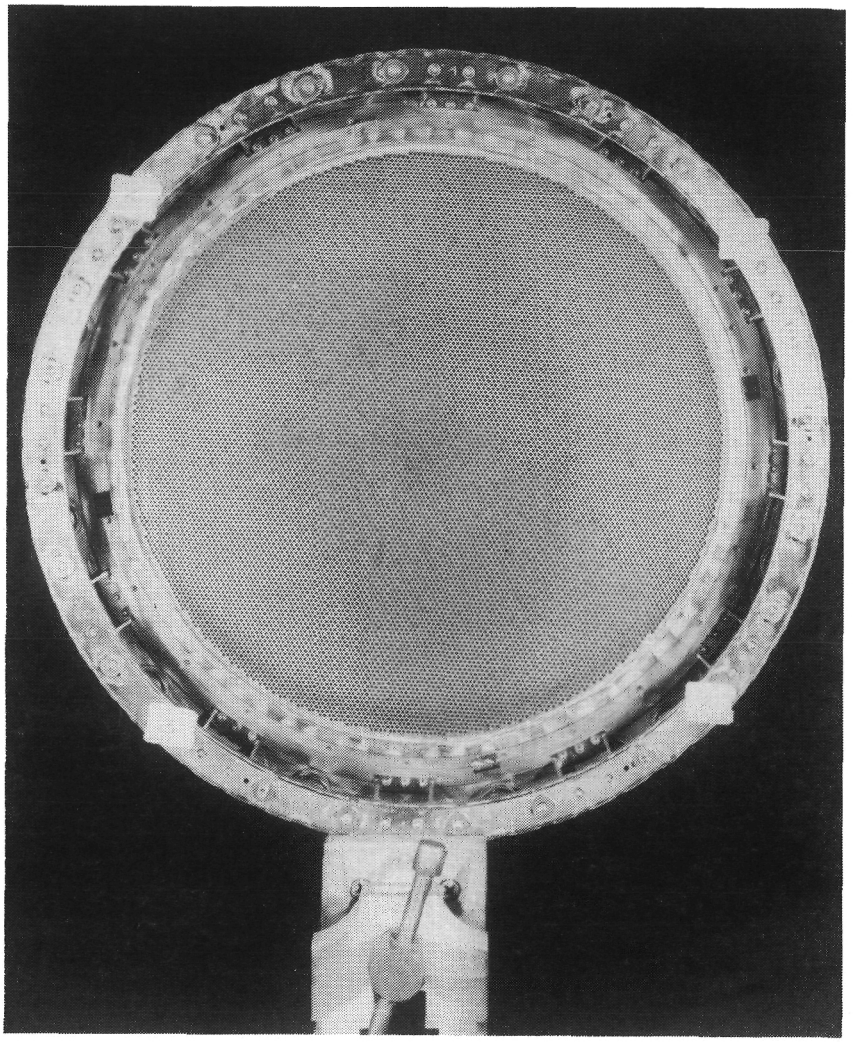

Figure A-78. Screen electrode, after test.

M10073

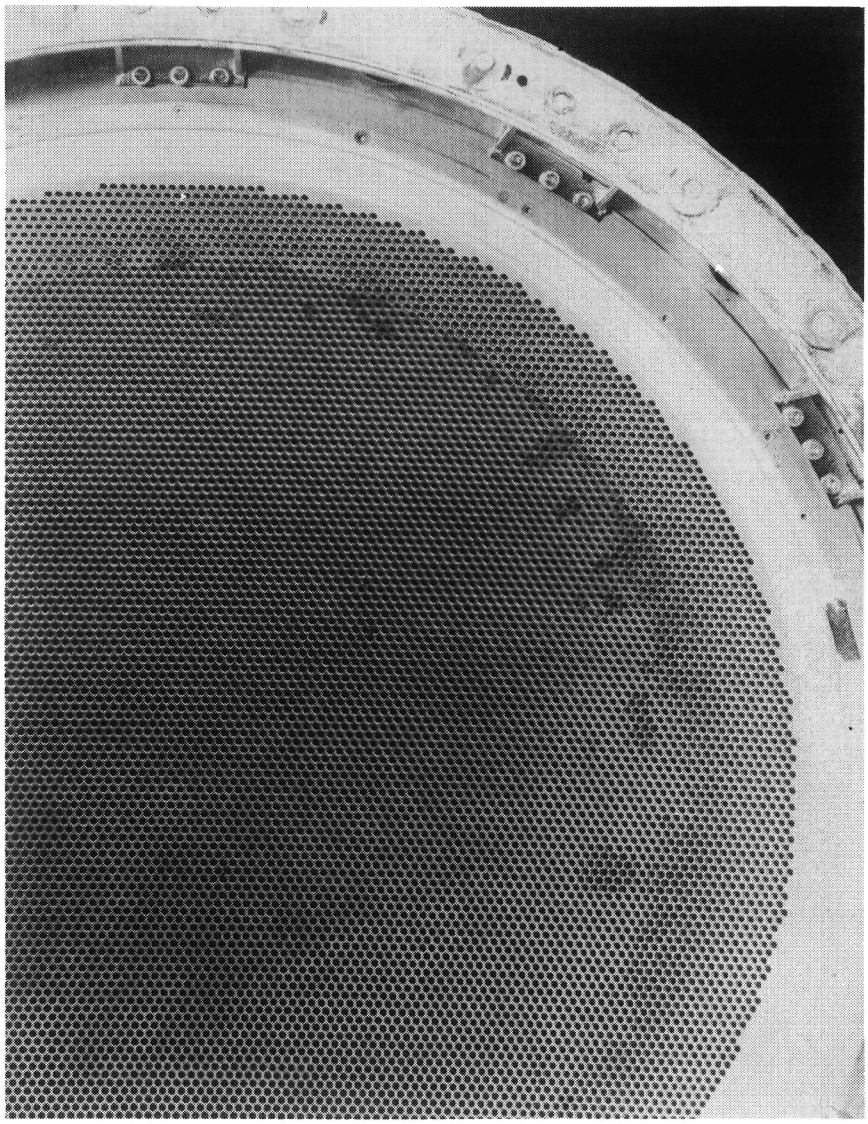

Figure A-79. Screen electrode, before test.

M11065

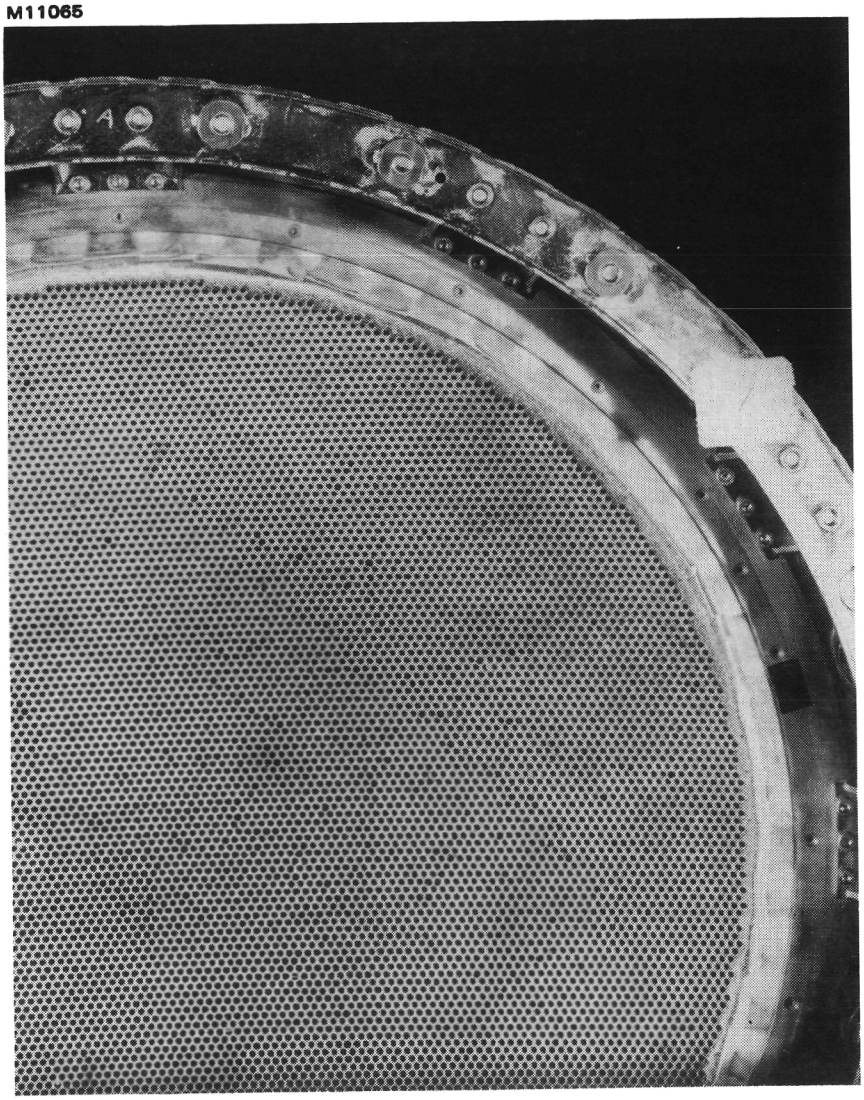

Figure A-80. Screen electrode, after test.

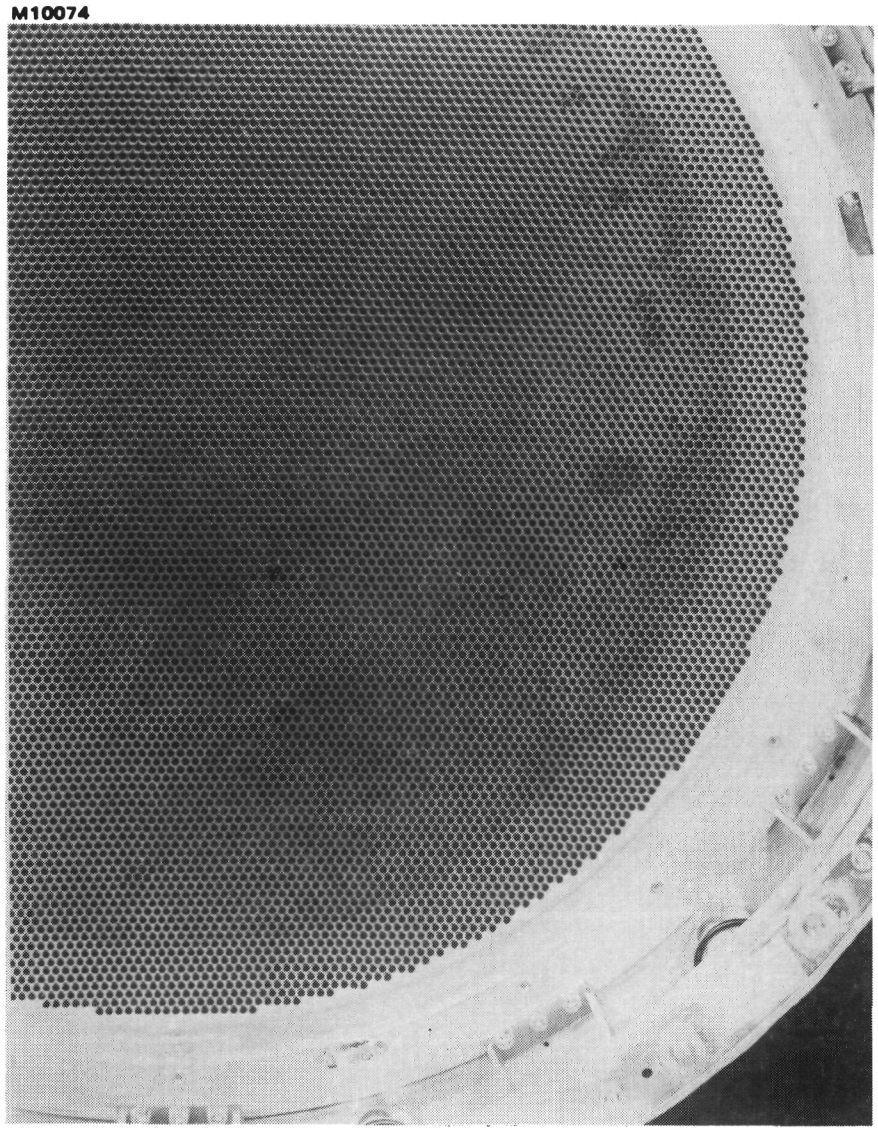

Figure A-81. Screen electrode, before test.

M11064

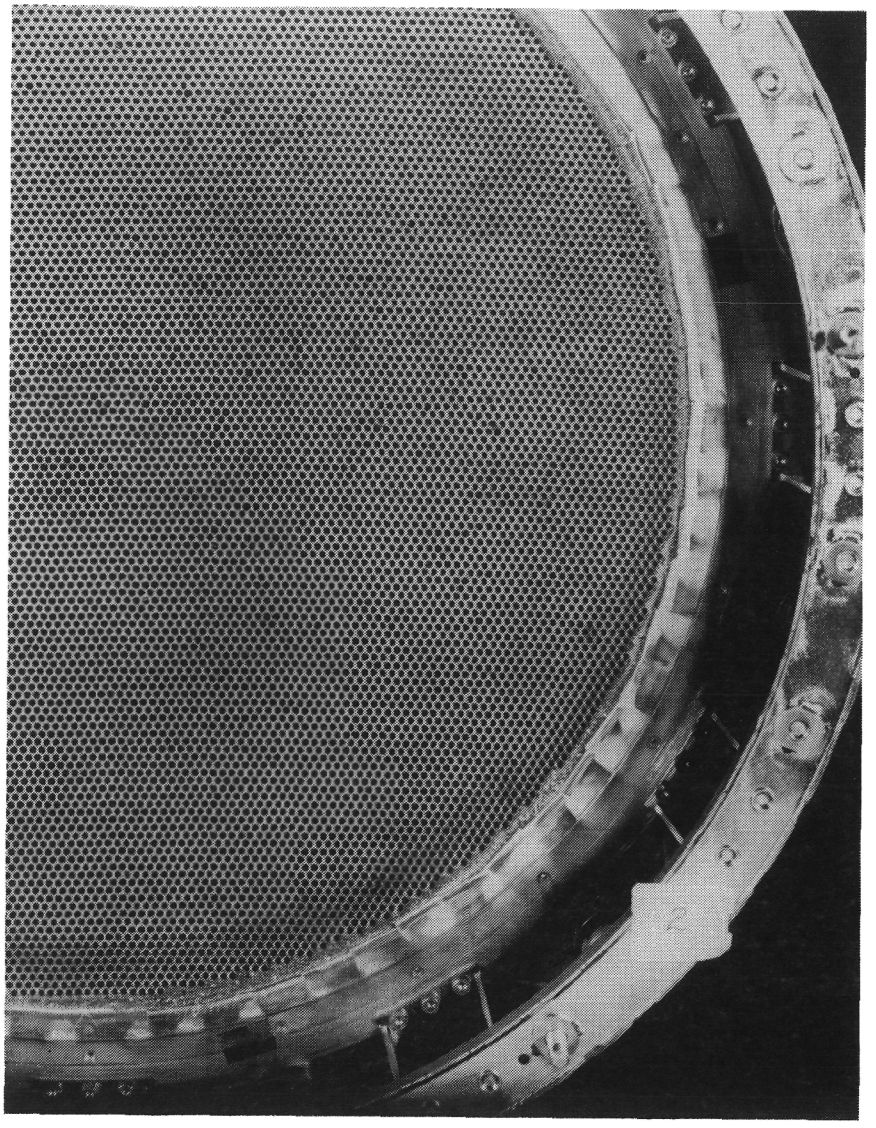

Figure A-82. Screen electrode, after test.

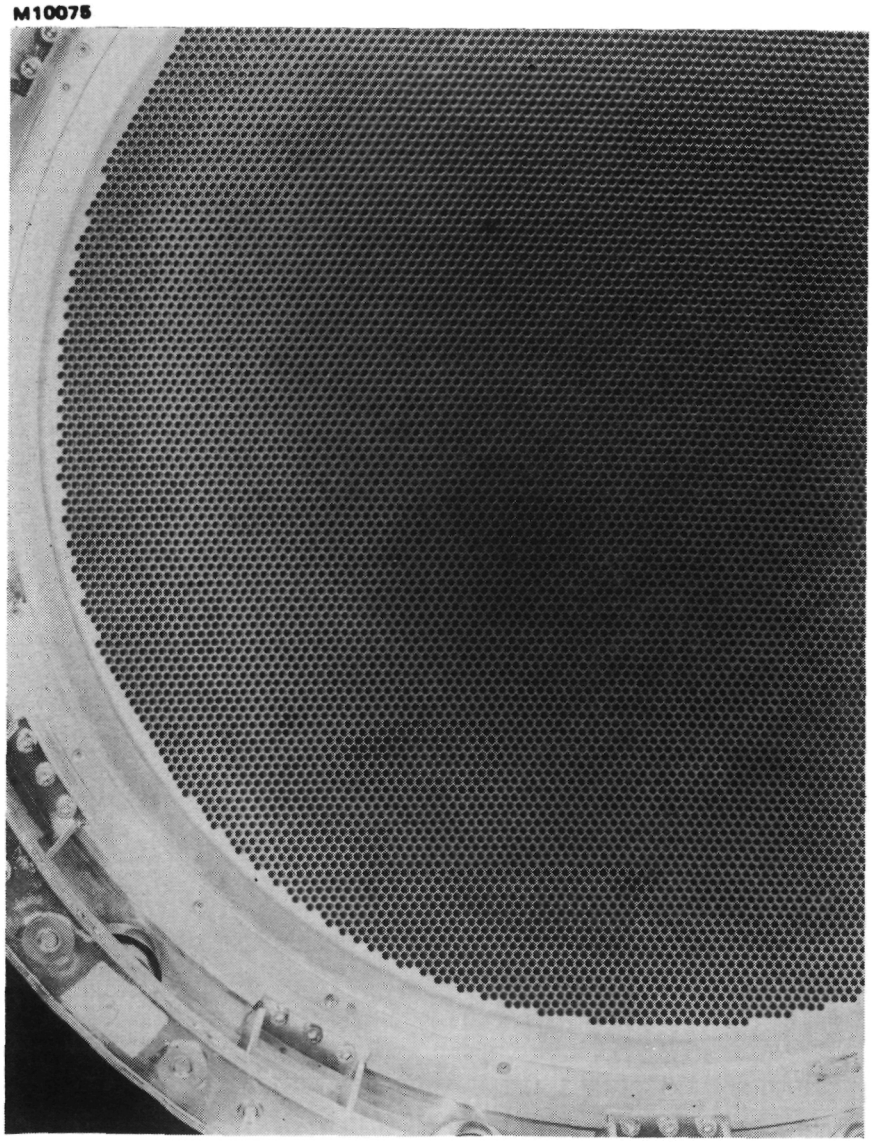

Figure A-83. Screen electrode, before test.

M11063

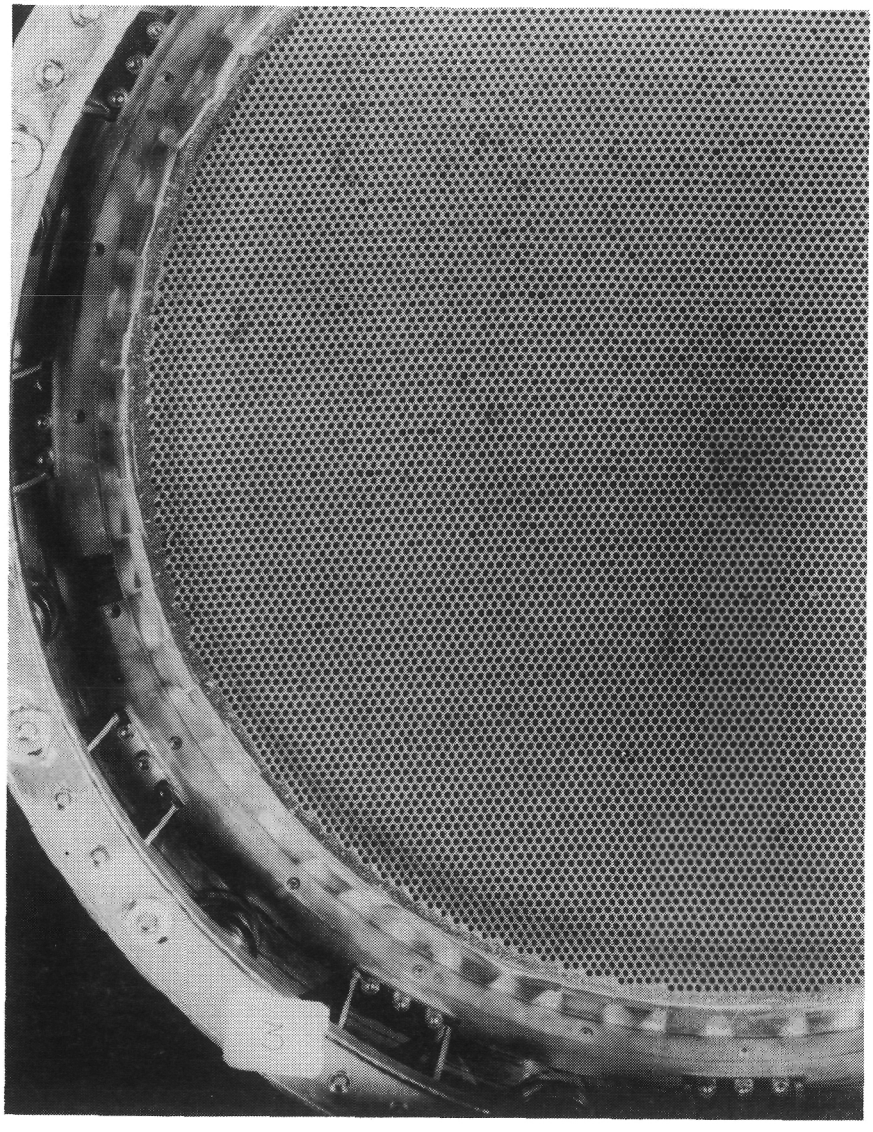

Figure A-84. Screen electrode, after test.

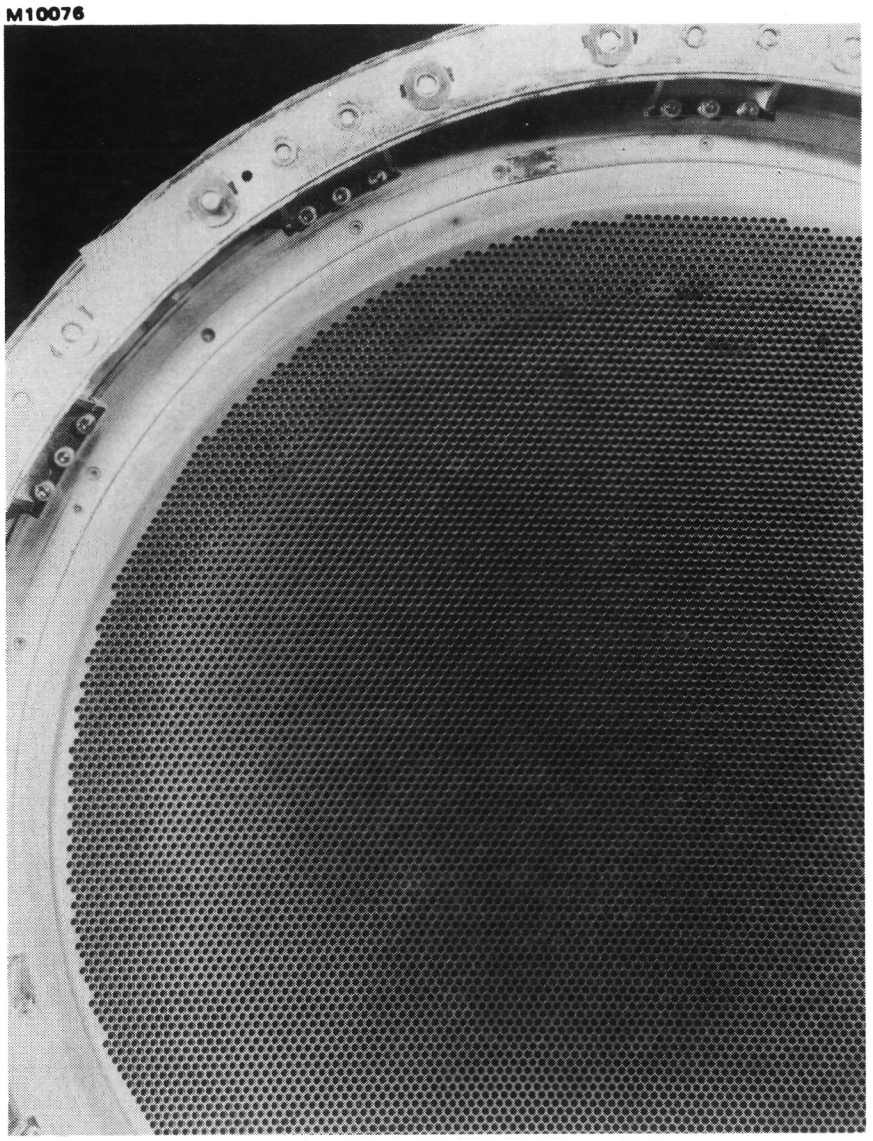

Figure A-85. Screen electrode, before test.

M11062 4893–264

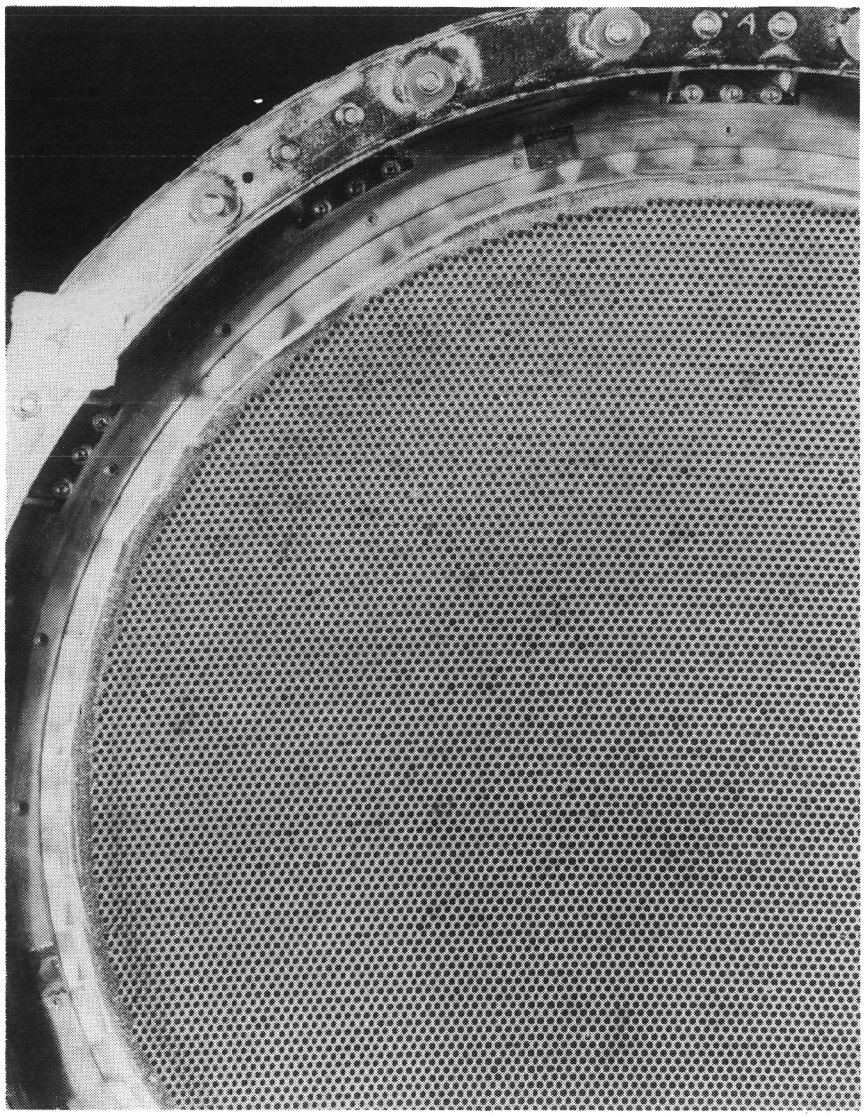

Figure A-86. Screen electrode, after test.

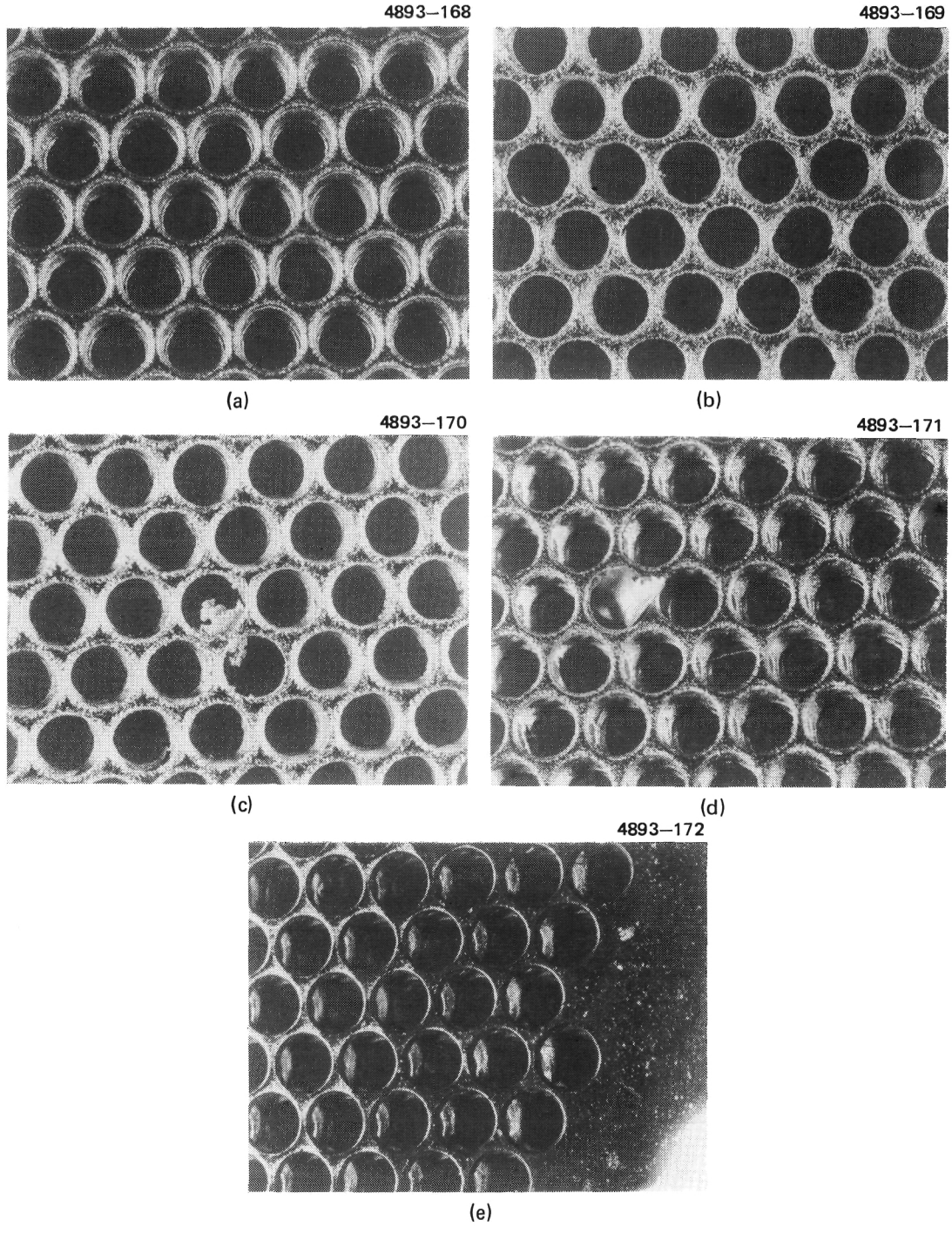

Figure A-87. Selected areas of upstream side of screen electrode.

chamfering is not present near the electrode edge. Figure A-87(c) and (d) are located about mid radius and show residual flakes on the grid. It was thought at first, that the screen grid electrode apertures were slightly enlarged nearer the center of the grid. Table A-10 gives measurements of the aperture diameters for the endurance test screen grid electrode. It is apparent that most apertures are smaller than the nominal 0.075 in. (0.191 cm) dimension specified by the design.

Table A-10.

Screen Grid Electrode Aperture Diameters Measured Along Several Radii of Endurance Test Grid SN 648				
Radius in.	Aperture Diameter[A] . in x 10^3			
0	74	—	—	—
1	75	76	74	76
2	72	73	72	74
3	73	73	73	73
4	72	75	73	72
5	73	72	73	73
(A) Print Specifies 75 ±1 x 10^{-3} in.				

T1859

Measurement of the electrode thickness showed the grid to be appreciably eroded and reduced in thickness nearer the center as documented in Fig. A-88. Measurements were performed using the same technique on a slightly used electrode (SN 645) which had been fabricated from the same material lot during the same time period as the endurance test electrode and these values are included in Fig. A-88 for comparison. The erosion seen, like that of the cathode pole piece and baffle, is thought to be a consequence of ion sputtering, predominantly by doubly charged ions. Figure A-89 shows unequivocally the extent of this erosion by comparing cross sections removed from the edge of the grid, in view (a), with several others taken from the center of the grid (views b, c, and d). The minimum thickness of the section shown in Fig. A-89(d) is only about 0.006 in. (0.015 cm) thick as compared to the 0.010 in. minimum thickness shown in Fig. A-88 (measured with micrometer). The difference in these values can be explained by the depression seen in view (d) and a coating on the downstream side of the grid that is about 0.001 in. thick. The coating on the downstream side of the screen grid electrode is readily seen in the magnified views shown in Fig. A-90. Figure A-90 also presents the electron beam microprobe scans which identify the elements composing the deposited layer. The molybdenum, iron, chromium and mercury are expected constituents while the silicon, aluminum and potassium originate in the glass used as a "potting" agent (to maintain sharp edges of the sectional sample). The origin of the barium and the chlorine is uncertain, however. Photographs of the entire downstream surface of the screen grid electrode are shown as Figs. A-91 through A-95. It is difficult to see any flakes or deposition in these photographs without magnification. Figure A-96 shows magnified views of what can be seen over the grid surface. Most of the electrode appears as shown in view (a) with a few "patchy" areas like the one shown in view (b). The electrode surface was examined for evidence of arcs, as was done with the accel, but the only marking found that has the appearance of damage caused by clearing a metallic flake is shown as view (c), (circled area). As a consequence of this relatively complete absence of grid damage like that usually caused when metallic

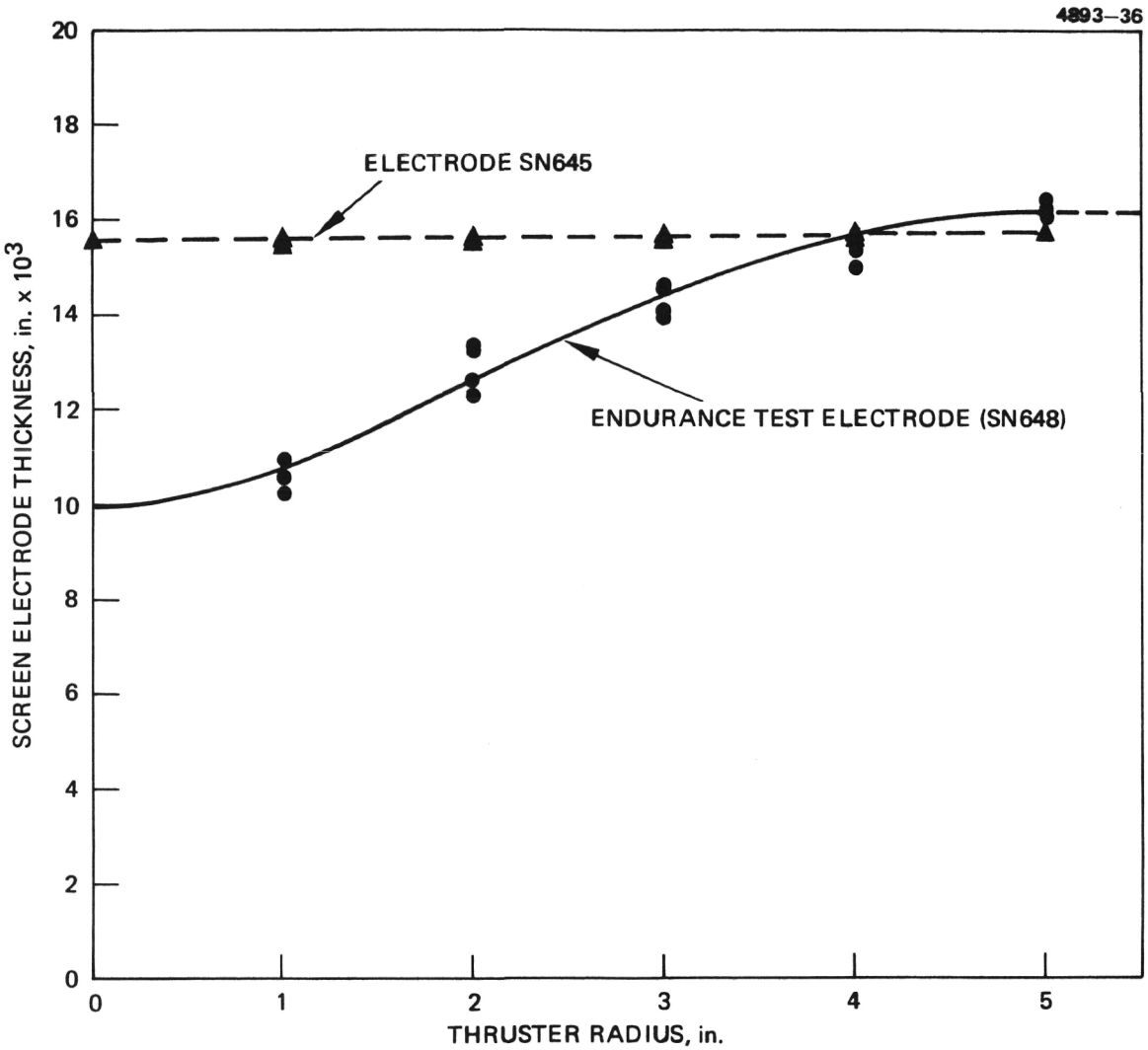

Figure A-88. Comparison of screen electrode thickness vs thruster radius for endurance test electrode (SN648) after 10,000 hours operation and slightly used screen electrode (SN645).

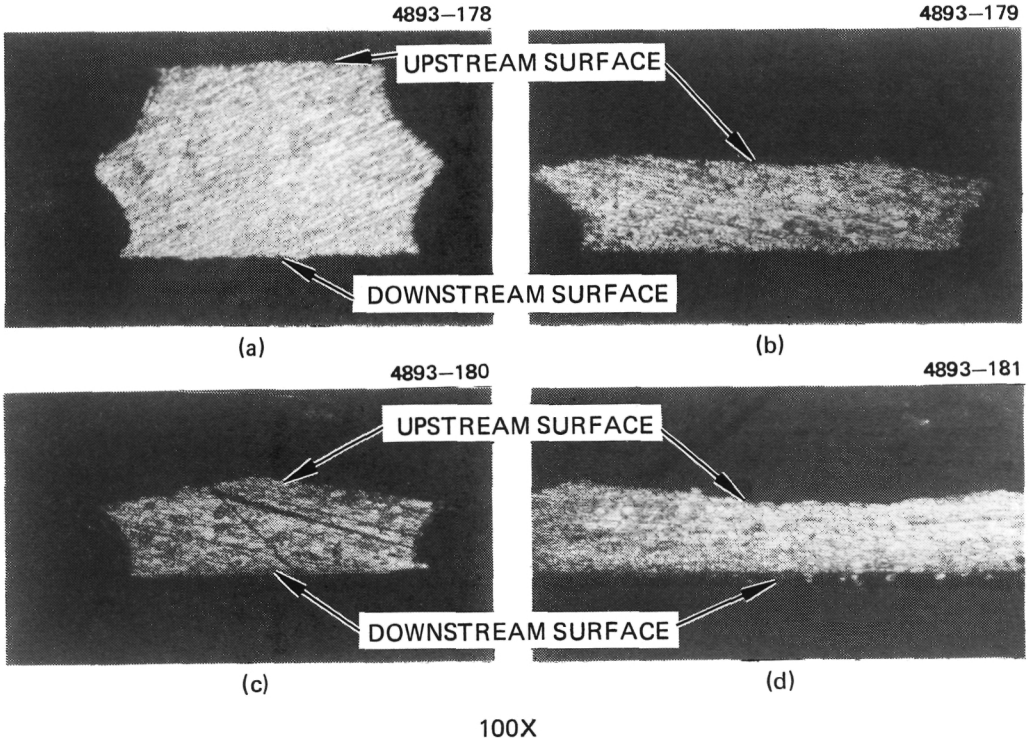

Figure A-89. Cross sections of screen electrode (a) edge of electrode; (b), (c) and (d) center of electrode.

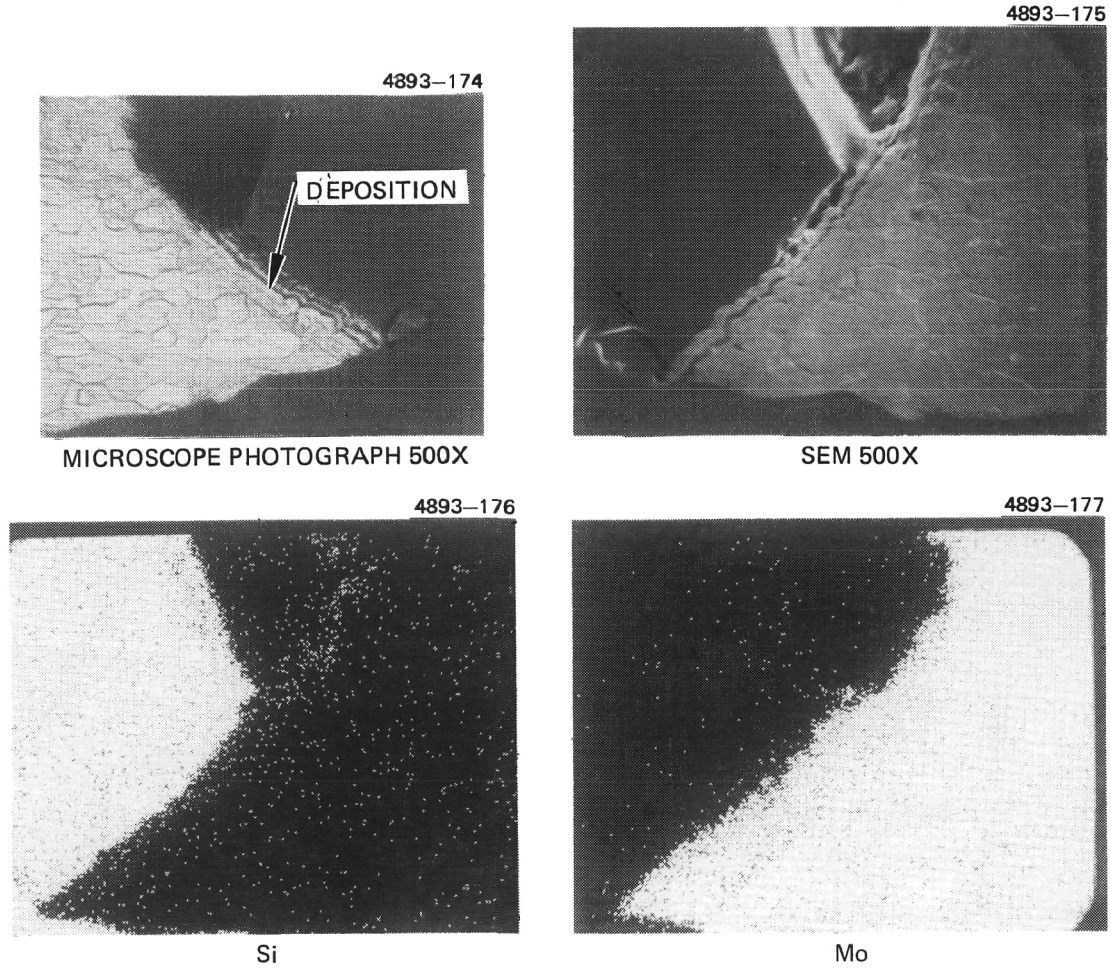

Figure A-90. Microscope photo, SEM. photo and electron beam microprobe analysis of screen electrode downstream coating.

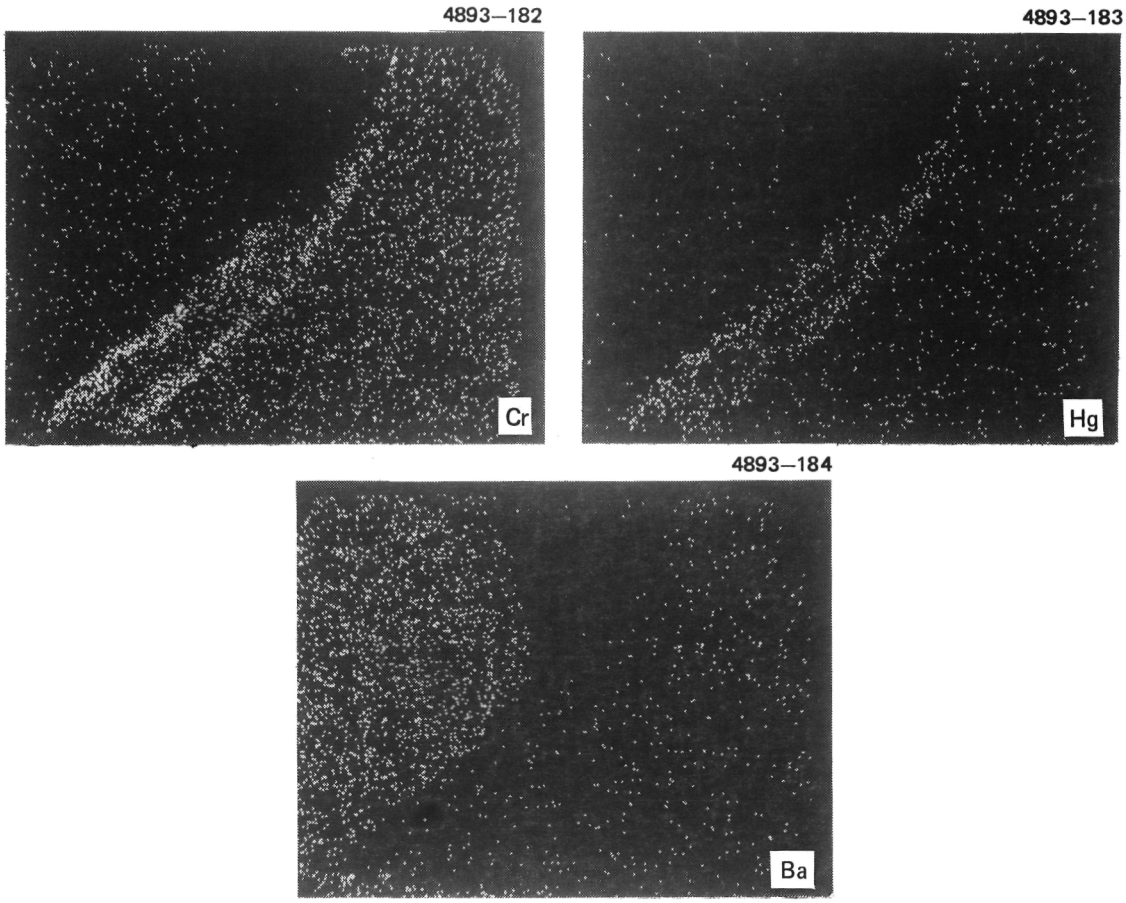

Figure A-90. (Continued).

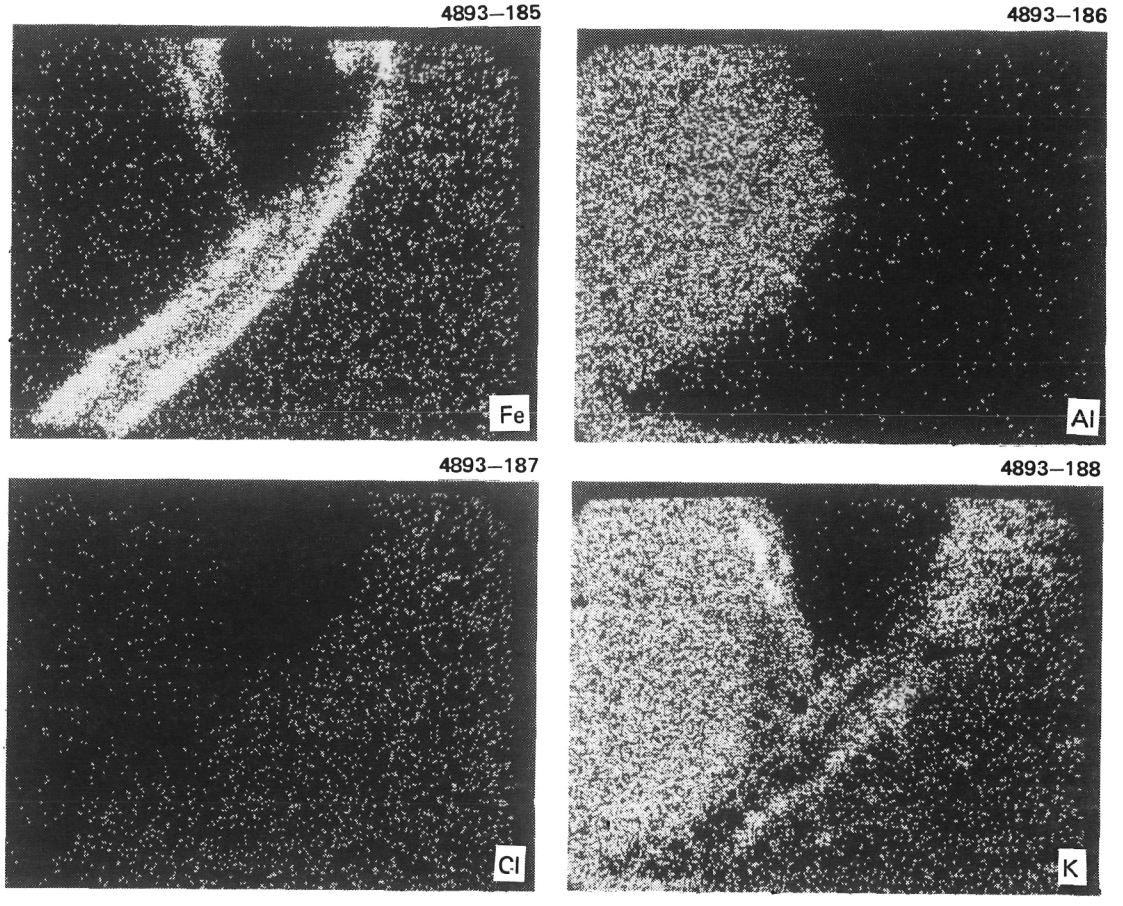

Figure A-90. (Continued).

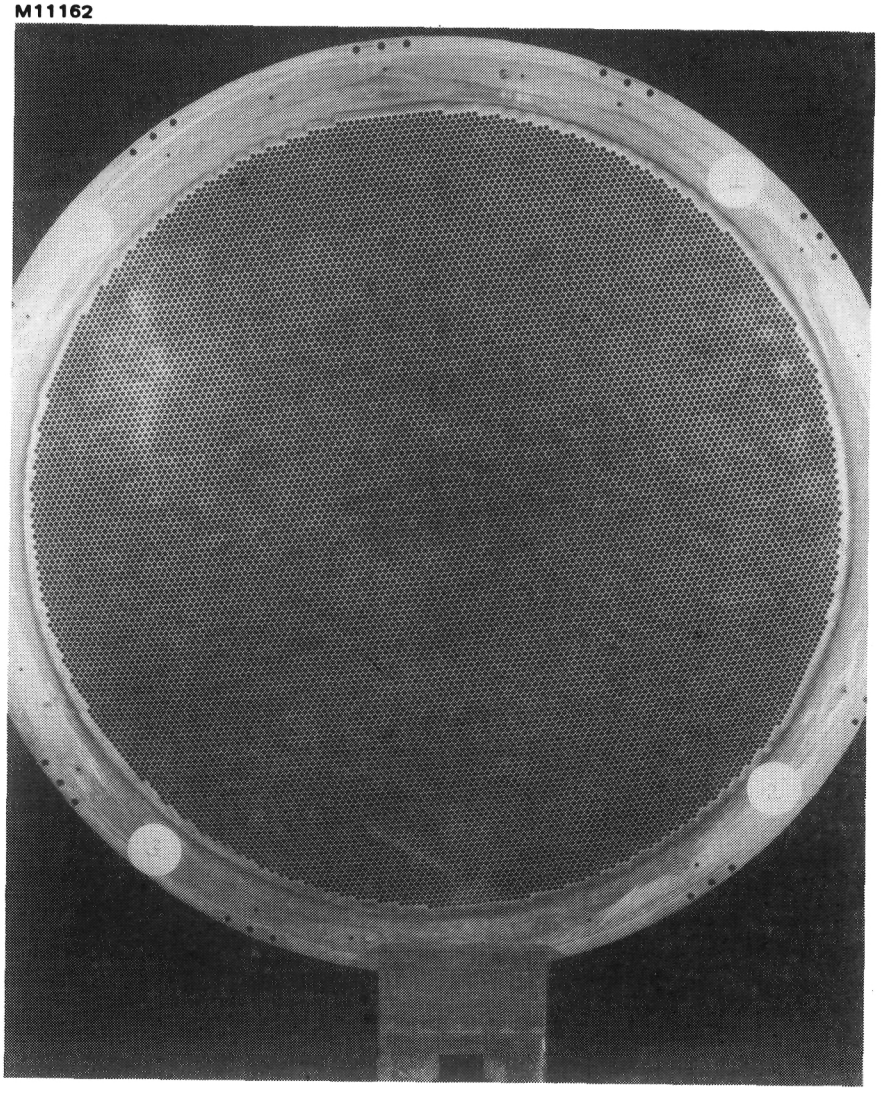

Figure A-91. Screen electrode, downstream side.

M11153

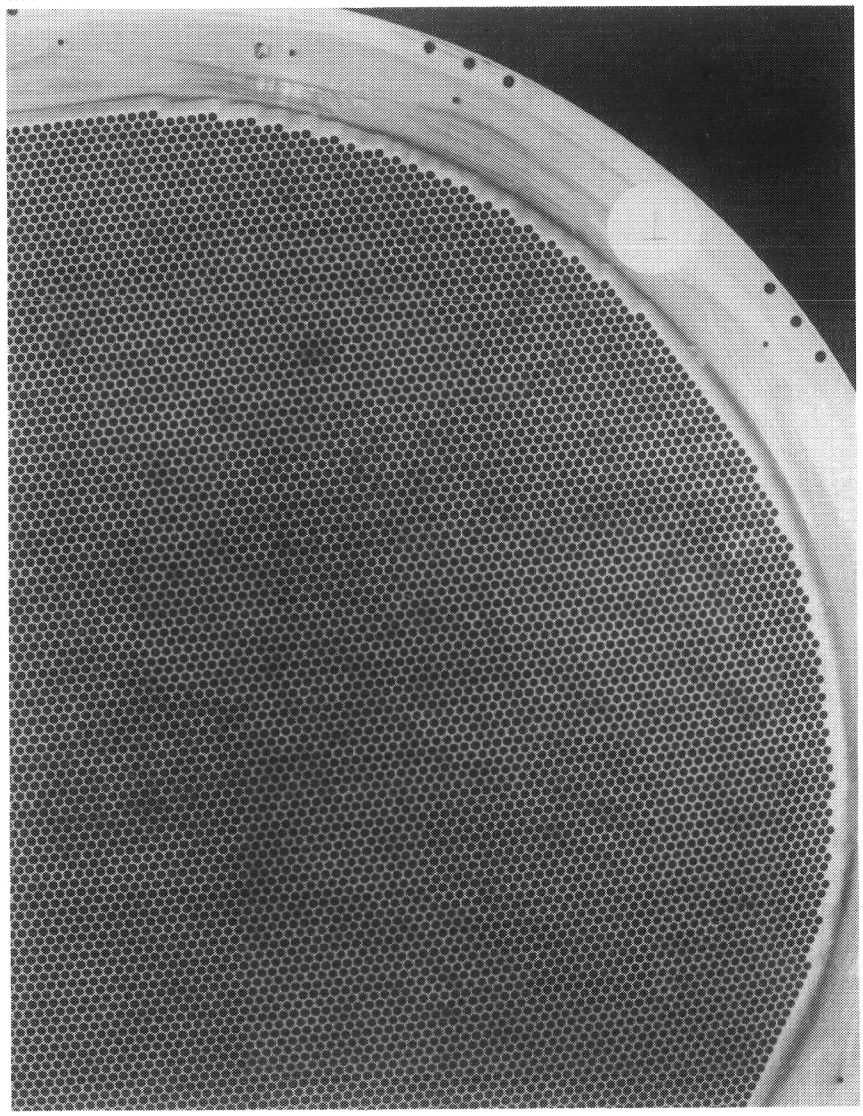

Figure A-92. Screen electrode, downstream side.

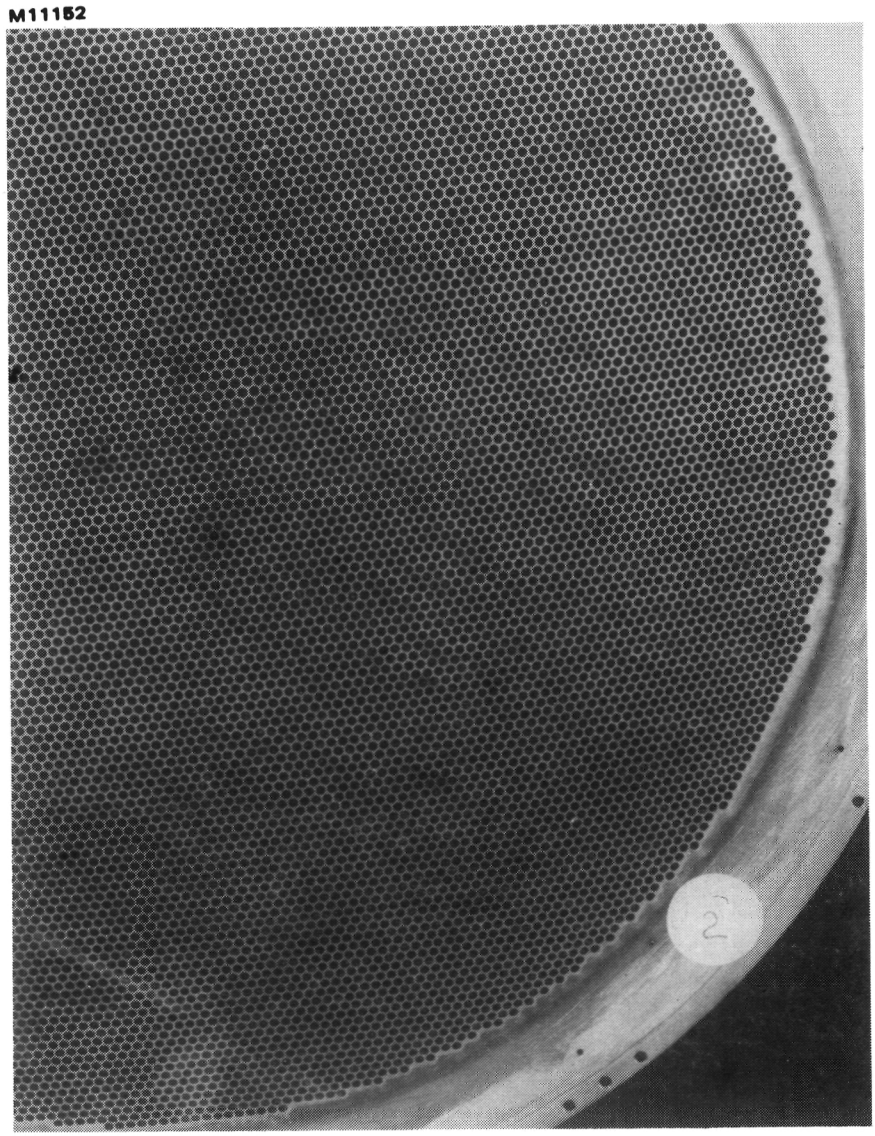

Figure A-93. Screen electrode, downstream side.

M11151

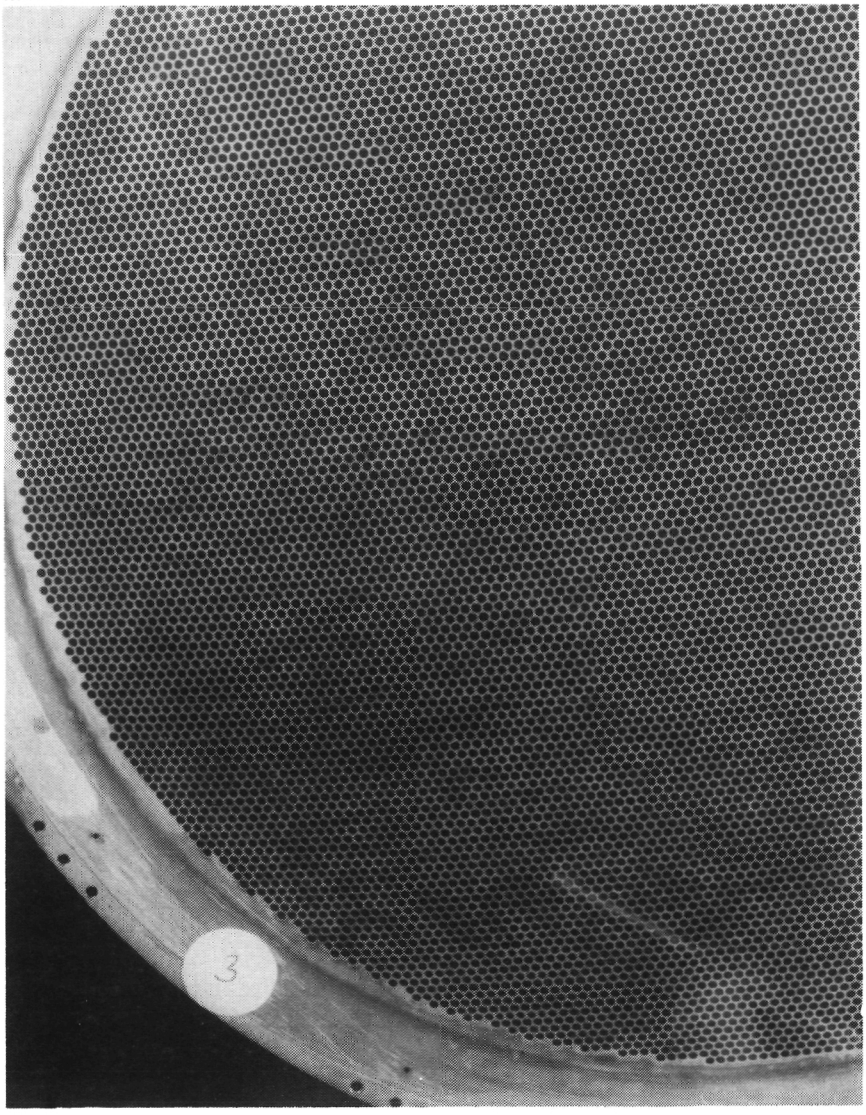

Figure A-94. Screen electrode, downstream side.

M11154 4893–263

Figure A-95. Screen electrode, downstream side.

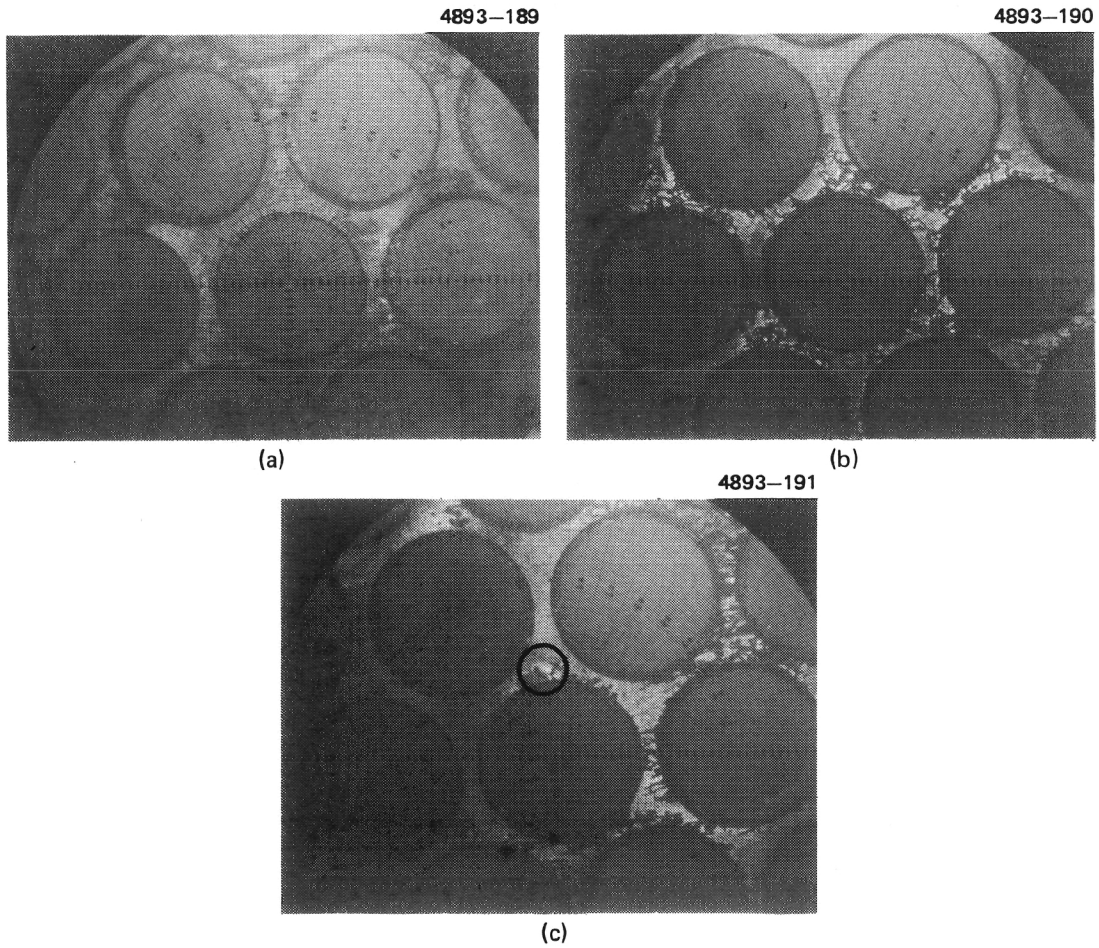

Figure A-96. Magnified view of selected areas of downstream surface of screen electrode.

shorts are removed by capacitive discharge, it is concluded that insignificant damage is caused by discharging a 1 μF capacitor charged to beam voltage (0.6 J) through a metallic grid short.

The ion optics electrode support structure used in this test has been replaced by a design that can be fabricated more readily. Consequently, only a few observations are commented on here. The primary purpose of this structure is to maintain a stable, uniform separation of the electrodes, establishing a voltage insulation to at least 2 kV. This structure demonstrated this property very well. One cause for concern is a series of markings seen on the insulator shields. These markings can be seen in Figs. A-97 through A-100 (arrows). While there is no real damage seen, it has not been possible to offer a convincing explanation of the origin of these marks. Presumably, the markings have been made by ions accelerated to these accelerator potential surfaces. It is possible that they were made during early testing before the installation of the tantalum gasket that prevents a direct path from the discharge chamber to these surfaces. If this is not the case, then some ion "leakage" from the discharge may still be occurring. The design of the support assembly which replaces the assembly tested here should eliminate most possible paths (unless the ions leak out between the optics electrodes).

The final figure presented in this section shows the support assembly with the grids removed (see Fig. A-101). Note the pristine condition of the insulators. It would be impossible to differentiate this assembly from one that had been tested only a few hours.

In summarizing this section on the ion optics assembly, the following major conclusions can be drawn.

- There is no evidence of excess charge exchange ion erosion associated with the neutralizer.
- Charge exchange ion erosion of the accelerator is a secondary factor in life limitation.
- Screen grid erosion by discharge ions is a significant factor in thruster wearout lifetime.
- Grid damage by sparks from metallic shorts is not a serious concern.

M11072

4893–192

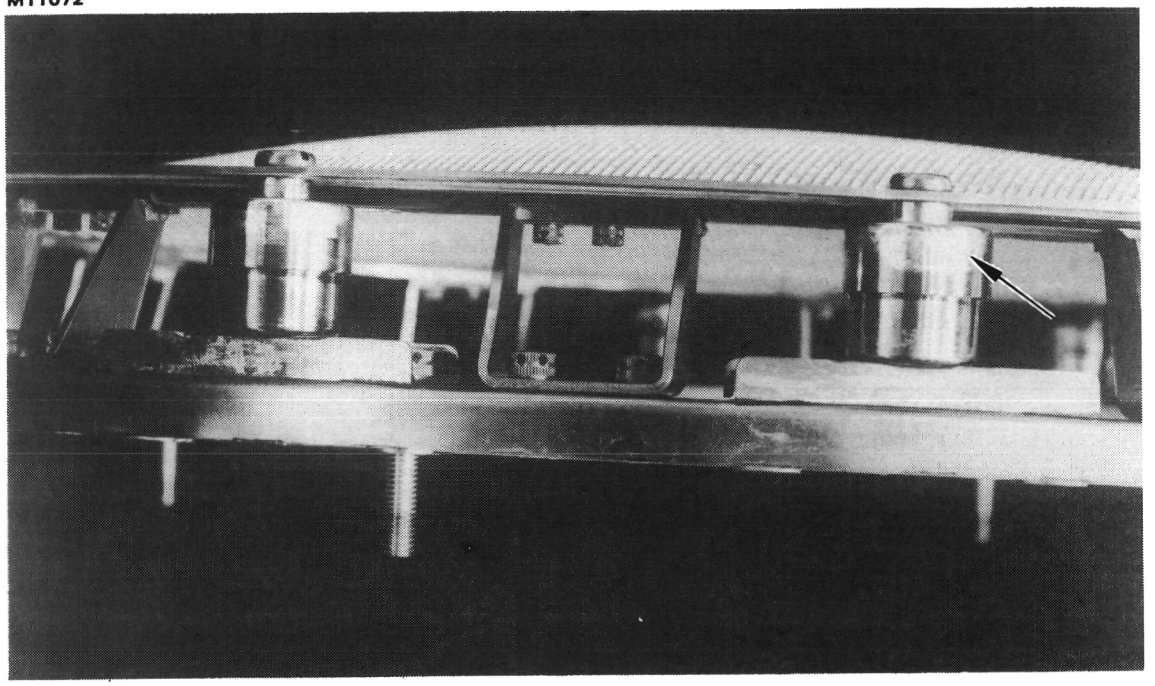

Figure A-97. Optics showing markings on insulator shields.

M11071

4893–193

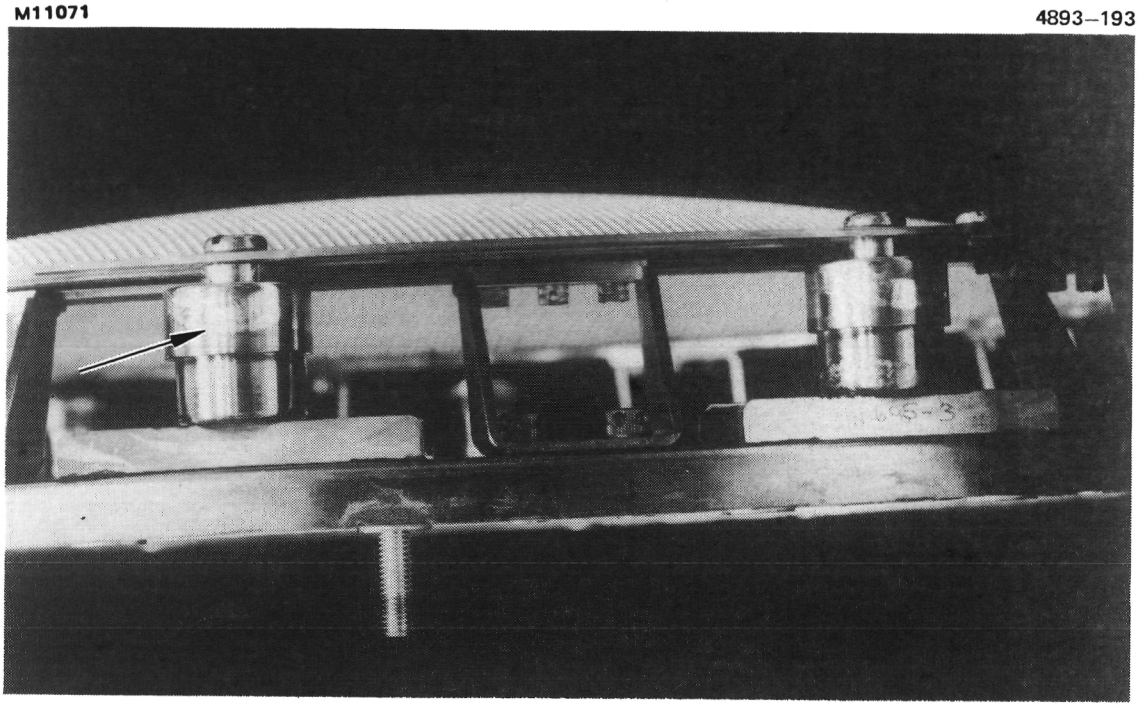

Figure A-98. Optics showing markings on insulator shields.

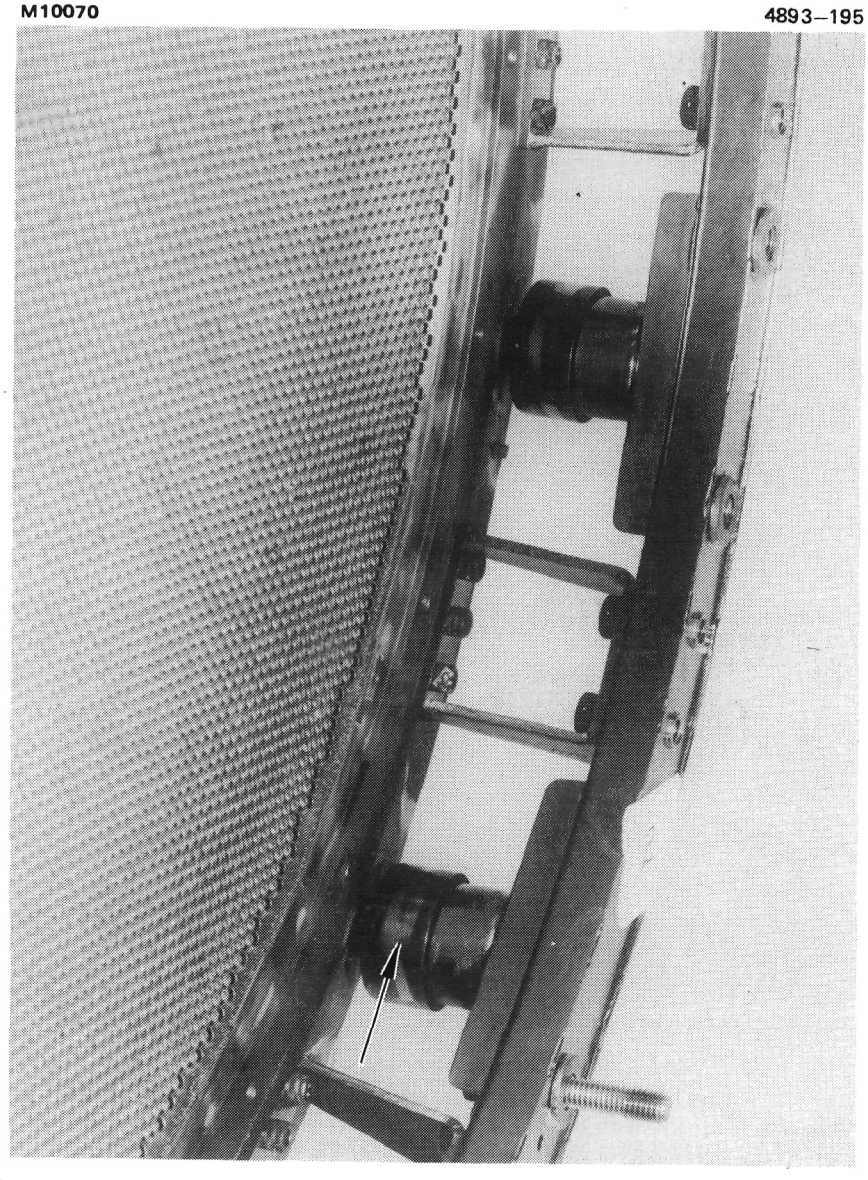

Figure A-99. Markings on optics insulator shields.

M11069 4893–194

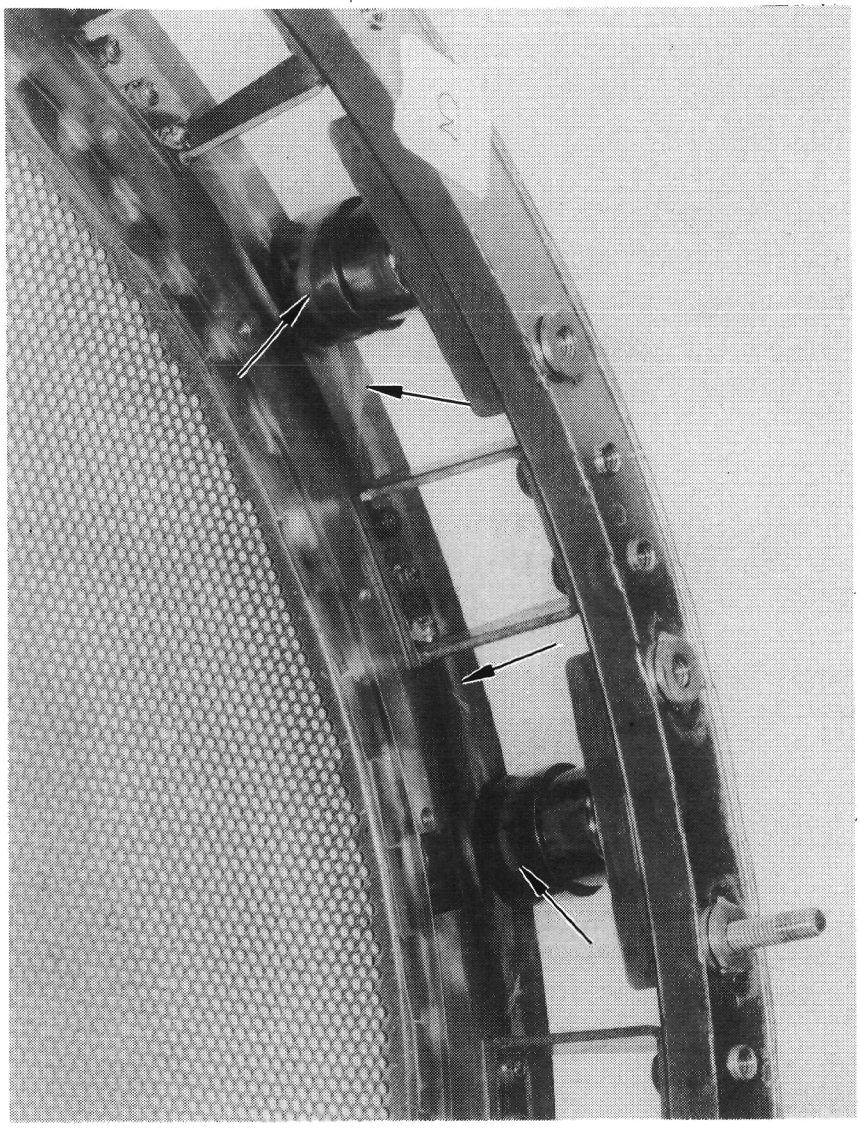

Figure A-100. Markings on optics insulator shields.

M11157

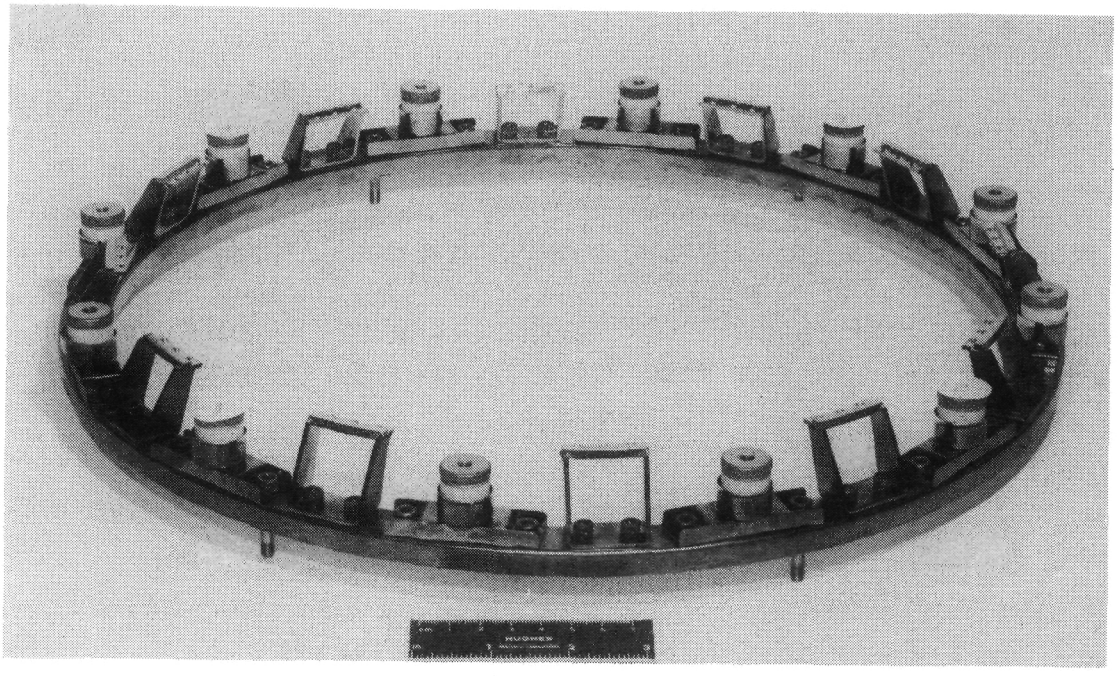

Figure A-101. Optics support assembly.

- Coating formation on the screen grid electrode (downstream side) may require special surface treatment of the electrode.

E. Neutralizer Assembly

Two neutralizer assemblies were mounted on Thruster SN 701 during the 10,000 hour test but only one, SN 701, was operated as a part of the test. The other neutralizer SN 415, was included as a back-up and was operated only for brief intervals both before and after the test to demonstrate that it was capable of operation. The components of the neutralizer that are of interest in this discussion are:

- the outer covering
- the keeper electrode
- the keeper and NIV support insulation
- electrical wiring and terminals
- the neutralizer isolator vaporizer subassembly (NIV).

Figures A-102 and A-103 show the portions of the neutralizer SN 701 outer covering that is of interest here. Note that there is no evidence of deposition and that the keeper cover is in fact eroded away at the downstream-most inboard surface. In contrast to this, Fig. A-104 shows that several surfaces of the neutralizer SN 415 outer cover are coated with both metallic deposits and finely divided mercury. Thus it appears that the active neutralizer is eroded while the inactive neutralizer has accumulated deposits. Figure A-105 compares dimensional parameters for the two neutralizers. Energetic ions with trajectories at angles up to 75° have been measured under the 2.5 kW Advanced Technology Ion Thruster Program (NAS 3-17831) and simulated by trajectory computations through variations in the shape of the neutralization plane. Consequently, it is concluded that the presence of erosion on the active neutralizer is related to the shape of the neutralization plane in the vicinity of the active neutralizer. A more definitive explanation would require further study of the observed high angle ion trajectories.

M3-5A 4893-267

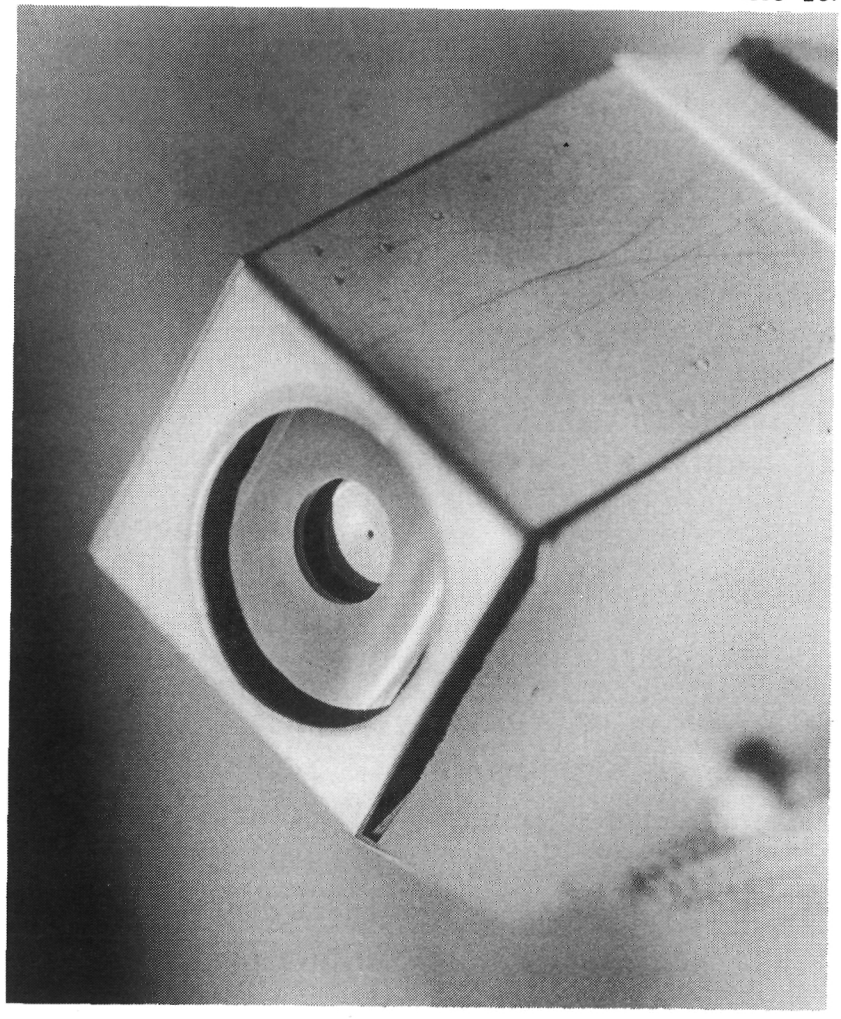

Figure A-102. Neutralizer 701 cover.

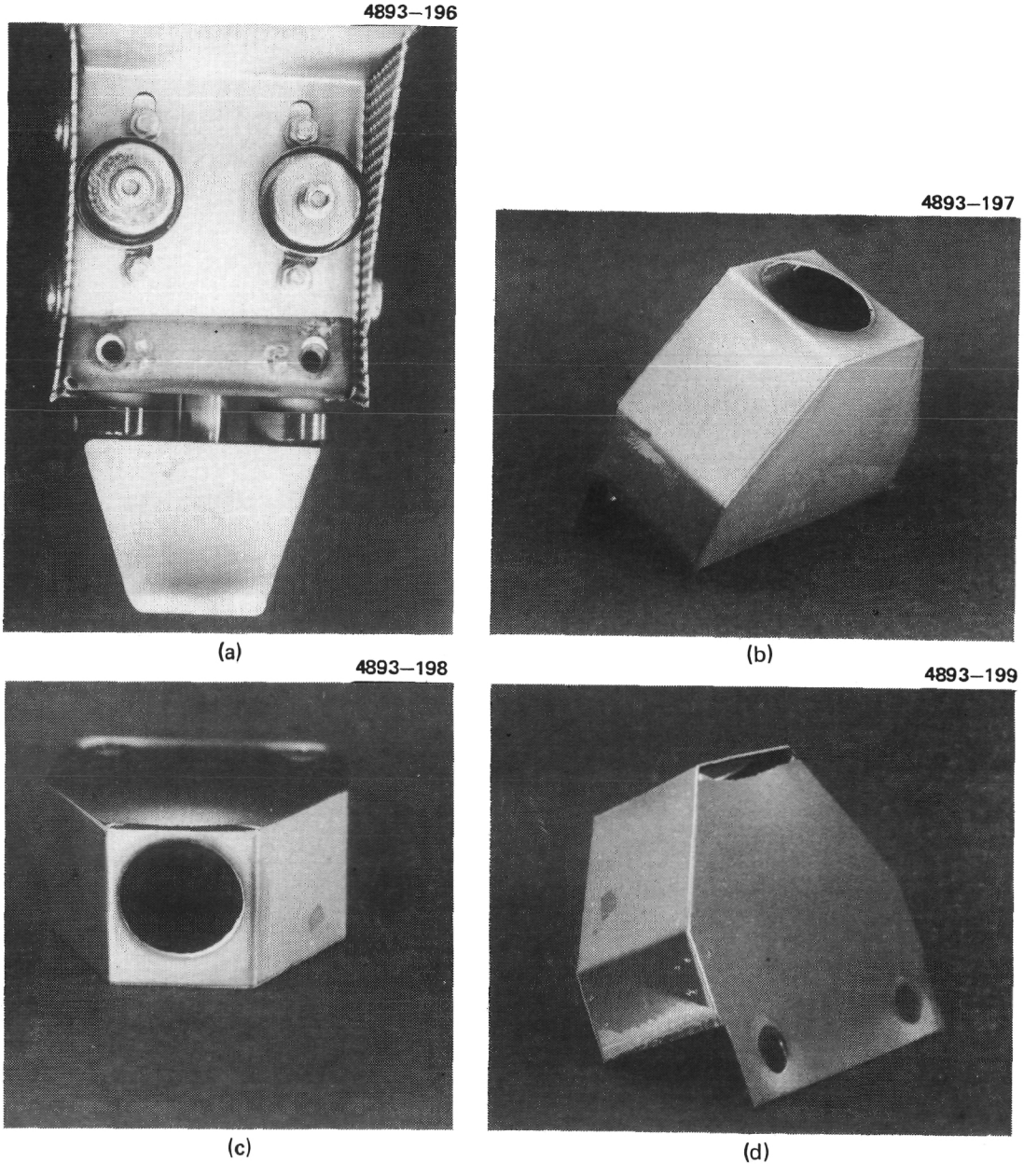

Figure A-103. Neutralizer 701 and keeper cover from neutralizer 701.

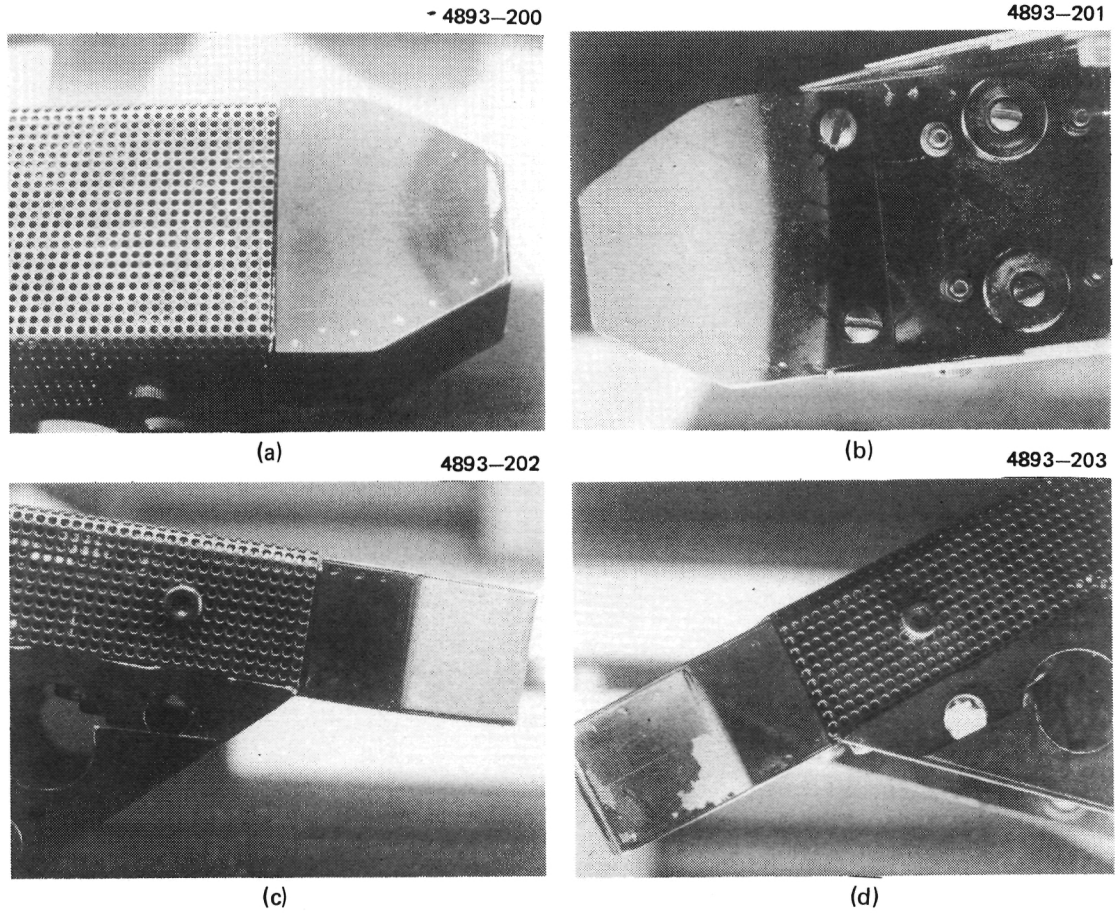

Figure A-104. Neutralizer 415.

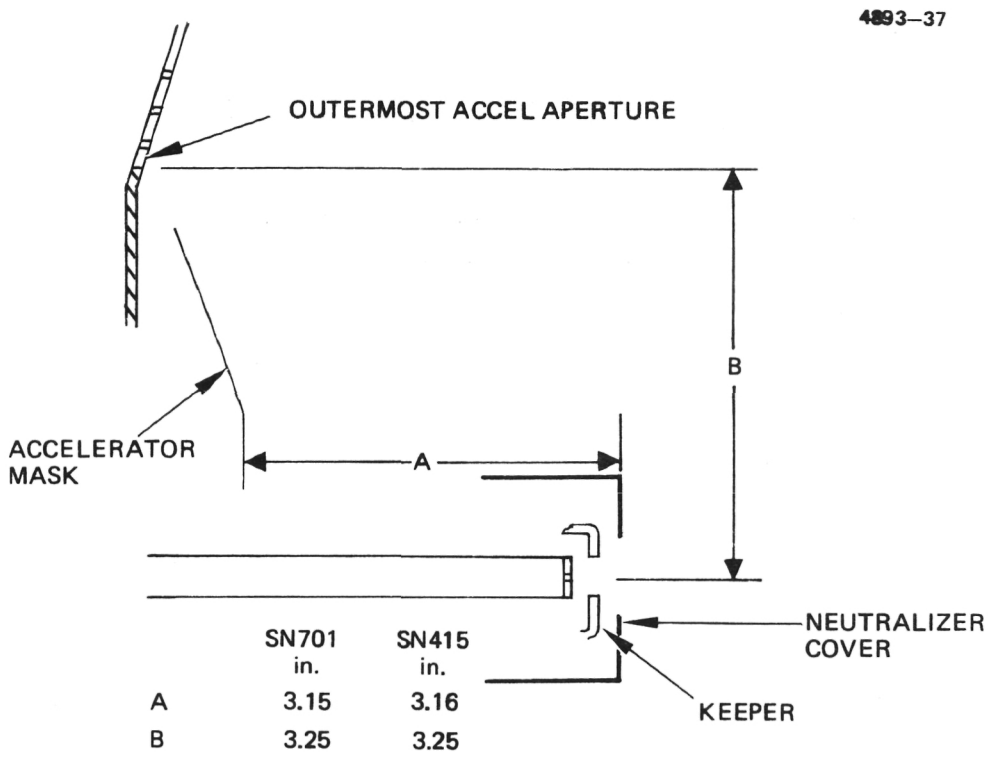

	SN701 in.	SN415 in.
A	3.15	3.16
B	3.25	3.25

a) NEUTRALIZER LOCATION

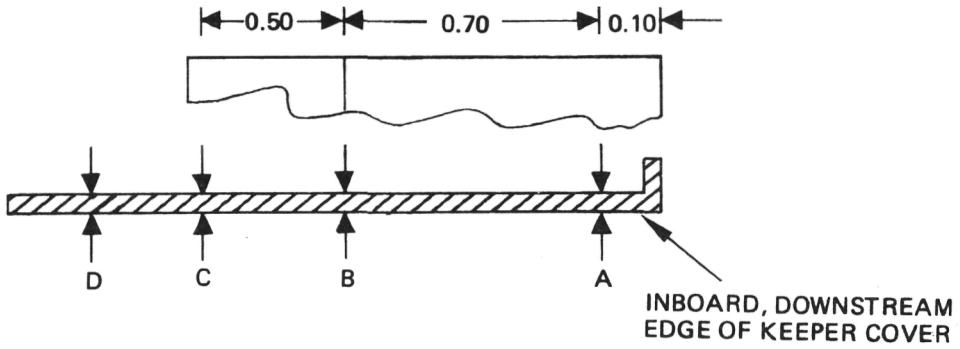

	SN701 in.	SN415 in.
A	0.004	0.018
B	0.017	0.019
C	0.019	0.020
D	0.023	0.022

b) NEUTRALIZER KEEPER COVER (SHIELD) CROSS SECTION DIMENSIONS

Figure A-105. Comparison of post test dimensions of neutralizers 701 and 415.

Figures A-106 and A-107 compare the appearance of the keeper electrodes on the active (SN 701) and reserve (SN 415) neutralizers. The SN 701 keeper electrode shows some discoloration on its exterior, but no substantial deposition such as that seen on SN 415. Both the weight and dimensions of the SN 701 keeper were unchanged (within measurement accuracy). Some copper colored deposition is also present on the inside of the SN 701 keeper electrode. This is thought to originate in the copper braze (now missing) of the tip heater support. A leakage resistance of 1 to 5 MΩ is present across the keeper support insulators for both assemblies. It is apparent in both Figs. A-107(a) and A-108(a), (b), that the unshielded support insulator located inside the neutralizer housing has been coated over. Loosening of the fastener holding the keeper lead wire for neutralizer SN 701 increased the leakage resistance from 1 MΩ to greater than 2000 MΩ. In either case, the neutralizer keeper insulator leakage was not a source of difficulty during the test. The remaining discussion in this section relates to 700 series design components.

Figure A-108 shows neutralizer SN 701 with the outer covering removed. Note the deterioration of the wiring and the discoloration of the insulators. Figure A-109 shows matching discoloration on both the interior and exterior surfaces of the outer covering parts. It is apparent that at least parts of the discoloration has its origin inside the neutralizer cover, and based on the decomposition seen in the wiring, the wiring insulation is a probable source. Thus, future designs should make better provision for routing polymide insulated wire such that high temperatures and consequently deterioration are avoided.

If the neutralizer is to be truly isolated from the spacecraft, then surfaces of the insulators that support the NIV, and the keeper electrode must be kept in good condition, in the same manner as the propellant isolator ceramics. Figure A-110 shows considerable darkening of the unshielded portions of all of these insulators. Note that the double shielded portion of the support insulator, shown in Fig. A-110(d) is clean. The NIV isolator (Fig. A-110(a), (b)) had a leakage resistance of 5 MΩ as measured with all leads disconnected.

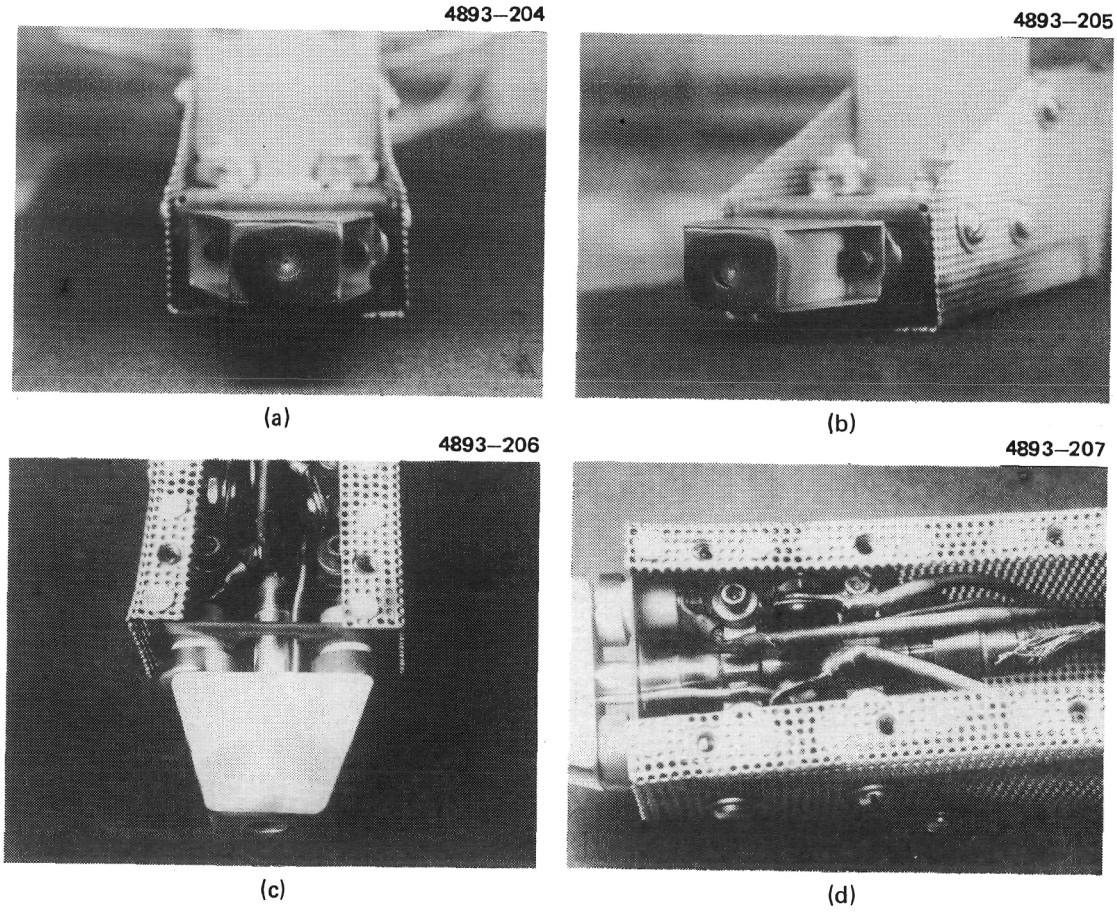

Figure A-106. Neutralizer 701.

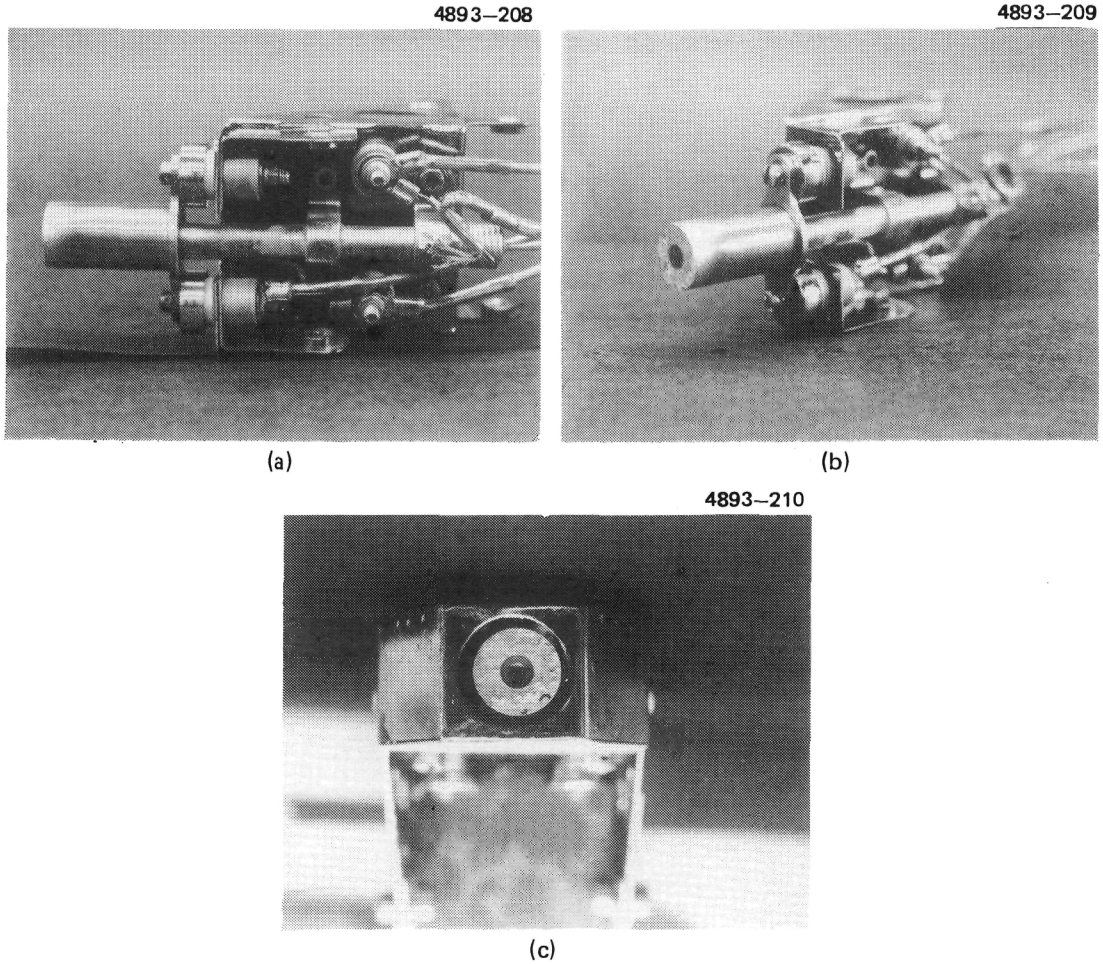

Figure A-107. Neutralizer 415.

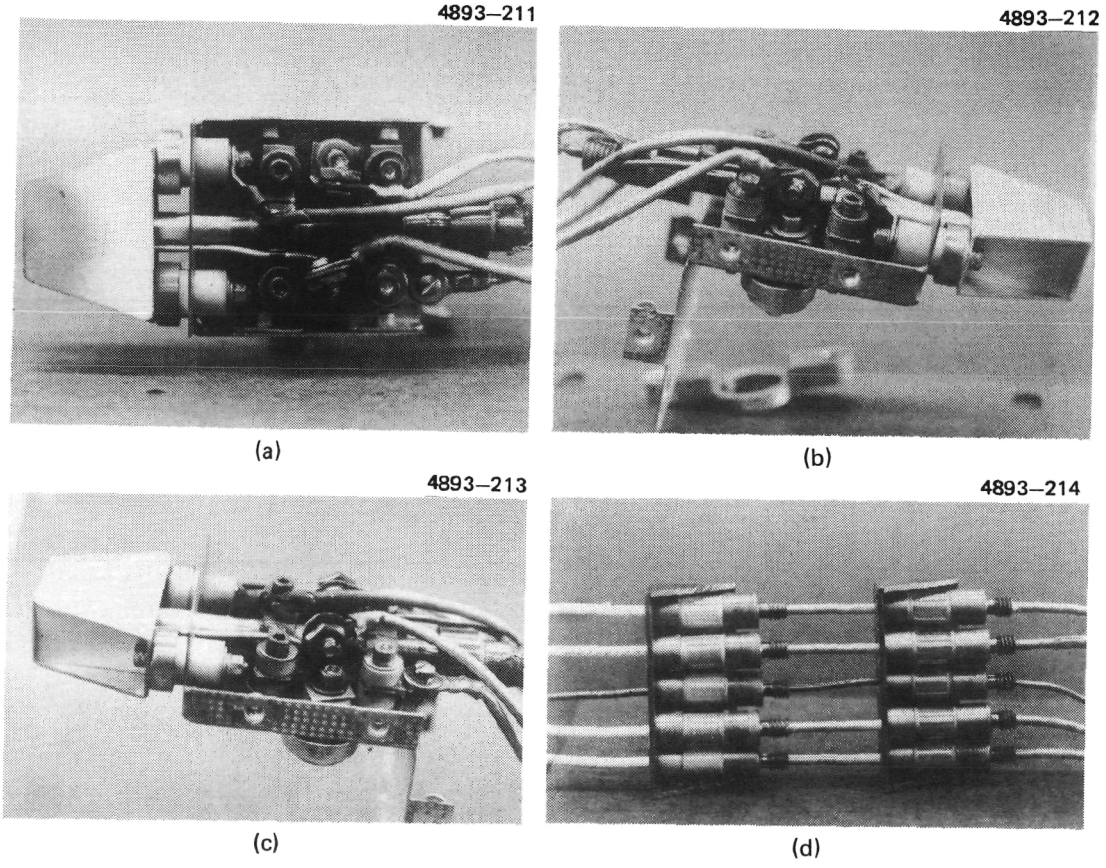

Figure A-108. Neutralizer 701.

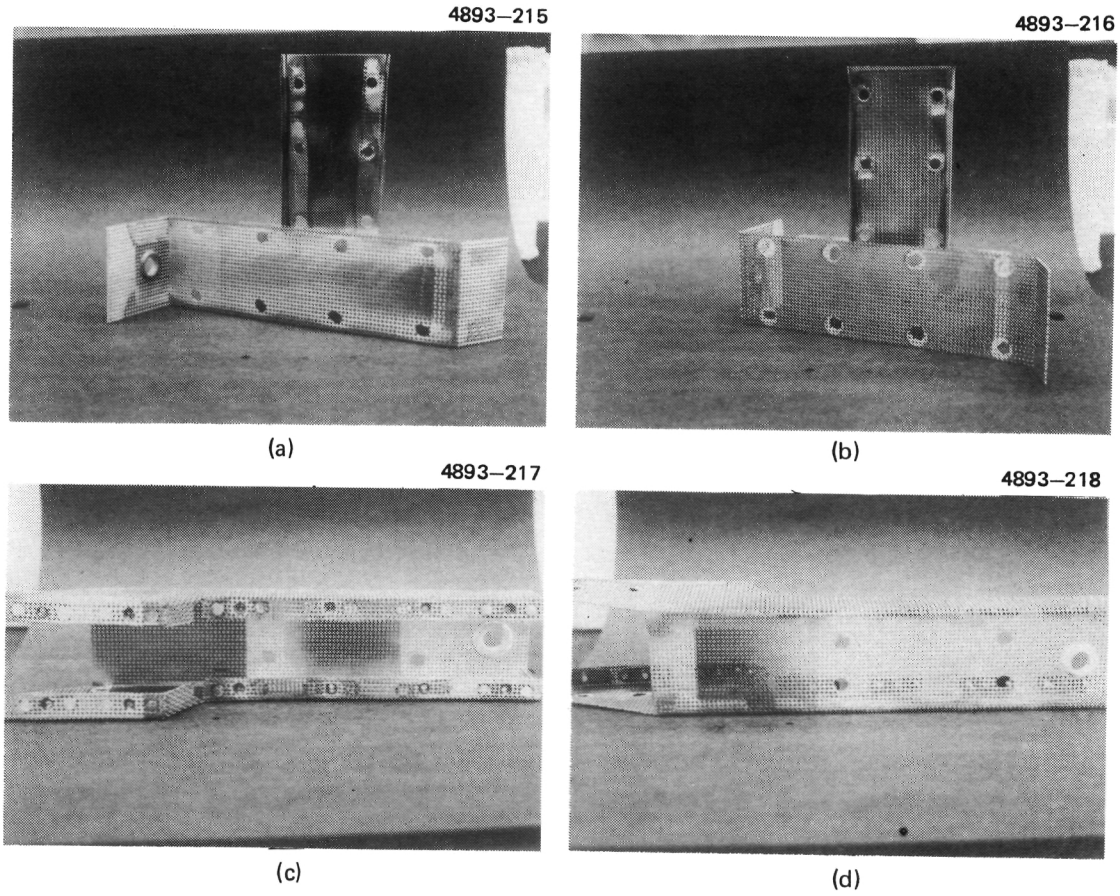

Figure A-109. Cover from neutralizer 701.

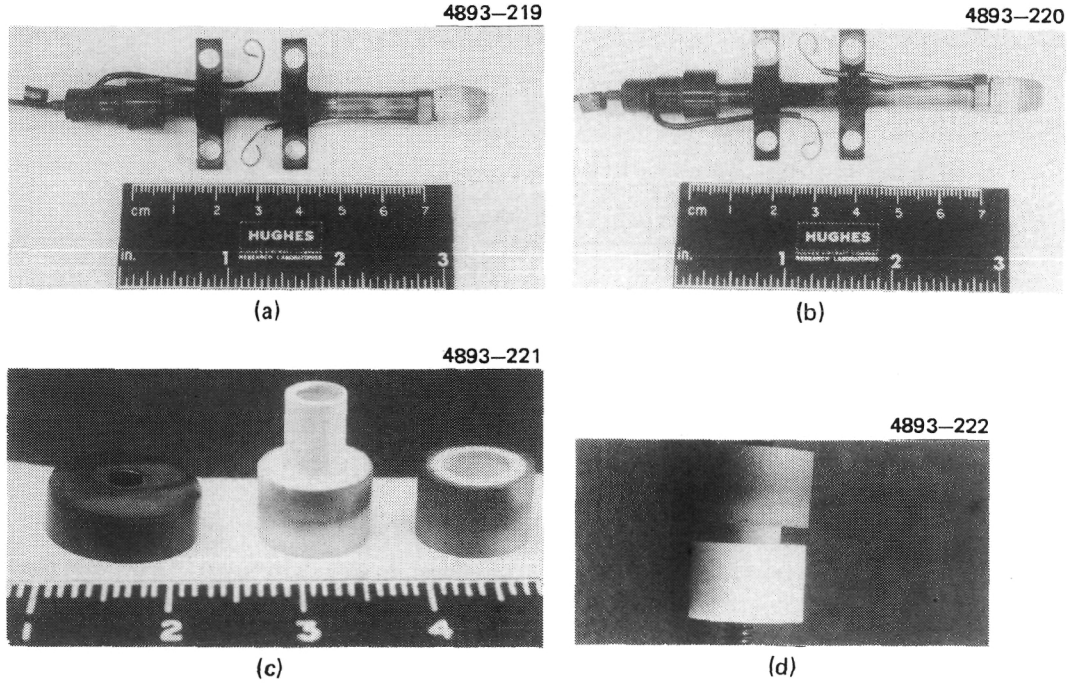

Figure A-110. (a) and (b) NIV 701; (c) and (d) neutralizer 701 keeper insulators.

The neutralizer assembly, as examined here is considered to have no major wear problems. Erosion of the keeper cover would be corrected most efficiently by eliminating or reducing the high angle trajectory ion flux. Otherwise, increasing the thickness of the cover would suffice to compensate for the erosion. Insulator deterioration can be readily eliminated by shielding of the exposed ceramic surfaces. Although the cathodes are discussed in detail in the following section, it is appropriate to note here that neutralizer cathode wear is relatively insignificant. Some operational anomalies observed during the test have resulted in a design change for the cathode insert, however.

F. Discharge and Neutralizer Cathodes

The hollow cathodes which serve as the electron sources for the discharge chamber and the neutralizer are considered to be critical components in determining thruster lifetime. Satisfactory cathode operation depends on the properties of three major elements as follows:

- Cathode orifice dimension
- Cathode insert
- Cathode tip heater.

Cathode orifice dimensions govern the internal mercury vapor pressure for a given flow rate and thereby control the operational characteristics. Small changes in dimensions are tolerable and do not significantly affect the overall performance or operational characteristics of either the discharge chamber or the neutralizer. Measurement of the discharge cathode orifice using wire gages show that the orifice diameter decreased slightly from 0.028 in. (0.071 cm) before testing to 0.026 in. (0.066 cm) after the test. Figure A-111 (a) through (d) compares photographs of the discharge cathode orifice and radiator taken before and after the test in views (a) through (d). It is apparent that the surfaces of the cathode and radiator have been eroded by ion sputtering. Cross sections of the cathode shown in Fig. A-111(e) and (f) indicate that the material removed is negligible. Figure A-111(f) shows evidence of a coating in the orifice region. The erosion seen is not considered

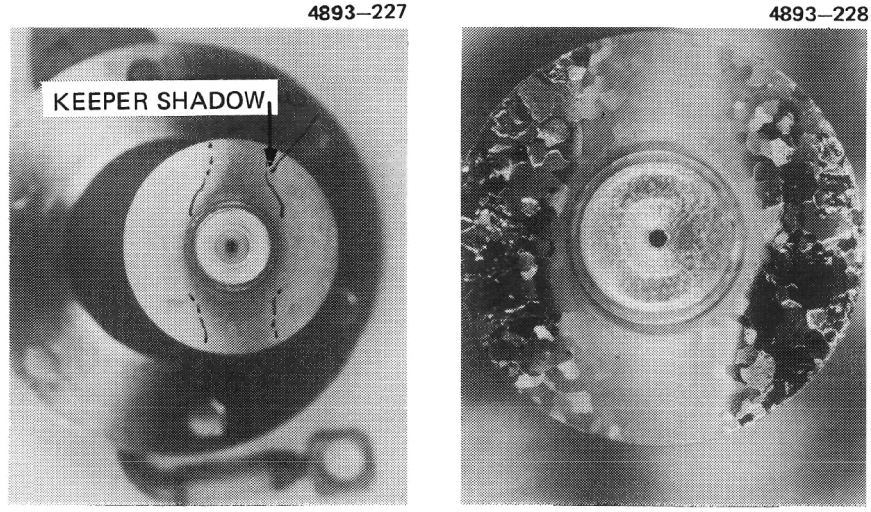

(a) BEFORE TEST (b) AFTER TEST

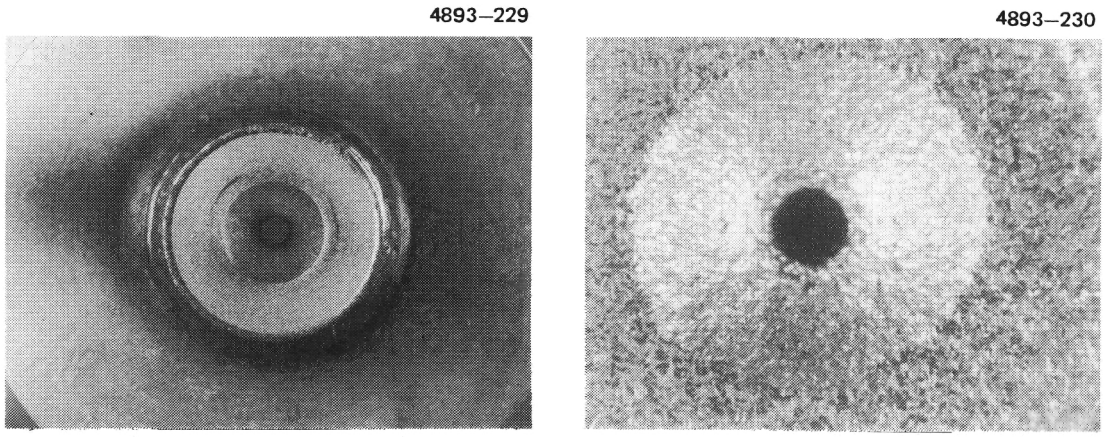

(c) BEFORE TEST (d) AFTER TEST

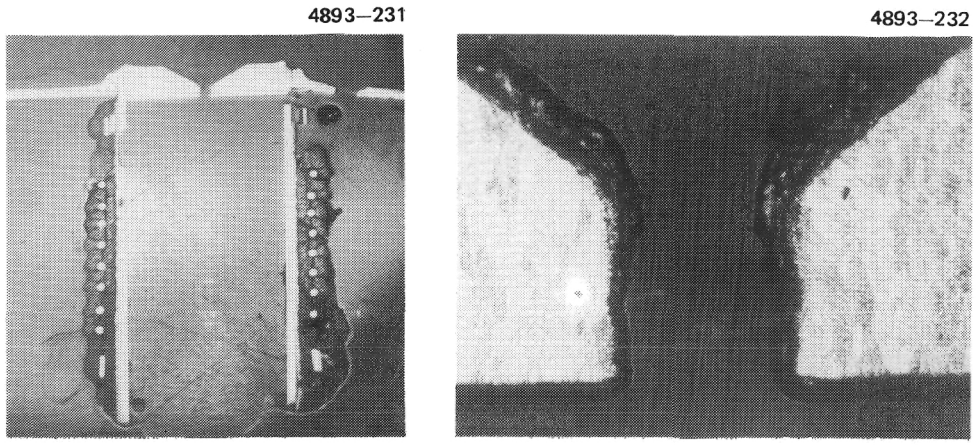

(e) (f)

Figure A-111. Cathode radiator and orifice before and after endurance test.

to be a life limiting factor at this time. This cross section does not pass exactly through the cathode center and consequently determination of the orifice diameter should not be attempted using Figs. A-111(e) and (f). The length of the orifice channel should be to scale, however, and is seen to be only 0.016 in. (0.041 cm) which is slightly smaller than the 0.020 ±0.003 in. (0.051 ±0.008 cm) in dimension specified. It is not known whether the initial dimension was low or whether this difference represents the erosion on the cathode face.

The neutralizer cathode orifice dimensions were not modified significantly during the test either. Figure A-112 compares photographs of the neutralizer orifice taken before and after testing in views (a) and (b). Again, some erosion by ion sputtering is evident and the cross sections shown in Fig. A-112(c) and (d) show the extent of the dimensional changes. As in the case of the discharge cathode these cross sections should not be used to determine the orifice diameter because the cut is neither parallel to the cathode axis nor does it pass through the orifice center. The orifice length is represented relatively accurately, however, and is seen to be reduced to 0.039 in. (0.0013 cm) by chamfering erosion as seen on the cathode face. The cathode plug still measures the original 0.051 in. (0.129 cm) at the edge. Again, the erosion seen is considered to be tolerable and both cathodes are thought capable of operating at least 10,000 hours more based on orifice wear and assuming that erosion processes are linear with time.

The cathode inserts used in this test were 0.0005 in. (0.0012 cm) thick tantalum foil coated with Baker R-500 triple carbonate mixture. Loss of the barium coating on the insert by evaporation or reaction with the tantalum has been considered a possible life limiting factor in the operation of hollow cathodes of this type. The downstream edge of the insert was positioned 0.25 in. upstream of the orifice in the discharge cathode and 0.375 in. upstream of the orifice in the neutralizer cathode. It is thought that the operating temperature of the inserts at these locations ranges between 850°C and 950°C. In this temperature range, the rates for evaporation and reaction of barium should provide long life. It was possible to remove both cathode inserts in relatively good

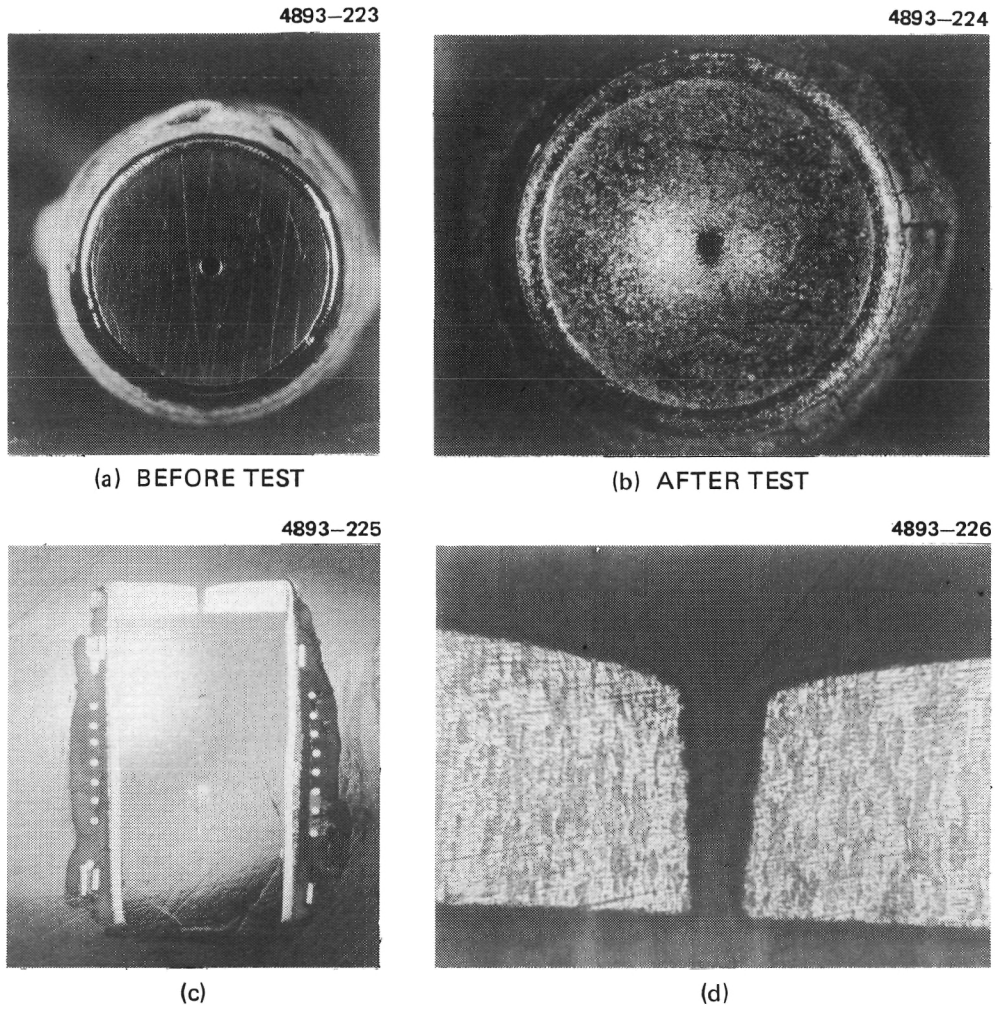

Figure A-112. Neutralizer 701 orifice before and after endurance test.

condition, although the powdery coating, thought to be the triple carbonate (or oxide) material, was extremely fragile and brushed off quite easily. The discharge cathode insert is shown in Fig. A-113 as it appeared on removal, and after it was unrolled. The downstream-most edge of the insert appeared "fused" and broke off during the unrolling process. The insert material was neither extremely brittle nor ductile but was "springy" and caution was required to prevent the foil from rolling up again. The weight of the insert was 0.359 g after the test as compared to the initial weight of 0.401 g. No attempt has been made to analyze this weight loss (42 mg) since a whitish, powdery coating, presumed to be a portion of the emissive coating material is found inside the cathode and on the downstream surface of the C-IV flange (see Figs. A-114 and A-115). Moreover, the foil insert design has been replaced by a barium aluminate impregnated porous tungsten material in 800 series thruster designs. This change has been made to improve the quality control and operational control of the neutralizer. Thus, the results of further quantitative analysis relating to the foil design are considered relatively unimportant.

The neutralizer cathode insert was removed in the same manner as the discharge cathode insert. A weight measurement was not attempted here because of the relatively large quantity of the coating that fell off as the insert was pulled from the cathode. Photographs of the neutralizer cathode insert are shown in Fig. A-116. On the basis of the amount of emissive material remaining and the absence of insert embrittlement, it is concluded that considerable additional cathode lifetime could be obtained from the inserts in both the neutralizer and discharge cathodes.

The cathode heaters are required primarily to ignite the hollow cathode discharge. Once ignited, the keeper discharge imparts sufficient power to the cathode to maintain emission. The cathode heaters used in the 700 series design make use of alumina encapsulated tungsten-rhenium wire. The alumina encapsulation is accomplished by flame-spraying the material over the heater. Fabrication of these cathodes in a controlled, reproducible manner has been difficult and a swaged heater design is being substituted for future thrusters. The cathode heaters

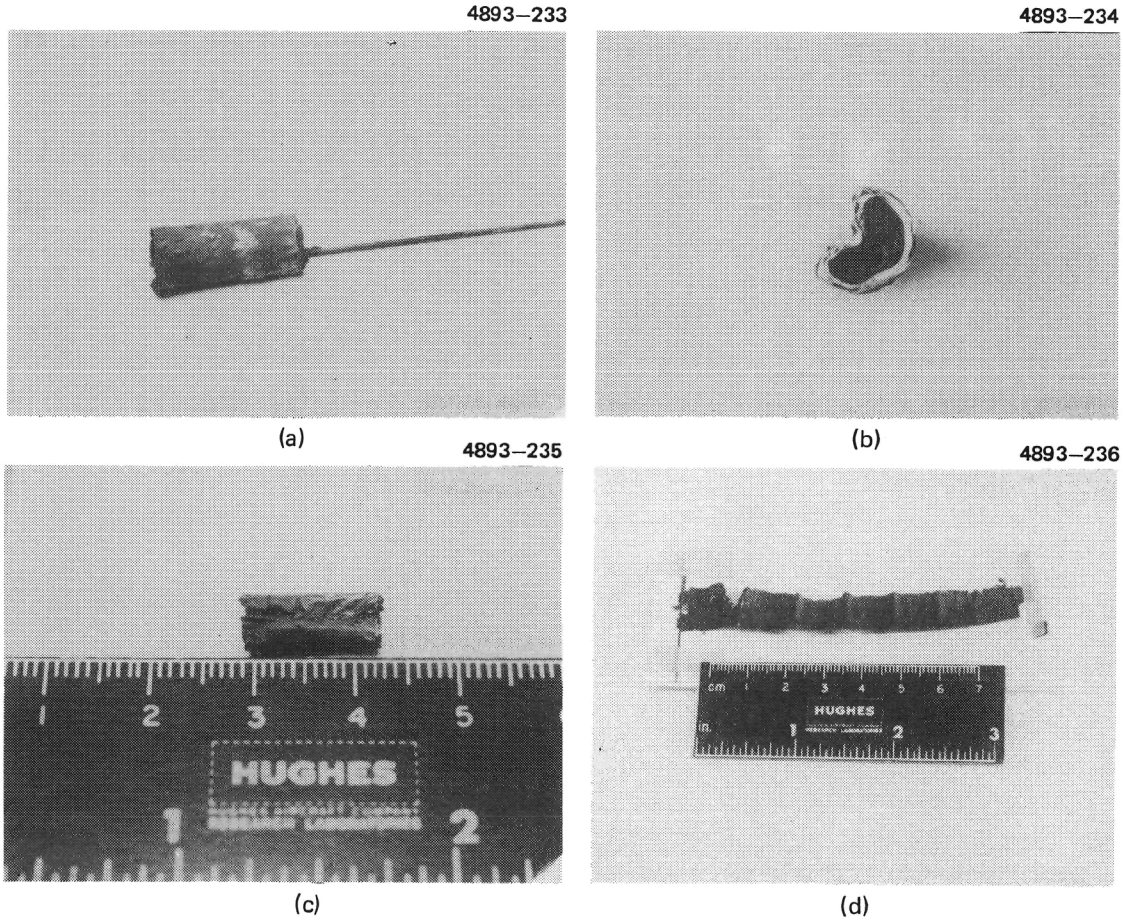

Figure A-113. Discharge cathode insert.

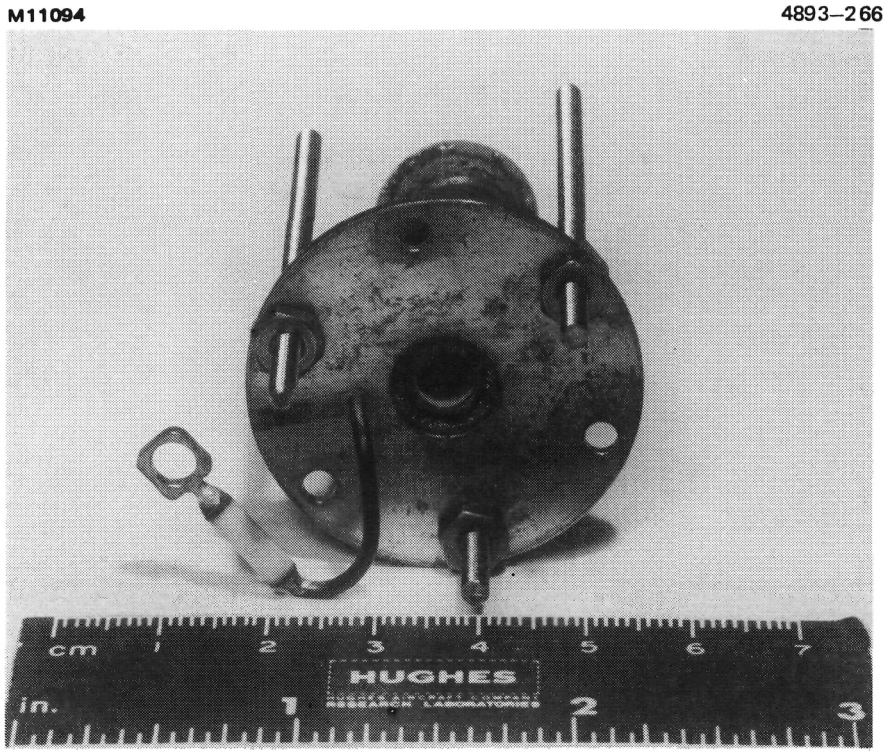

Figure A-114. Cathode assembly. Powder inside cathode is presumed to be emissive coating from insert.

M11116 4893–268

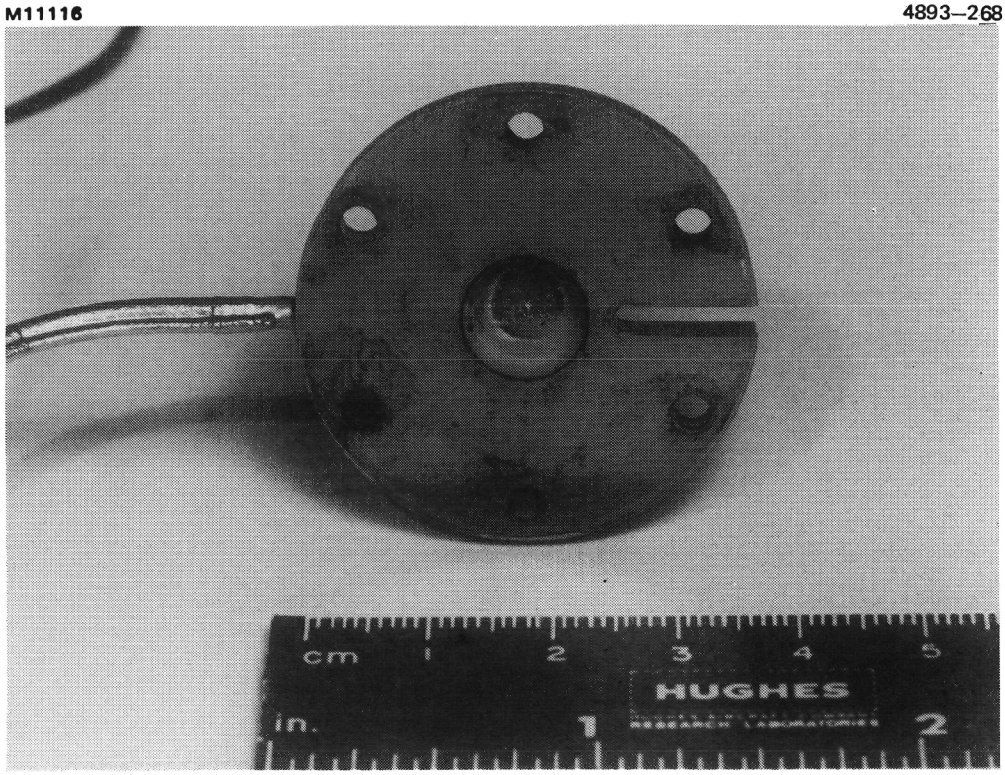

Figure A-115. Downstream surface of C-IV flange.

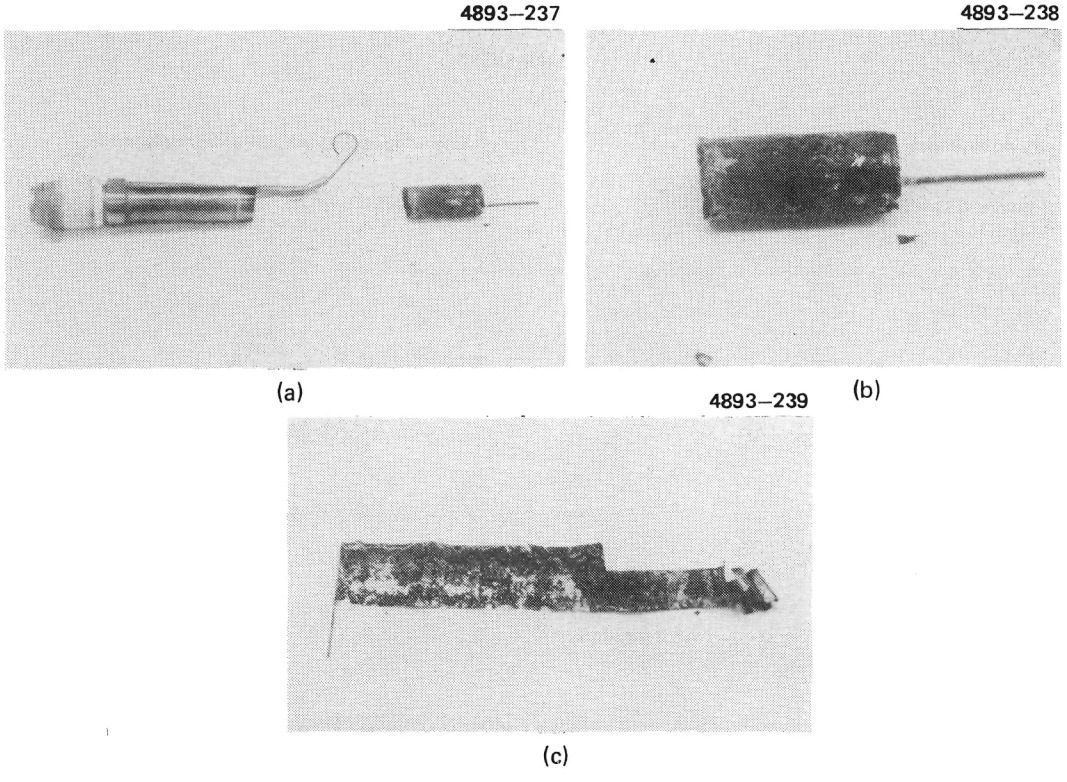

Figure A-116. Neutralizer 701 insert.

used in this test had been carefully selected as the best of a group and exhibited excellent performance throughout the test.

The discharge cathode requires heat shielding to enable the cathode to reach emissive temperature, primarily because the alumina bond between the heater coil and the cathode tube does not provide adequate thermal contact. As pointed out earlier, this heat shield was partially eroded by ion sputtering. It is thought that this ion sputtering is a consequence of operating with a damaged baffle, which permitted high energy discharge ions to enter the cathode pole region. Figure A-117 shows the extent of the erosion of the heat shield. Three of the five layers have been penetrated (see Fig. A-118), and if this type of erosion were continuous, the heat shield could probably furnish another 5000 hours of operation without difficulty. Figure A-119 shows the cathode heater with heat shields removed and compares the insulator as seen before and after testing. Notice that although the ceramic material is cracked, there is no loss of material or insulation between heater windings.

The neutralizer heater is shown in Fig. A-120 as seen before and after the test. Note that the cracks seen in the ceramic coating were present even before the test and the many cycles of start-up only increased the cracking somewhat. Both of these heaters performed excellently during the 10,000 hour test, without any change in power requirements.

To summarize, it is concluded that both the discharge chamber and neutralizer hollow cathodes have demonstrated the capacity for 10,000 hour operation without degradation and could be operated for substantially greater periods before wearout.

G. Isolator-Vaporizer Assemblies

There are three isolator-vaporizer assemblies in the 700 series EM thruster design which supply mercury vapor to the discharge cathode (C-IV), the discharge chamber (MIV) and the neutralizer cathode (NIV). The neutralizer isolator has been discussed earlier and will not be

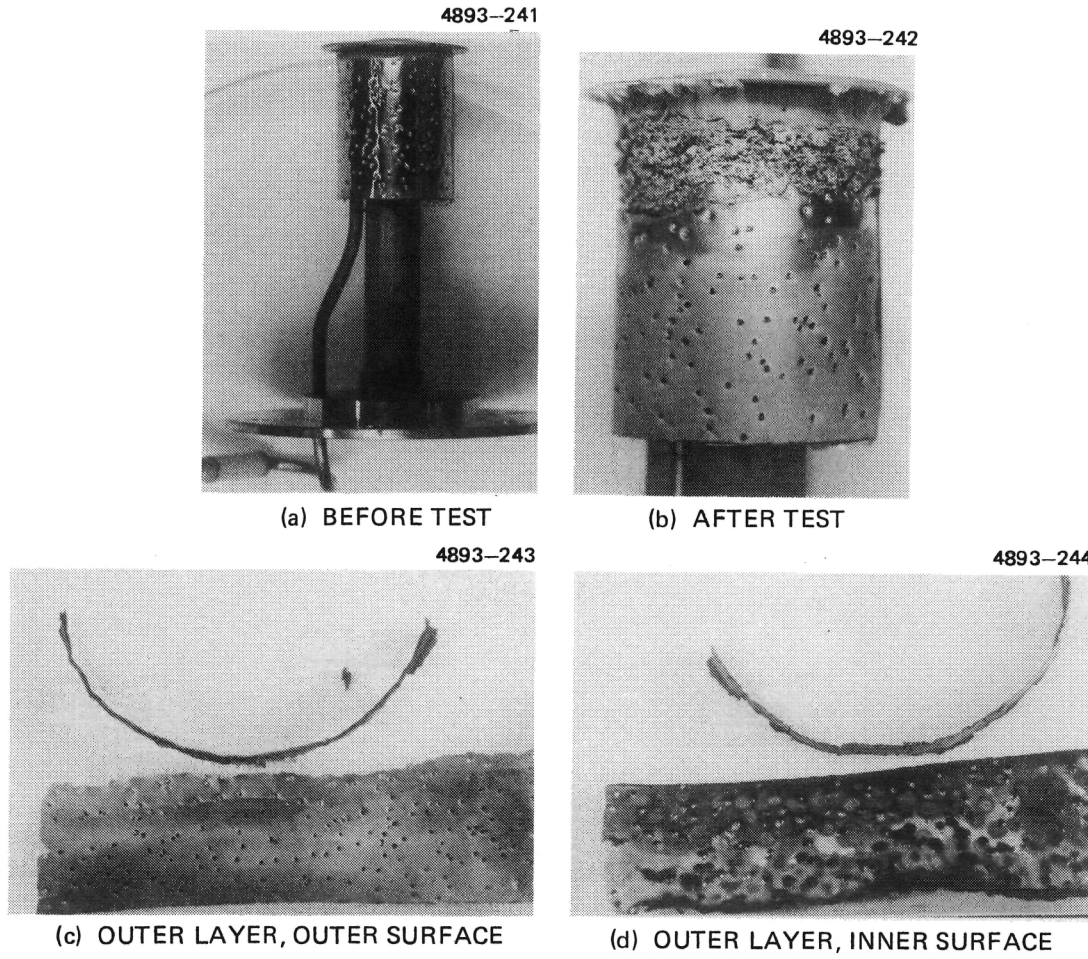

Figure A-117. Cathode heat shield before and after endurance test.

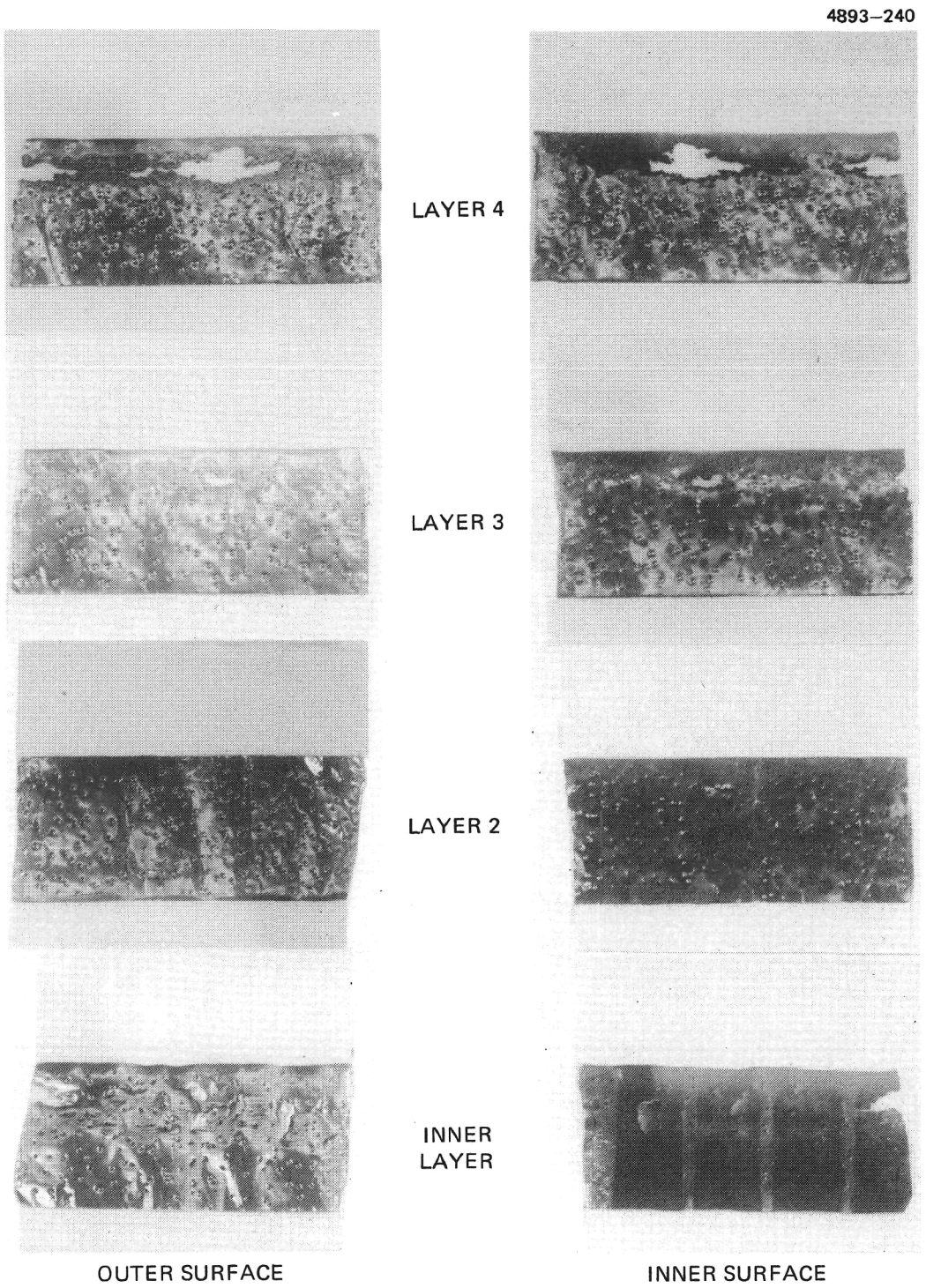

Figure A-118. Cathode heat shield after endurance test.

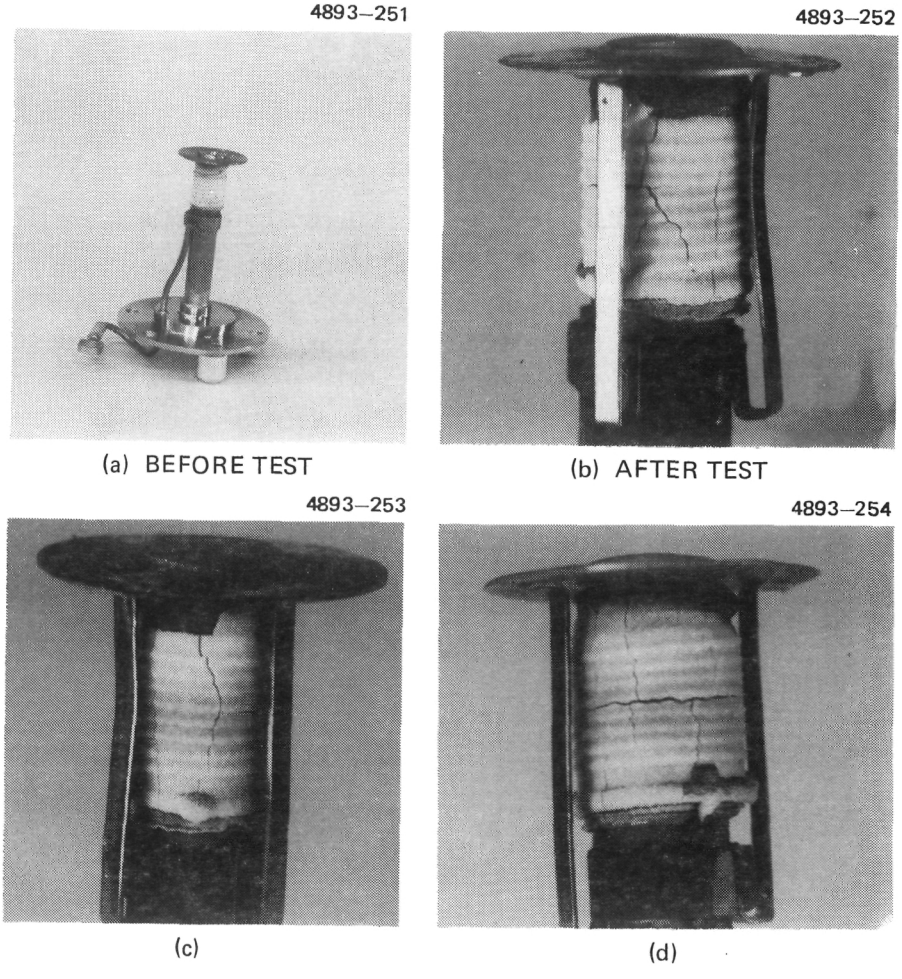

Figure A-119. Cathode tip heater before and after endurance test.

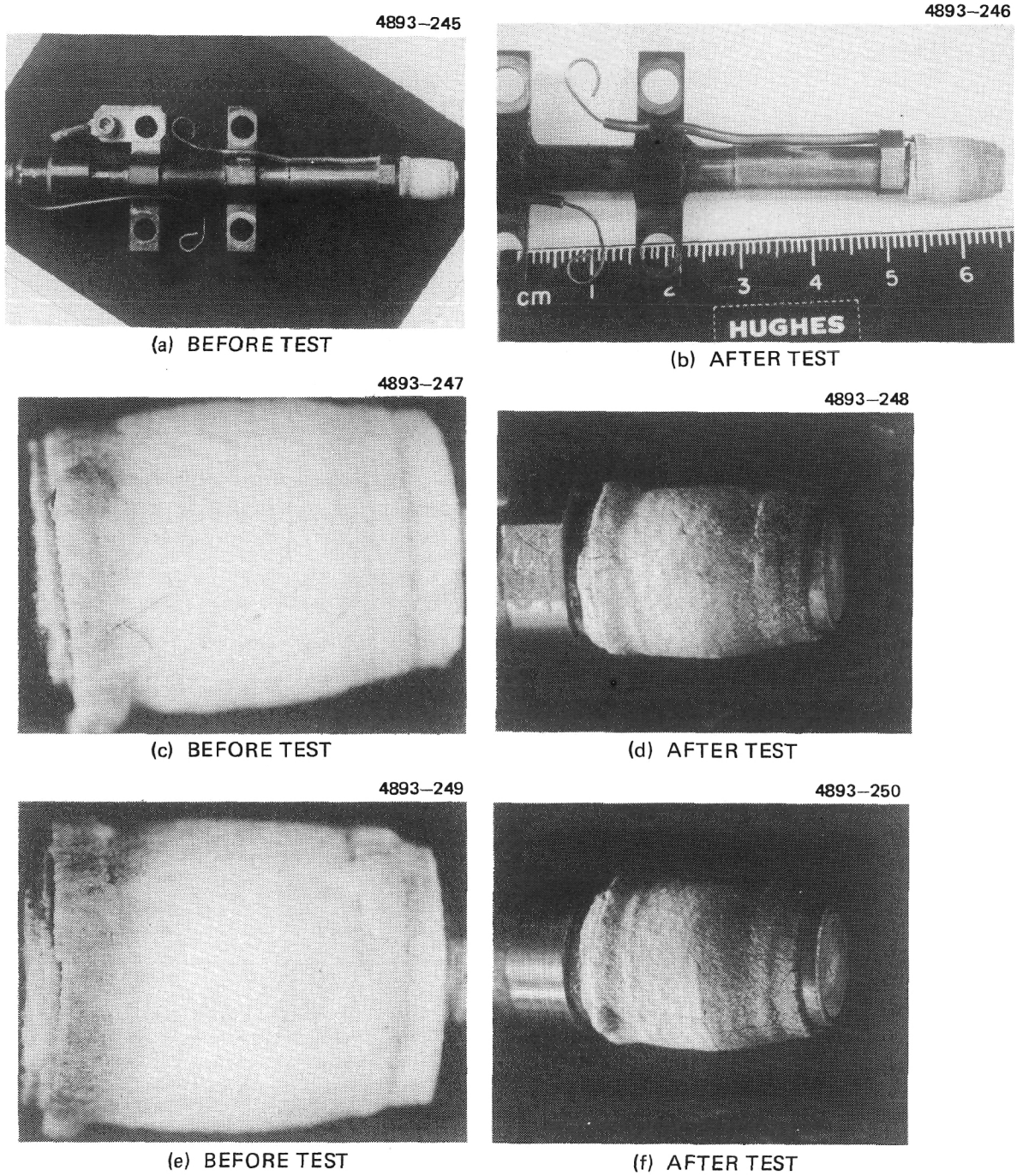

(a) BEFORE TEST

(b) AFTER TEST

(c) BEFORE TEST

(d) AFTER TEST

(e) BEFORE TEST

(f) AFTER TEST

Figure A-120. Neutralizer 701 tip heater before and after endurance test.

considered further here. These assemblies functioned according to specification throughout the test and except for the NIV, which has conductive deposits on the ceramic insulator of the isolator, the post test examination disclosed nothing that indicates wear or any form of life limitation. Thus, a problem area that existed earlier in endurance testing of a 400 series thruster design (insulation deterioration in the isolators) has been eliminated in the 700 series design. Photographs of the C-IV and MIV assemblies are included in this section to complete the post-test documentation.

Figure A-121 shows the C-IV as it appeared before the start of the test with the ceramic insulator shadow shields in place. Figure A-122 shows the same view after testing. Note that there is a slight darkening of the entire assembly. One can speculate that this slight deposition could cause insulator deterioration if the insulator were not protected by the re-entrant shadow shields. Figure A-123 shows the bottom side of the assembly; note the deposits in the transition that mates with the cathode assembly. Figures A-124 and A-125 compare the assembly before and after testing as seen without the protective shield that covers the ceramic insulator. Except for a few minute spots the insulator as seen in Fig. A-125 is as clean as any new assembly.

Post-test photographs of the MIV assembly are shown in Figs. A-126 through A-128. As in the case of the cathode isolator assembly, there is no evidence of anything that could be considered a life limiting factor. Further analysis of these assemblies is considered unnecessary.

M10066

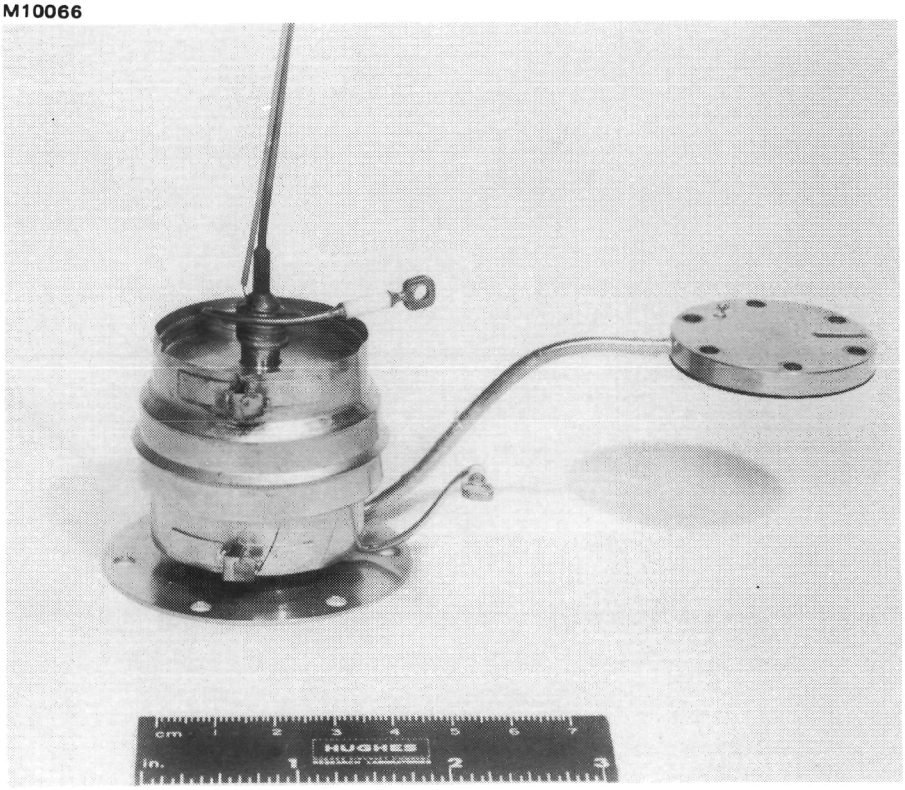

Figure A-121. C-IV before test.

M11118

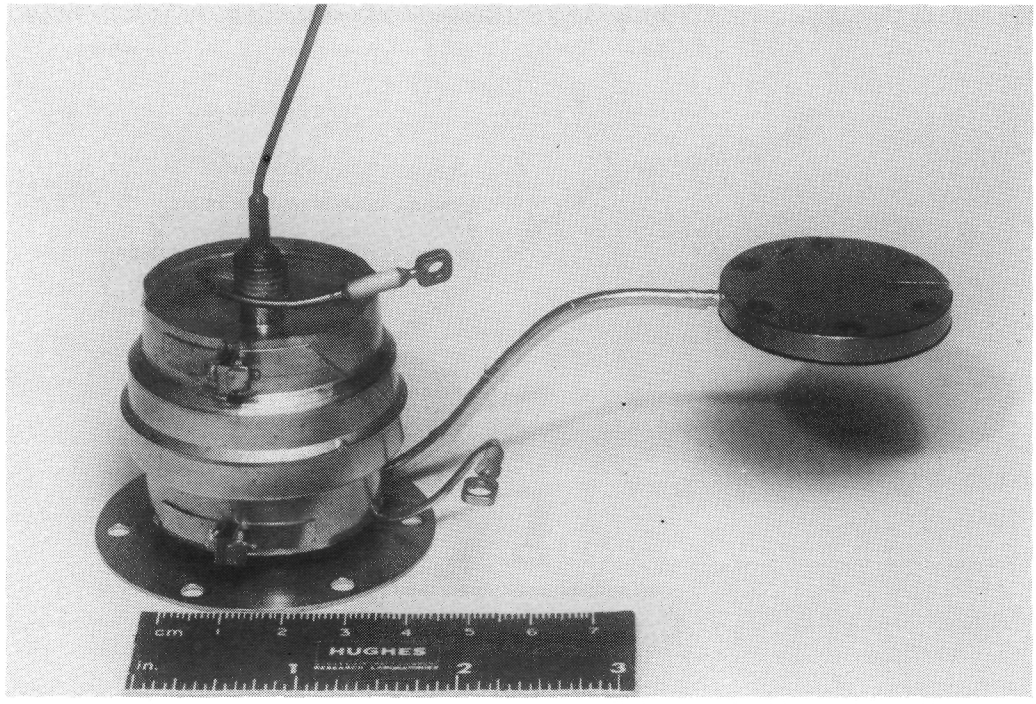

Figure A-122. C-IV after test.

M11117 4893–265

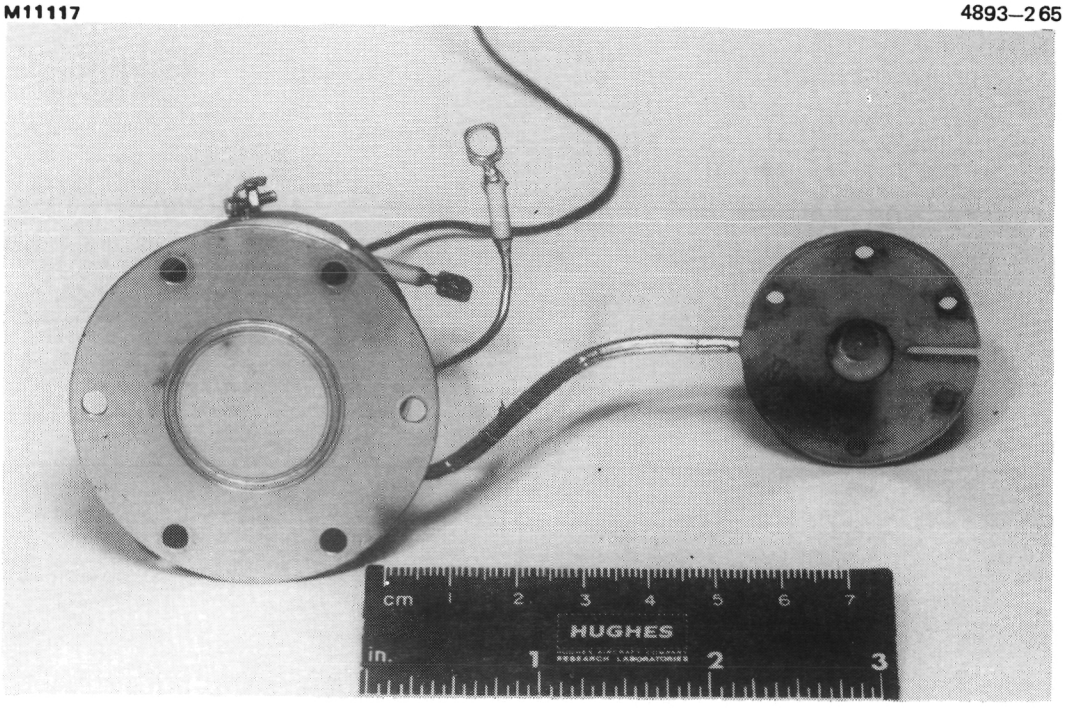

Figure A-123. Bottom of C-IV assembly after endurance test.

4893–255

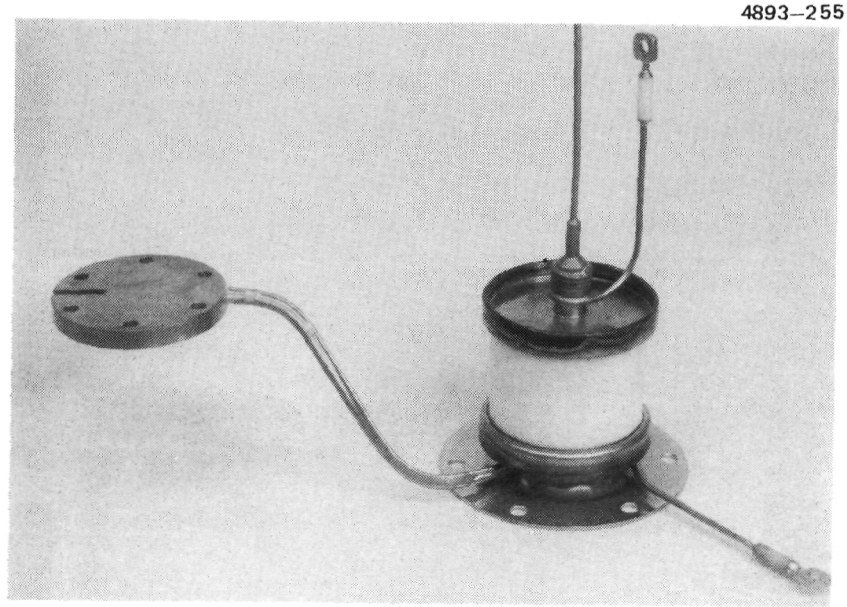

4893–256

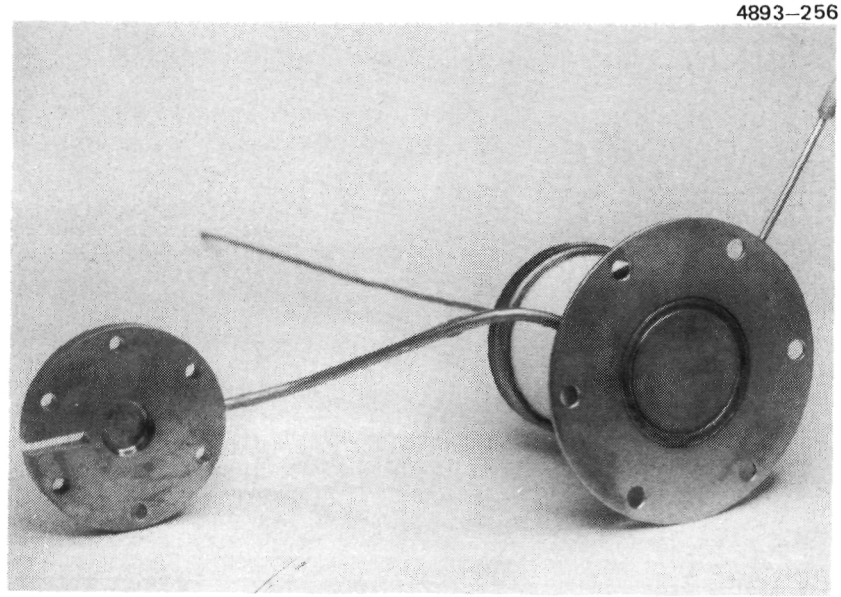

Figure A-124. C-IV before test.

M11143

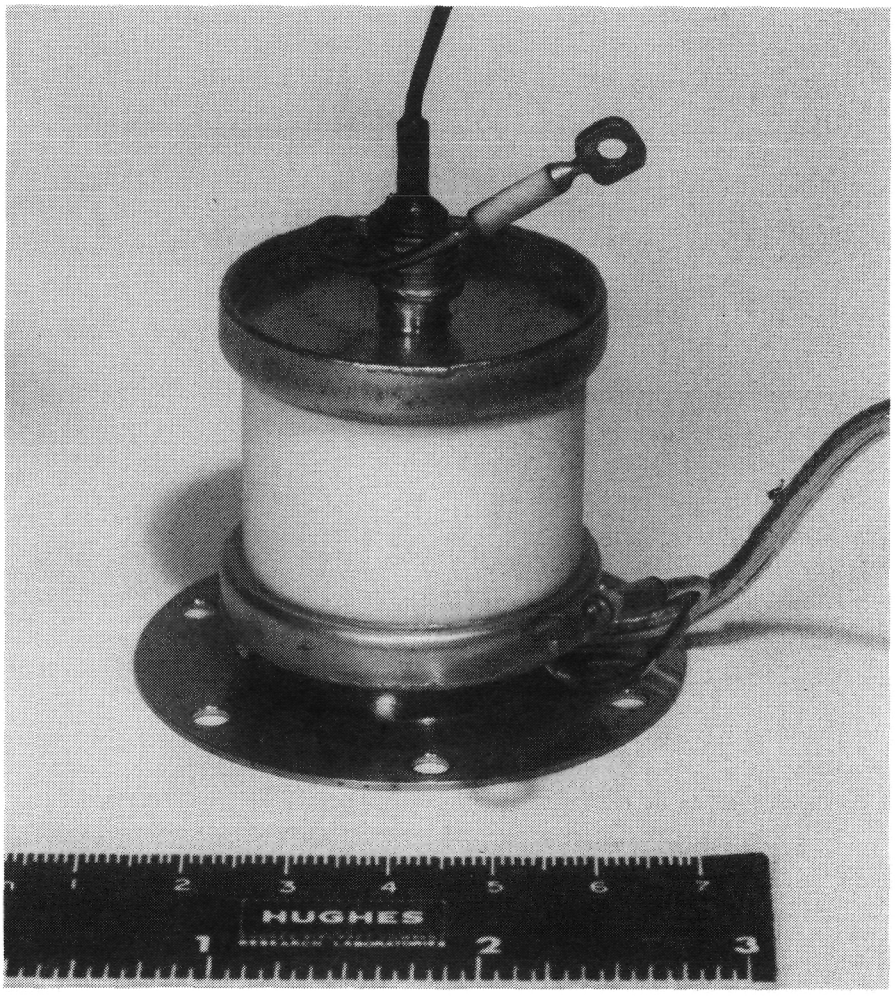

Figure A-125. C-IV after test.

M11114

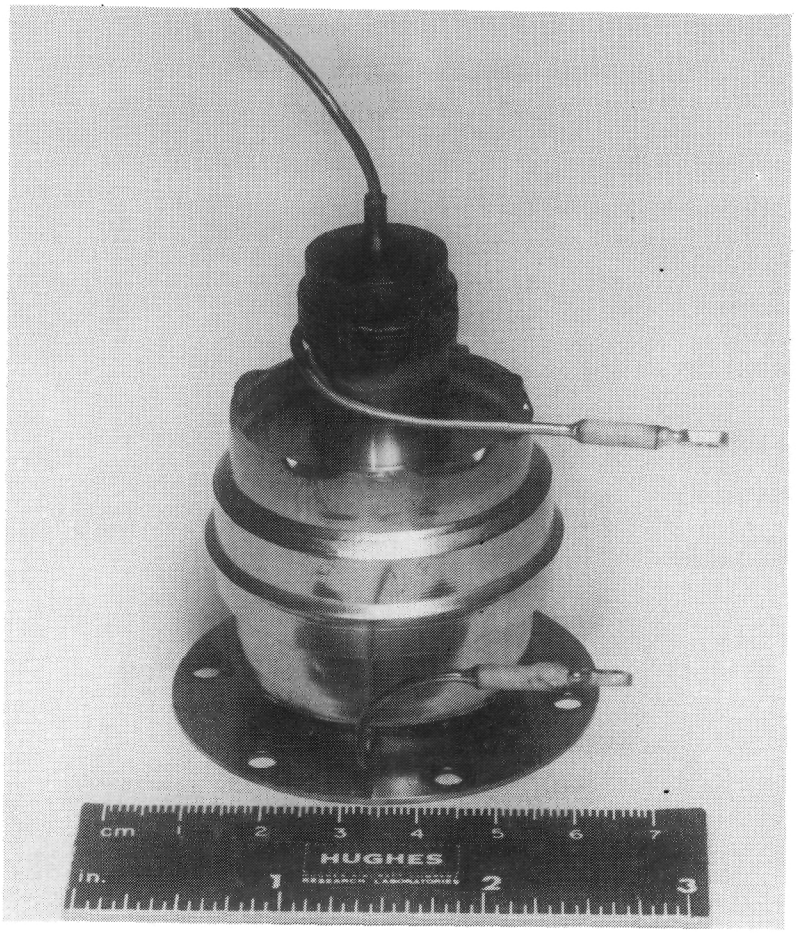

Figure A-126. MIV assembly after endurance test.

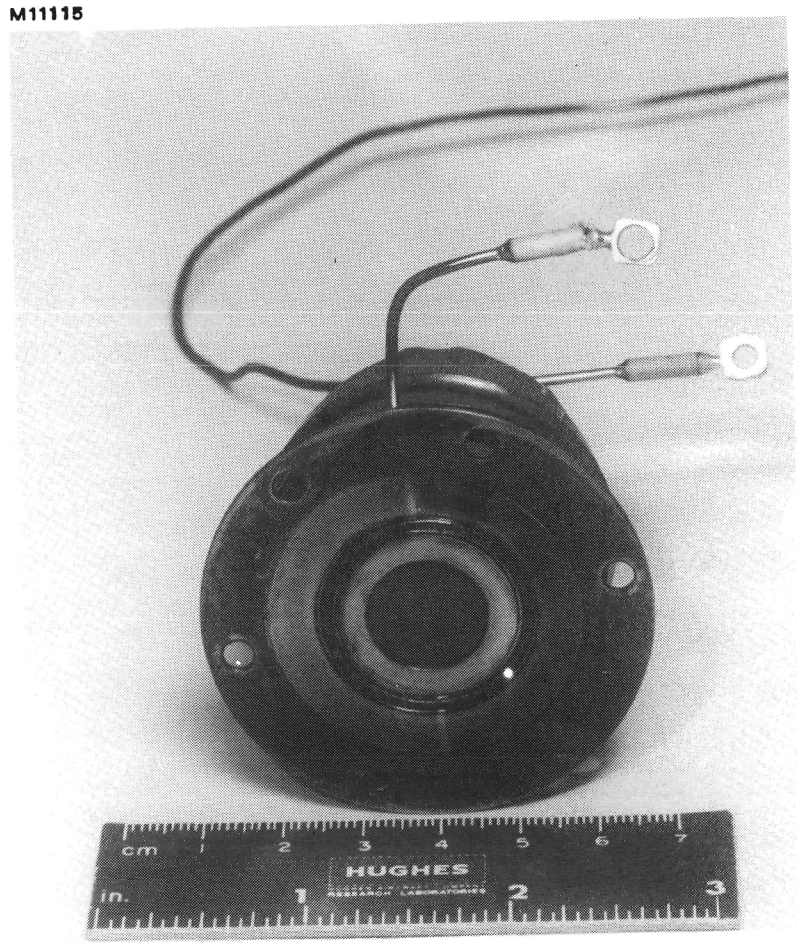

Figure A-127. MIV after endurance test.

MC11144

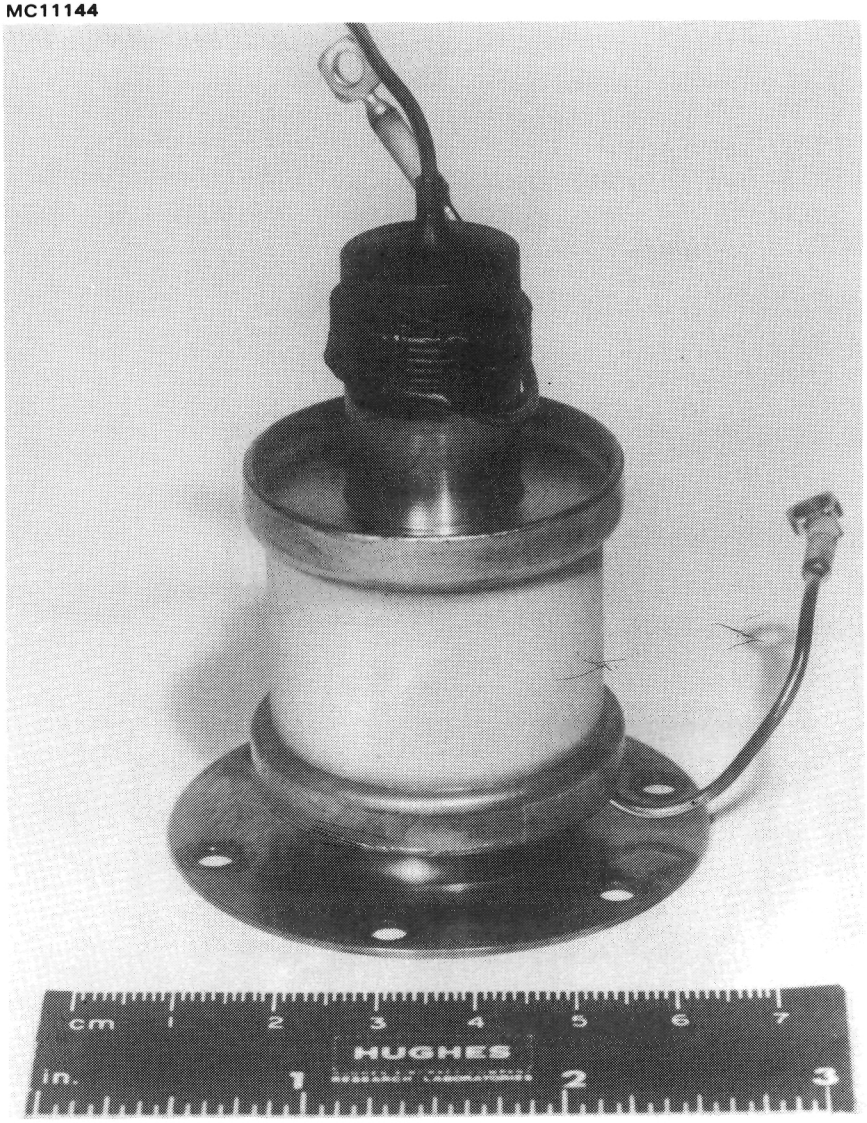

Figure A-128. MIV after endurance test.

REFERENCES

1. H. J. King et al., "Low Voltage 30 CM Thruster," NASA CR-120919, February 1972.

2. A. J. King et al., "Low Voltage 30 CM Ion Thruster Development," NASA CR-134731, October 1974.

3. D.E. Schnelker and C.R. Collett, "30-cm Engineering Model Thruster Design and Qualification Tests, AIAA Paper 75-341, March, 1975.

4. J.L. Power, "Solutions for Discharge Chamber Sputtering and Anode Deposit Spalling in Small Ion Thrusters," AIAA Paper 75-399, New Orleans, La., 1975.

5. M.A. Mantenieks and V.K. Rawlin, "Studies of Internal Sputtering in a 30-cm Ion Thruster," AIAA Paper 75-400, New Orleans, La., 1975.